

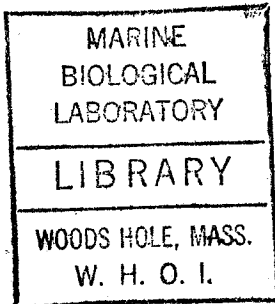
GC  
7.1  
A24  
1980

THE MARINE GEOCHEMISTRY OF THORIUM AND PROTACTINIUM

by

ROBERT FREDERICK ANDERSON

B.S., University of Washington  
(1975)



SUBMITTED IN PARTIAL FULFILLMENT  
OF THE REQUIREMENTS FOR THE  
DEGREE OF

DOCTOR OF PHILOSOPHY

at the

MASSACHUSETTS INSTITUTE OF TECHNOLOGY

and the

WOODS HOLE OCEANOGRAPHIC INSTITUTION

November, 1980

Signature of Author ..... ..

Joint Program in Oceanography, Massachusetts Institute  
of Technology-Woods Hole Oceanographic Institution,  
and Department of Earth and Planetary Sciences,  
Massachusetts Institute of Technology, November, 1980.

Certified by .. ..

Michael P. Bacon, Thesis Supervisor

Accepted by ..... ..

Chairman, Joint Oceanography Committee in the Earth  
Sciences, Massachusetts Institute of Technology-Woods  
Hole Oceanographic Institution.

THE MARINE GEOCHEMISTRY OF THORIUM AND PROTACTINIUM

by

Robert Frederick Anderson

Submitted to the Massachusetts Institute of Technology-Woods Hole Oceanographic Institution Joint Program in Oceanography on November 3, 1980 in partial fulfillment of the requirements of the Degree of Doctor of Philosophy.

ABSTRACT

Suspended particulate matter was collected by sediment traps deployed in the Sargasso Sea (Site S<sub>2</sub>), the north equatorial Atlantic (Site E), the north equatorial Pacific (Site P), and the Panama Basin (STIE Site). Additional samples of suspended particles were obtained by in situ filtration at Site E, at the STIE Site, and in the Guatemala Basin. Concentrations of dissolved Th and Pa were determined by extraction onto manganese dioxide adsorbers at Site P, at a second site in the Sargasso Sea (Site D), at the STIE Site and in the Guatemala Basin. Sediment samples were obtained from cores taken near Sites E and P.

Results have shown unequivocally that suspended particulate matter in the open ocean preferentially scavenges Th relative to Pa. This behavior could not have been predicted from the known physical chemistry of Th and Pa. Dissolved <sup>230</sup>Th/<sup>231</sup>Pa activity ratios were 3-5 at Sites P and D and 3-8 at the STIE Site. In contrast, unsupported <sup>230</sup>Th/<sup>231</sup>Pa ratios were 22-35 (average 29.7 for 7 samples) in sediment-trap samples from greater than 2000 m at Sites S<sub>2</sub>, E and P. Ratios were lower in particulate matter sampled at shallower depths. Particles filtered at 3600 m and 5000 m at Site E had ratios of 50 and 40. In contrast to the open ocean samples described above, samples collected by six sediment traps at depths of 667-3791 m in the Panama Basin had unsupported <sup>230</sup>Th/<sup>231</sup>Pa ratios of 4-8, and the deepest samples had the lowest ratios. Fractionation of Th and Pa that was observed at the three open ocean sites either does not occur or occurs to a very limited extent in the Panama Basin.

Particulate <sup>230</sup>Th/<sup>231</sup>Pa ratios were negatively correlated with the concentration of suspended particles. However, variable scavenging rates, as indicated by variable particle concentration, do not completely control the ratio at which Th and Pa are scavenged from solution. Major biogenic and inorganic components of trapped material were found in approximately the same proportions in the STIE samples and in samples from Sites E and S<sub>2</sub>. Lower <sup>230</sup>Th/<sup>231</sup>Pa ratios found in the STIE samples must therefore result from subtle changes in the chemical properties of the particles. Consideration of <sup>230</sup>Th/<sup>231</sup>Pa ratios in several depositional environments indicates that no single factor controls the ratio at which Th and Pa are adsorbed from seawater.

Fluxes of <sup>230</sup>Th and <sup>231</sup>Pa were less than their rates of production in the overlying water column in every trap at Sites S<sub>2</sub>, E,

1981-61701

and P. In the Panama Basin, fluxes measured with the same traps were greater than or equal to their rates of production. These results are a strong indication that even extremely reactive elements such as Th and Pa are redistributed within the oceans. Redistribution occurs because variable scavenging rates in different environments set up horizontal concentration gradients. Horizontal mixing processes produce a net horizontal transport of Th and Pa from areas of low scavenging rates to areas of high scavenging rates. Protactinium is redistributed to a greater extent than Th. Fluxes of  $^{230}\text{Th}$  can be used to set lower limits for horizontal transport of Pa even when absolute trapping efficiencies of the sediment traps are not known. Less than 50% of the Pa produced at the open ocean sites is removed from the water column by scavenging to settling particles. The remainder is removed by horizontal transport to other environments.

At Sites E and P,  $^{230}\text{Th}/^{231}\text{Pa}$  ratios were identical in the deepest sediment trap sample and in surface sediments. However,  $^{230}\text{Th}/^{232}\text{Th}$  and  $^{231}\text{Pa}/^{232}\text{Th}$  ratios were 2.5 times higher in trapped particles than in surface sediments. The  $^{230}\text{Th}/^{232}\text{Th}$  ratios were 5.5 times higher in particles filtered at 3600 m and 5000 m at Site E than in surface sediments. This observation is best explained by dissolution of most of the  $^{230}\text{Th}$  and  $^{231}\text{Pa}$  scavenged by settling particles during remineralization of labile biogenic phases.

The behaviors of certain other radioisotopes were also studied.  $^{232}\text{Th}$  is present only in detrital mineral components of trapped material. Concentrations of  $^{232}\text{Th}$  in trapped particles correlate closely with Al and K, at ratios approaching that of average shale or crustal abundances at Sites E and P and basalts at the STIE Site. High specific activities of  $^{228}\text{Th}$  and  $^{239+240}\text{Pu}$  were found in sediment trap samples throughout the water column at Sites E and P and in the Panama Basin. The dominant source of these isotopes is near the sea surface and also near the sea floor in the case of  $^{228}\text{Th}$ . Thus it appears that the bulk of the trapped material is recently derived from the sea surface where it incorporates these isotopes, with little loss during rapid transit through the water column. A bioauthigenic form of particulate uranium is produced at the sea surface and remineralized in the deep ocean along with its labile carrier phase(s). This flux of uranium to the deep ocean is  $0.25\text{--}1.0\text{ dpm/cm}^2 \cdot 10^3\text{ years}$ , which is insufficient to cause a measurable concentration gradient in the uranium distribution within the mixing time of the oceans. Increased concentrations and fluxes of particulate uranium were not found in the eastern equatorial North Pacific under areas of an intense oxygen minimum. Therefore, reduction of uranium to the tetravalent state with subsequent scavenging to settling particles in oxygen minima is not a mechanism removing uranium from the oceans.

Thesis Supervisor:

Dr. Michael P. Bacon  
Associate Scientist  
Department of Chemistry  
Woods Hole Oceanographic Institution  
Woods Hole, Massachusetts 02543

### ACKNOWLEDGEMENTS

Many people have assisted with various parts of this thesis research. Mike Bacon, my thesis advisor, provided my first exposure to marine radiochemistry the first day that I arrived at WHOI. Since then, he has not only provided guidance and direction for this research, but he labored through many drafts of first a thesis proposal and now this thesis. Many of the opportunities to obtain samples for this work came about through his initiatives.

Discussions with all of the members of the thesis committee, Mike Bacon, Peter Brewer, Ed Boyle, and Karl Turekian, during the past three years have lead to many of the ideas that were pursued in this thesis.

Alan Fleer has been a great help in developing the methods used in this thesis and in obtaining samples at sea. He is appreciated equally as much for his part in daily intellectually stimulating conversations in the lab.

This work relied heavily on the PARFLUX sediment trap samples. I am most grateful to Sus Honjo, Derek Spencer, and Peter Brewer for parting with portions of these samples that are many times more expensive than gold.

The in situ filtration systems used during this research functioned superbly thanks to the expertise of Pete Sachs.

The use of MnO<sub>2</sub> Nitex adsorbers to extract trace elements was initiated by Wei Min Hao. Much of the success of the continuance of this work can be attributed to the willingness of Werner Deuser to deploy and recover the sequential nitex samples which were attached to his sediment trap.

The Bowen group provided assistance with several aspects of this work. In particular, Hugh Livingston was very helpful in initiating the study of the fallout isotopes in the sediment trap samples. The plutonium results in this thesis would not have been obtained without his assistance.

Discussions with Bob Collier and Jim Bishop provided insight into the techniques of filtering large volumes of seawater in situ. The MIT-LVFS samples that they provided were the first samples of filtered particles that were obtained.

My wife, Christine, spent many days typing tables and preparing the final copy of this thesis. Her support during the last days of writing the thesis has prevented a sure case of depression on my part.

Leigh Volkman drafted most of the figures. Christine, Leigh, and Linda Botelho were of invaluable assistance in assembling the final copy of the thesis in the wee hours of the morning it was to be turned in.

In addition to the people noted above, Debbie, Becky, Susan, Edith, Hein, and my fellow chemistry students in general provided encouragement when it was needed during the writing of this thesis, and generally made everyday work a pleasant experience.

My parents provided me with encouragement and financial support through many years of being a student. My pursuit of an academic career is largely a result of their showing me at an early age that it is a joy to learn.

Financial support for parts of this work have come from many sources, including: National Science Foundation Grants OCE-7826318, OCE-7825724, and OCE-7727004; Department of Energy Contract EY-76-S-02-3566; a Cottrell Research Grant from the Research Corporation; the WHOI Ocean Industries Program; a fellowship from the WHOI Education Office, and the Paul Fye Fellowship.

TABLE OF CONTENTS

	Page
Title Page . . . . .	.1
Abstract . . . . .	.2
Acknowledgements . . . . .	.4
Table of Contents . . . . .	.6
List of Figures . . . . .	.8
List of Tables . . . . .	.11
CHAPTER 1. GENERAL INTRODUCTION . . . . .	13
Introduction . . . . .	13
History of Marine Radiochemical Research Leading to this Dissertation . . . . .	13
Early Comparisons of the Marine Geochemistry of Thorium and Protactinium . . . . .	18
Questions Concerning The Geochemical Behavior of Thorium and Protactinium . . . . .	20
Objectives of this Dissertation . . . . .	33
CHAPTER 2. METHODS . . . . .	35
Introduction . . . . .	35
Sample Preparation . . . . .	35
Analytical Techniques . . . . .	37
Sample Counting . . . . .	48
Sources of Error . . . . .	50
Accuracy and Precision . . . . .	66
Conclusions . . . . .	69
CHAPTER 3. PROCESSES REMOVING THORIUM AND PROTACTINIUM FROM SEAWATER: OPEN OCEAN ENVIRONMENTS . . . . .	70
Introduction . . . . .	70
Sample Procurement and Handling Procedure . . . . .	71
Results . . . . .	74
Discussion . . . . .	81
Chemical Behavior of Thorium-230 and Protactinium-231 . . . . .	85
Chemical Behavior of Other Isotopes . . . . .	119
Conclusions . . . . .	136
CHAPTER 4. CONCENTRATIONS OF THORIUM AND PROTACTINIUM IN SEAWATER DETERMINED BY ADSORPTION ONTO MANGANESE-OXIDE-COATED NITEX . . . . .	139
Introduction . . . . .	139
Laboratory Adsorption Experiments . . . . .	140
Methods and Sampling Locations . . . . .	144
Results . . . . .	144
Discussion . . . . .	
$^{230}\text{Th}/^{232}\text{Th}$ Ratios . . . . .	151
Particulate Thorium and Protactinium in the Nitex Samples . . . . .	151
$^{230}\text{Th}/^{231}\text{Pa}$ Activity Ratios . . . . .	154
Processes Removing Thorium and Protactinium from Seawater . . . . .	154

Short Term Variations in $^{230}\text{Th}$ and $^{231}\text{Pa}$ Concentrations at Site D . . . . .	.157
Residence Times of Thorium and Protactinium . . . . .	.160
Speculation About Growth Rates of Manganese Nodules . . . . .	.163
Conclusions . . . . .	.166
CHAPTER 5. PROCESSES REMOVING THORIUM AND PROTACTINIUM FROM SEAWATER: OCEAN-MARGIN ENVIRONMENTS . . . . .	168
Introduction . . . . .	.168
Sample Locations . . . . .	.170
Results . . . . .	.172
Discussion . . . . .	.180
Scavenging of Thorium and Protactinium in the Panama Basin . . . . .	.180
Scavenging of Thorium and Protactinium in the Guatemala Basin . . . . .	.195
Reversibility of Scavenging Processes . . . . .	.206
Residence Times of Thorium and Protactinium . . . . .	.207
Geochemical Behavior of Other Isotopes . . . . .	.215
Conclusions . . . . .	.225
CHAPTER 6. GENERAL SUMMARY . . . . .	228
Introduction . . . . .	.228
Some Aspects of the Solution Chemistry of Thorium and Protactinium . . . . .	229
Speculation About Processes Removing Thorium and Protactinium from Seawater . . . . .	.234
The Influence of Scavenging Rates on Particulate $^{230}\text{Th}/^{231}\text{Pa}$ Ratios . . . . .	.234
Composition of Particles as a Factor Controlling $^{230}\text{Th}/^{231}\text{Pa}$ Ratios . . . . .	.238
Depth Dependent Factors . . . . .	.252
Scavenging in Surface Seawater . . . . .	.254
Solution Chemistry . . . . .	.255
General Summary of Information Derived from this Thesis Research . . . . .	.257
REFERENCES . . . . .	262
APPENDIX A. Concentration of Actinides in Mono Lake Water . . . . .	274
Biographical Note . . . . .	287

FIGURE CAPTIONS

- Figure 1-1. The natural uranium and thorium decay series and the  $^{241}\text{Am}$  decay series.
- Figure 1-2. Inventories of unsupported  $^{231}\text{Pa}$  in deep-sea manganese nodules.
- Figure 1-3. Inventories of unsupported  $^{230}\text{Th}$  in deep-sea manganese nodules.
- Figure 1-4. Ratios of inventories of unsupported  $^{230}\text{Th}$  ( $\text{dpm}/\text{cm}^2$ ) to unsupported  $^{231}\text{Pa}$  ( $\text{dpm}/\text{cm}^2$ ) measured in deep-sea sediment cores.
- Figure 1-5. Unsupported  $^{230}\text{Th}/^{231}\text{Pa}$  activity ratio in surface sediments as a function of age and amount of reworked material.
- Figure 2-1. Radioactive decay of a  $^{233}\text{Pa}$  standard.
- Figure 2-2. A uranium spectrum from CH 75-2, Pilot Core 8, 0-4 cm.
- Figure 2-3. A thorium spectrum requiring corrections for peak tail overlap.
- Figure 2-4. A protactinium spectrum from PARFLUX P, KK1 Core 4, 4-5 cm.
- Figure 2-5. A plutonium spectrum from a sediment-trap sample: PARFLUX P, 5500 m.
- Figure 3-1. Locations of PARFLUX sediment trap sites.
- Figure 3-2. Concentrations of plutonium in sediment trap samples at Site P.
- Figure 3-3. Concentrations of  $^{230}\text{Th}$  in sediment trap samples at Sites E and P.
- Figure 3-4. Concentrations of  $^{231}\text{Pa}$  in sediment trap samples at Sites E and P.
- Figure 3-5. Unsupported  $^{230}\text{Th}/^{231}\text{Pa}$  activity ratios in sediment trap samples, filtered particles, and sediments at sites  $S_2$  and E.
- Figure 3-6. Unsupported  $^{230}\text{Th}/^{231}\text{Pa}$  activity ratios in sediment trap samples from Site P and KK1 Cores 1, 2, and 4.



- Figure 3-7. Flux of unsupported  $^{230}\text{Th}$  in the less than 1-mm size fraction of particles collected at Sites S<sub>2</sub>, E and P.
- Figure 3-8. Flux of unsupported  $^{231}\text{Pa}$  in the less than 1-mm size fraction of particles collected at Sites S<sub>2</sub>, E, and P.
- Figure 3-9. Concentration of particles at Site E.
- Figure 3-10. Concentration of particles at Site P.
- Figure 3-11. Correlation between  $^{232}\text{Th}$  and Al in sediment trap samples, sediments, and atmospheric dust at or near Site E.
- Figure 3-12. Correlation between  $^{232}\text{Th}$  and K in sediment trap samples, sediments, and atmospheric dust at or near Site E.
- Figure 3-13. Correlation between  $^{232}\text{Th}$  and Al in sediment trap samples from Site P.
- Figure 3-14. Particulate  $^{227}\text{Ac}/^{231}\text{Pa}$  ratio in sediment-trap samples.
- Figure 4-1. Concentrations of  $^{230}\text{Th}$  and  $^{231}\text{Pa}$  determined from the MnO<sub>2</sub>-Nitex adsorbers at Site D plotted against the flux of particles into a sediment trap at the same depth during each sampling period.
- Figure 5-1. Locations of stations occupied during KN 73-16, including the STIE Site (Station 1110).
- Figure 5-2. Thorium-230 content of sediment trap samples collected at the STIE site.
- Figure 5-3. Protactinium-231 content of sediment trap samples collected at the STIE site.
- Figure 5-4. Unsupported  $^{230}\text{Th}/^{231}\text{Pa}$  activity ratio in sediment trap samples from the STIE site.
- Figure 5-5. Flux of unsupported  $^{230}\text{Th}$  as a function of depth at the STIE site.
- Figure 5-6. Flux of unsupported  $^{231}\text{Pa}$  as a function of depth at the STIE site.
- Figure 5-7a. Concentrations of particulate  $^{230}\text{Th}$  along the KN 73-16 transect in the Guatemala Basin.
- Figure 5-7b. Concentration of particulate  $^{231}\text{Pa}$  along the KN 73-16 transect in the Guatemala Basin.
- Figure 5-8. Concentration of particulate  $^{230}\text{Th}$  at the KN 73-16 stations.

- Figure 5-9. Particulate  $^{230}\text{Th}/^{231}\text{Pa}$  activity ratios along the KN 73-16 transect into the Guatemala Basin.
- Figure 5-10. Concentrations of dissolved  $^{230}\text{Th}$  along the KN 73-16 transect into the Guatemala Basin.
- Figure 5-11. Concentration of particulate  $^{234}\text{Th}$  along the KN 73-16 transect into the Guatemala Basin.
- Figure 5-12a. Particulate  $^{230}\text{Th}$  as percent of the total  $^{230}\text{Th}$  along the KN 73-16 transect into the Guatemala Basin.
- Figure 5-12b. Particulate  $^{231}\text{Pa}$  as percent of the total  $^{231}\text{Pa}$  along the KN 73-16 transect into the Guatemala Basin.
- Figure 5-13. Thorium content plotted against aluminum for STIE sediment trap samples.
- Figure 5-14. Particulate  $^{228}\text{Th}/^{230}\text{Th}$  ratios along the KN 73-16 transect into the Guatemala Basin.
- Figure 6-1. Particulate  $^{230}\text{Th}/^{231}\text{Pa}$  activity ratios plotted against the concentration of suspended particles.
- Figure 6-2. Particulate Mn concentrations at stations along a transect across the Guatemala Basin.
- Figure 6-3. Particulate Mn/Al ratios at stations along a transect across the Guatemala Basin.
- Figure 6-4. Particulate aluminum concentrations at stations along a transect across the Guatemala Basin.
- Figure 6-5. Particulate calcium concentrations at stations along a transect across the Guatemala Basin.
- Figure 6-6. Particulate V/Al ratios at stations along a transect across the Guatemala Basin.

LIST OF TABLES

- Table 2-1. Results of Blank Analyses.
- Table 2-2. Duplicate Analyses of Volcanic Glass Standard OCB 66-15.
- Table 2-3. Duplicate Analyses of Sediment and Sediment Trap Samples.
- Table 3-1. Radiochemical Results for Sediment Trap Samples.
- Table 3-2. Concentrations of Radioisotopes in Filtered Particles at PARFLUX Site E.
- Table 3-3. Radiochemical Results for Cores Associated with PARFLUX Sites E and P.
- Table 3-4. Radionuclide Concentrations in Site S<sub>2</sub> and E Samples from Brewer et al. (1980).
- Table 3-5. Unsupported <sup>230</sup>Th and <sup>231</sup>Pa in Suspended Particles.
- Table 3-6. Scaled  $x_s^{231}\text{Pa}$  Deficiency.
- Table 3-7. Relative Importance of Vertical and Horizontal Transport Processes.
- Table 3-8. Bioauthigenic Uranium Content of Sediment Trap Material - Sites E and P.
- Table 3-9. <sup>227</sup>Ac/<sup>231</sup>Pa Ratios at PARFLUX Site P.
- Table 4-1. Adsorption of <sup>234</sup>Th and <sup>233</sup>Pa onto MnO<sub>2</sub>-Coated Nitex.
- Table 4-2. MnO<sub>2</sub>-Nitex Samples Analyzed for Thorium and Protactinium Isotopes.
- Table 4-3. Thorium and Protactinium Adsorbed to MnO<sub>2</sub>-Nitex - Sites P and D.
- Table 4-4. Concentrations of <sup>230</sup>Th and <sup>231</sup>Pa in Seawater.
- Table 4-5. <sup>230</sup>Th/<sup>232</sup>Th Activity Ratios in MnO<sub>2</sub>-Nitex Samples Compared to Ratios in Deep-Sea Manganese Nodules.
- Table 4-6. Unsupported <sup>230</sup>Th/<sup>231</sup>Pa Ratios in Manganese Nodules.
- Table 4-7. Residence Times of Thorium and Protactinium.
- Table 5-1. Fluxes of Particulate Material into STIE Sediment Traps.
- Table 5-2. Radioisotope Content of Sediment Trap Material: STIE Site.

- Table 5-3. KN73-16 In Situ Filtration Samples: Station Locations and Sample Sizes.
- Table 5-4. Effective Volumes of Seawater Sampled by MnO<sub>2</sub>-Nitex Adsorbers.
- Table 5-5. KN73-16: Dissolved Radioisotopes.
- Table 5-6. KN73-16: Particulate Radioisotope Concentrations - dpm/g.
- Table 5-7. KN73-16: Particulate Radioisotope Concentrations - dpm/10<sup>6</sup>l.
- Table 5-8. Unsupported <sup>230</sup>Th and <sup>231</sup>Pa in STIE Sediment Trap Samples.
- Table 5-9. Fluxes of Unsupported <sup>230</sup>Th and <sup>231</sup>Pa into STIE Sediment Traps.
- Table 5-10. Calculated MnO<sub>2</sub> in Sediment Trap Samples.
- Table 5-11. Residence Times of Dissolved <sup>230</sup>Th and <sup>231</sup>Pa.
- Table 5-12. Bioauthigenic Uranium in STIE Samples.
- Table 6-1. Compositions of Particles Collected at Four Sediment Trap Sites.

CHAPTER 1.

GENERAL INTRODUCTION

INTRODUCTION

The natural radioactive decay series, of which  $^{238}\text{U}$ ,  $^{235}\text{U}$ , and  $^{232}\text{Th}$  are the parents (Figure 1-1), have been present in the environment since the formation of the earth. Geochemical processes act upon the uranium- and thorium-series isotopes in the same manner as they act upon the stable elements. As geochemical processes separate elements with different chemical properties within the radioactive decay series, radioactive decay tends to restore radioactive equilibrium at a well defined rate. The degree of disequilibrium between a parent-daughter pair can then be used to determine the rate at which geochemical processes are separating the two elements.

Thorium-230 and protactinium-231 are valuable tracers of processes which scavenge reactive elements (elements that are rapidly adsorbed to particle surfaces) from seawater. Both isotopes are produced in seawater by radioactive decay of dissolved uranium, which has a long residence time ( $4 \times 10^5$  years; Brewer, 1975) in the oceans because of the stable complex it forms with carbonate ions (Starik and Kolyadnin, 1957; Langmuir, 1978). Because of its long residence time, the uranium concentration is constant throughout the open ocean (Turekian and Chan, 1971; Ku et al., 1977). Thus,  $^{230}\text{Th}$  and  $^{231}\text{Pa}$  are produced at constant rates throughout the ocean, greatly simplifying the modeling of the rates and mechanisms of removal of these isotopes from seawater.

History of Marine Radiochemical Research Leading to this Dissertation

Radioactive decay provides the ultimate clock against which all geological time scales must be set. Some of the earliest marine

U - 238 Series

Th - 232 Series

U - 235 Series

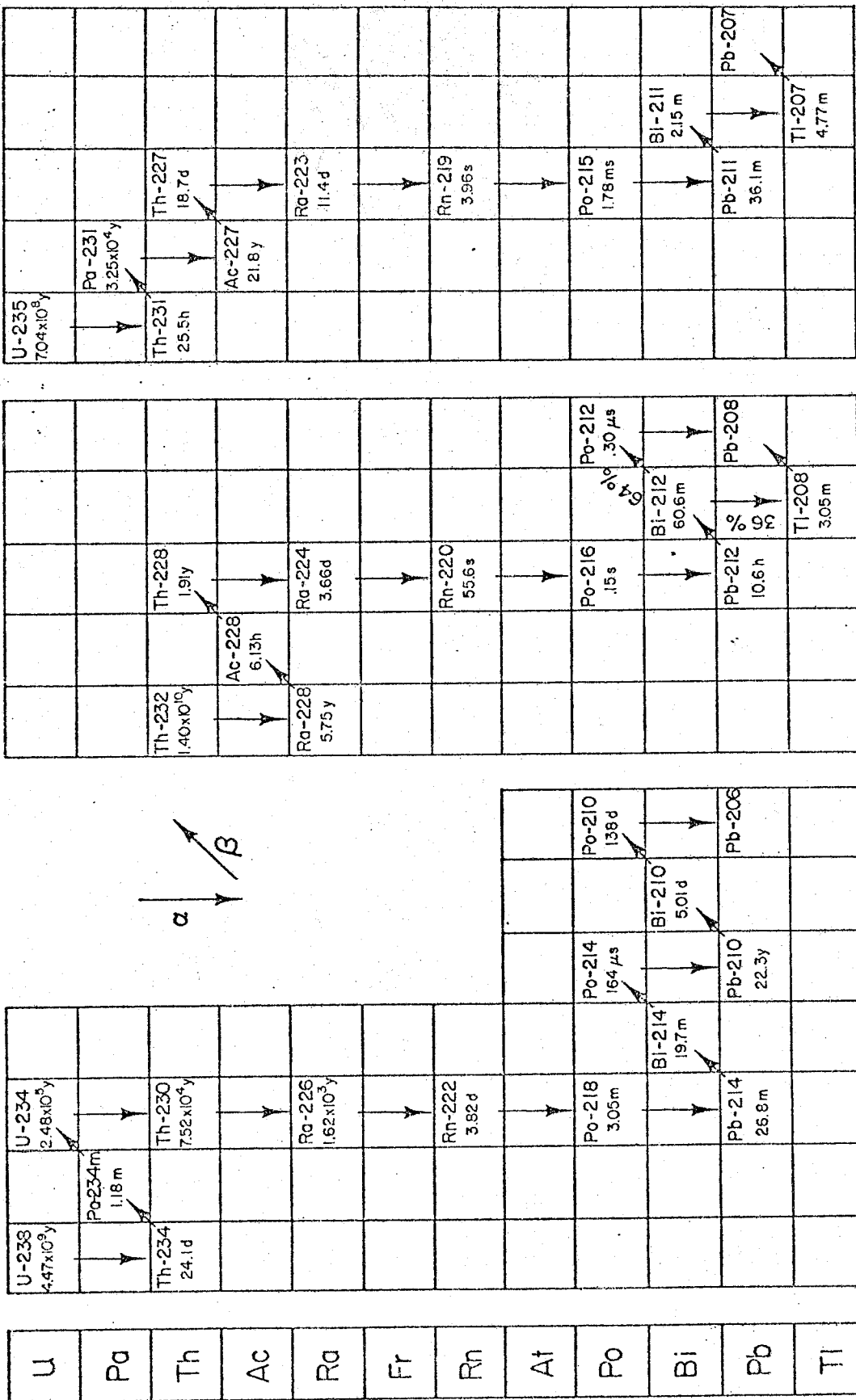
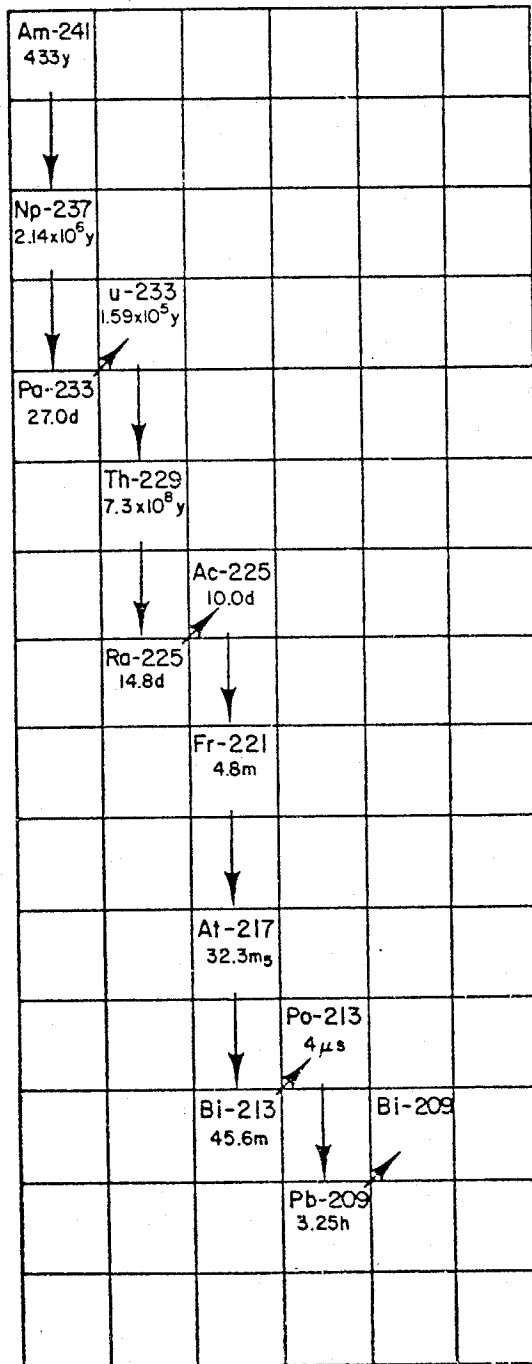


Figure 1-1a. The natural uranium and thorium decay series. Half-lives are from Lederer and Shirley (1978).

Figure 1-1b. The man-made  $^{241}\text{Am}$  decay series. Half-lives are from Lederer and Shirley (1978).

### Am - 241 Series



radiochemical research involved attempts to determine deep-sea sedimentation rates from uranium-series disequilibria. The early history of this field has been reviewed by several authors (Ku, 1966, 1976; Thomson and Walton, 1972; Goldberg and Bruland, 1974; Osmond, 1979). Only the history leading up to this research on the marine geochemistry of thorium and protactinium will be reviewed here.

The  $^{226}\text{Ra}$  content of deep-sea sediments was first measured by Joly (1908) and later by Pettersson (1930) and Piggot (1933). Radium was found to be present at much higher concentrations than in continental rocks. Based on the limited number of surface sediment analyses that had been carried out, Piggot (1933) suggested that in the deep, well oxygenated ocean uranium forms insoluble oxides which settle to the sea floor, producing the high  $^{226}\text{Ra}$  contents of sediments. Uranium could not be measured at that time and subsurface sediments were not available for analysis to determine if the radium contents remained high throughout the sediment column. Pettersson (1937) later suggested that the high radium contents result from the precipitation of ionium ( $^{230}\text{Th}$ ) from seawater after production by uranium decay. This was confirmed when radium distributions were measured in cores which had been dated by the lithological changes induced by glacial-interglacial cycles. Radium contents of sediments were observed to decrease according to the half-life of  $^{230}\text{Th}$  (Piggot and Urry, 1939, 1941, 1942 a,b). Pettersson (1937) and Piggot and Urry (1941) suggested that  $^{230}\text{Th}$  is scavenged from seawater by iron oxyhydroxides since  $\text{Fe}(\text{OH})_3$  was a well known carrier of thorium in laboratory studies.

By 1942 (Piggot and Urry, 1942a) the principles of the excess  $^{230}\text{Th}$  ( $^{230}\text{Th}$  unsupported by its uranium parent) method of determining



sedimentation rates were well known (see Ku, 1976, and Osmond, 1979, for a discussion of the method). Although  $^{230}\text{Th}$  could not yet be measured directly,  $^{226}\text{Ra}$  distributions were used to obtain sedimentation rates from the decay of its  $^{230}\text{Th}$  parent with depth in sediments. Problems associated with the method, including variable rates of precipitation of  $^{230}\text{Th}$  from seawater and variable sedimentation rates, were also discussed by Piggot and Urry (1942a). Kroll (1953, 1954) showed that diffusion of  $^{226}\text{Ra}$  in sediments may lead to disequilibrium between  $^{230}\text{Th}$  and  $^{226}\text{Ra}$ , so he (Kroll, 1953) encouraged Isaac and Picciotto (1953) to make the first direct measurement of  $^{230}\text{Th}$  in deep-sea sediments by an alpha track, nuclear emulsion technique. Picciotto and Wilgain (1954) refined the method, including a correction for alpha tracks produced by  $^{227}\text{Th}$ , a decay product of  $^{231}\text{Pa}$ , which they felt might be enriched in sediments by precipitation processes much like  $^{230}\text{Th}$ .

Several methods of normalizing  $^{230}\text{Th}$  contents in sediments to other elements or isotopes with a similar source by precipitation from seawater were developed to compensate for uncertainties resulting from variable sedimentation rates and variable rates of precipitation of reactive elements from seawater. Picciotto and Wilgain (1954) suggested normalization to  $^{232}\text{Th}$  while Baranov and Kuzmina (1957, 1958) normalized excess  $^{230}\text{Th}$  to Fe and Mn oxides. The  $^{230}\text{Th}/^{231}\text{Pa}$  method was suggested by Sackett (1960) and Rosholt et al. (1961). The basis of the method is that both isotopes are produced by uranium decay in seawater and both are rapidly removed from seawater to the sediments. Normalization of  $^{230}\text{Th}$  to  $^{231}\text{Pa}$  was thought to be superior to the other methods, as  $^{232}\text{Th}$  has a very different source than  $^{230}\text{Th}$ , and

Fe and Mn have very different chemistries than  $^{230}\text{Th}$ . If  $^{230}\text{Th}$  and  $^{231}\text{Pa}$  are affected equally by scavenging processes, then the unsupported  $^{230}\text{Th}/^{231}\text{Pa}$  ratio at any depth in the sediment would be only a function of time, and would not be affected by changes in sedimentation rate or changes in the uranium concentration of seawater.

Early Comparisons of the Marine Geochemistry of Thorium and Protactinium

Thorium and protactinium were soon shown not to have identical chemical behaviors in seawater. Unsupported  $^{230}\text{Th}/^{231}\text{Pa}$  ratios in surface sediments were often greater than 10.8, the ratio expected from their rates of production by uranium decay in seawater (Sackett, 1964; Ku, 1966). In contrast, ratios less than 10.8 were found at the surfaces of manganese nodules (Sackett, 1966; Ku and Broecker, 1969). Some type of chemical fractionation of thorium and protactinium was clearly occurring in the oceans.

Attempts at measurement of the  $^{230}\text{Th}$  and  $^{231}\text{Pa}$  content of seawater were of little help in understanding the nature of the fractionation. Early thorium measurements (Fovn et al., 1939; Koczy et al., 1957) were unsuccessful in accurately determining the low concentrations. They did, however, confirm that the  $^{230}\text{Th}$  activity in seawater is very low compared to the activity of its parent,  $^{234}\text{U}$ , because of the removal of thorium to sediments by scavenging processes. Koczy et al. (1957) produced the first indirect measurement of the low concentration of  $^{231}\text{Pa}$  in seawater. An upper limit for  $^{227}\text{Th}$  set during their thorium determination showed that either  $^{231}\text{Pa}$  or  $^{227}\text{Ac}$  was present in seawater at concentrations much lower than would be found if the  $^{235}\text{U}$  series was in radioactive equilibrium.

Very few measurements of Pa have been made. Levels of Pa measured by Sackett (1960) and Moore and Sackett (1964) were close to their detection limits, with very high analytical uncertainties. Measurements of Pa by Kuznetsov et al. (1966) and Imai and Sakanoue (1973) produced results that are questionable because of the high and internally inconsistent values that they obtained. Without reliable data on the Pa content of seawater, the fractionation of  $^{230}\text{Th}$  and  $^{231}\text{Pa}$  could not be explained. However, the work cited above, and the results of  $^{230}\text{Th}$  measurements by Somayajulu and Goldberg (1966) and Miyake et al. (1970), showed that Th and Pa are removed from seawater on a time scale of decades.

Some further understanding of the geochemistry of Th has been gained by the study of  $^{228}\text{Th}$  and  $^{234}\text{Th}$ . These isotopes are also produced by radioactive decay in seawater but are present at higher activities than  $^{230}\text{Th}$  because of their much shorter half-lives. Amin et al. (1974) found  $^{234}\text{Th}$  to be in radioactive equilibrium with  $^{238}\text{U}$  in the deep ocean. Therefore, Th is removed from the deep sea on a time scale much greater than the 24 day half-life of  $^{234}\text{Th}$ . Scavenging processes act at much greater rates in surface seawater and in nearshore environments, where Th residence times of months or less have been found (Bhat et al., 1969; Broecker et al., 1973; Matsumoto, 1975; Knauss et al., 1978; Santschi et al., 1979; Li et al., 1979; Minagawa and Tsunogai, 1980).

Attempts at constructing a mass balance for  $^{230}\text{Th}$  and  $^{231}\text{Pa}$  in the oceans have not been very successful (Ku, 1966; Scott, 1968; Ku and Broecker, 1969; Turekian and Chan, 1971). While Pa is preferentially incorporated into manganese nodules, there are not a sufficient number of nodules on the sea floor to balance the deficiency of  $^{231}\text{Pa}$  relative to

$^{230}\text{Th}$  in deep-sea sediments (Scott, 1968; Ku and Broecker, 1969). A source of  $^{230}\text{Th}$  other than by decay of uranium in seawater or a sink for  $^{231}\text{Pa}$  other than deep sea sediments and manganese nodules must be found.

Scott (1968) showed that rivers contribute an insignificant amount of excess  $^{230}\text{Th}$  to the oceans. Rydell and Prospero (1972) further showed that transport on atmospheric dust is also an insignificant source of excess  $^{230}\text{Th}$ . Thus the two most likely transport mechanisms were shown to be ineffective as  $^{230}\text{Th}$  sources. Nearshore and hemipelagic sediments were suggested as possible Pa sinks by the results of Joshi and Ganguly (1976a,b) and Kraemer (1975). However, the extremely limited nature of their results precluded any concrete demonstration of these environments as preferential sinks for Pa.

#### Questions Concerning the Geochemical Behavior of Thorium and Protactinium

Many questions remain regarding the mechanism by which sea floor deposits obtain their  $^{230}\text{Th}/^{231}\text{Pa}$  ratios. These include:

- 1) Do all particulate phases scavenge Th and Pa from seawater?
- 2) Do all particulate phases scavenge Th and Pa at the same Th/Pa ratio?
- 3) Are Th and Pa removed from the water column primarily by scavenging to large, rapidly settling particles, which dominate the particle flux, or by scavenging onto small particles, which form the bulk of the standing crop of particles (McCave, 1975; Bishop et al., 1977, 1978)?
- 4) As a corollary to the above questions, where does the fractionation of  $^{230}\text{Th}$  and  $^{231}\text{Pa}$  take place?
  - A) Do settling particles, or a component of settling particulate matter preferentially adsorb dissolved Th from seawater?

B) Do manganese nodules preferentially adsorb dissolved Pa from seawater?

C) Does fractionation occur by surface-surface competition as sediments come into contact with nodules?

D) Does some form of sediment diagenesis preferentially release dissolved Pa, which is then incorporated into manganese nodules?

E) Some combination of the above?

5) Are the high  $^{230}\text{Th}/^{231}\text{Pa}$  ratios in sediments and apparent mass balance problems an artifact of reworking of old sediments? The excess  $^{230}\text{Th}/^{231}\text{Pa}$  ratio increases with a doubling time of about 57,000 years. Reworking of old sediments could therefore produce, at least locally, high  $^{230}\text{Th}/^{231}\text{Pa}$  ratios.

Some of the above questions could be partially answered by a careful consideration of available data for sediments and nodules. Ku and Broecker (1969) and Krishnaswami and Cochran (1978) found higher concentrations of  $^{230}\text{Th}$  and  $^{231}\text{Pa}$  in the tops of nodules exposed to seawater than in the bottoms buried within the sediments. This suggested that nodules obtain their  $^{230}\text{Th}$  and  $^{231}\text{Pa}$  by adsorption from seawater rather than from the sediments.

Manganese nodules contain little of the  $^{230}\text{Th}$  and  $^{231}\text{Pa}$  produced in the overlying water column (Figures 1-2 and 1-3). Therefore, even if nodules fractionate Th and Pa during adsorption, they should have little effect on the ratio of the  $^{230}\text{Th}$  and  $^{231}\text{Pa}$  remaining in seawater. If nodules obtain their  $^{230}\text{Th}$  and  $^{231}\text{Pa}$  from settling particles, and if settling particles are the dominant transport mechanism removing  $^{230}\text{Th}$  and  $^{231}\text{Pa}$  from seawater, then the rate of supply of  $^{230}\text{Th}$  and  $^{231}\text{Pa}$  to the nodules should increase with depth. It can be seen in Figures 1-2

Figure 1-2. Inventories of unsupported  $^{231}\text{Pa}$  in deep-sea manganese nodules. Data are from Ku and Broecker (1969). The solid line represents the rate at which  $^{231}\text{Pa}$  is produced (atoms per minute/  $\text{cm}^2$ ) in the overlying water column by decay of uranium.

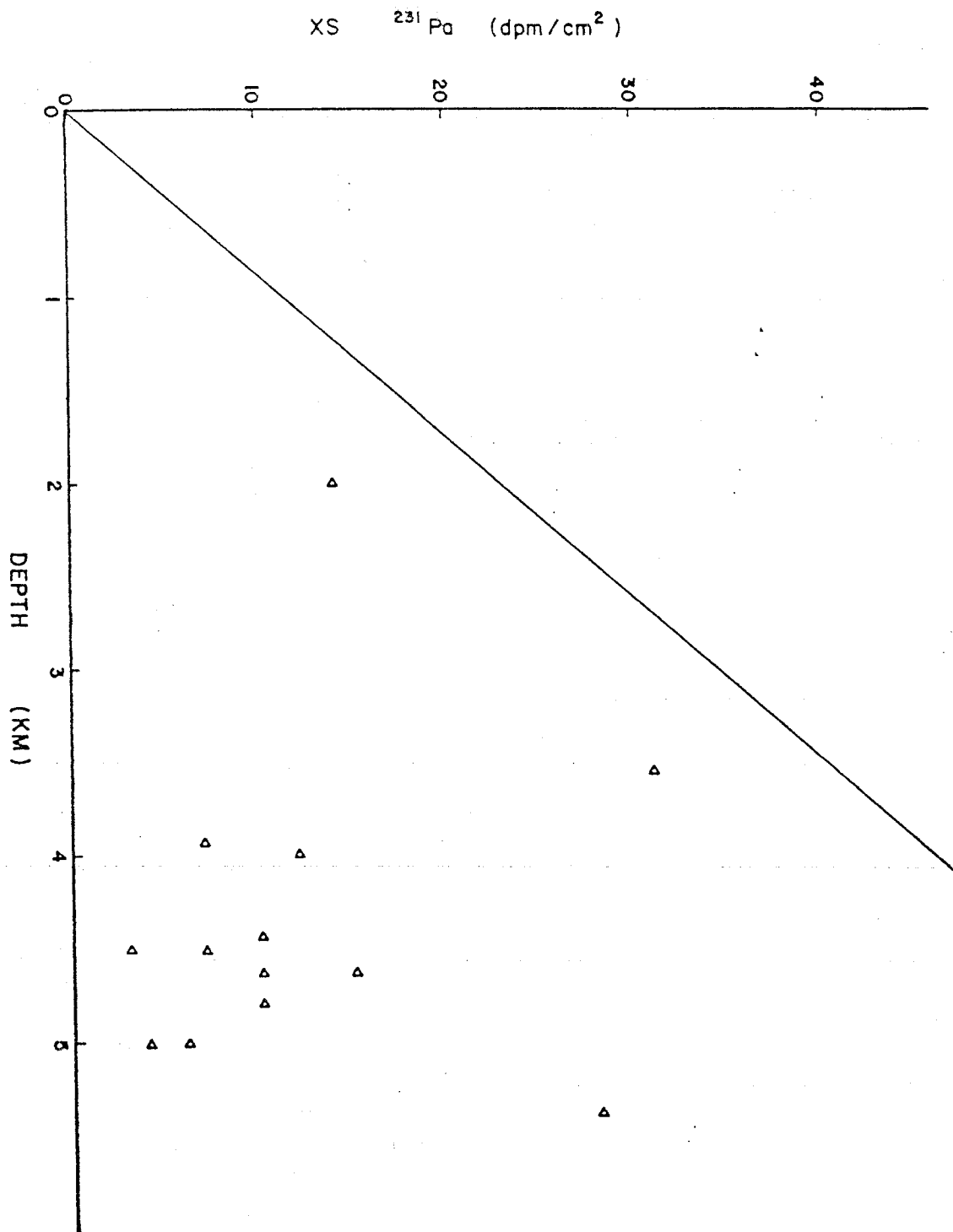
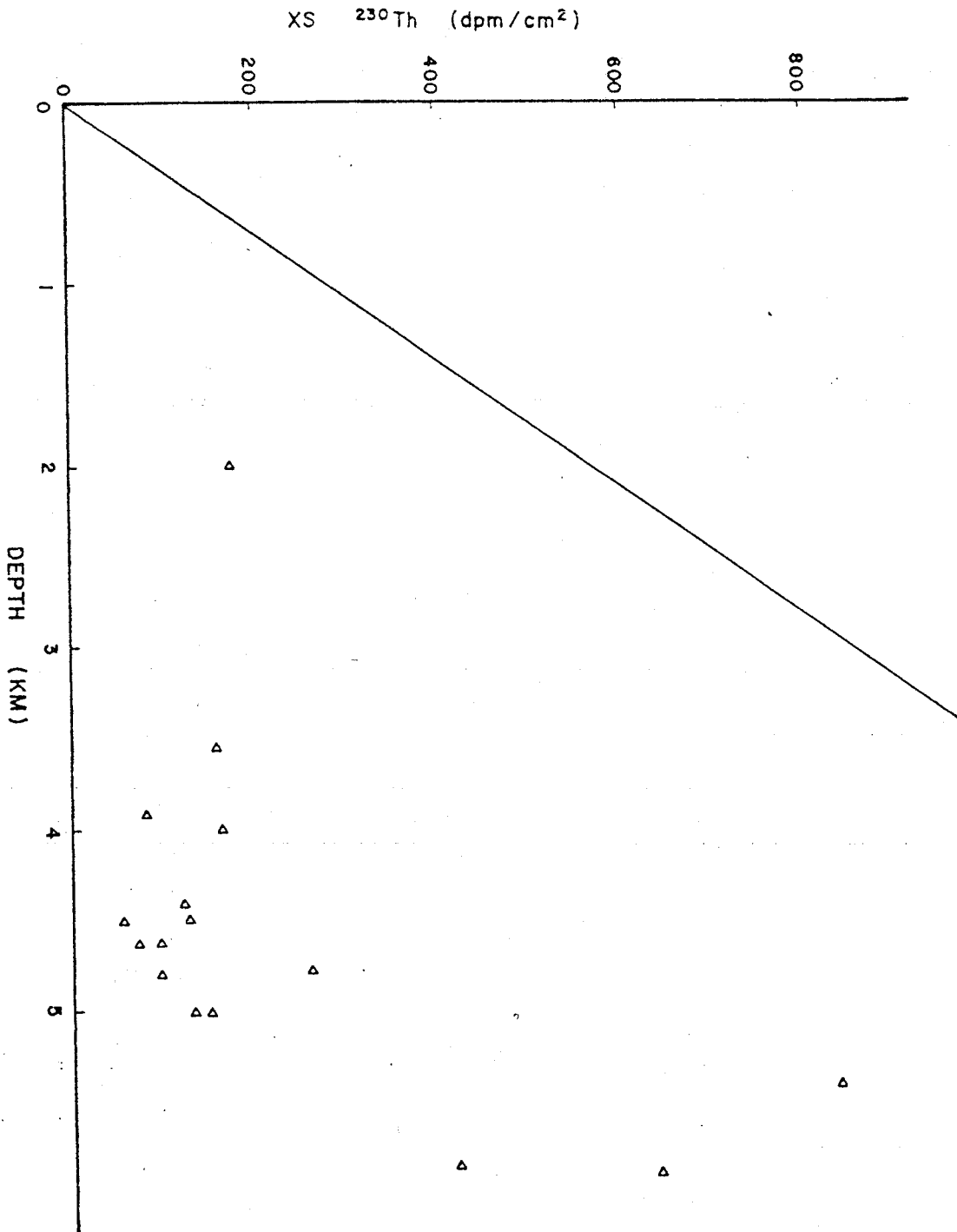


Figure 1-3. Inventories of unsupported  $^{230}\text{Th}$  in deep-sea manganese nodules. Data are from Ku and Broecker (1969). The solid line represents the rate at which  $^{230}\text{Th}$  is produced (atoms per minute/  $\text{cm}^2$ ) in the overlying water column by decay of uranium.





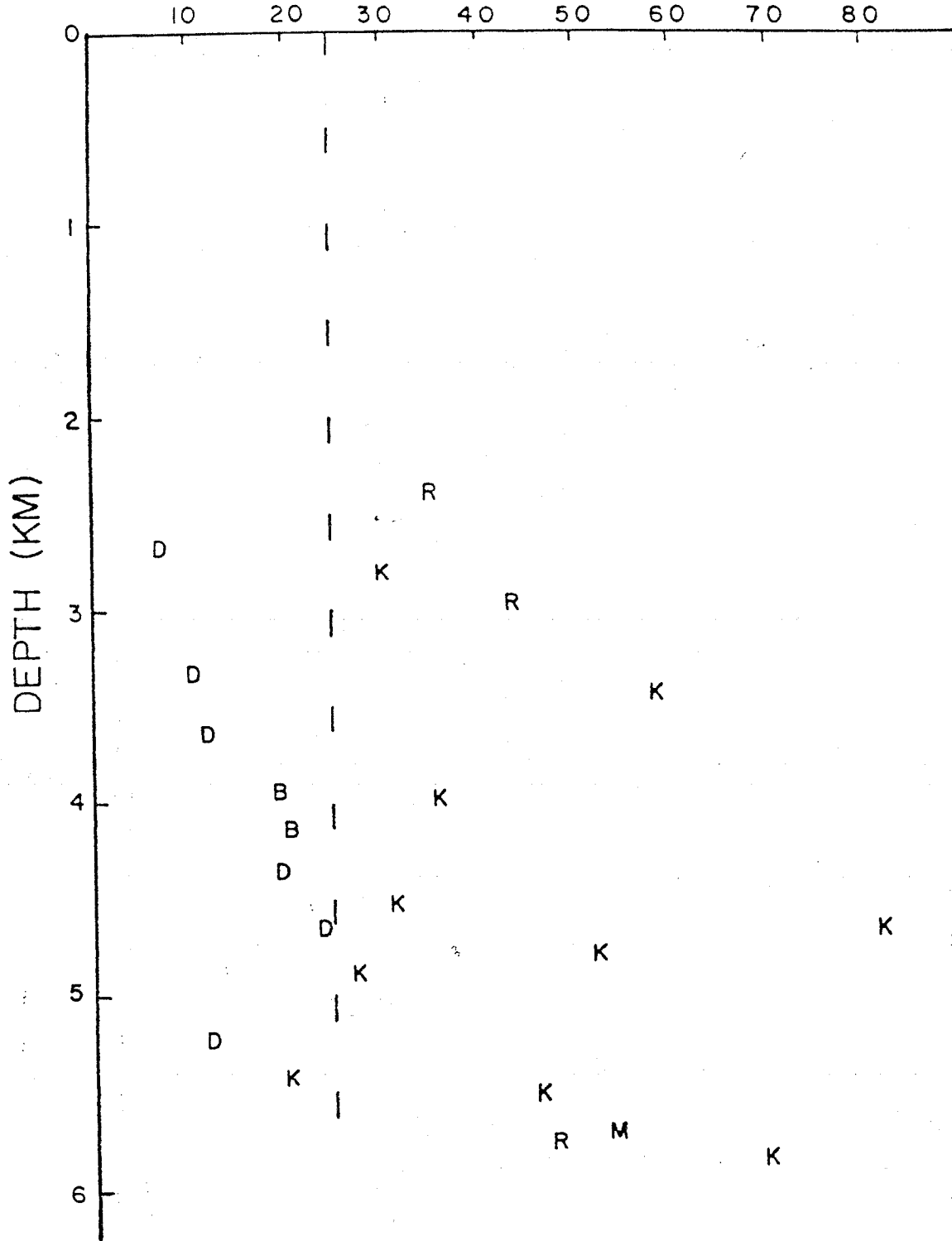
and 1-3 that inventories in nodules do not increase with depth, further suggesting that nodules do not obtain their  $^{230}\text{Th}$  and  $^{231}\text{Pa}$  from particles or sediments.

Two studies within limited areas of the oceans have shown highly variable unsupported  $^{230}\text{Th}$  inventories in sediment cores taken within the same depth range (Cochran and Osmond, 1976; DeMaster, 1979). Thus, scavenging of  $^{230}\text{Th}$  is not a strictly vertical process whereby settling particulate matter removes Th from the water column to underlying sediments. Calculated inventories of  $^{230}\text{Th}$  are very sensitive to sediment densities assumed in the calculation. Therefore, absolute inventories will not be discussed further. Ratios of the inventory of excess  $^{230}\text{Th}$  to the inventory of excess  $^{231}\text{Pa}$  are not sensitive to errors in assumed sediment density. These ratios, determined for several cores, are shown in Figure 1-4. There is no evidence that processes fractionating Th and Pa are a function of depth. Most of the cores in Figure 1-4 contain sediments with a ratio of the inventory of excess  $^{230}\text{Th}$  to the inventory of excess  $^{231}\text{Pa}$  greater than 25, the ratio that would be expected from their rates of production in seawater (the  $^{234}\text{U}/^{235}\text{U}$  activity ratio in seawater is 25). Of the cores with ratios less than 25, all but two, those designated by B, are from areas of siliceous oozes in the Antarctic.

Several arguments can be made against reworking of old sediments as a mechanism producing high  $^{230}\text{Th}/^{231}\text{Pa}$  ratios in surface sediments. Ku (1966) found that excess  $^{230}\text{Th}$  and  $^{231}\text{Pa}$  distributions in sediments generally gave concordant sedimentation rates, even in cores with high  $^{230}\text{Th}/^{231}\text{Pa}$  ratios at the surface. He used this as evidence against reworking, because it would require a constant supply of

Figure 1-4. Ratios of inventories of unsupported  $^{230}\text{Th}$  (dpm/cm<sup>2</sup>) to unsupported  $^{231}\text{Pa}$  (dpm/cm<sup>2</sup>) measured in deep-sea sediment cores. The dashed line represents the ratio that would be expected from the rates of production of  $^{230}\text{Th}$  and  $^{231}\text{Pa}$  in seawater ( $^{234}\text{U}/^{235}\text{U}$  activity ratio is 25) if thorium and protactinium were removed to sediments without fractionation. Symbols indicate the references from which the cores were taken: K: Ku (1966); B: Broecker and Ku (1969); R: Ku et al. (1972); M: Mangini and Sonntag (1977); D: DeMaster (1979).

INTEGRATED  $x_s^{230}\text{Th}/x_s^{231}\text{Pa}$  (ACTIVITY RATIO)



reworked material with a constant  $^{230}\text{Th}/^{231}\text{Pa}$  ratio for several hundred thousand years at the sites studied.

It can be shown by a simple calculation that  $^{230}\text{Th}/^{231}\text{Pa}$  ratios of 20-30 do not likely result from a mixture of modern settling particles, with a  $^{230}\text{Th}/^{231}\text{Pa}$  ratio of 10.8, and aged sediment eroded from another location. If the eroded sediment initially had a ratio of 10.8, and initially had  $^{230}\text{Th}$  and  $^{231}\text{Pa}$  specific activities equal to modern settling particles, then the resulting ratio can be expressed as

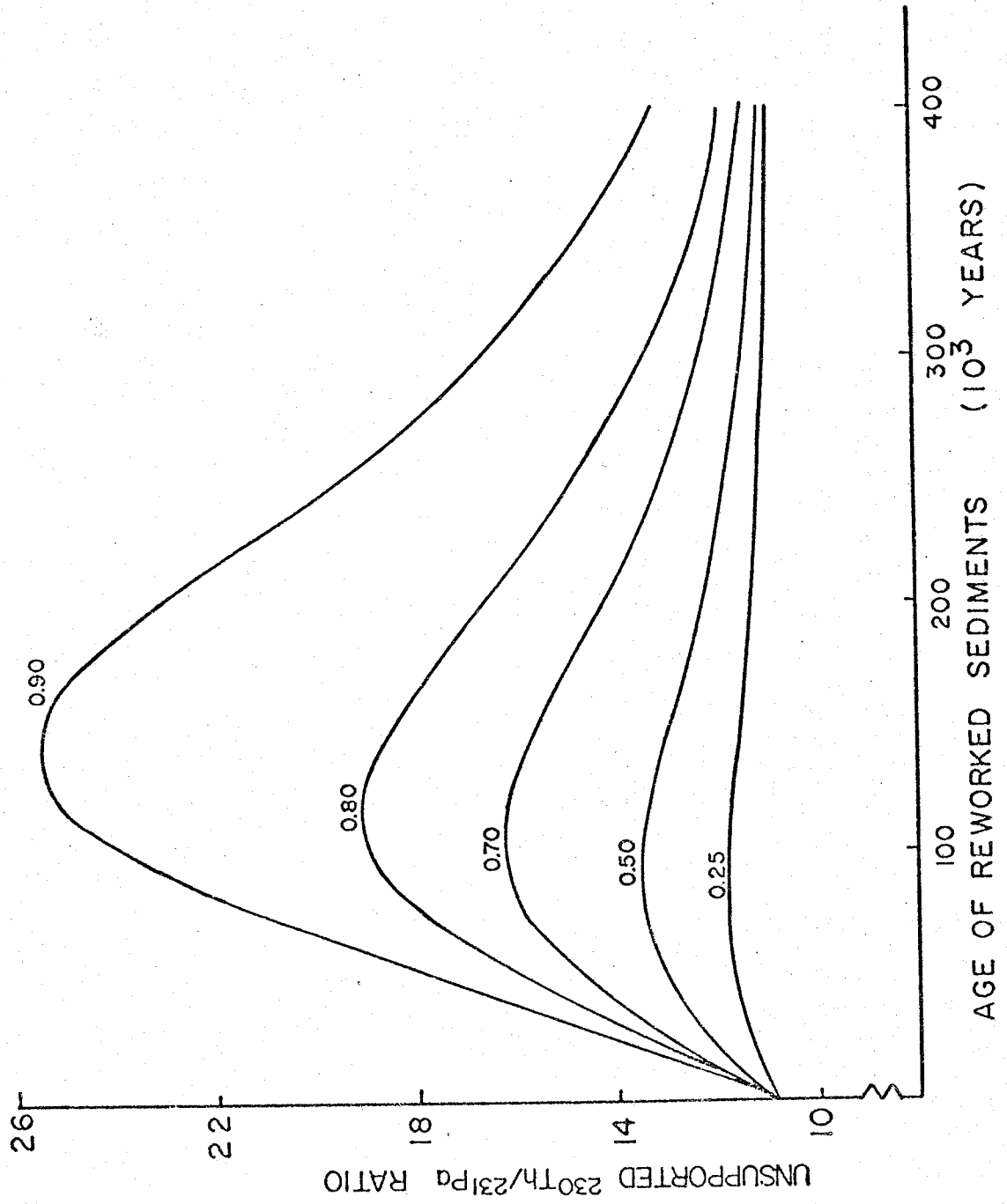
$$x_s \frac{^{230}\text{Th}}{^{231}\text{Pa}} = \frac{(1-X)A_0^{\text{Th}} + XA_0^{\text{Th}} e^{-\lambda_{\text{Th}} t}}{(1-X)A_0^{\text{Pa}} + XA_0^{\text{Pa}} e^{-\lambda_{\text{Pa}} t}} \quad (1)$$

where  $x_s$  refers to  $^{230}\text{Th}$  and  $^{231}\text{Pa}$  in excess of their uranium parents,  $X$  is the fraction of surface sediment made up of reworked material,  $A_0$  is the initial activity,  $A_0^{\text{Th}}/A_0^{\text{Pa}} = 10.8$ ,  $\lambda$  is the radioactive decay constant, and  $t$  is the age of the reworked sediment. A plot of the ratio against  $t$  for several values of  $X$  is shown in Figure 1-5. Even if 80% of surface sediments consist of reworked material, the maximum ratio at  $t = 120,000$  years is about 19, still much less than ratios that have been measured (Ku, 1966; Ku et al., 1972; this work). This model is overly simplistic in that it assumes mixing of two end members of discrete ages. However, it does show that unreasonably large amounts of eroded sediments are required to produce the unsupported  $^{230}\text{Th}/^{231}\text{Pa}$  ratios of 20-30 measured in surface sediments over large areas of the ocean.

Bioturbation also mixes particles settling to the surface sediments with older material. The effect of bioturbation on the unsupported  $^{230}\text{Th}/^{231}\text{Pa}$  ratio in the mixed layer can be shown by the following

Figure 1-5. Unsupported  $^{230}\text{Th}/^{231}\text{Pa}$  activity ratio in surface sediments as a function of age and amount of reworked material. The percent of total sediment consisting X% reworked material of age on the abscissa and (1-X)% modern sediment with a ratio of 10.8. Curves are drawn for different values of X assuming equal initial specific activities of modern and reworked sediment.

Figure 1-5.



calculation. The steady state distributions of unsupported  $^{230}\text{Th}$  and  $^{231}\text{Pa}$  can be represented as

$$SA_o^{\text{Th}} = \lambda_{\text{Th}} A_m^{\text{Th}} X_m + SA_m^{\text{Th}} \quad (2)$$

and

$$SA_o^{\text{Pa}} = \lambda_{\text{Pa}} A_m^{\text{Pa}} X_m + SA_m^{\text{Pa}} \quad (3)$$

where  $S$  is the sedimentation rate,  $A_o$  is the unsupported activity of the settling particles,  $A_m$  is the unsupported activity in the mixed layer, and  $X_m$  is the depth of the mixed layer. If high unsupported  $^{230}\text{Th}/^{231}\text{Pa}$  ratios in the mixed layer result entirely from bioturbation, i.e.  $A_o^{\text{Th}}/A_o^{\text{Pa}} = 10.8$ , then Equations (2) and (3) can be combined to give

$$\frac{A_m^{\text{Th}}}{A_m^{\text{Pa}}} = 10.8 \frac{(\lambda_{\text{Pa}} X_m + S)}{(\lambda_{\text{Th}} X_m + S)} \quad (4)$$

The depth of bioturbation is probably less than 10-15 cm (Nozaki et al., 1977; Cochran, 1980), and values of  $S$  for cores studied by Ku (1966) and Ku et al. (1972) with unsupported  $^{230}\text{Th}/^{231}\text{Pa}$  ratios of 20 or more in surface sediments range from 3-10 mm/10<sup>3</sup>y. Inserting these values of  $S$  and a maximum  $X_m$  of 15 cm into Equation (4) gives a range of  $A_m^{\text{Th}}/A_m^{\text{Pa}}$  of 13-16, much less than ratios measured in surface sediments. Therefore, neither redeposition of eroded sediments nor bioturbation can completely account for the high ratios commonly found in surface sediments, and the high ratios must result from some process fractionating the two isotopes between their production in seawater and their burial in sediments.



Objectives of this Dissertation

Several investigations of the marine geochemical behavior of Th isotopes have been carried out with the objective of better understanding the fates of reactive elements in the oceans (Broecker et al., 1973; Li et al., 1979). It is implicit in the use of Th as an analog of other reactive elements that all reactive elements follow the same pathway of removal from seawater. Thorium-230 and  $^{231}\text{Pa}$  are ideal for the study of scavenging processes in seawater. Their source by decay of dissolved uranium is better known, and better quantified, than for any other element.

Most of the studies of the geochemical behavior of Th have been carried out in surface or nearshore waters, where residence times with respect to scavenging are a few months or less. Thorium may act as an analog for other elements in these environments where many elements are rapidly removed from seawater onto particulate phases. Geochemical identities of different elements may be obscured in nearshore or surface waters because of temporal variability in scavenging processes associated with changes in primary productivity, rates of resuspension of sediments, or other factors. Scavenging processes occur on a much slower time scale in the deep ocean, so subtle variations in scavenging processes between different environments, or between different elements, may become measurable.

A study of the processes removing Th and Pa from the deep sea was initiated because of the information that it would provide about the rates and mechanisms of removal of reactive elements from the oceans. Specifically, the means by which two extremely reactive elements, Th and Pa, are fractionated in seawater was to be determined. Since  $^{230}\text{Th}$  and

$^{231}\text{Pa}$  are produced by the same source in seawater, their distributions are valuable as an indicator of the limitations of the use of one element, for example Th, to predict the fate of other reactive elements introduced into the deep oceans. More generally, a study of the scavenging of these elements in different environments would show to what extent factors such as particle flux, particle composition, and proximity to ocean margins affect the removal of reactive elements from seawater. Since the rates of production of  $^{230}\text{Th}$  and  $^{231}\text{Pa}$  in seawater are well-known, fluxes of  $^{230}\text{Th}$  and  $^{231}\text{Pa}$  into sediment traps can be used to set constraints on the trapping efficiency of the sediment traps. Finally, a better understanding of the geochemical behaviors of  $^{230}\text{Th}$  and  $^{231}\text{Pa}$  could help explain discrepancies in chronologies determined by the two isotopes, and even open up some new opportunities for their use in paleoceanography.

## CHAPTER 2.

### METHODS

#### INTRODUCTION

Uranium, thorium, and protactinium have been measured in environmental samples for many years. However, analytical methods described in the literature tend to be very time consuming or require elaborate laboratory facilities (Ku, 1966; Rosholt and Szabo, 1969; Kraemer, 1975; Sill, 1978). Initial work on this dissertation involved the development of a simpler analytical procedure for the measurement of U, Th and Pa isotopes in small environmental samples. As the work progressed, the method was altered to allow the measurement of  $^{227}\text{Ac}$ ,  $^{241}\text{Am}$ , and the alpha-emitting Pu isotopes.

Objectives of this method are basically the same as in the references listed above. Samples must be brought into solution to allow isotopic equilibration of the natural isotopes with isotopes added as yield monitors. Elements of interest are first separated from the major elements constituting the bulk of the sample and subsequently from each other to allow counting without interferences. Each purified element is then plated as a thin source suitable for alpha spectrometry. Isotopes of interest were shown in their radioactive decay schemes in Figure 1-1.

#### SAMPLE PREPARATION

Little preparation was required for sediment samples, which were taken so as to avoid contamination at the edges of gravity and piston cores and the bottoms of box cores. Several grams of sediment were dried at  $110^{\circ}\text{C}$  to a constant weight, ground with an agate mortar and pestle, and stored in air-tight plastic vials.

A detailed description of the procedures for recovery of sediment trap samples at sea, transport of the samples to Woods Hole, and distribution of sample fractions to various investigators has been given by Honjo (1978, 1980). A portion of each sample for chemical analysis was obtained from the less than 1-mm size fraction of the trapped particles. These sample fractions were vacuum filtered on 0.45- $\mu$ m Nuclepore filters, dried to a constant weight at 60°C, removed from the filters, ground with an agate mortar and pestle, and stored in plastic vials in a desiccator.

Samples obtained by the Massachusetts Institute of Technology Large Volume Filtering System (M.I.T.-L.V.F.S.) were handled according to the procedure of Bishop and Edmond (1976). These samples were collected on Mead 935-BJ glass fiber filters.

Samples of particulate matter obtained on R/V KNORR Cruise 73, Leg 16, and R/V OCEANUS Cruise 78, Leg 1, were obtained by in situ filtration with 293-mm Nuclepore filters with a 1.0- $\mu$ m pore diameter. Filtering was carried out by means of battery-powered pumps which have been described by Spencer and Sachs (1970) and Krishnaswami et al. (1976). Filters were pre-weighed after equilibration with air for several days. Immediately upon recovery of the pumps at sea, the filters were rinsed with distilled water, folded, and stored wet in plastic bags for return to Woods Hole. Filters were dried at room temperature in a constant humidity weighing room and weighed periodically until they reached a constant weight. The weights were used to determine the quantities of particulate matter filtered. Dried filters were stored in plastic bags until time of analysis.

Manganese oxide-coated Nitex was exposed to seawater to allow adsorption of Th and Pa isotopes as a means of determining their concentration. Similar methods have been used for several years (Moore and Reid, 1973; Moore, 1976; Knauss et al., 1978; Reid et al., 1979 a,b). Nitex fabric (Tobler, Ernst and Traber, Inc.) was coated with  $MnO_2$  according to the method of W. M. Hao (personal communication). Sheets of 62-micron mesh Nitex fabric of approximately 30 cm x 80 cm were leached in 0.1N HCl for 24 hours. Upon removal from the HCl, the Nitex was washed with distilled water and then soaked in 0.3N  $KMnO_4$  for 19 hours. This formed a thin coating of cryptomelane (R. Burns, personal communication to P. Brewer) on the Nitex. The  $MnO_2$ -coated Nitex was then washed with distilled water, dried, and stored in plastic bags. Upon recovery from seawater, the  $MnO_2$ -Nitex samples were stored wet in plastic bags until time of analysis.

#### ANALYTICAL TECHNIQUES

##### Dissolution of Sediment and Sediment Trap Samples

Dried sediment, sediment trap, and glass fiber filter samples were first weighed in Teflon beakers. Glass beakers were avoided throughout this procedure to prevent adsorption of Pa. Sample sizes were 0.1-0.6 g of sediment trap material and 1-3 g of sediment. Appropriate amounts of  $^{236}U$ ,  $^{229}Th$ , and  $^{233}Pa$  tracers were added, along with enough 9N HCl to dissolve any  $CaCO_3$  present and to initiate the breakdown of the aluminosilicate matrices. Certain samples also received  $^{242}Pu$  and  $^{243}Am$  tracers and stable Sr and Cs carriers. Samples were then evaporated to near dryness, whereupon 5-15 ml 70%  $HClO_4$ , depending on sample size, was added, and heating was continued to fuming  $HClO_4$  to destroy organic matter. After fuming in covered beakers for 20-30

minutes, the samples were cooled briefly and 15-20 ml 48% HF was added. To insure that all of the Si was volatilized as  $\text{SiF}_4$ , three additions of HF, with subsequent heating to  $\text{HClO}_4$  fumes, were made. Beakers were then rinsed with concentrated  $\text{HNO}_3$  and taken to fuming  $\text{HClO}_4$  twice to remove all traces of HF. This is important, because protactinium forms stable fluoride complexes (Keller, 1966) which could interfere at later stages of the procedure. Finally, samples were dissolved in the minimum amount of 2N HCl required to achieve complete dissolution of the  $\text{HClO}_4$  sludge. If the  $\text{HClO}_4$  was heated to a crust, heating in a larger volume of 2N HCl for 1-2 hours was required to bring the samples back into solution.

Precipitates of unknown composition occasionally formed later in the procedure, particularly in  $\text{HNO}_3$  solutions. Since isotopic equilibrium should have been achieved once samples were in solution, no special efforts were made to prevent later precipitates from forming. Chemical yields were not seriously affected on occasions when these precipitates formed.

#### Dissolution of Nuclepore Filters

A slower and more gentle dissolution procedure was required for Nuclepore filters. Filters placed in hot, concentrated  $\text{HNO}_3$  oxidize rapidly (burn), leaving charred, soot-covered beakers. Filters placed in hot, fuming  $\text{HClO}_4$  explode, resulting in loss of samples.

Dried, weighed filters were folded into 50 ml Teflon beakers, and appropriate yield monitors were added. Decomposition of Nuclepore filters was initiated by soaking in concentrated  $\text{NH}_4\text{OH}$  for approximately 12 hours. Ammonia was driven off by repeatedly heating the samples to near dryness and adding water. Organic residues from the

filters were gently oxidized by adding 4N HNO<sub>3</sub> and heating to gradually concentrate the HNO<sub>3</sub> as the samples evaporated. Concentrated HNO<sub>3</sub> was added as the samples neared dryness, and the beakers were covered with Teflon watchglasses to reflux the HNO<sub>3</sub>. When residues were removed from the sides of the beakers and it appeared that the samples were in solution, watchglasses were removed, approximately 5 ml concentrated HClO<sub>4</sub> was added, and the samples were heated slowly to fuming HClO<sub>4</sub>. Explosions were successfully avoided by this slow oxidation procedure. HF was added to remove Si, and the samples were heated to concentrated HNO<sub>3</sub> and then fuming HClO<sub>4</sub> to remove HF. Samples in fuming HClO<sub>4</sub> were heated to a crust to remove as much Cl as possible and were subsequently dissolved in 5 ml 1.6N HNO<sub>3</sub>. Aliquots (2%) were removed and evaporated on 37-mm Nuclepore filters, which were then pelletized for neutron activation. The remaining 98% of each sample was heated again to a HClO<sub>4</sub> crust, dissolved in a minimum amount of 2N HCl, and treated thereafter like sediment and sediment trap samples.

#### Coprecipitation of Hydrolyzable Metals

Alkali and alkaline earth metals were separated from the actinides by coprecipitation of hydrolyzable metals. The samples, now in 2N HCl, were brought to pH 7 with concentrated NH<sub>4</sub>OH. Aluminum and iron were the major cations forming hydroxide precipitates, and even in the case of the smallest amount of filtered particulate material, there was sufficient precipitate to carry the actinides. Only during blank determinations was it necessary to add Fe to carry the tracer isotopes through the coprecipitation steps. Precipitates were centrifuged, decanted, resuspended in distilled water, and centrifuged again. Samples were

further purified by re-dissolving with 9N HCl and repeating the coprecipitation procedure.

Certain sediment trap samples were analyzed for  $^{90}\text{Sr}$  and  $^{137}\text{Cs}$ . These were the samples to which stable Cs and Sr carriers were added along with the radioisotope yield monitors. Strontium and cesium are not significantly coprecipitated with Al and Fe hydroxides. Supernates from the coprecipitations and distilled water washes were combined and saved for analysis of  $^{90}\text{Sr}$  and  $^{137}\text{Cs}$  in the laboratory of Dr. V. T. Bowen at W.H.O.I. according to published methods (Wong et al., 1970).

#### Ion Exchange Procedure for Sediment and Particulate Samples

Most of the remaining purification of the actinides was carried out by selectively using the anion exchange resin Dowex AG 1X8, 100-200 mesh. Both chloride and nitrate forms of the resin were used to make columns of 10-12 cm length and 7 or 13 mm internal diameter. Larger diameter columns were used for the first and second columns in the analysis of large sediment samples. For smaller samples and subsequent clean-up steps the 7-mm diameter columns were used. Slightly different elution schemes were used, depending on whether or not plutonium was to be measured.

Columns were prepared by pouring resin suspended in distilled water into the columns and rinsing the resin with several column volumes of distilled water. Resin in the first column for each sample was converted to the chloride form by washing with 3-4 column volumes of 9N HCl. Sample precipitates were dissolved in enough concentrated HCl to bring the total volume to at least 9N in HCl, and samples were loaded on the columns. Several column volumes of 9N HCl were added in small increments to wash the bulk of the samples through the columns. If Pu was to be



measured, concentrated HCl was substituted for 9N HCl. Thorium, Am and Ac passed through the resin along with Al, which constituted the bulk of the sample at this point. Some Pa also passed through the resin in HCl when large samples were analyzed. Protactinium retained by the resin was eluted with 9N HCl+0.13N HF, or with concentrated HCl+0.13N HF if Pu was to be measured. Plutonium was eluted with 6N HCl+0.26N HF, and U and Fe were eluted with 0.1N HCl<sup>(1)</sup>. Uranium was separated from Fe and other contaminants on 7-mm diameter nitrate columns prepared like the chloride columns described above except that 8N HNO<sub>3</sub> was used to wash the resin rather than 9N HCl. The 0.1N HCl fractions from the first columns were evaporated, taken to concentrated HNO<sub>3</sub>, diluted with distilled water to approximately 8N in HNO<sub>3</sub>, and placed on nitrate columns. Iron was eluted with several increments of 8N HNO<sub>3</sub> wash and U was eluted with 0.1N HCl. The 0.1N HCl fractions were again taken to small volumes of concentrated HNO<sub>3</sub>. At this point U fractions were usually clean enough to electroplate. If too much Fe remained, as judged from experience, nitrate columns were repeated before plating. Iron fractions were saved for certain sediment trap samples for analysis of <sup>55</sup>Fe in the laboratory of V. T. Bowen by the method of Labeyrie et al. (1975).

---

<sup>1</sup>Two alternatives to the method in the above paragraph have been tried and discarded. First, ethyl and isopropyl ether were used individually to extract most of the Fe from the 9N HCl before the first column. This step was replaced by using the wider diameter columns which could accommodate all of the Fe in any of the samples analyzed. Ether extraction of Fe was not quantitative and another column was necessary to separate U from residual Fe whether or not an ether extraction was performed. Second, it would have been desirable to have used the nitrate form of the resin in the initial column since theoretically U, Th, and Pa should be retained by the resin while most other elements pass through. However, some Pa passed through the initial nitrate column and low U yields resulted when a nitrate column was used first.

Sample fractions containing Th, Am, Ac, and some Pa were heated to evaporate the HCl. When precipitates began to form, 3-4 times that volume of concentrated HNO<sub>3</sub> was added. As HCl boiled off, more white precipitate often formed, particularly in large sediment samples. After samples had been heated to concentrated HNO<sub>3</sub>, equal volumes of distilled water were added so that the resulting solutions were approximately 8N in HNO<sub>3</sub>. Precipitates usually dissolved with gentle heating if sufficient 8N HNO<sub>3</sub> was used. After cooling to room temperature, 8N HNO<sub>3</sub> fractions were placed on 7- or 13-mm diameter nitrate columns, depending on sample size. When large sediment samples were analyzed, only about one column volume of 8N HNO<sub>3</sub> wash was passed through the columns after the samples since Pa would eventually begin to elute in 8N HNO<sub>3</sub>. Thorium was eluted next with 9N HCl. Once the washing solutions were changed to 9N HCl, Pa was strongly bound to the resin and Th could be eluted with 4-5 column volumes of 9N HCl. Protactinium was eluted with 3-4 column volumes of 9N HCl+0.13N HF and combined with the Pa fractions from the first (chloride) columns. Plutonium and americium were only measured on small samples where Pa was strongly bound by the resin so that several column volumes of 8N HNO<sub>3</sub> wash could be used. The 8N HNO<sub>3</sub> fractions contained Am and Ac and were saved for later analysis.

Poor retention of Pa by the resin in 9N HCl and 8N HNO<sub>3</sub> was a problem only for large sediment samples. Protactinium was strongly bound by the resin in both acid solutions when smaller sediment trap and filtered particle samples were analyzed. Poor retention of Pa by the resin in HCl was also observed by Kraemer (1975), and it appears that Pa is less strongly adsorbed to the resin, or more easily displaced from

resin binding sites, in more concentrated sample solutions. It is not clear whether this is due to competition for resin binding sites or if the speciation of Pa is changed in the more concentrated solutions.

Thorium fractions were heated to concentrated  $\text{HNO}_3$ , diluted with distilled water to approximately 8N  $\text{HNO}_3$ , and placed on 7-mm diameter nitrate columns. Enough 8N  $\text{HNO}_3$  wash was used to remove essentially all interfering elements. Thorium was eluted with 9N HCl, heated to small volumes of concentrated  $\text{HNO}_3$ , and electroplated. Any Pa that may have been in the Th fractions after the first nitrate columns was eluted with 9N HCl + 0.13N HF. Usually no Pa was found, as determined by gamma-counting  $^{233}\text{Pa}$ . When  $^{234}\text{Th}$  was measured, it was essential that no  $^{233}\text{Pa}$  be present in the Th fractions to interfere with the beta-counting. Therefore, when  $^{234}\text{Th}$  was measured, the Th fractions were put through third nitrate columns, identical to the second, to remove any residual Pa.

Macroscopic amounts of impurities present in the Pu fractions after the first ion exchange columns necessitated additional clean-up columns before Pu could be electroplated. Plutonium fractions were heated to near dryness several times in concentrated  $\text{HNO}_3$  to remove any HF, taken up in concentrated HCl, and heated to remove as much  $\text{HNO}_3$  as possible. Samples in concentrated HCl were cooled and placed on 7-mm diameter chloride columns. Impurities were washed off with 9N HCl, and Pu was eluted with 6N HCl + 0.26N HF. If residue was still present on heating the Pu fraction to dryness, the clean-up columns were repeated. However, this was seldom necessary, and the Pu fractions at this point were ready to electroplate.

Manganese Oxide-Coated Nitex Samples

An acid-reducing agent was used to bring the  $\text{MnO}_2$ -Nitex samples into solution. Appropriate amounts of tracer isotopes were added to samples in Teflon or polypropylene beakers. Manganese oxide was dissolved by leaching in a mixture of 200 ml 3%  $\text{HNO}_3$ , 10 ml 20%  $\text{NH}_2\text{OH-HCl}$ , and 1 ml 48% HF. Leaching solutions were decanted from the Nitex into 250 ml Teflon beakers and evaporated. Meanwhile, the Nitex was leached again in 200 ml 3%  $\text{HNO}_3$  + 1 ml 48% HF. The second leachates were added to the first, and third leaches were performed using 200 ml 3%  $\text{HNO}_3$ . Each leach required about 12 hours. Leachates were combined and evaporated to small volumes of concentrated  $\text{HNO}_3$ . Beakers were washed several times with concentrated  $\text{HNO}_3$  and heated to near dryness to remove all HF. If samples were accidentally heated to dryness, concentrated HCl was required to dissolve the precipitates and the samples were heated back to concentrated  $\text{HNO}_3$ . Distilled water was added to bring the solutions to 8N  $\text{HNO}_3$  and samples were loaded on 7 mm x 12 cm nitrate columns, prepared as previously described. The bulk of the samples consisted of Mn leached from the Nitex. Manganese passed through the resin in 8N  $\text{HNO}_3$ , along with Am, Ac, Ra, and any transition metals which may have been adsorbed from seawater onto the  $\text{MnO}_2$ -Nitex. Several column volumes of 8N  $\text{HNO}_3$  were used to rinse the Teflon beaker and wash the column, and the combined 8N  $\text{HNO}_3$  was stored for later analysis. Thorium was eluted with concentrated HCl, Pa with concentrated HCl + 0.13N HF, Pu with 6N HCl + 0.26N HF, and U with 0.1N HCl. Approximately 20-25 ml wash was used in each elution. Subsequent purification followed the anion exchange procedures described above. Protactinium was strongly retained by the resin prior to its elution step.

Actinium and Americium

Actinium was measured indirectly by allowing its daughter,  $^{227}\text{Th}$  ( $t_{1/2} = 18.7$  days), to grow into radioactive equilibrium for 3-5 months. The  $^{227}\text{Th}$  initially present in the samples was isolated with the Th fractions. Attempts to count  $^{227}\text{Th}$  in the Th fractions of several samples proved unsuccessful because of interferences in the Th alpha spectra by  $^{229}\text{Th}$  and  $^{228}\text{Th}$  daughters. Thorium-free  $^{227}\text{Ac}$  was eluted from the first nitrate columns in the above procedure in 8N  $\text{HNO}_3$ . Thorium-230 tracer was added to the samples in 8N  $\text{HNO}_3$ , and after ingrowth of  $^{227}\text{Th}$ , the samples were passed through 7 mm x 12 cm nitrate columns. Actinium and Am passed through the resin, while Th was retained. Thorium was eluted with 9N HCl and electroplated. Counting of the  $^{227}\text{Th}$  samples was started four days after plating to allow  $^{212}\text{Pb}$  and its alpha-emitting daughter  $^{212}\text{Bi}$ , which interferes with  $^{227}\text{Th}$ , to decay.

It is necessary to assume a quantitative recovery of Ac, since no Ac yield monitors were added to the samples. To test the assumption, a sample of Pacific red clay from several centimeters below the sediment surface was analyzed for  $^{231}\text{Pa}$  and  $^{227}\text{Ac}$ . This sediment was sufficiently old that  $^{227}\text{Ac}$  and  $^{227}\text{Th}$  should have been in radioactive equilibrium with  $^{231}\text{Pa}$ . The  $^{231}\text{Pa}$  and  $^{227}\text{Ac}$  ( $^{227}\text{Th}$ ) were identical within counting error ( $^{227}\text{Ac} = 2.17 \pm .19$  dpm/g,  $^{231}\text{Pa} = 2.23 \pm .05$  dpm/g). Similar agreement of the two methods has been observed by Y. Nozaki (personal communication).

After isolation of  $^{227}\text{Th}$ , americium was measured in certain samples in the laboratory of V. T. Bowen according to published methods (Wong et al., 1970; Livingston et al., 1975; Anonymous, 1975).

#### Solvent Extraction and Plating of Protactinium

Protactinium required purification beyond the above ion exchange steps, since its activity was much lower than other potentially interfering isotopes. Five drops of concentrated  $\text{H}_2\text{SO}_4$  were added to Pa fractions, which were heated first to concentrated  $\text{HNO}_3$  and then to fuming  $\text{H}_2\text{SO}_4$  to remove all of the HF. After a brief cooling, samples were taken up in 7.2N HCl and transferred to Teflon separatory funnels. A second portion of 7.2N HCl was used to rinse the beakers and was added to the separatory funnels so that the combined volume of HCl +  $\text{H}_2\text{SO}_4$  was 10 ml. Protactinium was extracted twice with 6 ml of methyl isobutyl ketone (MIBK) and then back extracted from the combined MIBK with two washings of 5-6 ml 7N HCl + 2N HF.

One drop of concentrated  $\text{H}_2\text{SO}_4$  was added to the combined HCl + HF washes. Samples were heated first to concentrated  $\text{HNO}_3$  to oxidize residual MIBK and then to fuming  $\text{H}_2\text{SO}_4$  to remove any remaining HF.

Samples in one drop of  $\text{H}_2\text{SO}_4$  were taken up in 1.5 ml 0.01N  $\text{HNO}_3$  and Pa was extracted into 0.4M TTA (Thenoyltrifluoroacetone or 4,4,4-Trifluoro-1-(2-thienyl)-1,3-butanedione) in benzene. The organic phase was evaporated onto silver discs, which were then flamed. Two 1-1.5-ml TTA extractions were sufficient to remove at least 90-95% of the

Pa from the acid phase. Silver discs were used for uniformity since all of the other elements were electroplated onto silver discs<sup>(2)</sup>.

### Electroplating

Electroplating was carried out on 1-inch diameter silver discs in a cell designed by C. L. Smith and S. Tsunogai. A coil of platinum wire placed horizontally above the silver disc within the plating solution served as the anode. Plating solutions were stirred continuously by means of a magnetic stir bar placed on top of the anode. Uranium, Th, and Pu samples<sup>(3)</sup> were heated to small drops of concentrated  $\text{HNO}_3$ ,

---

<sup>2</sup>Protactinium was mounted for alpha-counting by three different methods during the course of this work. Initial attempts to electroplate Pa by the method used for U, Th, and Pu were unsuccessful, so other methods were developed. Two methods were used on some early samples. In one case, the drop of  $\text{H}_2\text{SO}_4$  was taken up in 1 ml 1.5N  $\text{HNO}_3$  and extracted into 1.0-1.5 ml 0.4M TTA-benzene. The organic phase was evaporated on a stainless steel disc and flamed. In the other case, the  $\text{H}_2\text{SO}_4$  was taken up in 1 ml 6N HCl and Pa was extracted into MIBK, which was also evaporated onto a stainless steel disc and flamed. The TTA-benzene gave a much cleaner plate after flaming but required three extractions from the acid, and even then up to 30% of the Pa remained in the acid phase. Protactinium extracted quantitatively into the MIBK in one extraction, but some residue remained on the disc after flaming. The small amount of residue did not appear to affect the resolution of the alpha spectrum of Pa.

Extraction into TTA-benzene proceeded to a much greater extent if the drop of  $\text{H}_2\text{SO}_4$  was taken up in 0.01N  $\text{HNO}_3$  than in higher concentrations of  $\text{HNO}_3$ .

<sup>3</sup>A method of electroplating Pa was developed part-way through the work. To the drop of cooled  $\text{H}_2\text{SO}_4$  was added 100  $\mu\text{l}$  of 9N HCl + 0.13N HF. Plating then proceeded exactly as for the other samples. Pure Pa tracer would plate well by the standard method described above. However, following isolation from a sample less than 10% of the Pa would plate without the addition of HCl + HF. Unfortunately, the electroplating method was not selective for Pa, as was the TTA-benzene extraction, and there was frequent cross-contamination of small amounts of Th in the electroplated Pa fractions. The electroplating method for Pa was only used on a few sediment samples and was abandoned in favor of the TTA extraction to prevent cross-contamination.

taken up in 1 ml of 0.01N HNO<sub>3</sub>, and transferred to the electroplating cell. Beakers were washed with 3 ml of 2N NH<sub>4</sub>Cl (taken to pH 2 with HCl) and this was also transferred to the cell. Electrical current was provided by a Hewlett-Packard 6296A DC power supply. Plating started at 0.8 amps and 3-4 volts, and was terminated after about one hour when the current had dropped to 0.3 amps at 7.0 volts.

#### SAMPLE COUNTING

##### Alpha Spectrometry

Counting of alpha-emitting isotopes was by alpha spectrometry with silicon surface-barrier detectors (Princeton Gamma-Tech PD-400-26-100) mounted inside Kicksort vacuum counting chambers. Vacuum was provided by a GCA/Precision Scientific Model DD-20 vacuum pump. Detectors had an active surface area of 400 mm<sup>2</sup> and a minimum depletion thickness of 100 microns. Detector bias was supplied by a Kicksort Model 504 N Quad Bias Supply. Signals from the detectors were amplified by Kicksort Model 601 FET preamps and Model 211 Q Quadamps.

Two multichannel analyzer systems were used during the work. For the early samples, the amplified signals were sorted by a Tracor Northern Model TN 1710-5 four-input multiplexer-router and fed into a Tracor Northern Model TN 1710 4096-channel pulse-height analyzer. The majority of the samples were counted on an expanded counting system in which the amplified signals were fed through a Tracor Northern NS-459 D sixteen-input multiplexer-router into a Tracor Northern NS-720 4096-channel pulse-height analyzer. Spectra were printed out by a Computer Terminal Corporation Model 3300P thermal printer.



### Beta and Gamma Counting

Beta-counting of most the  $^{233}\text{Pa}$  tracers and some of the  $^{234}\text{Th}$  samples was performed on a Nuclear Measurements Corporation Model PCC-11T proportional counter coupled to a NMC Model DS-1T decade scaler/timer/high voltage supply. Union Carbide 10% methane/ 90% argon was used as the counting gas. Background for beta counting was 10-12 cpm in the plateau region of 1750V. During the course of this work it was necessary to change the center wire and preamplifier of the proportional counter, after which the beta plateau was shifted to a higher voltage and counting was carried out at 1950V.

During the later part of this work a low-level, anticoincidence beta-counting system was acquired. The detector was similar to that described by Lal and Schink (1960). Voltage was supplied to the sample detector and a guard detector by Canberra Model 3002 High Voltage Supplies. Signals from the sample and guard detectors were first amplified by Pelagic Electronics Model 7030-2 preamplifiers. Sample signals were further amplified by a Canberra Model 2012 amplifier. Signals from the guard detector were sent to a Pelagic Electronics Model 7030-4 Gate Driver set for a 100-microsecond gate. Amplified signals from the sample detector were fed through a Canberra Model 2032 dual discriminator, which was coupled to the Gate Driver, and further through a Canberra Model 2035A single-channel analyzer and a Canberra Model 1476A scaler. Sample and guard counts were recorded by a Canberra Model 1790C Counter/Timer. Most of the  $^{234}\text{Th}$  and some of the  $^{233}\text{Pa}$  counting was performed on this system.

Protactinium could be followed through the procedure by gamma-counting the  $^{233}\text{Pa}$  tracer in various sample fractions. Sample solutions were placed in test tubes and counted in a NMC Model US-1B NaI(Tl) well-type scintillation counter coupled to the DS-17 scaler/timer/voltage supply. Background was 250-300 cpm at 1300V. During alteration of the procedure to allow measurement of Pu isotopes,  $^{237}\text{Pu}$  was used to monitor the Pu behavior through the various steps of the method. Gamma-counting of  $^{233}\text{Pa}$  and  $^{237}\text{Pu}$  greatly simplified the development of the methods for Pa and Pu.

#### SOURCES OF ERROR

##### Sample Size

Dried sediment and sediment-trap samples used for radioisotope analyses were accurately weighed on a Mettler semi-micro balance. Errors in weighing were negligible compared to other errors. Weights given for sediment samples include residual sea salt from pore waters. Sediment trap samples were split while still wet with a precision of better than 1% for particles less than 62 microns, and 6% for 250 micron particles (Honjo, 1978). One-quarter splits of the samples were filtered, dried, and weighed as described under sample preparation. Total amounts of material collected in the traps were calculated from the weights of one-quarter splits. Other errors in sample preparation prior to weighing are unknown, but should be small.

Large Volume Filtration System samples were weighed at MIT by R. Collier. Weights of particulate matter are given to two significant figures, although the precision is unknown. A better indicator of sample size is the volume of water filtered, which is known to  $\pm 3\%$  (Bishop and Edmond, 1976).

Volumes of seawater filtered and weights of particulate matter collected were measured for samples obtained using the battery-powered pumps. Several small sources of error in sample size exist, the magnitude of which cannot be accurately determined. Flow meters used with the pumps (Kent Meter Sales, Tampa, FL) to determine the volumes of seawater filtered were accurate to within  $\pm 2\%$  (P. Sachs, personal communication). No leaks in the pumping systems were ever detected. Unfortunately, particulate matter could not be quantitatively recovered on the filters. Water within the filter holders was agitated as the pumping systems were brought on deck. Some particulate material was resuspended from the filters and adsorbed to the filter holders. This material could not be observed directly on the filter holders, but became visible on wiping the filter holders with a white tissue paper. Quantities of material lost in this way were very small relative to the total sample sizes but cannot be accurately determined.

Errors in weighing Nuclepore filters most likely result from incomplete equilibration of the dried filters with air in the weighing room. Unexpected changes in the humidity of the weighing room air could also cause errors in the weights of the filters. Filters were weighed repeatedly to minimize this error, which was probably less than 10% of the calculated weight of particulate material.

Effective volumes of seawater sampled by  $\text{MnO}_2$ -Nitex adsorbers were calculated from the measured amounts of adsorbed  $^{234}\text{Th}$  with the assumption that  $^{234}\text{Th}$  is in radioactive equilibrium with  $^{238}\text{U}$  in the deep ocean (Amin et al., 1974; Bacon, unpublished data) at 2.5 dpm/l (Ku et al., 1977). Particulate  $^{234}\text{Th}$  was determined in samples obtained by in situ filtration. Effective volumes of seawater sampled by

MnO<sub>2</sub>-Nitex adsorbers placed in-line behind the filters were calculated from a dissolved <sup>234</sup>Th concentration estimated as the total concentration (2.5 dpm/l) less the measured particulate concentration. Effective volumes of seawater sampled by MnO<sub>2</sub>-Nitex adsorbers attached to sediment trap moorings were calculated using the total <sup>234</sup>Th concentration (2.5 dpm/l). If no particulate <sup>234</sup>Th was sampled by the adsorbers on the moorings, the error introduced by this calculation is about 2%, as the concentration of particulate <sup>234</sup>Th measured at open-ocean stations on KN 73-16 was about 0.05 dpm/l (Chapter 5). A 2% uncertainty is small compared to counting errors. Absolute amounts of <sup>234</sup>Th in the samples were calculated from the ratio of sample <sup>234</sup>Th activities to standard <sup>234</sup>Th activities (see below) where both were plated and counted under identical conditions. Therefore, corrections were not necessary for counting efficiency and geometry factors. Chemical yields for Th in samples counted for <sup>234</sup>Th were determined from the recovery of the added <sup>229</sup>Th tracer. Detector efficiencies used to calculate <sup>229</sup>Th recoveries were determined by counting <sup>239</sup>Pu and <sup>241</sup>Am standards. Errors reported for <sup>234</sup>Th measurements, and apparent volumes of seawater sampled by MnO<sub>2</sub>-Nitex, are the result of propagation of counting errors through several steps, including beta-counting <sup>234</sup>Th and determination of thorium chemical yields, which includes uncertainties in the alpha-detector efficiencies. Other uncertainties in the method are discussed in Chapter 4.

#### Counting Statistics

The standard counting error ( $1-\sigma$ ) is given by  $\sqrt{N}$ , where N is the number of counts (Friedlander et al., 1964). Propagation of counting errors in a derived result,  $f(x,y)$ , is made by use of the equation

For example,

$$\sigma_{F(x,y)}^2 = \left(\frac{\partial f}{\partial x}\right)^2 \sigma_x^2 + \left(\frac{\partial f}{\partial y}\right)^2 \sigma_y^2$$

$$\sigma_{x/y} = \frac{x}{y} \left( \frac{\sigma_x^2}{x^2} + \frac{\sigma_y^2}{y^2} \right)^{1/2}$$

Detector Calibration and Chemical Yields

Counting efficiencies of the detectors used for alpha spectrometry were determined to within  $\pm 1\%$  by counting  $^{239}\text{Pu}$  and  $^{241}\text{Am}$  standard sources that were borrowed from the laboratory of V. T. Bowen (W.H.O.I.). Detector efficiencies were needed to calculate sample  $^{231}\text{Pa}$  activities since the  $^{233}\text{Pa}$  added as a chemical yield monitor was a beta emitter. There are no alpha-emitting Pa isotopes available to use as a yield monitor for  $^{231}\text{Pa}$ . Detector efficiencies were also required to determine the chemical yield of Th in samples for which  $^{234}\text{Th}$  was to be measured. Natural alpha-emitting U, Th, and Pu isotopes were measured relative to known amounts of alpha-emitting tracer isotopes added to the samples. It was assumed that chemical yields and detector efficiencies were the same for all alpha-emitting isotopes of an element in a given sample fraction.

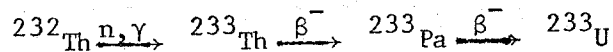
Chemical yields of Pa were determined by beta-counting samples and standards plated on the same kind of disc. Thus, unknown detector efficiency and geometry factors would cancel in yield calculations. Back-scatter of beta particles is a function of the atomic weight of the element on which samples are plated and can give an increased apparent counting efficiency in a  $2\pi$  proportional counter. Back-scatter ranges from 30% for an Al disc to 80% for a Pb disc (Friedlander et al., 1964, p. 108).

Preparation and Calibration of Standards

Uranium-236 and  $^{229}\text{Th}$  tracers (Oak Ridge National Laboratory) were calibrated against standard solutions prepared from weighed amounts of

$^{238}\text{U}$  ( $\text{U}_3\text{O}_8$ , NBS 950A) and  $^{232}\text{Th}$  ( $\text{ThO}_2$ , Lindsay Code 116, 99.9% minimum purity, American Potash and Chemical Company). Standard  $^{234}\text{Th}$  plates were prepared periodically from the  $\text{U}_3\text{O}_8$  standard solution in which  $^{234}\text{Th}$  had grown into radioactive equilibrium. Thorium-230 tracer was added to known amounts of the  $\text{U}_3\text{O}_8$  solution and Th was separated from U and electroplated. Chemical yields for the standard Th plates were determined by alpha-counting the  $^{230}\text{Th}$ .

Preparation of  $^{233}\text{Pa}$  was by neutron activation of 1-5 mg  $\text{Th}(\text{NO}_3)_4 \cdot 4\text{H}_2\text{O}$  which had been pressed into a pellet in a Nuclepore filter. Irradiation was performed at the M.I.T. Nuclear Reactor in a neutron flux of  $8 \times 10^{12}$  n/cm<sup>2</sup>-sec for 8 hours, resulting in a  $^{233}\text{Pa}$  activity of about 5-20  $\mu\text{Ci}$ . The irradiation reaction is



After irradiation, the pellet was fragmented in hot, concentrated  $\text{NH}_4\text{OH}$  for several hours before wet combustion in hot, concentrated  $\text{HNO}_3$ .

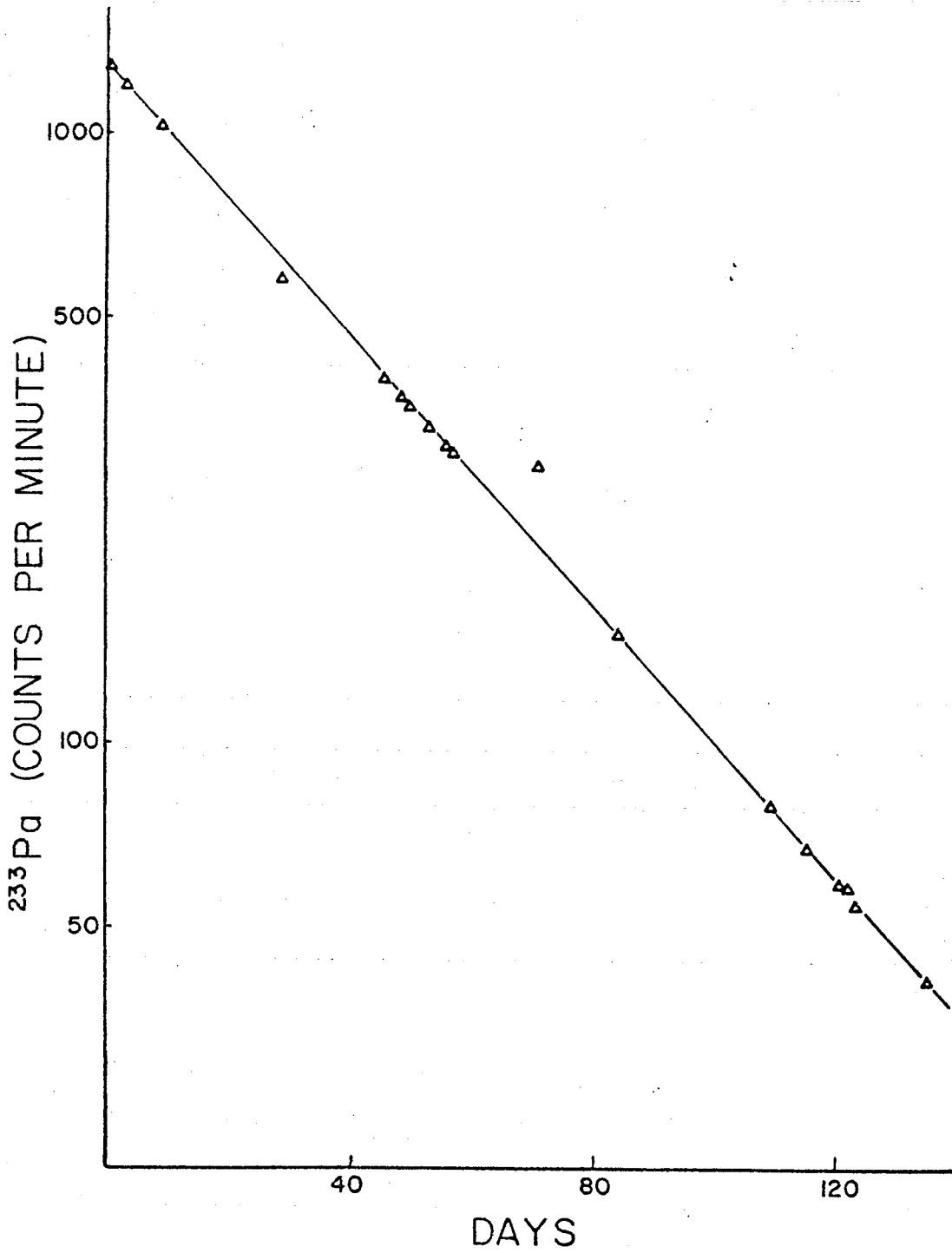
Only a small amount of the  $^{232}\text{Th}$  was converted to  $^{233}\text{Pa}$ . To remove the Th, the  $\text{HNO}_3$  was heated to dryness, taken up in 9N HCl, and placed on a Dowex AG 1X8  $\text{Cl}^-$  column. Thorium was eluted with 9N HCl and Pa with 9N HCl + 0.13N HF. The Pa fraction was heated to concentrated  $\text{HNO}_3$  to remove HF, and the above column procedure was repeated.

Complete removal of  $^{232}\text{Th}$  was verified by alpha spectrometry.

Radioactive decay of one  $^{233}\text{Pa}$  standard plate over a period of five months is shown in Figure 2-1. A least squares fit through the points is indistinguishable from the  $^{233}\text{Pa}$  half-life of twenty-seven days.

Standard  $^{233}\text{Pa}$  plates were made by pipetting tracer solution directly into an electroplating cell and plating, as the  $^{233}\text{Pa}$  solution

Figure 2-1. Radioactive decay of a  $^{233}\text{Pa}$  standard. A least squares fit through the points gives the correct half-life of 27 days.



could not be evaporated on a silver disc. Several plates were made from each batch of  $^{233}\text{Pa}$  tracer. All of the plates usually agreed within counting statistics. Any that did not agree were discarded. It was assumed that electroplating efficiency was 100%. One of the purposes of testing the accuracy of this procedure (see below) was to insure that the  $^{233}\text{Pa}$  standard plates were properly prepared.

Calibrated  $^{242}\text{Pu}$  and  $^{243}\text{Am}$  tracers used during this work were obtained from the laboratory of V. T. Bowen.

#### Peak Overlap

Typical U, Th, Pa and Pu spectra are shown in Figures 2-2, 2-3, 2-4, and 2-5. Energy resolution, expressed as peak width at half maximum height, was 30-40 KeV for monoenergetic alpha-emitting isotopes. Tail corrections were sometimes necessary in Th spectra, particularly for samples in which one Th isotope was present in a much greater activity than the others. Occasionally, small amounts of impurities remained in the samples when they were electroplated, causing degraded peak resolution. Tail corrections were made by assuming that the tails of all of the isotopes in a given spectrum have the same shape. These corrections seldom amounted to more than a few per cent, so it was assumed that differences in peak tail shapes of the different isotopes added a negligible error to the calculations. An example of a Th spectrum for which tail corrections were necessary was given in Figure 2-3. Overlap of  $^{229}\text{Th}$  and  $^{230}\text{Th}$  peaks was the most common correction of this type and was seldom greater than shown in Figure 2-3. Similarity of peak tail shapes is also illustrated in Figure 2-3. A Th tail correction was required for the Th spectra of the standard OCB 66-15 during the test of the accuracy of the method (see below). Results



Figure 2-2. A uranium spectrum from CH75-2, Pilot Core 8, 0-4 cm.

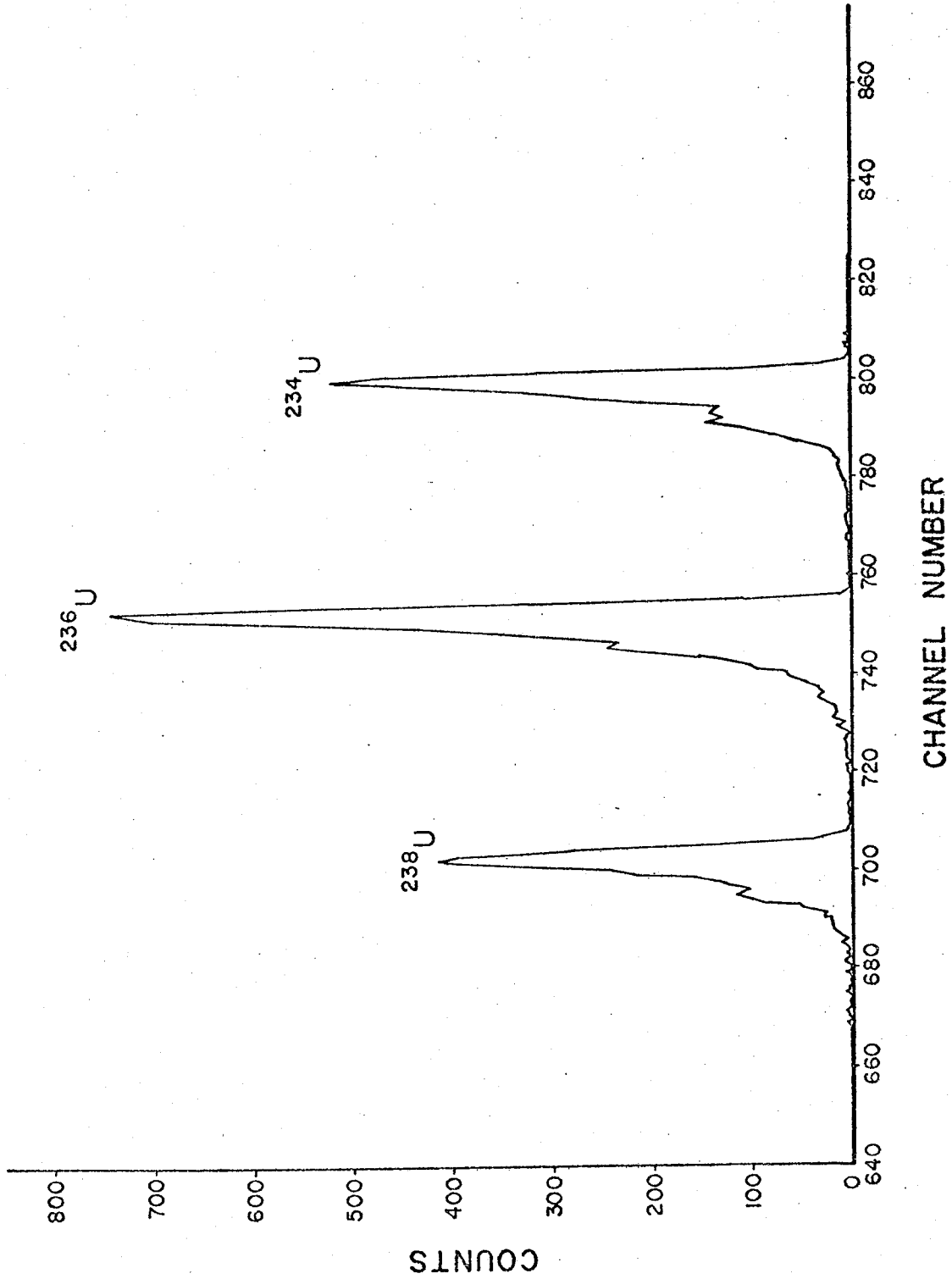


Figure 2-3. A thorium spectrum requiring corrections for peak tail overlap: CH75-2, Pilot Core 8, 0-4 cm.

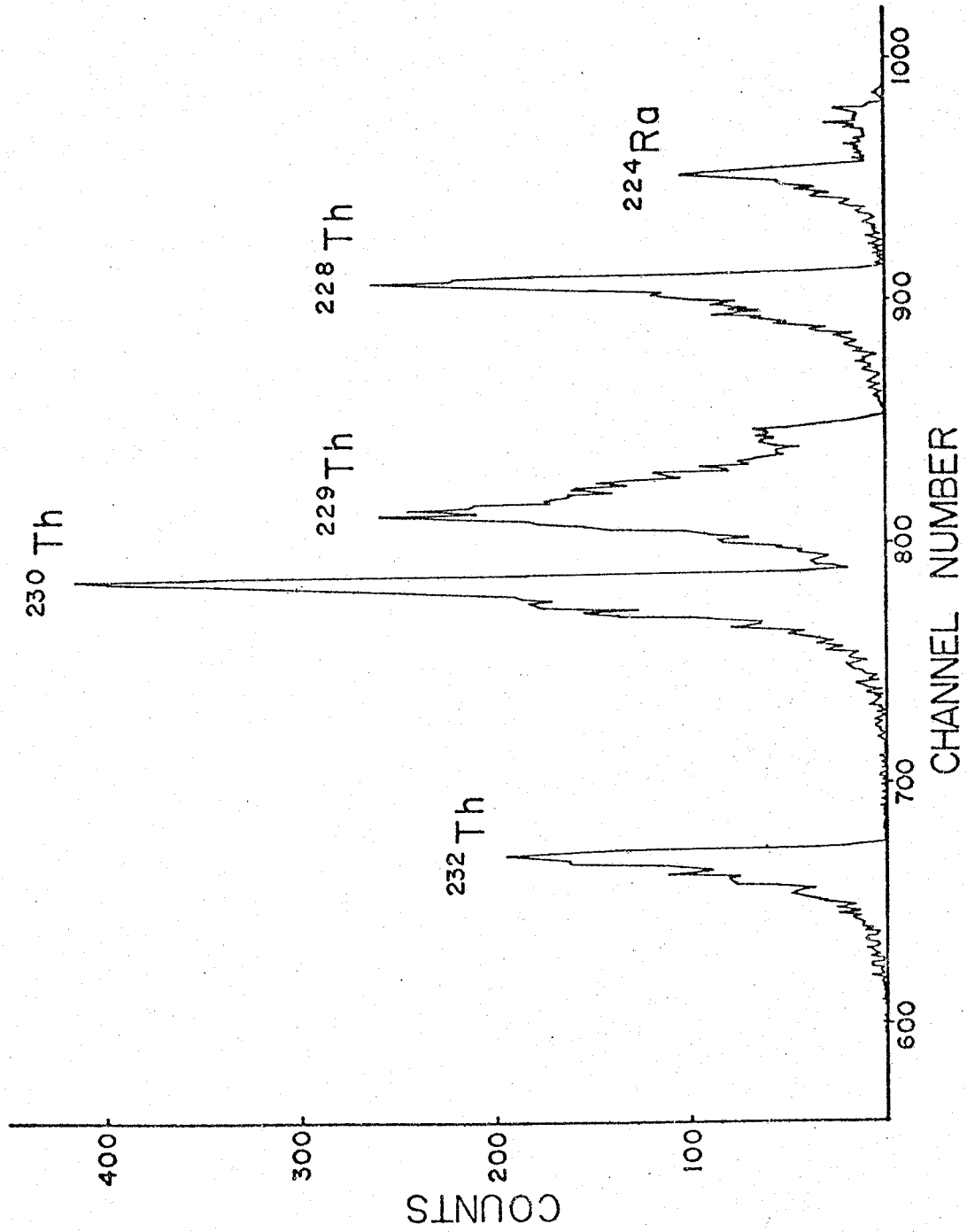


Figure 2-4. A protactinium spectrum from PARFLUX P,  
KK1 Core 4, 4-5 cm.

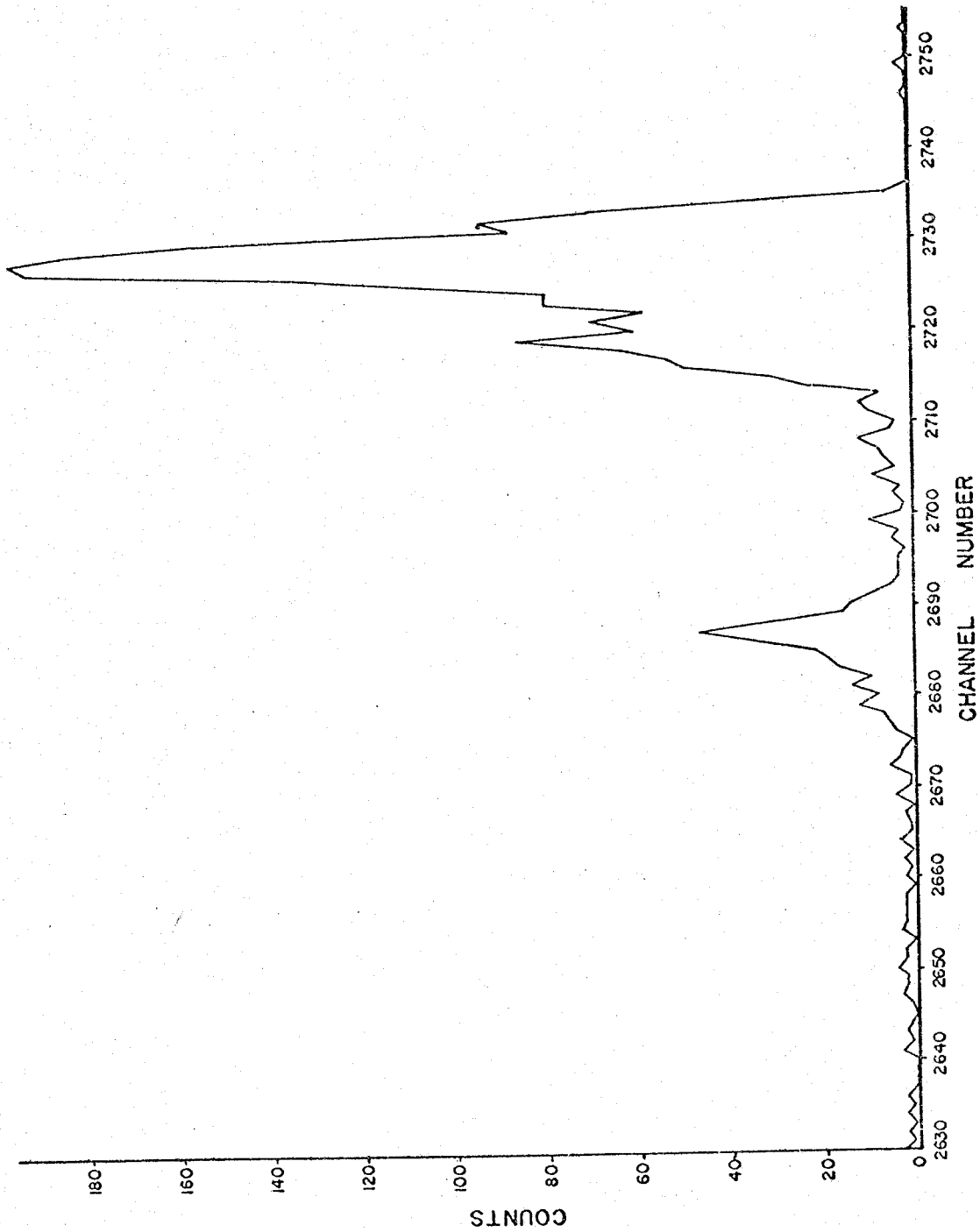
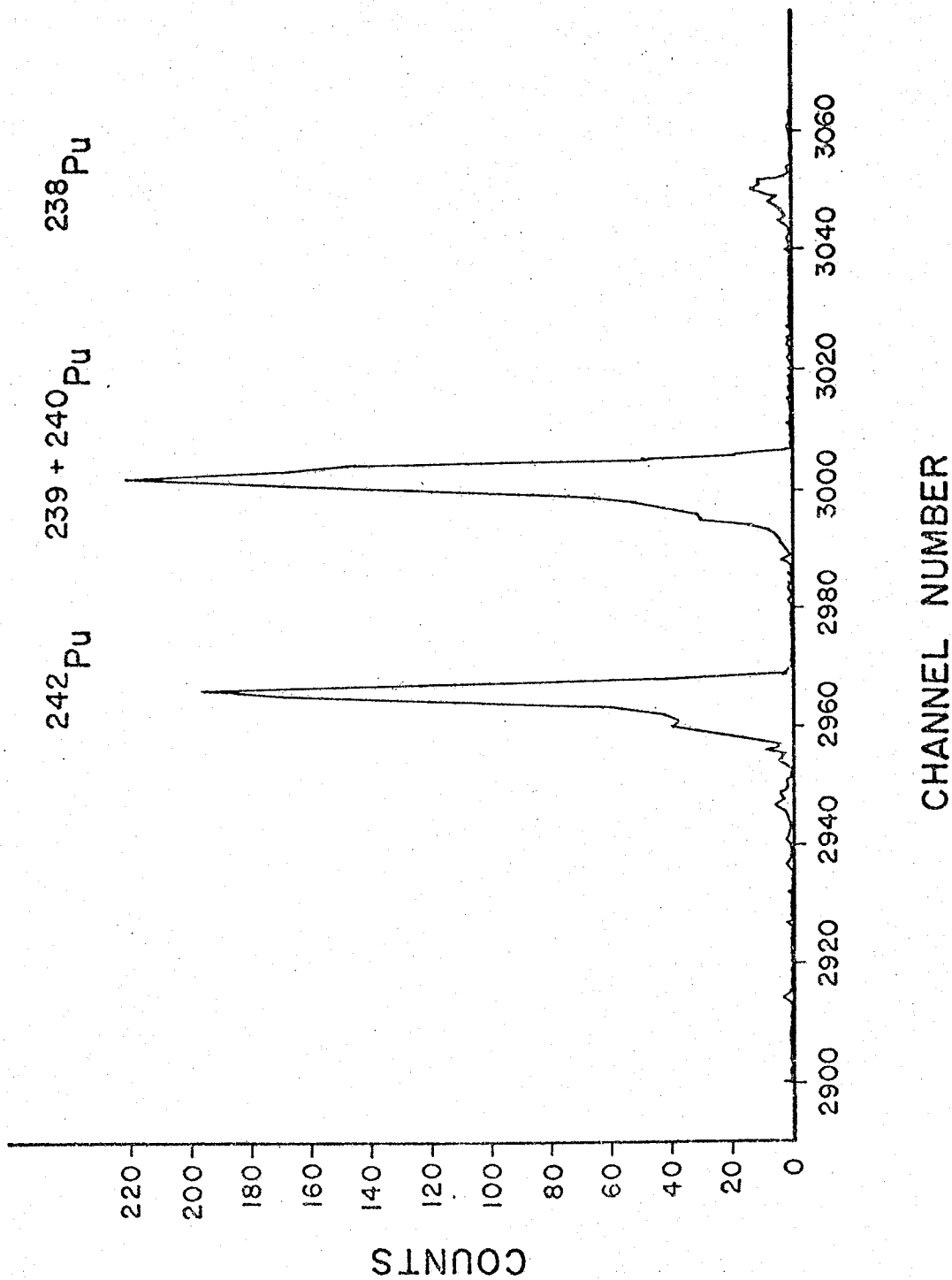


Figure 2-5. A plutonium spectrum from a sediment trap sample: PARFLUX P, 5500 m.



calculated after the tail corrections were made agreed with the published Th values within the error of the counting statistics.

Well-purified samples with the best resolution had some unavoidable peak overlaps. In Th spectra, 5% of  $^{224}\text{Ra}$  activity ( $t_{1/2} = 3.66\text{d}$ , daughter of  $^{228}\text{Th}$ ) occurred at an energy that was not resolvable from  $^{228}\text{Th}$ . Since the main  $^{224}\text{Ra}$  peak was cut off at the high energy end of most Th spectra, this contribution was subtracted as 4.5% of the total  $^{228}\text{Th}$  peak. Similarly, 0.4% of the  $^{229}\text{Th}$  peak fell under the  $^{230}\text{Th}$  peak. Finally, about half of the  $^{235}\text{U}$  peak fell under the  $^{236}\text{U}$  peak. Correction for the  $^{235}\text{U}$  contribution to the  $^{236}\text{U}$  peak was based on the natural  $^{235}\text{U}/^{238}\text{U}$  activity ratio.

#### Background Corrections

Initial background count rates on detectors used for alpha spectrometry were near zero. Significant background contamination built up over time due to recoil of daughter isotopes onto the detectors. Short-lived daughters of  $^{229}\text{Th}$  and  $^{228}\text{Th}$  (Figure 1-1) were responsible for virtually all of the background counts except for two detectors on which  $^{232}\text{U}$  had been counted and its daughter,  $^{228}\text{Th}$ , was present as a contaminant. Although the peak energies of these daughters were higher than the energies of the isotopes being studied, they did contribute an increased background at all lower energies. This increased background was most significant for counting Pa because of its low activity in these samples, so separate detectors were maintained on which Th samples and  $^{232}\text{U}$  were not counted.

Background for beta counting on the proportional counter was 10-12 cpm. Sufficient  $^{233}\text{Pa}$  tracer was used so that background corrections were very small. Background corrections were more significant for

$^{234}\text{Th}$  counting, but were still less than 20% on the proportional counter. Background on the low-level beta counter was  $0.52 \pm 0.02$  cpm. No  $^{234}\text{Th}$  samples were counted on the low level counter at a net count rate of less than 1 cpm, so the uncertainty in the background correction was small.

#### Contributions from Tracers

Tracer isotopes  $^{236}\text{U}$  and  $^{229}\text{Th}$  used in this work contained some impurities. The  $^{236}\text{U}$  contained a  $^{234}\text{U}$  activity in an amount equal to 12.4% of the  $^{236}\text{U}$  activity as well as small amounts of  $^{238}\text{Pu}$  and  $^{239}\text{Pu}$  or  $^{240}\text{Pu}$ . The  $^{229}\text{Th}$  initially contained  $^{228}\text{Th}$  in an amount equal to 7.7% of the  $^{229}\text{Th}$  activity. Contributions of  $^{234}\text{U}$  and  $^{228}\text{Th}$  in the tracers were determined to within  $\pm 1\%$  and were subtracted from the sample activities. Plutonium was removed from the  $^{236}\text{U}$  tracer after the first few Pu analyses. Because nearly all of the Pu in the  $^{236}\text{U}$  was  $^{238}\text{Pu}$ ,  $^{239+240}\text{Pu}$  could be determined in samples to which the unpurified  $^{236}\text{U}$  had been added.

Protactinium-233 decays to  $^{233}\text{U}$ , which could interfere with measurement of  $^{234}\text{U}$ . This was a problem with some particulate samples with very low U activities, and uranium blanks, where the  $^{234}\text{U}/^{238}\text{U}$  ratios could not be determined. A more serious problem resulted in certain particulate samples with very low  $^{231}\text{Pa}$  contents. A significant amount of  $^{233}\text{U}$  was produced between the time Pa was plated and the time it was counted. The  $^{231}\text{Pa}$  alpha spectrum is divided roughly into two parts (Figure 2-3), a high energy part containing 89% of the total activity and a low energy part containing 11% of the activity. Decay of  $^{233}\text{U}$  occurs at the same energy as the part containing 11% of the  $^{231}\text{Pa}$  activity. Therefore, it was sometimes necessary to calculate

$^{231}\text{Pa}$  activities based on the 89% peak. This resulted in an additional uncertainty of approximately 2% in the calculated  $^{231}\text{Pa}$  activity since any degradation of the resolution of the Pa spectra tended to cause less than 89% of the total activity to be found in the high energy peak.

#### Blanks

Distilled, deionized water and reagent grade acids were used throughout this work. Several sets of blanks were run. Blank corrections of more than a few percent of sample activities were seldom necessary except for samples obtained with the in situ filtration systems.

Blanks were determined for the Mead glass fiber and Millipore HA filters (Table 1-1) before a reagent-only blank analysis could be carried out. Blanks for the Millipore filters plus reagents and  $\text{FeCl}_3$  carrier were so low that even if the entire blanks were due to reagents, they would be negligible compared to the activities of the samples requiring reagent-only blank corrections (sediments and sediment-trap samples).

Several types of glass fiber filter material were tested during this work. All had unacceptably high contents of uranium and thorium series isotopes, so glass fiber filters were not used except for the two M.I.T.-L.V.F.S. samples. Blanks for  $^{232}\text{Th}$  were 40 and 47%, for uranium 60 and 70%, for  $^{230}\text{Th}$  24 and 27%, and for  $^{228}\text{Th}$  7 and 9% of total activities of the two M.I.T.-L.V.F.S. samples. A Pa peak could not be resolved above the background noise in the Pa spectrum of the Mead glass fiber blank. Sample Al65-Pa and the Pa blank were counted consecutively on the same detector. Background and filter blank were subtracted together in this case. Sample Al63-Pa was counted on a different detector. Protactinium was assumed to be in radioactive equilibrium with

TABLE 2-1  
Results of Blank Analyses.

Description of Blank	232Th	230Th	231Pa	238U	228Th <sup>a</sup>	234U <sup>a</sup>
<u>Millipore Filters<sup>b</sup></u>						
dpm/3x142 mm filters	0.005±.004	0.005±.004	0.000±.002	0.005±.003	0.064±.013	0.008±.008
dpm/g filter	0.002±.002	0.002±.002	0.000±.001	0.002±.001	0.025±.005	0.003±.003
<u>Mead Glass Fiber Filters<sup>c</sup></u>						
dpm/g filter	0.056±.004	0.125±.007	0.016±.003 <sup>d</sup>	0.153±.010	0.094±.009	0.151±.010
<u>Nuclepore Filter<sup>e</sup></u>						
dpm/filter	0.0020±.0008	0.012±.002	0.011±.002 <sup>d</sup>	0.010±.005	0.008±.003	ND <sup>g</sup>
			0.0013±.0011 <sup>f</sup>			
<u>MnO<sub>2</sub>-Nitex</u>						
dpm/sheet	A	0.004±.003	0.083±.010 <sup>i</sup>	0.0021±.0004 <sup>d</sup>	ND <sup>h</sup>	0.016±.009
	B	0.005±.003	0.006±.003	0.0041±.0014	0.011±.006	ND <sup>g</sup>

ND = Not Determinable.

<sup>a</sup>Errors include correction for 228Th and 234U in the added tracers.

<sup>b</sup>Three 142-mm 0.45-micron HA filters were combined for the blank. Total weight was 2.55 g.

<sup>c</sup>Average weight of glass fiber material in samples analyzed in this work was 1.8 g.

<sup>d</sup>Values represent cpm of blank plus background when blank activity was not resolvable above background.

<sup>e</sup>Blanks are from a 293-mm 1.0-micron pore size filter taken to sea. The filter was torn while placing it in a filter holder,

so it was returned to Woods Hole for as a blank.

<sup>f</sup>Background corrected. Not significantly different from zero.

<sup>g</sup>Contamination by U-233 prevented accurate measurement of U-234.

<sup>h</sup>Counted on a detector contaminated with Th-228. Corrected blank Th-228 activity was indistinguishable from zero with large

counting errors.

<sup>i</sup>May include contamination from the electroplating cell. See text.



its parent  $^{235}\text{U}$  in the glass fiber material and this value was used as the Pa blank. Both methods of blank correction gave similar results for sample Al65-Pa.

Blank values for a 293-mm diameter Nuclepore filter and two analyses of  $\text{MnO}_2$ -Nitex are also presented in Table 2-1. Uranium and  $^{230}\text{Th}$  were found in significantly greater amounts than in the Millipore blank. The higher  $^{230}\text{Th}$  blank in one Nitex analysis may have resulted from contamination in the electroplating cell. During the early part of this work, the same cell was used for all samples. An effort was made throughout this work not to plate a Th sample after another Th sample, particularly a Th sample to which a  $^{230}\text{Th}$  tracer had been added. In addition to standard washing procedures, plating reagents alone were plated in cells after samples with large amounts of added  $^{230}\text{Th}$  or  $^{234}\text{Th}$  tracers as a precaution against contamination from previous samples. Later in this work, when the second Nitex blank and filtered particles from KN 73-16 and OC 78-1 were analyzed, a separate plating cell was used for samples with low activities.

Blank corrections were most significant for samples obtained with the in situ filtration systems. Nuclepore filter blanks reported in Table 2-1 amounted to 4-16% (average 9%) of sample activities for  $^{230}\text{Th}$ . Nitex blanks for  $^{230}\text{Th}$  were a maximum of 20% of the activity of two samples. The average Nitex blank correction for  $^{230}\text{Th}$  samples obtained with the in situ filtration systems was about 9%. Corrections for Pa blanks were a maximum of about 28% in one filtered-particle sample and 22% in two Nitex samples. Filter and Nitex Pa blank corrections averaged about 10% and 13% of sample activity respectively. Particulate and dissolved  $^{232}\text{Th}$  and particulate uranium are present at extremely

low concentrations in seawater, and large blank corrections were usually required. Blanks for dissolved and particulate  $^{232}\text{Th}$  ranged from less than 20% to more than 100% (not by more than the counting error) of the total sample activities. Blanks were approximately  $30 \pm 10\%$  of the total uranium activity in filtered particle samples. Concentrations of dissolved and particulate  $^{228}\text{Th}$  are very low at mid depth in the open ocean, and maximum blank corrections for particulate and dissolved  $^{228}\text{Th}$  were 16% (average 8%) and 35% (average 16%) respectively. The major emphasis of this study is on  $^{230}\text{Th}$  and  $^{231}\text{Pa}$  for which blank corrections were overall the least significant. The average blank corrections listed above only refer to Nitex samples obtained with the in situ filtration systems. Nitex blanks were less significant for samples obtained from the sediment trap moorings (Sites P and D, Chapter 4) as the effective volumes sampled, and therefore the total activities sampled, tended to be greater than for the samples obtained by in situ filtration.

#### ACCURACY AND PRECISION

Accuracy of the method was determined by duplicate analyses of the volcanic glass OCB 66-15 in which the U and Th isotopes have been measured both by mass spectrometry and alpha spectrometry, and  $^{230}\text{Th}$  was found to be in equilibrium with  $^{234}\text{U}$  and  $^{238}\text{U}$  (Rosholt et al., 1971). It was assumed that  $^{231}\text{Pa}$  should therefore also be in equilibrium with  $^{235}\text{U}$ . Results by this method are compared with the published results in Table 2-2. Agreement is within errors due to counting statistics.

Precision of the method was determined by replicate analyses of several sediment samples and one sediment-trap sample. A box-core sample

TABLE 2-2

Duplicate Analyses of Volcanic Glass Standard OCB 66-15.

	Literature <sup>a</sup>	<sup>232</sup> Th	<sup>238</sup> U	<sup>230</sup> Th <sup>b</sup>	<sup>231</sup> Pa <sup>b</sup>
U (ppm)	6.70±0.11		6.67±.15	6.71±.16	6.24±.25
			6.76±.12	6.70±.16	6.94±.20
Th (ppm)	29.7±0.7	30.39±.62			
		30.68±.68			

Activity Ratios

<sup>234</sup>U/<sup>238</sup>U

<sup>228</sup>Th/<sup>232</sup>Th

0.998±.027

0.996±.024

0.992±.012

0.965±.020<sup>c</sup>

<sup>a</sup>Rosholt et al., 1971.

<sup>b</sup>Equivalent ppm U based on measured isotope activity.

<sup>c</sup>Poor high energy resolution on detector used.

TABLE 2-3  
Duplicate Analyses of Sediment and Sediment Trap Samples.

Analysis	Count	232Th	230Th	228Th	238U	234U	231Pa
<u>Activity dpm/gram</u>							
<u>KN 69-1, Station 13, Box Core 13, 0-3 cm</u>							
A	1	1.845±.043	2.195±.049	1.750±.042	1.220±.046	1.126±.043	
	2	1.791±.041	2.200±.047	1.759±.040	1.262±.050	1.221±.049	
B	1	1.940±.049	2.192±.054	1.906±.048	1.277±.033	1.159±.030	0.128±.004
	2	1.862±.046	2.195±.052	1.713±.044	1.294±.033	1.181±.030	
<u>PARFLUX Site E, 389-m Sediment Trap</u>							
A		0.21±.012	0.36±.02	13.9±.2	0.7±.01	0.82±.02	0.026±.003
E		0.18±.015	0.37±.02	12.1±.7	0.67±.04	0.71±.04	0.023±.005

was analyzed twice for U and Th, and each plate was counted twice on different detectors. The results are presented in Table 2-3.

Variability due to counting errors is as great as the variability between replicate analyses. Agreement between duplicate analyses of the standard OCB 66-15 mentioned above is further evidence for the good precision of the method.

Sediment trap samples were generally too small to allow duplicate analyses for U, Th, and Pa. However, sample sizes from PARFLUX Site E were sufficiently large to allow duplicate analysis of one sample as part of this work. Material from 389 m at Site E was chosen since it had the lowest specific activities and therefore was considered likely to be the most difficult sample to precisely measure. Results of duplicate analyses are given in Table 2-3. Errors are larger on the second analysis because a smaller sample size was used. Agreement between the two analyses was good.

#### CONCLUSIONS

This procedure allows the accurate and precise measurement of U, Th, Pa, Pu, Am, and Ac isotopes in small environmental samples. It is also possible to include the measurement of  $^{90}\text{Sr}$ ,  $^{137}\text{Cs}$ , and  $^{55}\text{Fe}$ . The portion of this procedure for analysis of U, Th, and Pa isotopes is simpler and shorter than methods in the literature.

CHAPTER 3.

PROCESSES REMOVING THORIUM AND PROTACTINIUM FROM SEAWATER:

OPEN OCEAN ENVIRONMENTS

INTRODUCTION

Thorium-230 and  $^{231}\text{Pa}$  are produced in seawater by radioactive decay of dissolved uranium isotopes. Once produced in seawater, both are rapidly hydrolyzed and subsequently removed to sediments in times much shorter than their radioactive half-lives ( $^{230}\text{Th}$ =75200 years;  $^{231}\text{Pa}$ =32500 years; Lederer and Shirley, 1978). Production rates are well known for several thorium isotopes from the known distributions of their radioactive parents in the oceans. Several investigators have taken advantage of these well known sources and the rapid removal of thorium to model the scavenging of reactive elements from seawater based on the distributions of thorium isotopes (Broecker et al., 1973; Krishnaswami et al., 1976; Li et al., 1979; Brewer et al., 1980).

In spite of their short residence times in seawater,  $^{230}\text{Th}$  and  $^{231}\text{Pa}$  are chemically fractionated during their incorporation into sea floor deposits. If there were no fractionation, thorium and protactinium would be removed from seawater at a  $^{230}\text{Th}/^{231}\text{Pa}$  activity ratio of 10.8, a ratio fixed by the constant concentration and isotopic composition of uranium in the oceans. However, many deep-sea surface sediments have activity ratios of 20-30 or higher (e.g. Sackett, 1964; Ku, 1966; Ku et al., 1972; this chapter), whereas manganese nodules and some sediments have surface ratios less than 10.8, occasionally as low as three (Ku and Broecker, 1969; DeMaster, 1979; Cochran, 1979). Particulate  $^{230}\text{Th}$  and  $^{231}\text{Pa}$  distributions measured at three open ocean sites are used in this chapter to determine where the separation of

$^{230}\text{Th}$  and  $^{231}\text{Pa}$  is taking place, and to determine the effectiveness with which settling particles remove Th and Pa from seawater.

#### SAMPLE PROCUREMENT AND HANDLING PROCEDURE

Most of the samples discussed here were taken as part of the PARFLUX program (Honjo, 1978, 1980; Spencer et al., 1978; Brewer et al., 1980). Locations of the PARFLUX sediment-trap Sites S, F, and P are shown in Figure 3-1. Water depths and site coordinates are presented in Table 3-1. Sediment trap samples used in this study were from the second occupation of Site S, designated S<sub>2</sub>. Two samples of particulate material were collected by filtration in situ at Site E during the sediment-trap recovery cruise with the Massachusetts Institute of Technology Large Volume Filtration System (MIT-LVFS; Bishop and Edmond, 1976). Site E was reoccupied in February, 1980, during R/V Oceanus, Cruise 78-1. Large volumes of seawater were filtered in situ (293-mm diameter, 1.0- $\mu\text{m}$  pore size, Nuclepore filters) with a battery-powered pump described by Spencer and Sachs (1970) and Krishnaswami et al. (1976).

Sediment samples were available in the WHOI core library from a piston core and a pilot gravity core taken 50 km to the north of Site E at a slightly greater water depth on R/V Chain, Cruise 75-2. Three box cores were taken on the sediment trap deployment cruise near Site P. Two cores were red clay from deeper than 5800 m, and the third was taken at a depth of 2701 m approximately 100 km south of Molokai Island.

Hydrographic conditions at Site S were described by Spencer et al. (1978). Site E is between GEOSECS stations 36 and 37 and is hydrographically similar to those stations. Site P will be described by Brewer et al. (in preparation).

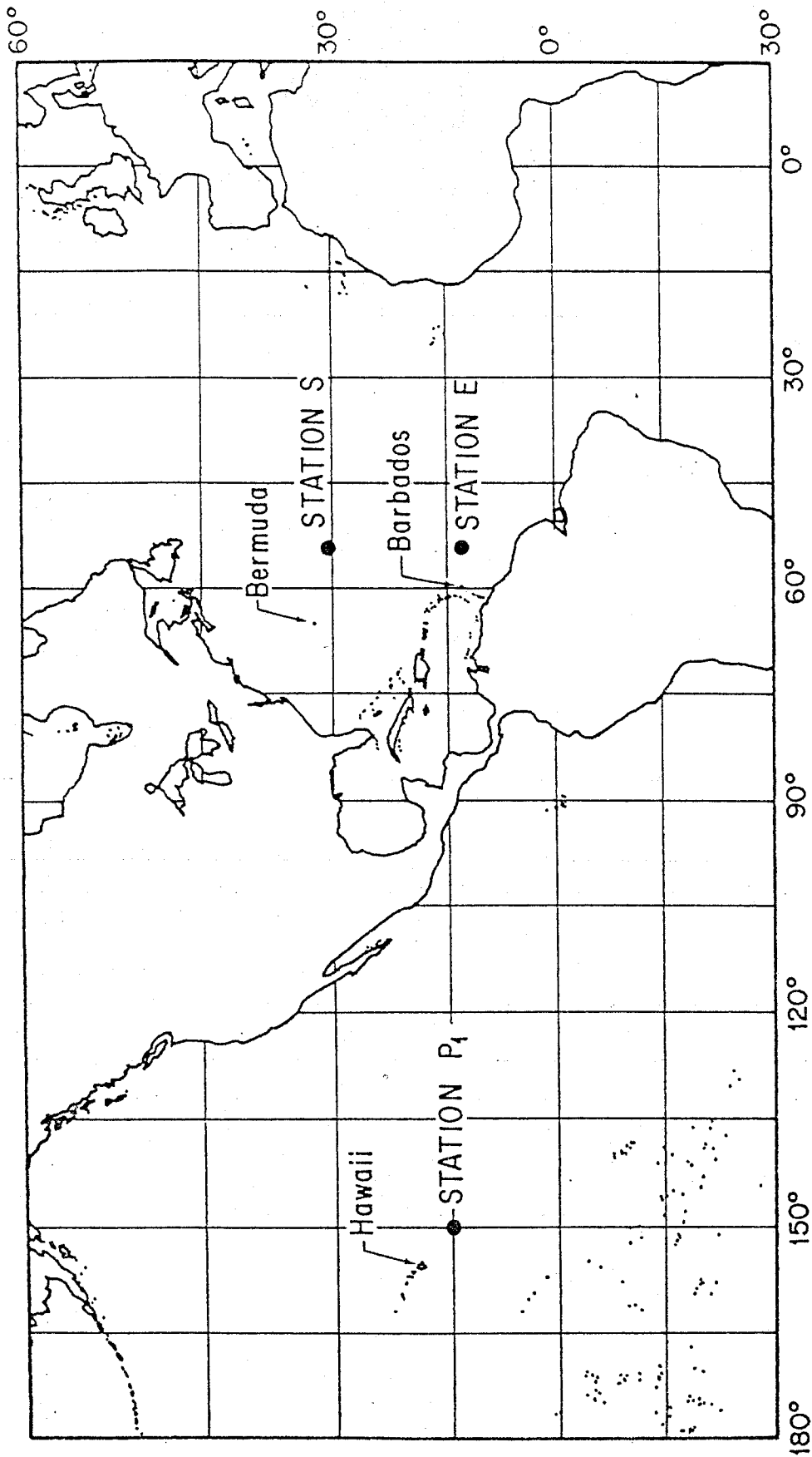


Figure 3-1. Locations of PARFLUX sediment trap sites.



All of the sediment trap results reported here are from the less than 1-mm size fraction. The greater than 1-mm size fraction was a significant portion of the total sample only in the shallowest trap at each site (Honjo, 1980).

Sediment-trap samples were kept refrigerated from the time of their collection until they were returned to Woods Hole, where they were split wet into four equal subsamples by a rotating sample splitter (Honjo, 1978). One or two quarters of the less than 1-mm size fractions, depending on the sample, were filtered onto 0.5-micron Nuclepore filters, rinsed with distilled water, dried, and weighed (Brewer et al., 1980). Weighed samples were homogenized in an agate mortar and dispensed to various investigators. Filtered particle samples obtained with the MIT-LVFS were handled according to standard procedures (Bishop et al., 1977). Filtered particles obtained with the battery-powered pump were rinsed with distilled water immediately upon recovery at sea. Excess water was removed from the filters by suction supplied with an aspirator. Wet filters were folded into eighths and stored in plastic bags for return to WHOI, where filters were dried and weighed.

Samples collected with the MIT-LVFS were prefiltered through 53-micron mesh Nitex fabric. Prefilters were not used with the battery-powered pump. However, since the bulk of the standing crop of marine particulate matter is of less than 53-micron diameter (Bishop and Edmond, 1976), filtered samples should consist predominantly of the less than 53-micron fraction whether or not a prefilter was used.

The chemical procedure for the analysis of U, Th, Pa, Ac, and Pu isotopes is described in Chapter 2.

## RESULTS

Mass fluxes of the less than 1-mm size fractions and radiochemical results for sediment-trap samples are given in Table 3-1. Errors reported are one standard deviation counting statistics. There was too little sample material to run duplicate analyses on each sediment-trap sample. The Site E-389 m sample was chosen for duplicate analysis since it had the lowest specific activities of samples with sufficient material for duplicate analysis, and was therefore considered the most difficult for which to obtain reproducible results. Good agreement was found for all isotopes.

An accurate measurement of the flux in the Site S<sub>2</sub> 5206-m trap could not be made because the sample contained large amounts of aluminum hydroxide precipitate that resulted from the corrosion of the sliding door sealing the sample container at the end of the deployment period. The volume of seawater from which actinides were scavenged by the aluminum hydroxide was estimated to be only a few liters, as indicated by the quantity of uranium collected. Assuming that U is scavenged with the same efficiency as Th and Pa, the Th and Pa isotope ratios in the trapped particles were not significantly affected by dissolved isotopes scavenged by the aluminum hydroxide.

Plutonium was initially measured in samples from Sites S<sub>2</sub> and E with <sup>238</sup>Pu (present as an impurity in the <sup>236</sup>U spike) as a yield monitor. The <sup>239+240</sup>Pu/<sup>238</sup>Pu ratio in the spike was approximately 0.05. Since the natural <sup>238</sup>Pu/<sup>239+240</sup>Pu ratio could not be measured in the samples, it was assumed to be 0.04 (Hardy et al., 1974). Uncertainty in this ratio resulted in a small additional uncertainty in the Pu values. The activity of <sup>238</sup>Pu added was of the same order of

TABLE 3-1  
 Radiochemical Results for Sediment Trap Samples.  
 All Activities are Given in dpm per g of Dried Sediment.

Depth (m)	Mass Flux (mg/cm <sup>2</sup> yr)	238U	230Th	231Pa	232Th	228Th	239,240Pu	234U/238U	235Pu/239,240Pu	Activity Ratio	
										dpm/g	
<u>Site S<sub>1</sub>, 31.5°N, 55.0°W, 5580 m</u>											
3694	0.741	1.0±.04	7.7±.20	0.2±.02	0.57±.04	46.8±.7	0.48±.02	1.18±.07		ND	
5206a	--	6.8±.19	1.4±.05	0.04±.005	0.5±.03	4.8±.09	--	1.14±.04		ND	
<u>Site F, 13.5°N, 54.0°W, 5283 m</u>											
389-A	1.888	0.7±.01	0.3±.02	0.02±.003	0.21±.01	13.9±.2	0.18±.03	1.15±.04		ND	
389-B	--	0.6±.04	0.37±.02	0.02±.005	0.18±.02	12.1±.7	0.20±.03	1.06±.08		ND	
988	1.510	0.7±.03	1.2±.03	0.087±.006	0.60±.02	13.8±.1	0.14±.02	1.01±.07		ND	
3755	1.956	0.81±.03	4.80±.08	0.22±.010	0.97±.03	14.1±.2	0.15±.02	0.98±.07		ND	
5086	1.808	0.83±.03	5.69±.15	0.20±.009	1.2±.05	21.7±.5	0.12±.02	1.06±.06		ND	
<u>Site P, 15.3°N, 151.5°W, 5792 m</u>											
378	0.182	3.78±.14	0.38±.03	< .03	0.06±.02	0.7±.1	0.28±.03	1.20±.07		0.05±.036	
978	0.268	0.6±.04	1.9±.06	0.10±.009	0.07±.01	5.5±.1	1.61±.09	1.20±.12		0.03±.007	
2778	0.606	0.41±.02	10.4±.2	0.34±.007	0.11±.01	5.9±.1	2.0±.1	1.29±.13		0.038±.005	
4280	0.584	0.34±.02	16.6±.3	0.48±.02	0.12±.01	5.4±.1	2.4±.1	1.28±.13		0.036±.005	
5582	0.355	0.44±.04	27.4±.5	0.91±.04	0.23±.02	10.0±.2	2.2±.1	1.10±.19		0.049±.007	

This sample contained a large quantity of corrosion product from the trap door.

ND = Not Determined.

magnitude as the activity of  $^{239+240}\text{Pu}$  in the samples, so the  $^{239+240}\text{Pu}$  added with the spike was small relative to the amounts in the samples. Plutonium was measured in Site P samples with a  $^{242}\text{Pu}$  yield monitor and a Pu-free  $^{236}\text{U}$  solution so that  $^{238}\text{Pu}$  could be measured. Measured  $^{238}\text{Pu}/^{239+240}\text{Pu}$  ratios ranged between 0.038 and 0.054 (Table 3-1).

Results from particulate samples obtained by in situ filtration at Site F are presented in Table 3-2. Depths given in Table 3-2 represent wire out during pumping. True depths of the battery-powered pump (OC78-1, 3600 m and 5000 m) could not be determined, and probably varied somewhat during the course of the 10-12 hour pumping periods due to changes in the rate of ship drift. Errors in the estimated depths are probably not too large as wire angles were kept vertical at the surface and wire angles at depth were small during Niskin casts as determined from reversing thermometer data.

Of the samples discussed in this chapter, blank corrections were significant only for filtered particle samples. Glass fiber material contained fairly high amounts of uranium and thorium series isotopes. Nuclepore filter blanks were much lower, but because of the smaller sample sizes, the blanks were significant. Glass fiber filter blanks for the two samples in Table 3-2 (975 m and 1400 m) averaged 65% of total sample activity for the uranium isotopes, 43% for  $^{232}\text{Th}$ , 25% for  $^{230}\text{Th}$ , and 8% for  $^{228}\text{Th}$ . A protactinium blank could not be resolved above background. Nuclepore filter blank corrections for the two samples in Table 3-2 (3600 m and 5000 m) averaged 7% for  $^{232}\text{Th}$ , 2% for  $^{228}\text{Th}$ , 4% for  $^{230}\text{Th}$ , and 15% for  $^{231}\text{Pa}$ .

TABLE 3-2  
 Concentrations of Radioisotopes in Filtered Particles at PARFLUX Site E.

Sample Depth (m); Volume (l); Weight (mg)	232Th	228Th	230Th	231Pa	238U	234U	230Th/ <sup>231</sup> Pa
<b>MIT-LVFS</b>							
975 m	0.80±.10	10.8±.3	3.53±.17	0.261±.027	0.48±.17	0.75±.17	13.5±1.8
10350 l							
200 mg	15±2	20.9±.6	68±3	5.0±.5	9±3	14±3	
<b>MIT-LVFS</b>							
1400 m	0.79±.07	7.32±.14	3.01±.12	0.222±.018	0.60±.13	0.63±.13	13.6±1.2
11500 l							
270 mg	18±1.6	17.2±.3	71±3	5.2±.4	14±3	15±3	
<b>OC 78-1</b>							
3600 m	1.26±.18	13.2±1.0	11.87±.64	0.255±.060	ND	ND	47±11
3373 l							
23.5 mg	8.8±1.3	92±7	78±4	1.57±.42			
<b>OC 78-1</b>							
5000 m	1.78±.19	39.1±2.2	15.86±.69	0.418±.068	ND	ND	38±6
4276 l							
25.1 mg	10.4±1.1	229±13	93±4	2.20±.40			

Radioisotope results from sediments taken near Sites E and P are presented in Table 3-3. Only results from the pilot core of CH 75-2, Core 8 were used as it appeared that the top of the piston core was lost. Results from three box cores taken during the Site P sediment trap deployment cruise are also given in Table 3-3. KKI Core 2 was a hard, compacted sediment, very different from Core 1, which consisted of normal deep-sea clay. The compact nature and low specific activities of unsupported  $^{230}\text{Th}$  and  $^{231}\text{Pa}$  suggest that Core 2 may have been taken in an area of outcropping Tertiary sediments which occur in the equatorial Pacific (Johnson, 1972). Two cores from near Site P studied by Riedel and Funnell (1964) contained Eocene sediments within a few centimeters of the surface. Core 4 was taken at a depth of 2701 m on the slope of Molokai Island to compare the sediment trap sample at 2778 m with sediment accumulating at a similar depth on the sea floor.

Sediment trap samples from Sites S<sub>2</sub> and E were analyzed for radioisotopes by Brewer et al. (1980) by slightly different analytical procedures. Their results are reproduced in Table 3-4. Agreement of the two sets of results is generally good. Smaller relative errors reported here result in part from the much larger sample sizes used in this work (100-500 mg vs. approximately 50 mg), and in part because their errors include variability between Yale and WHOI results.

Uranium isotope activities in the shallowest sediment-trap samples at Sites E and P were greater than the activities of their  $^{230}\text{Th}$  and  $^{231}\text{Pa}$  daughters (Table 3-1), suggesting that part of the uranium was recently derived from seawater. It was necessary to resolve the contributions of detrital and seawater-derived uranium in the samples to determine the amounts of  $^{230}\text{Th}$  and  $^{231}\text{Pa}$  scavenged from seawater. It

TABLE 3-3  
Radiochemical Results for Sediment Cores Associated with PARFLUX Sites E and P.

Depth (cm)	$^{232}\text{Th}$	$^{230}\text{Th}$	$^{238}\text{U}$	$^{234}\text{U}$	$^{231}\text{Pa}$	$^{210}\text{Pb}$	$\frac{^{230}\text{Th}/^{231}\text{Pa}}{\text{ACTIVITY RATIO}}$
			(dpm/g)				
KK1, Core 1, 14.07°N, 153.10°W, 5926 m							
0-1	1.9±.08	93.5±1.5	1.5±.05	1.3±.05	3.73±.11	NA	25.2±0.9
KK1, Core 2, 15.20°N, 151.34°W, 5802 m							
0-3	0.506±.011	9.9±.15	0.556±.020	0.514±.020	0.337±.010	NA	30.2±1.1
KK1, Core 4, 100 km Due South of Molokai Islands, 2701 m							
0-2	0.260±.012	15.09±.23	0.69±.018	0.77±.019	1.43±.09	38.0±7.2	10.3±.7
10-15	0.244±.011	14.4±.20	0.67±.021	0.82±.025	1.36±.05	11.86±.54	10.4±.4
19-21	0.247±.017	14.2±.20	0.66±.017	0.69±.017	1.33±.04	14.91±.51	10.5±.4
CH 75-2, Core 8, 14.1°N, 54.1°W, 5342 m							
2-4	3.25±.08	6.6±.13	1.69±.04	1.7±.04	0.23±.009	NA	31.5±2.0

NA = Not Analyzed.

<sup>a</sup>Radar fix only.

TABLE 3-4

Radionuclide Concentrations (dpm/g).  
(From Table 5 in Brewer et al.)

Trap Depth	PARFLUX E. Site			PARFLUX S <sub>2</sub> Site		
	389 m	988 m	3755 m	5086 m	1694 m	
Nuclide						
<sup>234</sup> Th	4320±343	3589±79	3251±20	3411±326		5458±1284
<sup>228</sup> Th	13.5±1.9	12.9±2.6	12.5±1.1	18.4±2.8		50.5±9.8
<sup>230</sup> Th	0.5±0.8	1.45±0.07	4.2±0.29	5.37±0.80		8.04±1.14
<sup>232</sup> Th	0.37±0.13	0.69±0.08	0.9±0.11	1.20±0.22		0.77±0.12
<sup>210</sup> Pb	9±6	148±14	331±41	376±38		47±39
<sup>210</sup> Po	12±5	104±12	49±15	667±20		87±10
<sup>226</sup> Ra	3.47±0.10	2.57±0.23	1.87±0.48	1.60±0.85		7.06±0.40
<sup>238</sup> U	1.2±0.17	1.0±.15	1.0±0.13	1.1±0.15		1.28±0.10
<sup>231</sup> Pa	ND	0.09±0.007	0.25±0.04	0.27±0.02		ND

ND = Not Determined.



was assumed that the detrital  $^{238}\text{U}/^{232}\text{Th}$  ratio was constant at each site and equal to the ratio measured in surface sediments. It was also assumed that the uranium series were in secular equilibrium in the detrital phases. Excess  $^{230}\text{Th}$  (that scavenged from seawater, designated  $x_s^{230}\text{Th}$ ) was calculated for each sample of suspended particles as

$$x_s^{230}\text{Th}_z = {}^{230}\text{Th}_z - [({}^{238}\text{U}/{}^{232}\text{Th})_{\text{sed}} \times {}^{232}\text{Th}_z] \quad (1)$$

Unsupported  $^{231}\text{Pa}$  was calculated as

$$x_s^{231}\text{Pa}_z = {}^{231}\text{Pa}_z - 0.046 [({}^{238}\text{U}/{}^{232}\text{Th})_{\text{sed}} \times {}^{232}\text{Th}_z] \quad (2)$$

where z identifies the sample and sed refers to the ratio measured in the sediments. Sediment samples were not available at Site  $S_2$ , so the U/Th ratio from Site E was used. Results of these calculations are presented in Table 3-5. Uranium-supported  $^{230}\text{Th}$  and  $^{231}\text{Pa}$ , calculated from Equations 1 and 2, amounted to 6-20% of the total sample activities at Sites  $S_2$  and E. With the exception of the 378-m sample, the corrections for Site P samples were less than 10% of the total sample activities.

Much of the seawater-derived uranium is remineralized in the water column (see discussion section), so it must be associated with very labile particle phases that would not remain for long periods of time at the sediment surface. While it cannot be proven that all of the uranium in the sediments is detrital, the above procedure was the best available means of estimating the detrital uranium content of suspended particles.

## DISCUSSION

### Particle Fluxes

The flux of particulate material (Table 3-1) was constant throughout the water column at Site E and was more than two times higher than at

TABLE 3-5  
 Unsupported  $^{230}\text{Th}$  and  $^{231}\text{Pa}$  in Suspended Particles<sup>a</sup>.

Sample	$x_s^{230}\text{Th}$ dpm/g	$x_s^{231}\text{Pa}$	$x_s^{230}\text{Th}/x_s^{231}\text{Pa}$ Activity Ratio
Site S <sub>2</sub> , 3964 m	7.41±.20	0.270±.017	27.4±1.9
Site S <sub>2</sub> , 5206 m	1.14±.05	0.034±.005	33.5±5.1
Site E, 389 m	0.250±.018	0.021±.003	11.9±1.9
Site E, 988 m	0.907±.033	0.073±.006	12.4±1.1
Site E, 3755 m	4.28±.08	0.197±.010	21.7±1.2
Site E, 5086 m	5.04±.15	0.170±.009	29.6±1.8
MIT-LVFS, 975 m	3.11±.18	0.242±.027	12.9±1.6
MIT-LVFS, 1400 m	2.59±.13	0.203±.018	12.8±1.3
OC 78-1, 3600 m	11.19±.64	0.226±.060	50±13
OC 78-1, 5000 m	14.94±.68	0.375±.068	40±7
Site P, 378 m	0.331±.046	< .03	> 11
Site P, 978 m	1.88±.07	0.103±.009	18.3±1.7
Site P, 2778 m	10.34±.21	0.341±.007	30.3±0.9
Site P, 4280 m	16.46±.32	0.472±.021	34.9±1.7
Site P, 5582 m	27.25±.52	0.899±.043	30.3±1.6

<sup>a</sup>Calculated as described in text.

Site S<sub>2</sub>, whereas concentrations of suspended particles measured in Niskin bottle water samples were about two times higher at Site S (Spencer et al., 1978; Brewer et al., 1980). Fluxes of particles through the water column are not strictly correlated with the concentrations of particles measured in standard water samples. Therefore, the efficiency of removal of reactive elements from the water column by settling particles may likewise not be proportional to the measured concentration of particles.

Fluxes at Site P were less at all depths than at the Atlantic sites, as would be expected from its remote location and low biological productivity. A mid-depth maximum in the particle flux was observed at Site P. It is not possible to determine if this was an artifact of variable trapping efficiency or if it was due to horizontal input of particles.

The mid-depth flux maximum probably did not result from sampling a slow moving wave or pulse of increased particle flux that happened to be at mid-depth during the deployment. Pulses of increased particle flux, such as are induced by seasonal variability in primary productivity, travel with sufficient rapidity (Deuser and Ross, 1980; Deuser et al., in preparation) that they would have been sampled equally by traps at all depths.

#### Nature of the Particles

Sediment-trap samples were dominated by large, rapidly settling particles of sea surface origin (Honjo, 1980). Plutonium and <sup>228</sup>Th results support this conclusion. The plutonium distribution in the Pacific exhibits a pronounced maximum at 500-800 m (Bowen et al., 1980). Plutonium specific activities in trap samples at Site P were low at 378 m

and increased by a factor of 6-8 to a nearly constant value below this depth (Figure 3-2). Most of the plutonium in samples below 378 m must have been scavenged between 378 m and 978 m, as the plutonium concentration deeper in the water column is very low. These observations are consistent with a near surface origin for the bulk of the particles trapped at all depths.

Specific activities of  $^{228}\text{Th}$  were nearly constant in the upper three traps at Site E and in the middle three traps at Site P (Table 3-1). There is little production of  $^{228}\text{Th}$  at mid-depths in the open ocean because significant amounts of its parent,  $^{228}\text{Ra}$ , are present only near the sea surface and the sea floor (Trier et al., 1972; Sarmiento et al., 1976). In order to maintain the constant specific activities in particles trapped at mid-depths, particles must have scavenged  $^{228}\text{Th}$  at or near the sea surface and then settled through the water column in considerably less time than the 1.9-year radioactive half-life of  $^{228}\text{Th}$ .

An average particle settling rate of 21 m/d (7665 m/yr) was calculated by Brewer et al. (1980) for samples at Site E. Settling velocities of 20000 m/yr or more can be inferred from the "immediate" reflection of seasonal surface productivity cycles in sediment traps placed at 3200 m in the Sargasso Sea (Deuser and Ross, 1980; Deuser et al., in preparation). These rates are consistent with the rapid settling velocities predicted from the radioisotope distributions discussed above.

#### CHEMICAL BEHAVIOR OF THORIUM-230 AND PROTACTINIUM-231

##### Scavenging by Settling Particles

Specific activities of  $^{230}\text{Th}$  and  $^{231}\text{Pa}$  in trapped particles increased with depth at Sites E and P (Figures 3-3 and 3-4), with the

Figure 3-2. Concentration of plutonium in sediment trap samples at Site P. Error bars indicate one standard deviation counting statistics.

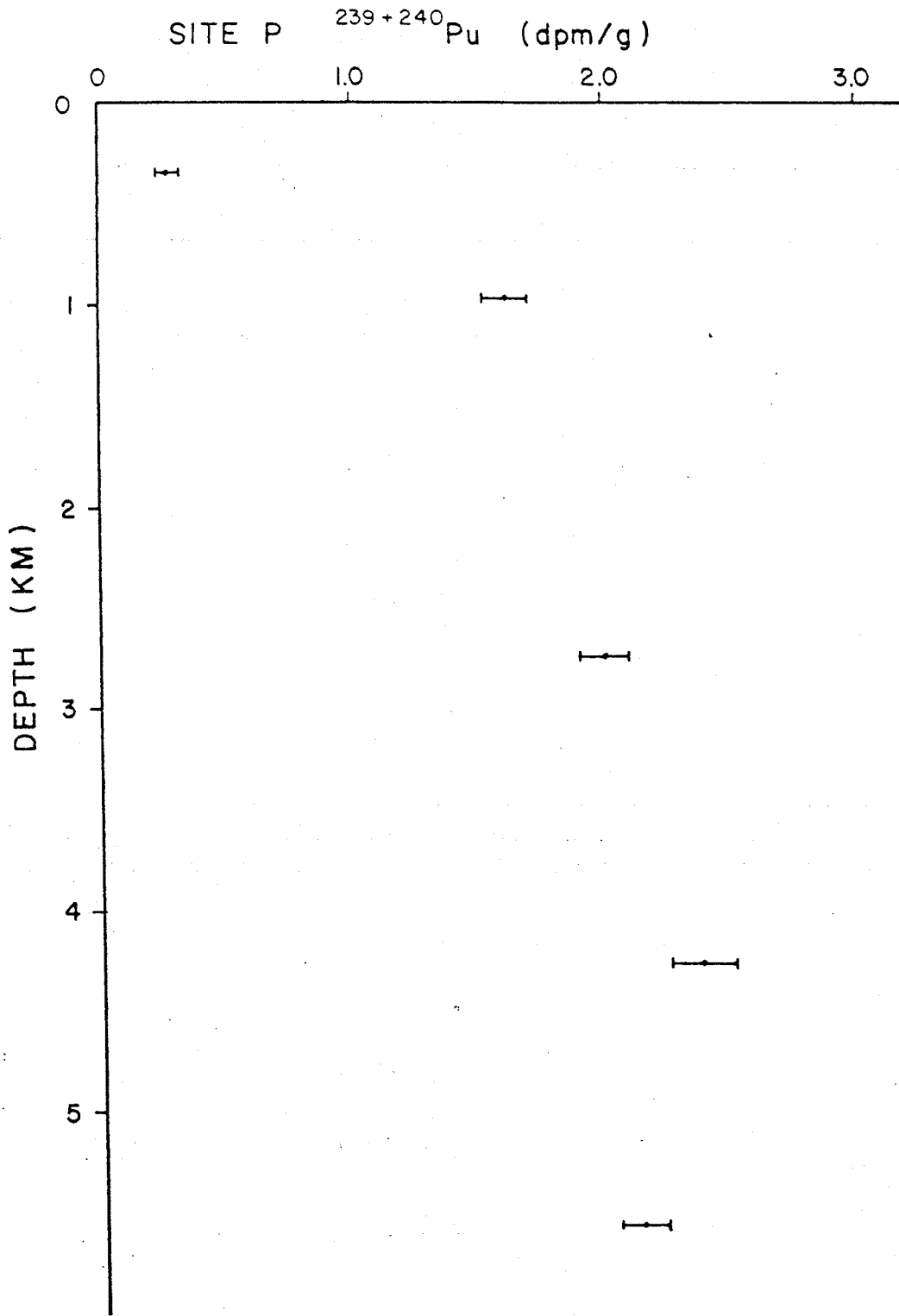


Figure 3-3. Concentrations of  $^{230}\text{Th}$  in sediment trap samples at Sites E and P. Error bars indicate one standard deviation counting statistics. Where error bars are not drawn, the size of the symbol approximately indicates the counting error.

Figure 3-3.

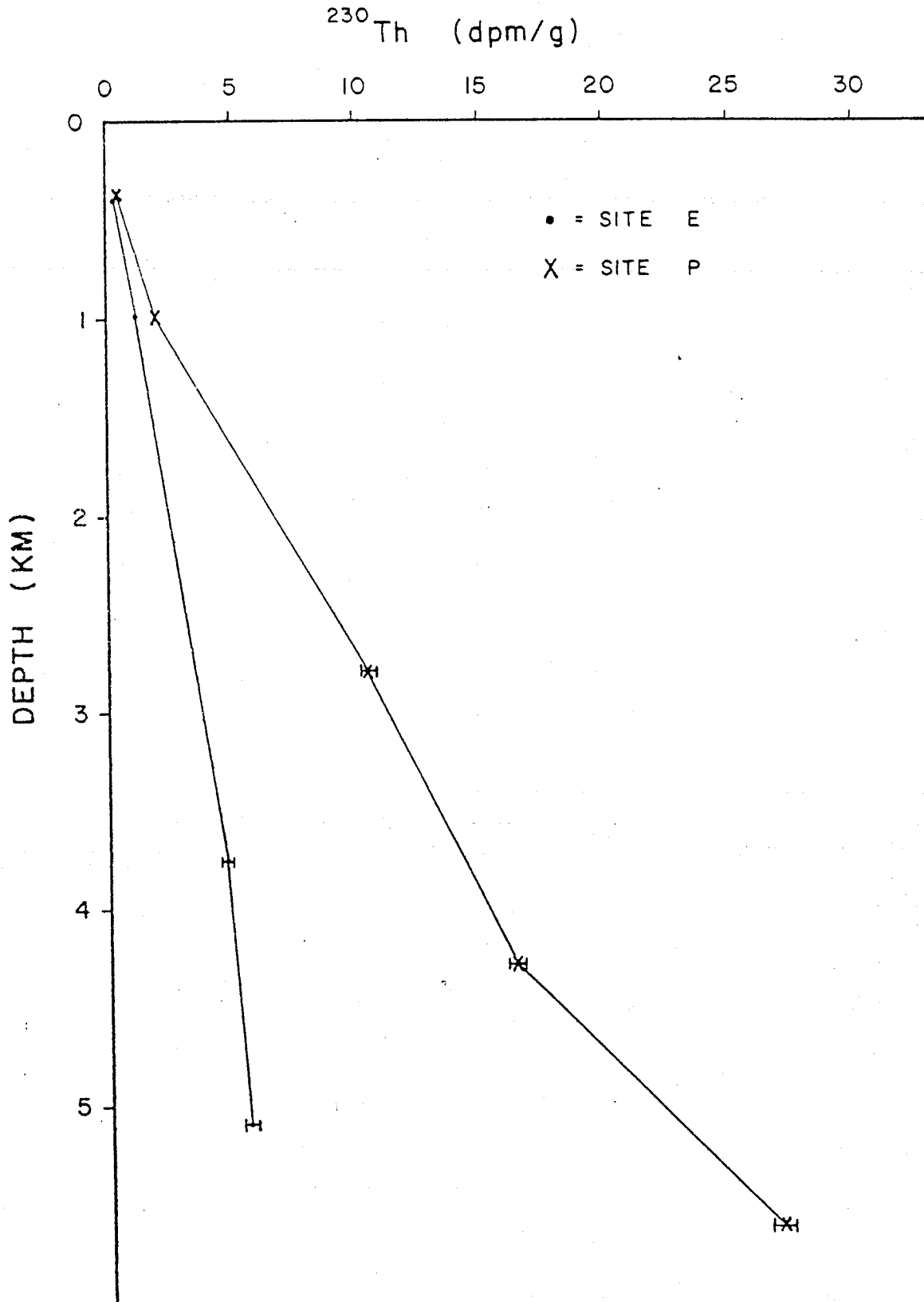
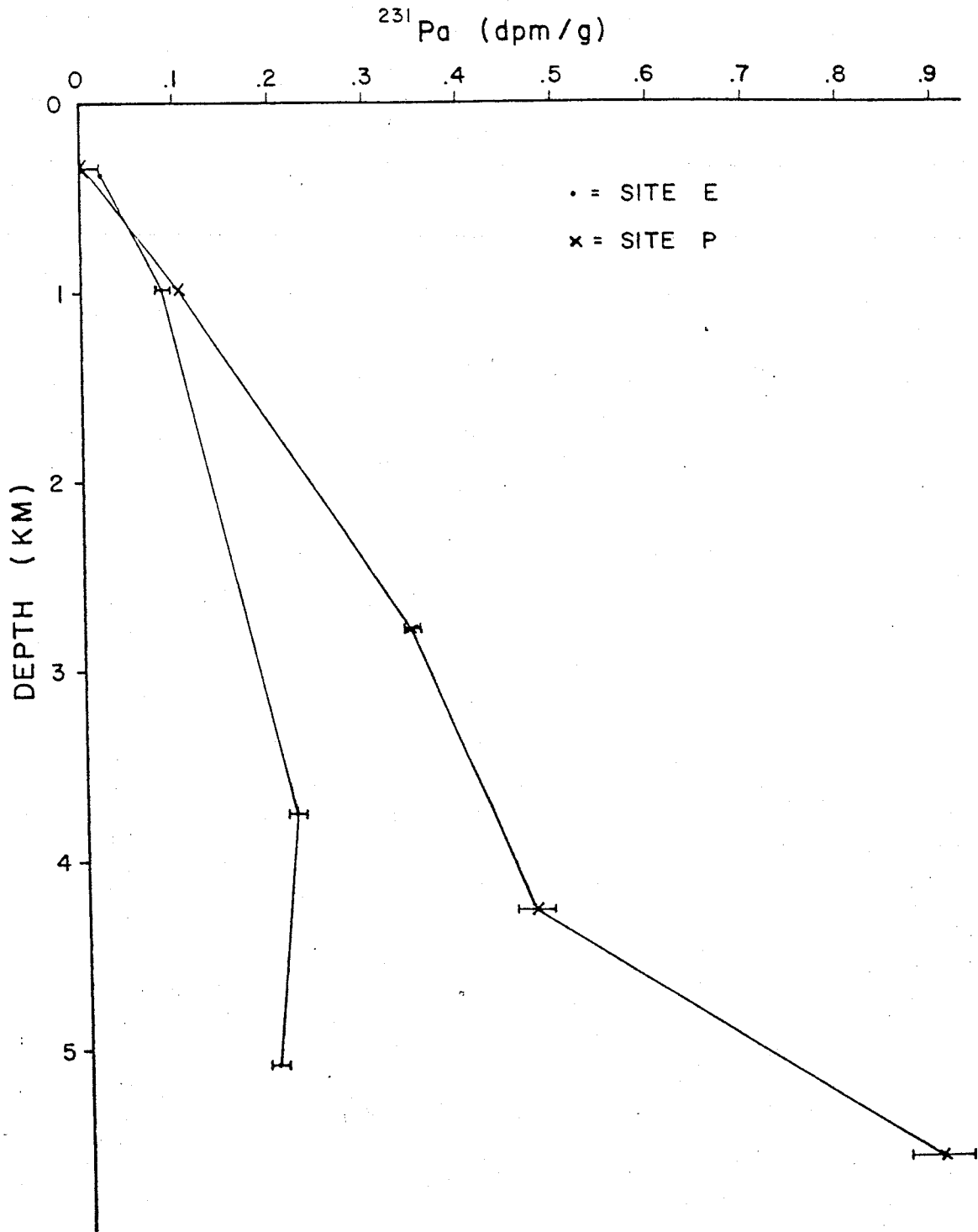


Figure 3-4. Concentrations of  $^{231}\text{Pa}$  in sediment trap samples at Sites E and P. Error bars indicate one standard deviation counting statistics. Where error bars are not drawn, the size of the symbol approximately indicates the counting error.



Figure 3-4.



exception of the deepest  $^{231}\text{Pa}$  sample at Site E. This behavior is consistent with continuous scavenging of these isotopes as particles settle through the water column, and is in contrast with the behavior of Pu (Figure 3-2) which has its primary source in the upper 1000 m. The near linear increase with depth in the specific activities of  $^{230}\text{Th}$  and  $^{231}\text{Pa}$  at Site P suggests that the particles accumulate  $^{230}\text{Th}$  and  $^{231}\text{Pa}$  at a constant rate over any depth interval.

Unsupported  $^{230}\text{Th}/^{231}\text{Pa}$  activity ratios from Sites  $S_2$  and E are shown in Figure 3-5. Two samples of trapped particles and two samples of filtered particles above 1500 m at Site E had nearly identical ratios at about  $12 \pm 1.5$ . Below 1500 m the ratio increased with depth to 30 in sediment trap samples and sediments and 40-50 in filtered particles. Similar results were observed in sediment trap samples at Site P (Figure 3-6). Sample P-378 m was too small to accurately measure  $^{231}\text{Pa}$ . Only an upper limit for  $^{231}\text{Pa}$  could be set with a corresponding lower limit for the  $^{230}\text{Th}/^{231}\text{Pa}$  ratio. The  $^{230}\text{Th}/^{231}\text{Pa}$  ratio increased with depth as it did at Site E; although at Site P the ratio was two times higher at 1000 m than at Site E, and it decreased in the bottom trap at Site P.

Suspended particles more than 1500 m above the sea floor contained unsupported  $^{230}\text{Th}/^{231}\text{Pa}$  ratios of 27 or higher at all three sites. Similar ratios are commonly found in deep-sea surface sediments, and are 5-10 times greater than dissolved  $^{230}\text{Th}/^{231}\text{Pa}$  ratios (Chapters 4 and 5). Filtered particles at Site E and trapped particles at Site P contained higher unsupported  $^{230}\text{Th}/^{231}\text{Pa}$  ratios than underlying sediments (Figures 3-5 and 3-6). Resuspended sediments, with a ratio of 30, cannot be mixed with a primary flux of particles with a ratio of 10.8

Figure 3-5. Unsupported  $^{230}\text{Th}/^{231}\text{Pa}$  activity ratios in sediment trap samples, filtered particles, and sediments at Sites S<sub>2</sub> and F. The vertical dashed line indicates the ratio at which Th and Pa are produced by uranium decay. Hatched areas represent water depths.

Figure 3-5.

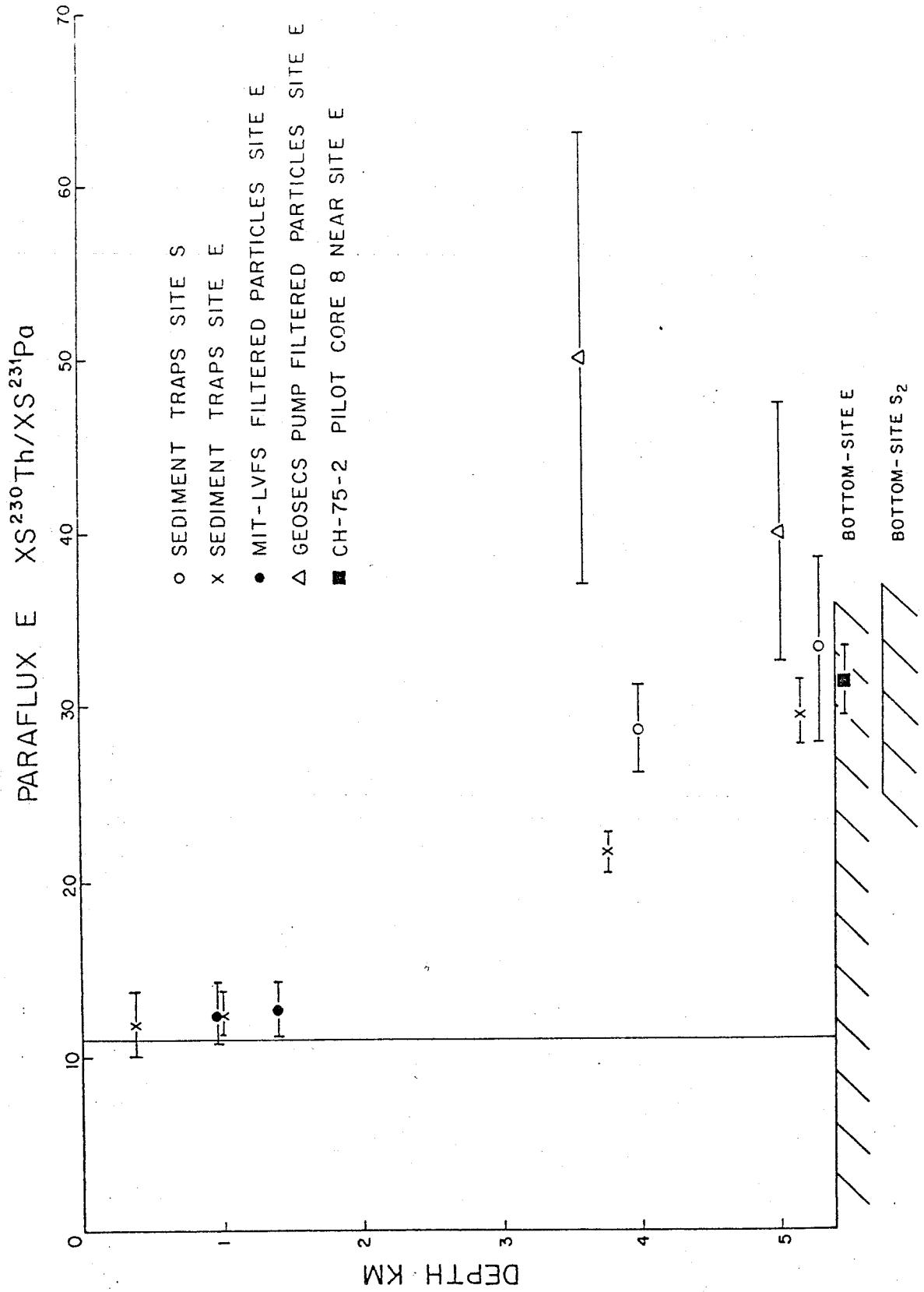
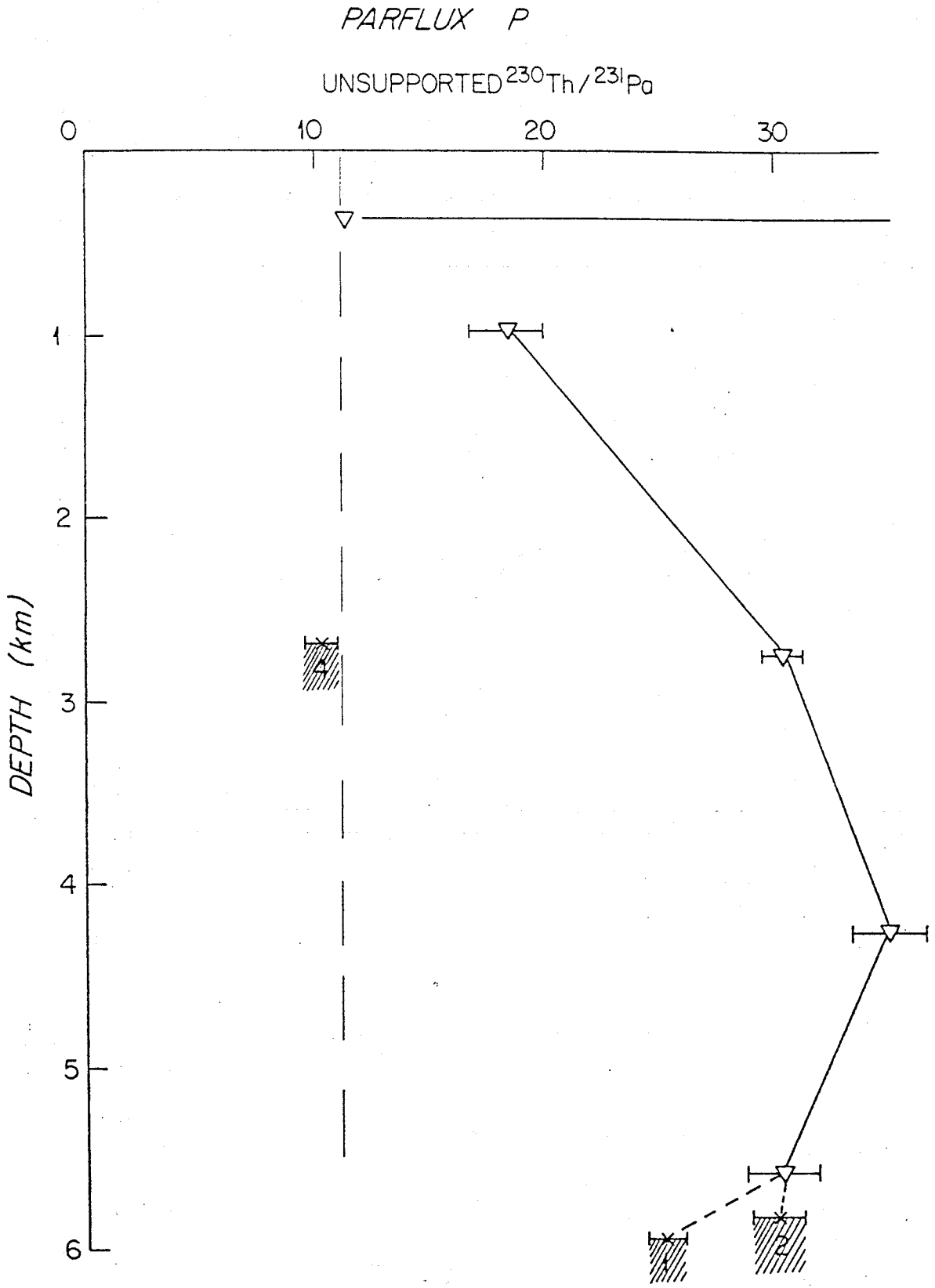


Figure 3-6. Unsupported  $^{230}\text{Th}/^{231}\text{Pa}$  activity ratios in sediment trap samples from Site P and KKI Cores 1, 2, and 4. The vertical dashed line indicates the ratio at which Th and Pa are produced by uranium decay. Hatched areas represent water depths.

Figure 3-6.



to produce ratios of 35 (Site P-4280 m trap) or 40-50 (Site E, filtered particles). Therefore, processes fractionating Th and Pa are not of sedimentary origin, but must be occurring in the water column. Settling particulate matter preferentially scavenges Th relative to Pa from seawater in open ocean environments.

Activity ratios in surface sediments of three box cores taken in association with Site P are also shown in Figure 3-6. Core 1 was taken approximately 180 km southwest of Site P and represents recent sediment accumulation in the area. Core 2 was taken within a few kilometers of the sediment trap site. Sediments in both cores contained unsupported  $^{230}\text{Th}$  and  $^{231}\text{Pa}$  at a ratio consistent with a source by settling particles like those collected with the sediment traps. Although Core 2 may have been taken in exposed Tertiary sediments, as previously mentioned, it contained measurable amounts of unsupported  $^{230}\text{Th}$  and  $^{231}\text{Pa}$  in a ratio identical to that found in the deepest trap. If erosion ceased at the end of the last glaciation (Johnson, 1972) and if the sedimentation rate is less than  $1 \text{ mm}/10^3 \text{ yr}$ , then perhaps only one cm of recent sediment has accumulated since erosion ceased. Bioturbation to a depth of approximately 10 cm would disperse recently accumulated material within a much greater volume of old sediment, producing the low unsupported  $^{230}\text{Th}$  and  $^{231}\text{Pa}$  activities. The  $^{230}\text{Th}/^{231}\text{Pa}$  ratio would not have changed much from that in the sediment trap samples if renewed sedimentation had only occurred for a few thousand years. Alternatively, there may be no net accumulation of sediment even today, in which case unsupported  $^{230}\text{Th}$  and  $^{231}\text{Pa}$  present in the sediment would have been adsorbed directly from seawater by surface sediments. Unsupported  $^{230}\text{Th}/^{231}\text{Pa}$  ratios in KKI Core 4 were much lower than in Cores 1 and 2 and will be discussed later.

Regeneration of Thorium-230 and Protactinium-231

Specific activities of uranium isotopes,  $^{232}\text{Th}$ ,  $^{230}\text{Th}$  and  $^{231}\text{Pa}$  were lower in trapped particles than in surface sediments at Sites E and P (Tables 3-1 and 3-3). Higher specific activities of  $^{230}\text{Th}$  and  $^{231}\text{Pa}$  in the sediments indicates that either most of the Th and Pa are scavenged by the refractory fraction of the trapped material, or part of the Th and Pa scavenged by biogenic particles remains with the detrital material as the biogenic particles are remineralized. However, the excess  $^{230}\text{Th}/^{232}\text{Th}$  ratio was 2.6 and 2.5 times greater in the deepest trap sample than in sediments at Sites E and P respectively. If the decrease is due to radioactive decay of excess  $^{230}\text{Th}$ , the calculated age of the sediment is 105,000 years. The excess  $^{230}\text{Th}/^{231}\text{Pa}$  ratio increased only slightly, if at all, between the 5086 m trap sample and the sediments at Site E and may have actually decreased between the 5582 m trap sample and the sediments at Site P, contradicting the sediment age calculated from the change in the excess  $^{230}\text{Th}/^{232}\text{Th}$  ratio.

Filtered particles had an excess  $^{230}\text{Th}/^{232}\text{Th}$  ratio 5.5 times greater than surface sediments at Site E. If the lower ratio in sediments is due to radioactive decay of excess  $^{230}\text{Th}$ , the calculated age of the sediments is 185,000 years, and there should be little or no excess  $^{231}\text{Pa}$  remaining in the sediments. However, the excess  $^{230}\text{Th}/^{231}\text{Pa}$  ratio was lower in surface sediments than in particles filtered in the overlying water column. These changes in isotope ratios between suspended particles and sediments clearly cannot be explained by radioactive decay.

Thorium-230 and  $^{231}\text{Pa}$  are probably adsorbed to the surfaces of all types of particles whereas  $^{232}\text{Th}$  is associated with detrital minerals



(see discussion below). Two processes could be responsible for lower  $^{230}\text{Th}/^{232}\text{Th}$  and  $^{231}\text{Pa}/^{232}\text{Th}$  ratios in surface sediments compared to sediment trap samples. First, if the flux of detrital minerals, the carrier of  $^{232}\text{Th}$ , is today only 40% of the average flux during the late Quaternary, and if  $^{230}\text{Th}$  and  $^{231}\text{Pa}$  are removed from seawater at the same rate regardless of the flux of detrital minerals, then the higher ratios in trapped particles may simply result from the present lower flux of  $^{232}\text{Th}$ . Alternatively, since sediments at Sites P and E contain negligible amounts of biogenic material compared to the sediment-trap samples, some of the  $^{230}\text{Th}$  and  $^{231}\text{Pa}$  scavenged by suspended material may be regenerated with the labile biogenic particles, resulting in lower excess  $^{230}\text{Th}/^{232}\text{Th}$  and excess  $^{231}\text{Pa}/^{232}\text{Th}$  ratios in the sediments.

While the former possibility cannot be disproven, the latter is chosen on the basis of two recent studies. Bowen et al. (1980) found an increase in plutonium concentration near the sea floor at several stations in the North Pacific. After a careful consideration of circulation patterns, they concluded that the concentration maximum at the bottom did not result from sinking of shallow water with higher plutonium contents. Rather, the plutonium must have been released during remineralization of biogenic particles at the sea floor which had scavenged the plutonium from seawater at shallower depths.

Nozaki (in preparation) has recently measured a profile of  $^{230}\text{Th}$  concentrations at a station in the central north Pacific. The concentration increased with depth from 1000 m to the sea floor (about 5500 m) with a gradient of  $3-5 \times 10^{-9}$  dpm  $^{230}\text{Th}/1\text{-cm}$ . A flux of  $^{230}\text{Th}$ ,  $F_{\text{Th}}$ , away from the sea floor can be calculated

$$F_{Th} = K_z (dA_{Th} / dz) \quad (3)$$

where  $K_z$  is the apparent vertical eddy diffusivity near the sea floor and  $A_{Th}$  is the concentration of  $^{230}Th$ , and  $z$  is the depth.

$K_z$  has been determined from  $^{222}Rn$  profiles at several locations (Sarmiento et al., 1976), and of the stations at which  $K_z$  was measured, the one closest to the site studied by Nozaki had a  $K_z$  of  $45 \text{ cm}^2/\text{sec}$ . The apparent vertical eddy diffusivity is largely determined by mixing along isopycnals (Sarmiento and Rooth, 1980). Since the flux of regenerated  $^{230}Th$  away from the sediment-seawater interface is to be calculated,  $K_z$  is the appropriate parameter to use. It is of no consequence whether mixing away from the sea floor occurs along or across isopycnals.

It is estimated from the decrease in the  $^{230}Th/^{232}Th$  ratio between trapped particles and surface sediments at Sites E and P that about 60% of the scavenged  $^{230}Th$  is regenerated.  $F_{Th}$  calculated from equation (3) with the data of Nozaki is  $4.3-7.0 \text{ dpm/cm}^2-10^3$  years, which is 30-50% of the rate of production of  $^{230}Th$  by uranium decay in a 5500 m water column. Other factors may also be involved.  $K_z$  varies from site to site (Sarmiento et al., 1976), so the calculated  $F_{Th}$  is only as good as the approximation of  $K_z$ .  $F_{Th}$  should be compared with the rate of delivery of  $^{230}Th$  to the sea floor by settling particles rather than its rate of production by uranium decay. Part of the  $^{230}Th$  produced by uranium decay at the site where the  $^{230}Th$  profile was measured may be removed from the water column by horizontal mixing processes (see discussion below) without ever having been scavenged by particles, in which case  $F_{Th}$  would be more than 30-50% of the rate of delivery of particulate  $^{230}Th$  to the sea floor. These uncertainties are of minor importance. The concentration gradient measured by Nozaki is consistent with regeneration at the sea floor

of a large portion of the  $^{230}\text{Th}$  delivered by settling particles.

Sarmiento et al. (1976) showed that  $K_z$  decreases by an order of magnitude or more above the bottom mixed layer. The nearly linear  $dA_{\text{Th}}/dz$  measured by Nozaki (in preparation) throughout the water column implies that the vertical flux of  $^{230}\text{Th}$  also decreases by an order of magnitude, and consequently there must be a sink for  $^{230}\text{Th}$  at the upper boundary of the mixed layer. It is difficult to reconcile such a sink with present understanding of scavenging processes. A detailed study of near-bottom  $^{230}\text{Th}$  concentration gradients coupled with measurements of mixing rates from  $^{222}\text{Rn}$  distributions will be required to accurately assess the magnitude of the flux of  $^{230}\text{Th}$  away from the sea floor.

Unsupported  $^{230}\text{Th}/^{231}\text{Pa}$  ratios were nearly the same in the deepest trap sample and in surface sediment at Sites E and P while filtered particles<sup>1</sup> had a higher excess  $^{230}\text{Th}/^{231}\text{Pa}$  ratio than the underlying sediments at Site E (Figures 3-5 and 3-6). Therefore, if sediments are formed almost entirely by particles similar to those collected by the sediment traps, then  $^{230}\text{Th}$  and  $^{231}\text{Pa}$  are regenerated with equal efficiency. Alternatively, if particles similar to those sampled by in situ filtration form a significant portion of the accumulating sediments, then  $^{230}\text{Th}$  must be preferentially regenerated relative to Pa.

---

(1) The  $^{230}\text{Th}/^{231}\text{Pa}$  and  $^{230}\text{Th}/^{232}\text{Th}$  ratios in filtered particles may actually be biased too low. Site E was reoccupied as the last station of R/V Oceanus, Cruise 78-1 and the only remaining, functioning pressure switch was activated at a water depth of 1000m. Therefore, seawater was pumped through the filters between 1000m and the indicated depth of the sample. The pump was raised and lowered at 50 m/min and pumped at depth for 10 hours so that most of each sample was collected at the indicated depth. Particles filtered at 975 m and 1400m had lower  $x_s^{230}\text{Th}/x_s^{231}\text{Pa}$  and  $x_s^{230}\text{Th}/x_s^{232}\text{Th}$  ratios than particles filtered at 3600 m and 5000 m. Thus contamination of the deep samples by particles sampled at shallower depths would tend to reduce the true difference between filtered particles and sediments.

### Efficiency of Scavenging by Settling Particles

Particles obtained with sediment traps clearly scavenge thorium and protactinium from seawater. An estimate of the efficiency of removal of  $^{230}\text{Th}$  and  $^{231}\text{Pa}$  by these particles can be made by comparing their fluxes into sediment traps with their production rates in overlying seawater. In every case, fluxes of unsupported  $^{230}\text{Th}$  and  $^{231}\text{Pa}$  were less than their rates of production (Figures 3-7 and 3-8). Variable undertrapping of the true flux of particles could have been responsible, in part, for the low fluxes of  $^{230}\text{Th}$  and  $^{231}\text{Pa}$ . However, if the total particle flux into each trap is scaled up until the flux of  $^{230}\text{Th}$  exactly equals its production, the scaled-up  $^{231}\text{Pa}$  flux into the deeper traps at all three sites is still less than 50% of its rate of production in overlying seawater (Table 3-6). High  $^{230}\text{Th}/^{231}\text{Pa}$  ratios in the filtered particles at Site E reveal that protactinium is not preferentially adsorbed to small particles which might be less efficiently collected by the sediment traps. Protactinium that is not removed by the vertical flux of particles must be removed from seawater by another process, since radioactive decay in the water column is insignificant relative to its rate of production (Chapter 4).

### Horizontal Transport of Thorium-230 and Protactinium-231

Bacon et al. (1976) showed that  $^{210}\text{Pb}/^{226}\text{Ra}$  disequilibria in seawater decrease with distance, both vertically and horizontally, from the sediment-seawater interface. They concluded that mixing of dissolved  $^{210}\text{Pb}$  to ocean basin margins, with subsequent scavenging at the sediment-seawater interface, is an important process removing  $^{210}\text{Pb}$  from the deep ocean. Similar processes appear to be affecting  $^{230}\text{Th}$  and  $^{231}\text{Pa}$ .

Figure 3-7. Flux of unsupported  $^{230}\text{Th}$  in the less than 1-mm size fraction of particles collected at Sites S<sub>2</sub>, E, and P. The solid line is the rate at which  $^{230}\text{Th}$  is produced in overlying seawater by uranium decay. Error bars indicate one standard deviation counting statistics. Where error bars are not drawn, the size of the symbol approximately indicates the counting error.

Figure 3-7

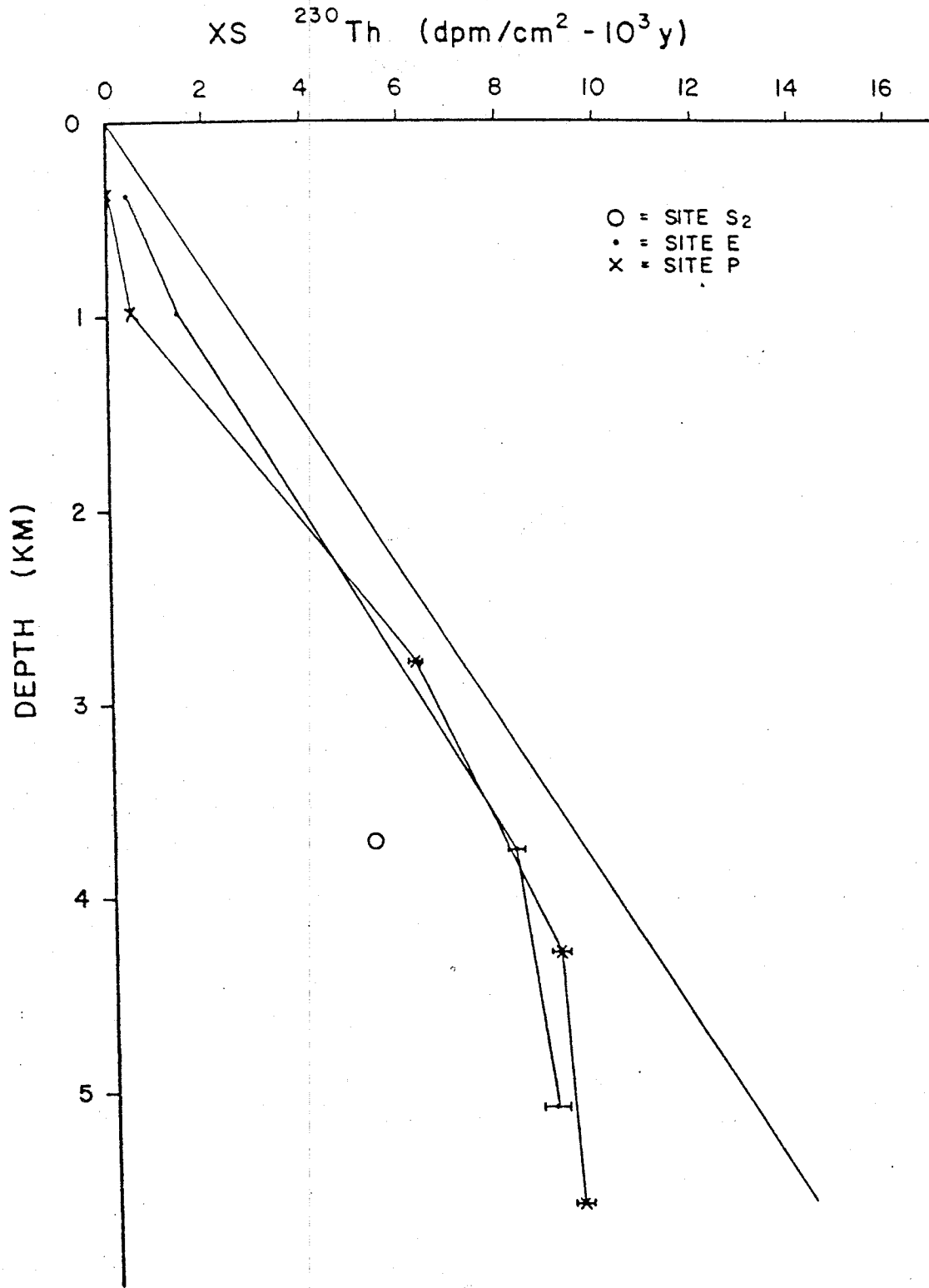


Figure 3-8. Flux of unsupported  $^{231}\text{Pa}$  in the less than 1-mm size fraction of particles collected at Sites S<sub>2</sub>, E, and P. The solid line is the rate at which  $^{231}\text{Pa}$  is produced in overlying seawater by uranium decay. Error bars indicate one standard deviation counting statistics. Where error bars are not drawn, the size of the symbol approximately indicates the counting error.

Figure 3-8.

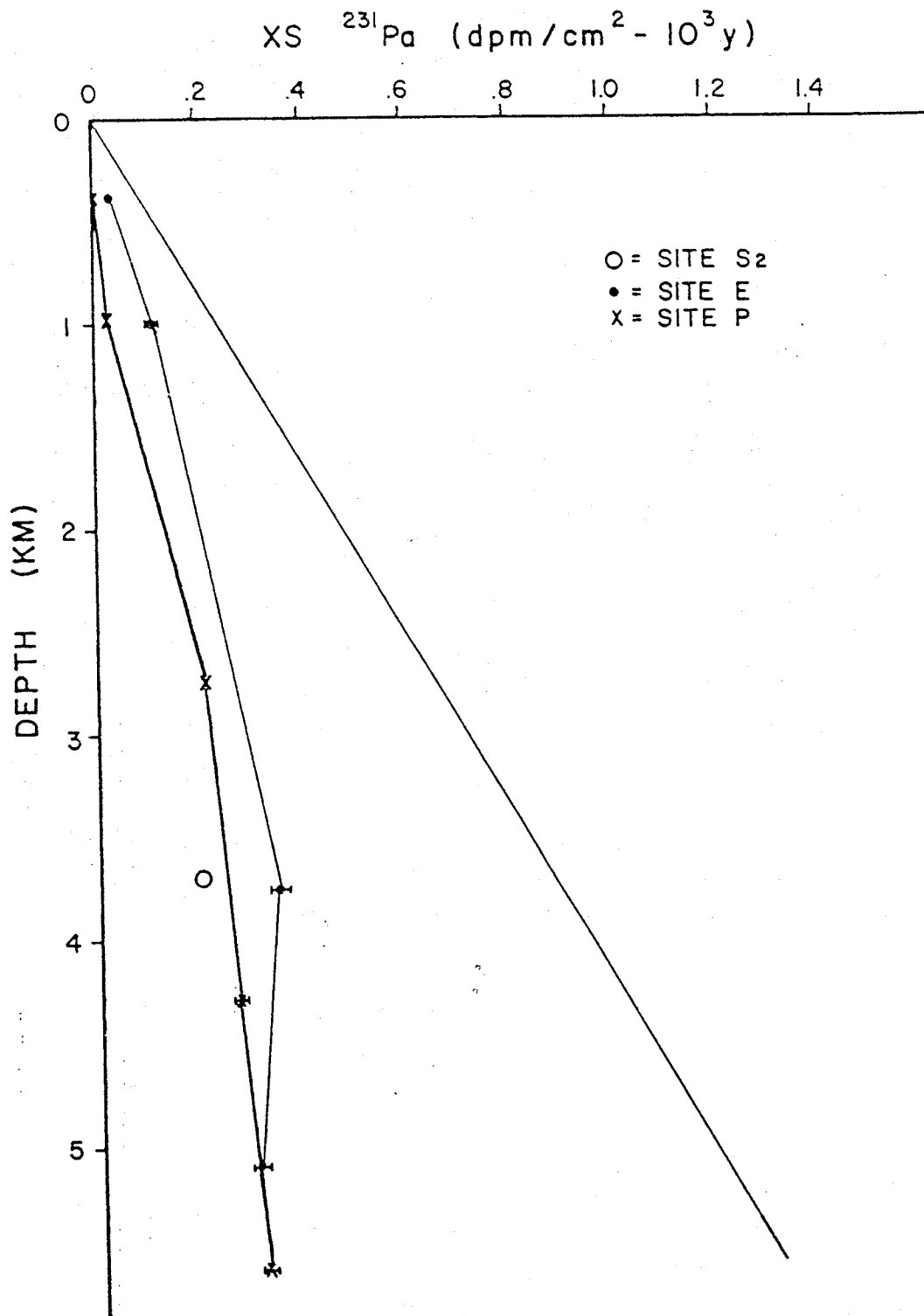




TABLE 3-6  
Scaled  $x_s^{231}\text{Pa}$  Deficiency<sup>a</sup>.

<u>Atlantic</u>		<u>Pacific</u>	
Sample	Deficiency (% of Production)	Sample	Deficiency (% of Production)
Site S <sub>2</sub> , 3694 m	61	Site P, 378 m	ND <sup>b</sup>
Site E, 389 m	9	Site P, 978 m	40
Site E, 988 m	12	Site P, 2778 m	64
Site E, 3755 m	50	Site P, 4280 m	69
Site E, 5086 m	63	Site P, 5582 m	64

<sup>a</sup>The deficiency is calculated as:

$$\left[ 1 - \left( \frac{{}^{230}\text{Th Production}}{x_s {}^{230}\text{Th Flux}} \right) \left( \frac{x_s {}^{231}\text{Pa Flux}}{{}^{231}\text{Pa Production}} \right) \right] \times 100$$

<sup>b</sup>Not Determinable.

Approximate limits can be set for the relative importance of scavenging onto settling particles and horizontal mixing as mechanisms removing Th and Pa from seawater. One limit is set by assuming that sediment traps are 100% effective at trapping the true vertical flux of particles. Another limit is set by assuming that  $^{230}\text{Th}$  is completely removed from seawater by settling particles, and that the low flux to production ratios in Figure 3-7 are a result of undertrapping the true flux of particles. The relative importance of vertical and horizontal removal of  $^{230}\text{Th}$  and  $^{231}\text{Pa}$  at these two extremes is presented in Table 3-7. Removal attributed to horizontal processes is simply the production rate of the isotope less its measured or calculated flux into the sediment traps. The horizontal flux of  $^{231}\text{Pa}$  in the  $^{230}\text{Th}$ -normalized model is then equal to the scaled Pa deficiency in Table 3-6.

Three points can be made from the above discussion. First, at these sediment trap sites, horizontal mixing and scavenging to particles remove roughly equal amounts of the  $^{231}\text{Pa}$  produced by uranium decay at Sites S<sub>2</sub>, E, and P. Second, because of the preferential adsorption of Th by particles, horizontal mixing is less effective at redistributing  $^{230}\text{Th}$  than  $^{231}\text{Pa}$ . Third, if sediment traps overtrap the true flux of particles, then thorium and protactinium are removed by horizontal mixing to a greater extent than predicted by the two models in Table 3-7.

It has been assumed in models in the literature (Krishnaswami et al., 1976; Brewer et al., 1980) that the rate of scavenging of reactive radioisotopes onto settling particles can be approximated by their rates of production by decay of their radioactive parents. Horizontal mixing accounts for over half of the removal of  $^{231}\text{Pa}$  in the open ocean, and

TABLE 3-7

Relative Importance of Vertical and Horizontal Removal Processes.

	Vertical (%) <sup>a</sup>	Horizontal (%) <sup>b</sup>
<u>100% Trap Efficiency Model</u>		
<u>Sites S<sub>2</sub> and E</u>		
<sup>230</sup> Th	47-86	14-53
<sup>231</sup> Pa	20-50	50-80
<u>Site P</u>		
<sup>230</sup> Th	6-87 (67-87) <sup>a</sup>	13-96 (13-33) <sup>c</sup>
<sup>231</sup> Pa	12-31 (24-31) <sup>a</sup>	69-88 (69-76) <sup>c</sup>
<u><sup>230</sup>Th-Normalized Model</u>		
<u>Sites S<sub>2</sub> and E</u>		
<sup>230</sup> Th	100	0
<sup>231</sup> Pa	36-92	8-64
<u>Site P</u>		
<sup>230</sup> Th	100	0
<sup>231</sup> Pa	30-60	40-70

<sup>a</sup>By scavenging to settling particles.

<sup>b</sup>By horizontal mixing down concentration gradients.

<sup>c</sup>Three deepest traps.

conversely, represents a source of  $^{230}\text{Th}$  and  $^{231}\text{Pa}$  to environments which act as sinks for horizontally transported elements. Therefore, the above approximation is in error by more than a factor of two for Pa, and may be generally inaccurate.

#### Consequences for Calculated Sediment-Trap Trapping Efficiencies

Brewer et al. (1980) calculated trapping efficiencies of the sediment traps at Sites  $S_2$  and E from the measured  $^{230}\text{Th}$  flux into each trap as

$$TE = F_{\text{Th}} / P_{\text{Th}} \quad (4)$$

where TE is the trapping efficiency,  $F_{\text{Th}}$  is the measured flux of excess  $^{230}\text{Th}$ , and  $P_{\text{Th}}$  is integrated rate of production of  $^{230}\text{Th}$  by uranium decay in the water column above the trap. It is assumed in the use of Equation (4) that all of the  $^{230}\text{Th}$  produced by uranium decay is scavenged locally by settling particles, and that production by uranium decay is the only source of  $^{230}\text{Th}$ .

A more accurate representation of TE would be

$$TE' = F_{\text{Th}} / S_{\text{Th}} \quad (5)$$

where  $S_{\text{Th}}$  is the integrated rate of adsorption of  $^{230}\text{Th}$  to settling particles in the water column above the trap. Horizontal mixing may act locally as a source or a sink for  $^{230}\text{Th}$  and the upward flux of  $^{230}\text{Th}$  regenerated at the sea floor also acts as a source of  $^{230}\text{Th}$ .

Horizontal mixing probably acts as a sink for  $^{230}\text{Th}$  at Sites  $S_2$  and E as it does for  $^{231}\text{Pa}$ . If the flux of regenerated  $^{230}\text{Th}$  is negligible at these sites, then  $S_{\text{Th}} < P_{\text{Th}}$  and TE' will be underestimated by an amount equal to the percent of the  $^{230}\text{Th}$  production that is removed by horizontal mixing (Table 3-7).

The magnitude of the upward flux of regenerated  $^{230}\text{Th}$  at Sites  $S_2$  and E is unknown, but a reasonable limit of its effect on the calculated

trapping efficiency can be set. If horizontal transport of  $^{230}\text{Th}$  is assumed to be negligible, if 60% of the flux of particulate  $^{230}\text{Th}$  is regenerated ( $^{230}\text{Th}/^{232}\text{Th}$  in surface sediments is 40% of the ratio in the deepest sediment trap sample), and if regenerated  $^{230}\text{Th}$  is rescavenged equally throughout the water column, then  $S_{\text{Th}} = 1.6 P_{\text{Th}}$ , and the trapping efficiency is overestimated by  $TE = 1.6 TE'$ .

The above two sources of error have counteracting effects on the estimated trapping efficiency at Sites  $S_2$  and E and may be of similar magnitude. Quantification of these fluxes of  $^{230}\text{Th}$  will allow more accurate estimates of trapping efficiencies to be made from measured fluxes of particulate  $^{230}\text{Th}$ .

#### Locations of Sinks for Horizontally Transported Elements

If more than half of the Pa produced in the deep ocean is removed by horizontal mixing, then some environments must exist where: 1) the rate of incorporation of Pa into sediments is greater than its rate of production in the overlying water column, and 2) the excess  $^{230}\text{Th}/^{231}\text{Pa}$  ratio is less than 10.8. KKI Core 4, taken near Site P is one example of such an environment. Specific activities of  $^{230}\text{Th}$  and  $^{231}\text{Pa}$  were constant to a depth of 20 cm (Table 3-3), which was the maximum depth of core penetration. If the constant activities are not a result of bioturbation or some other sediment mixing process, then a minimum sedimentation rate of  $3 \text{ cm}/10^3 \text{ yr}$  is derived from the excess  $^{231}\text{Pa}$  distribution. Activities of  $^{210}\text{Pb}$  measured in three samples (Table 3-3) show an excess of  $^{210}\text{Pb}$  with respect to  $^{230}\text{Th}$  at the surface, a deficiency at 10-15 cm, and equilibrium at 19-21 cm. This reflects an input of excess  $^{210}\text{Pb}$  at the surface, a  $^{226}\text{Ra}$  deficiency deeper in the core, and finally radioactive equilibrium of  $^{230}\text{Th}$

daughters at 20 cm, similar to cores studied by Cochran (1979). Therefore, bioturbation is not active below 10 cm, and the constant  $^{230}\text{Th}$  and  $^{231}\text{Pa}$  activities result from rapid sediment accumulation.

Fluxes of  $^{230}\text{Th}$  and  $^{231}\text{Pa}$  into Core 4 are at least four times their rates of production in the overlying seawater given the above estimate for the sedimentation rate. Even if the sedimentation rate is overestimated by a factor of two because of bioturbation above 10 cm, the fluxes of  $^{230}\text{Th}$  and  $^{231}\text{Pa}$  are greater than their rates of production. Therefore, the first criterion above for a sink for horizontally transported Th and Pa is satisfied. However, the second, that the excess  $^{230}\text{Th}/^{231}\text{Pa}$  ratio must be less than 10.8 is only partially fulfilled. The ratio in Core 4 is about 10, much less than in typical deep-sea sediments such as KKI Cores 1 and 2, but these sediments do not provide a preferential sink for Pa relative to Th.

A situation similar to that observed in Core 4 has been reported for two cores from the FAMOUS area on the mid-Atlantic ridge (Cochran, 1979) where nearly constant  $^{230}\text{Th}$  and  $^{231}\text{Pa}$  activities were found to a depth of at least 20 cm. Fluxes of  $^{230}\text{Th}$  and  $^{231}\text{Pa}$  into the sediments were greater than their rates of production in the overlying seawater, while the excess  $^{230}\text{Th}/^{231}\text{Pa}$  ratio ranged from 4-8. Thus both criteria for a sink for horizontally transported Th and Pa were satisfied.

An extreme example of one of these sinks was found in the area of rapidly accumulating siliceous oozes in the Antarctic (DeMaster, 1979). Sediment inventories of unsupported  $^{230}\text{Th}$  and  $^{231}\text{Pa}$  were up to six and fourteen times their respective production rates in overlying seawater. Activity ratios as low as three were found, and ratios less

than eleven occurred as deep as 15 m in some of the cores studied. DeMaster (1979) also studied a core from the Argentine Basin where sediments contained an excess  $^{230}\text{Th}/^{231}\text{Pa}$  ratio of about 10 to a depth of 500 cm. The sedimentation rate could not be unambiguously determined from the  $^{230}\text{Th}$  and  $^{231}\text{Pa}$  distributions, but it was very high, and  $^{230}\text{Th}$  and  $^{231}\text{Pa}$  are accumulating in these sediments at rates much greater than their rates of production by uranium decay in the overlying water column.

A final example was found in the Panama Basin (Chapter 5). Fluxes of  $^{230}\text{Th}$  and  $^{231}\text{Pa}$  into sediment traps identical to those used at Sites S<sub>2</sub>, E, and P were greater than their rates of production in overlying seawater, and  $^{230}\text{Th}/^{231}\text{Pa}$  ratios in filtered and trapped particles as low as 3-5 were observed.

One factor common to all of the areas described above where low  $^{230}\text{Th}/^{231}\text{Pa}$  ratios (less than 10.8) have been found in sediments and suspended particles is that  $^{230}\text{Th}$  and  $^{231}\text{Pa}$  are both accumulating in sediments or in sediment traps at rates greater than their rates of production by uranium decay in the overlying water column. Therefore, areas where Th and Pa are scavenged at low ratios also act as sinks for Th and Pa transported horizontally from the open ocean. Scavenging rates must be greater in these areas than in the open ocean, setting up concentration gradients down which Th and Pa are transported by mixing processes.

#### Particulate $^{230}\text{Th}/^{231}\text{Pa}$ Ratios: The Effect of Scavenging Rate

Scavenging rates are much higher in surface waters than in the deep ocean. Residence times for  $^{234}\text{Th}$ ,  $^{228}\text{Th}$ , and  $^{210}\text{Pb}$  in the surface layer of the oceans are as low as a few months (Bhat et al., 1969;

Matsumoto, 1975; Bacon et al., 1976; Nozaki et al., 1976; Knauss et al., 1978; Li et al., 1979) where biological activity results in the incorporation of reactive elements into large, rapidly sinking fecal matter (Turekian et al., 1974; Cherry et al., 1975; Kharkar et al., 1976; Beasley et al., 1978; Bishop et al., 1977, 1978; K. Bruland, personal communication). Scavenging onto settling particles is probably the dominant process removing reactive elements like Th and Pa from surface seawater. Scavenging rates are too rapid to allow for redistribution by horizontal transport to be effective. If the sea surface acts as a closed system, with only one process removing Th and Pa, then the rates of removal of Th and Pa must equal their rates of production or input. Production by uranium decay is the only significant source of  $^{230}\text{Th}$  and  $^{231}\text{Pa}$  to surface seawater. Consequently, the average  $^{230}\text{Th}/^{231}\text{Pa}$  activity ratio in particles settling from the sea surface must correspond to the ratio at which they are produced by uranium decay, 10.8.

Samples were not obtained in the surface mixed layer at any of the sediment trap sites. However, this effect can be seen at Site E and to a lesser extent at Site P. In both cases, the  $^{230}\text{Th}/^{231}\text{Pa}$  ratio decreases towards the surface (Figures 3-4 and 3-5). At Site E, particulate ratios above 1500 m were within counting error of 10.8. Lower biological productivity at Site P may account for the lesser effect at that site.

Particles at the sea surface may fractionate Th and Pa to the same extent as particles in the deep ocean, where particulate  $^{230}\text{Th}/^{231}\text{Pa}$  ratios are approximately ten times greater than dissolved ratios (compare Table 3-1 with Table 4-3). If so, then the dissolved  $^{230}\text{Th}/^{231}\text{Pa}$  ratio in surface seawater must be about one. Dissolved ratios in surface



seawater have not been measured, but they should indicate whether or not fractionation occurs. In either case, when one mechanism dominates the removal of Th and Pa from a parcel of water, the ratio at which Th and Pa are removed must equal the ratio of their combined inputs. In surface seawater this ratio is 10.8.

In the deep ocean, horizontal transport may act as a source of dissolved Th and Pa at a ratio of 3-5 (Chapter 4). Therefore, in areas of the deep sea where scavenging onto particles is the only significant mechanism removing Th and Pa from the water column, the particulate  $^{230}\text{Th}/^{231}\text{Pa}$  ratios must be between 3-5 and 10.8, the ratios at which they are supplied by mixing and uranium decay respectively. However, increased scavenging rates alone cannot account for the low  $^{230}\text{Th}/^{231}\text{Pa}$  ratios in suspended particles in the Panama Basin (Chapter 5), and presumably in the other areas where low  $^{230}\text{Th}/^{231}\text{Pa}$  ratios have been found as well. Other factors affecting  $^{230}\text{Th}/^{231}\text{Pa}$  ratios in sediments and suspended particles will be discussed in more detail in Chapter 6.

#### Contributions to Trapped Material by Resuspended Sediments

In certain environments where intense bottom currents are present, sediment traps near the bottom have collected large amounts of resuspended sediments (Spencer et al., 1978; Richardson, 1980). Resuspended sediments in the trapped samples could be responsible for high  $^{230}\text{Th}/^{231}\text{Pa}$  ratios, regardless of the mechanism initially causing high ratios in sediments.

Several lines of evidence demonstrate that the observed  $^{230}\text{Th}/^{231}\text{Pa}$  ratios at sites E and P were not a result of incorporation of resuspended sediments. Concentrations of particulate

matter measured in Niskin bottle samples at Sites E and P (Figures 3-9 and 3-10) were low throughout the deep water, and although there was a slight increase near the bottom, values only reached 10  $\mu\text{g}/\text{kg}$ .

Particle fluxes were constant with depth at Site E and decreased with depth in the lower three traps at Site P (Table 3-1). Particle fluxes and concentrations would have increased near the bottom if there was a significant input of resuspended sediment.

Spencer et al. (1978) concluded that resuspended sediments constituted a large proportion of the material collected in a trap situated 214 m above the sea floor during the first occupation of Site S. Radioisotope results from Site S<sub>2</sub> samples support this conclusion. The  $^{228}\text{Th}/^{232}\text{Th}$  activity ratio in Site S<sub>2</sub> samples decreased dramatically from 82 at 3964m to 9 at 5206m because of dilution of the primary flux of particles with resuspended sediment lacking unsupported  $^{228}\text{Th}$ . If the  $^{228}\text{Th}/^{232}\text{Th}$  ratio was one in resuspended sediments at Site S<sub>2</sub>, and if the ratio in the primary flux of particles did not change between 3964 m and 5206 m, then about 90% of the  $^{232}\text{Th}$  in the 5206 m sample was resuspended from the bottom. As the ratio in the primary flux of particles probably increased near the bottom, as it did at the other sites, more than 90% of the  $^{232}\text{Th}$  was actually derived from resuspension. The proportion of the total trapped material derived from resuspension cannot be determined as the specific activities of the thorium isotopes in resuspended sediments are unknown and most of the S<sub>2</sub> 5206 m sample consisted of aluminum hydroxide. Contributions by resuspended sediments are not apparent at other sites where the  $^{228}\text{Th}/^{232}\text{Th}$  ratios increased near the bottom.

Figure 3-9. Concentration of particles at Site E.  
From Brewer et al. (1980).

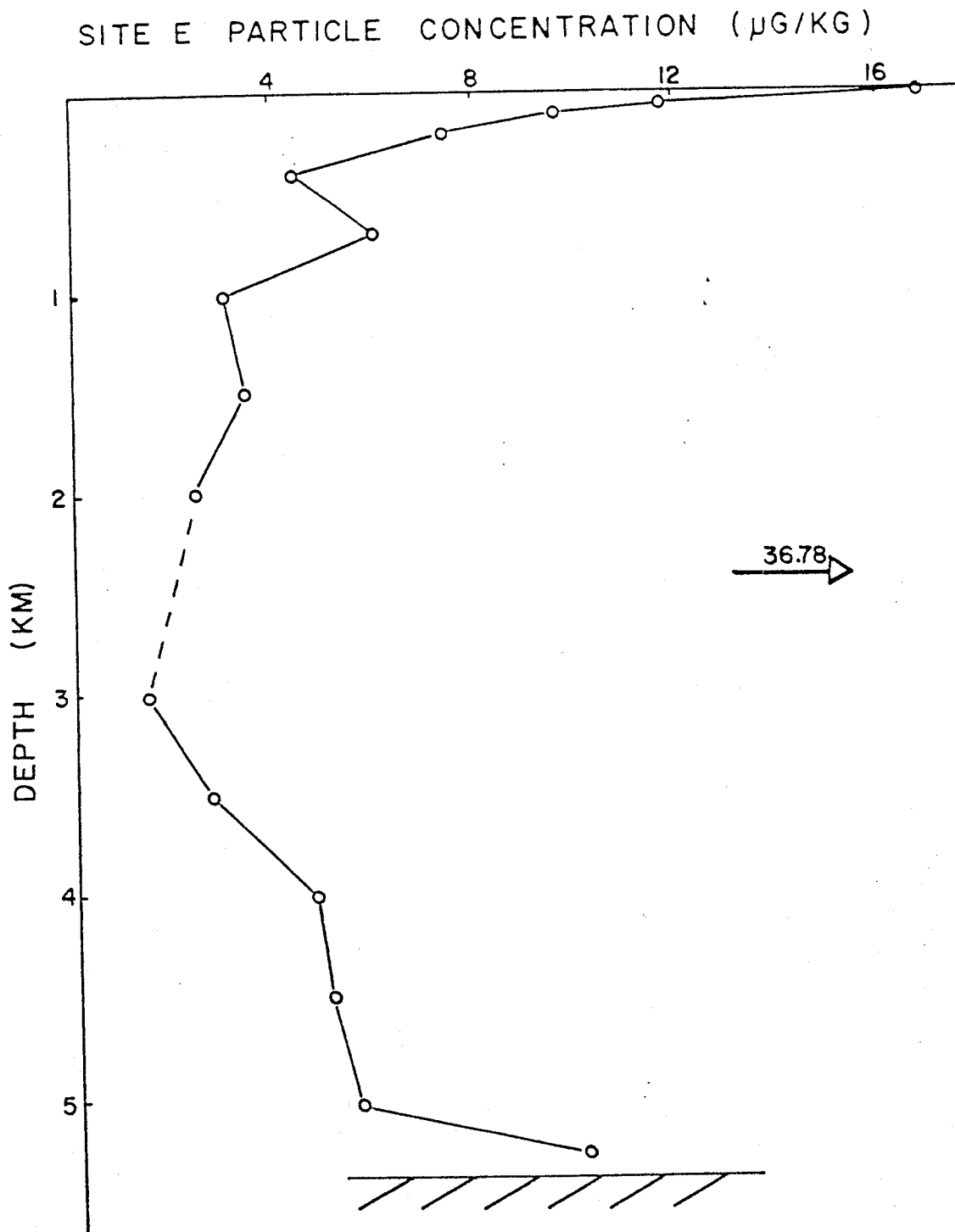
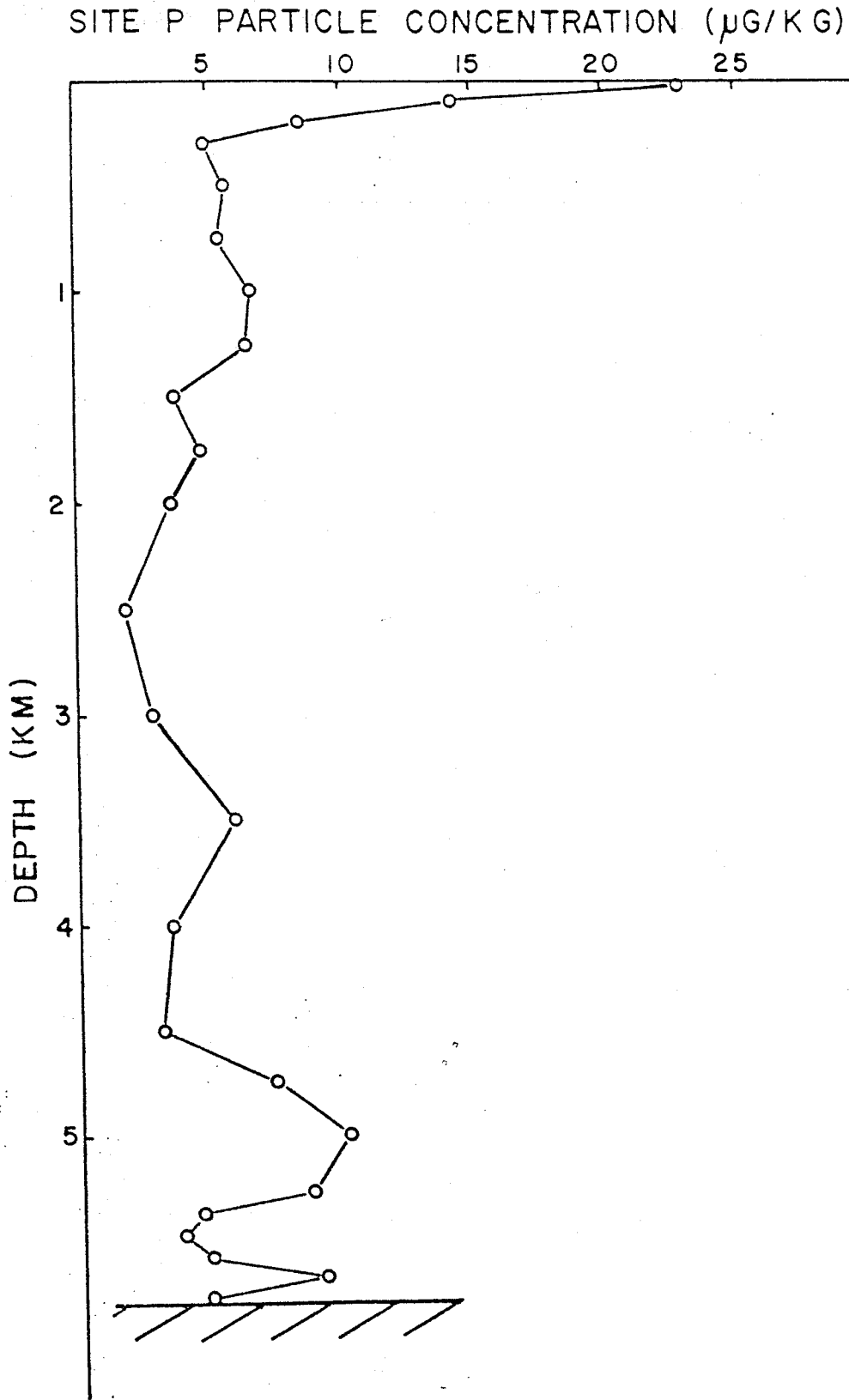


Figure 3-10. Concentration of particles at Site P.  
From Brewer et al. (in preparation).



Fluxes of detrital material increased with depth at Sites E and P (Honjo, 1980; Brewer et al., 1980, in preparation); however, detrital minerals constituted less than 10% of the total flux at Site P even in the deepest trap, so the portion of the total flux potentially derived by resuspension of surface sediments, which consist almost entirely of detrital minerals, would be negligible.

Concentrations of plutonium in deep-sea surface sediments are an order of magnitude lower in the Atlantic (Labeyrie et al., 1976) than in Site E samples, and two orders of magnitude lower in the Pacific (Bowen et al., 1976) than in Site P samples. Dilution of the primary flux of particles with resuspended sediments would have resulted in a decrease in plutonium concentrations with depth. However, plutonium concentrations were nearly constant in the deepest three trap samples at both sites, indicating that there was little, if any, contribution of resuspended sediments older than a few decades.

#### CHEMICAL BEHAVIOR OF OTHER ISOTOPES

##### Thorium-228

Many of the important aspects of the  $^{228}\text{Th}$  results have already been discussed. Concentrations of  $^{228}\text{Th}$  in sediment-trap samples are consistent with its source by decay of  $^{228}\text{Ra}$  in surface seawater and near the sea floor. The  $^{228}\text{Th}$  results were also used as evidence that most of the particles collected by sediment traps settle rapidly from the sea surface.

Particles collected with the sediment trap at 3755 m at Site E contained a  $^{228}\text{Th}/^{230}\text{Th}$  activity ratio of 2.9 while particles filtered at 3600 m at Site E contained a ratio of 1.1 (Tables 3-1 and 3-2). This is consistent with the source of the Th scavenged by the two samples of

particles. Trapped particles have settled rapidly from the sea surface where waters typically contain high  $^{228}\text{Th}/^{230}\text{Th}$  ratios (Knauss et al., 1978; Bacon, unpublished data) whereas smaller filtered particles have probably been at mid-depth (3600 m) where concentrations of  $^{228}\text{Ra}$ , the source of  $^{228}\text{Th}$ , are very low. Thus, filtered particles more accurately represent the ratio at which  $^{228}\text{Th}$  and  $^{230}\text{Th}$  are scavenged at 3600-3755 m than trapped particles.

Disaggregation of trapped particles at mid-depth would act as a source of particulate Th with a  $^{228}\text{Th}/^{230}\text{Th}$  ratio greater than would be expected if the particles had simply scavenged dissolved Th at the mid-depth dissolved  $^{228}\text{Th}/^{230}\text{Th}$  ratio. If adsorption of Th is a reversible process (see Chapter 5), then particles settling from the sea surface would act as a source of dissolved  $^{228}\text{Th}$  at mid-depths. Since Ra is not significantly scavenged by particles, an equivalent source of  $^{228}\text{Ra}$  from settling particles would not exist. Dissolved  $^{228}\text{Th}/^{228}\text{Ra}$  ratios greater than one at mid-depth would provide convincing evidence for the reversibility of thorium scavenging. Unfortunately, mid-depth dissolved  $^{228}\text{Th}/^{228}\text{Ra}$  ratios have yet to be measured.

#### Thorium-232

Specific activities of  $^{232}\text{Th}$  increased with depth at Sites E and P. Detrital components of trapped material also increased with depth at both sites, and detrital elements were present at constant ratios in all of the sediment trap samples at Site E (Brewer et al., 1980). Correlations of  $^{232}\text{Th}$  with Al and K in sediment trap samples are shown in Figures 3-11 and 3-12, and indicate an average shale-like rock as the source of the detrital minerals. Sediments from Ch 75-2 and atmospheric dust sampled at Barbados (Rydell and Prospero, 1972) follow the same Th/Al and Th/K

Figure 3-11. Correlation between  $^{232}\text{Th}$  and Al in sediment trap samples, sediments, and atmospheric dust (Rydell and Prospero, 1972) at or near Site E. Solid lines represent average ratios for crust (C), shale (S), basalt (B), and granite (G) from Krauskopf (1979).

Figure 3-11.

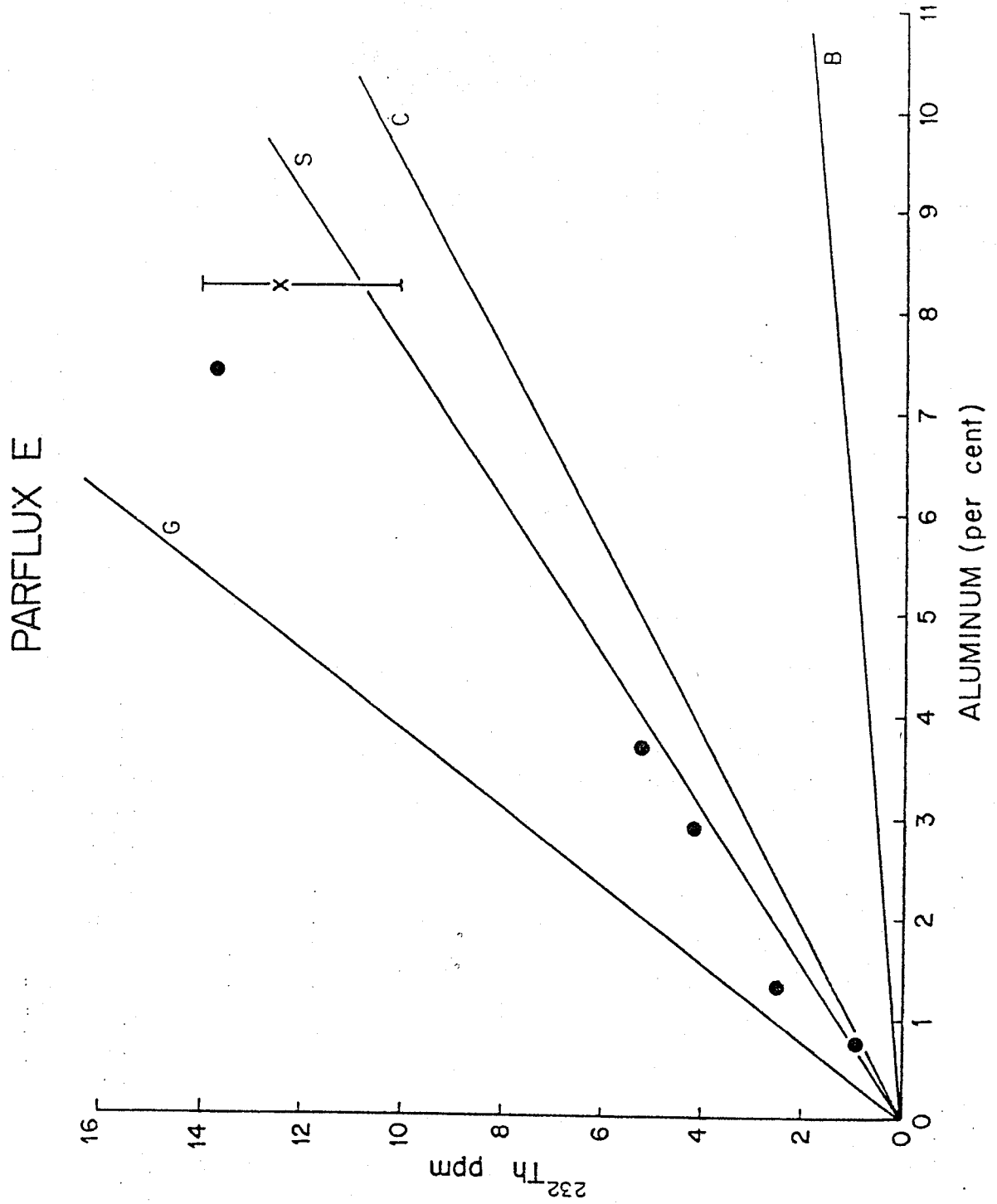
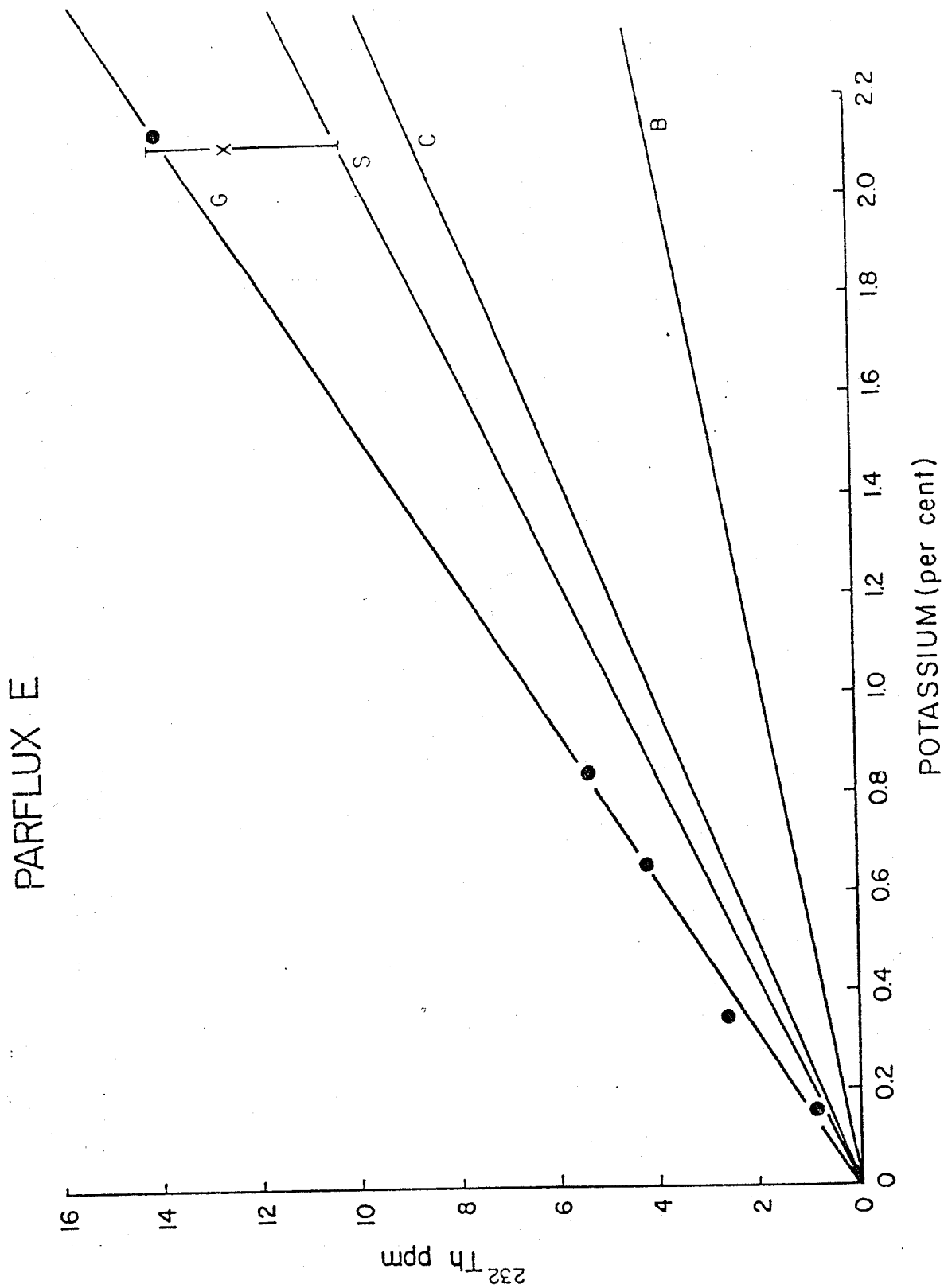




Figure 3-12. Correlation between  $^{232}\text{Th}$  and  $\text{K}$  in sediment trap samples, sediments, and atmospheric dust (Rydell and Prospero, 1972) at or near Site E. Solid lines represent average ratios for crust (C), shale (S), basalt (B), and granite (G) from Krauskopf (1979).

Figure 3-12.



correlations (Figures 3-11 and 3-12). The similarity in composition suggests that atmospheric transport of Saharan Dust, which also has a shale-like composition (Glaccum and Prospero, 1980), is an important source of the detrital material sampled at Site E. Furthermore, the increase in the  $^{232}\text{Th}$  content of trapped material with depth was simply a result of the increasing abundance of detrital minerals, and it is not necessary to postulate scavenging of dissolved  $^{232}\text{Th}$  from seawater.

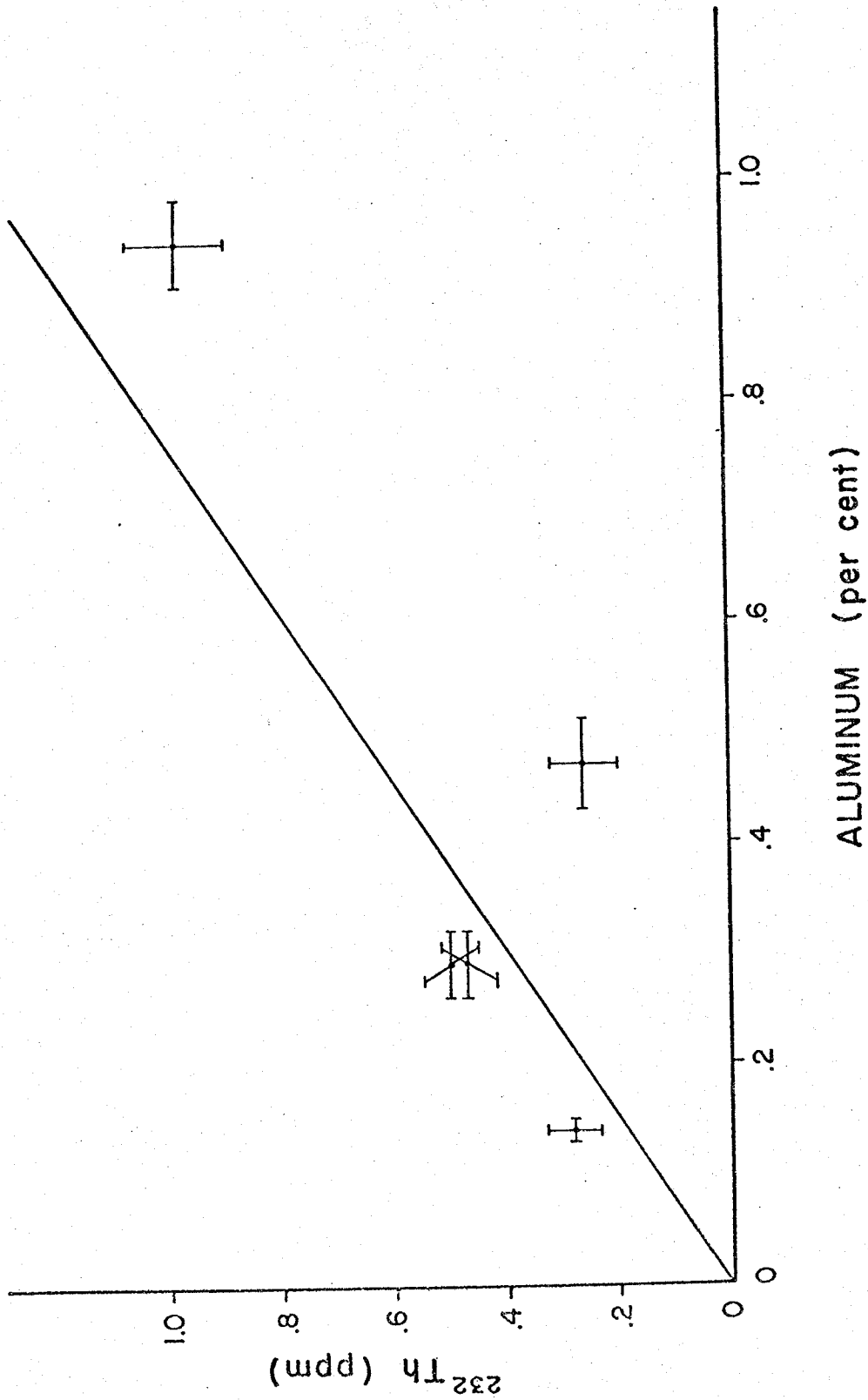
With the exception of the shallowest sample at Site P, the Th/Al ratio is similar to that at Site E (Figure 3-13), with a composition consistent with average crustal rocks or shales as a source. However, the correlation is not as good as at Site E. Brewer et al. (in preparation) found that the correlation among other detrital elements at Site P was likewise not as good as at Site E. If horizontal transport influences the distribution of detrital particles at Site P, then the variable composition of the detrital elements may indicate that detrital particles are transported from different sources, i.e. from different directions, at different depths.

#### Uranium

Uranium concentrations in trapped particles were nearly constant with depth, with the exception of samples S<sub>2</sub>-5206 m and P-378 m. Uranium in the S<sub>2</sub>-5206 m sample was scavenged from seawater by the aluminum hydroxide precipitate, which could not be separated from normal sediment. The P-378 m sample may have become anoxic from decomposition of organic material before processing (A. Fleer, personal communication). Uranium would then have been reduced from the (VI) to the (IV) valence state and scavenged by trapped material. There was

Figure 3-13. Correlation between  $^{232}\text{Th}$  and Al in sediment trap samples from Site P. Solid line is the slope through the points at Site E. Note change of scale from Figure 3-11.

Figure 3-13.



ample uranium in the seawater in the two liter sample cup to have provided the amount of uranium in the sampled particles.

It was previously shown that some of the uranium in sediment-trap samples must have been recently derived from seawater. Bioauthigenic uranium (Table 3-8) was calculated as the difference between total and detrital uranium:

$$U_{BA-z} = U_{T-z} - (U/^{232}\text{Th})_{\text{sed}} \times ^{232}\text{Th}_z \quad (6)$$

where  $U_T$  is the total uranium,  $z$  is the sample depth, and  $\text{sed}$  refers to the ratio in sediments. Values of  $U_{BA}$  were similar at Sites E and P, even though  $U_T$  was about two times greater at Site E because of the greater contribution of detrital uranium. Site P lacks a source of detrital material as pronounced as the transport of Saharan dust by the trade winds to Site E.

Bioauthigenic uranium cannot be an artifact of incomplete removal of sea salt from the sediment trap material or scavenging of dissolved uranium from seawater in the sample containers. Trapped material had higher specific activities of uranium than would be found in pure sea salt. Sample sizes and volumes of seawater in which the samples were stored were about the same for all of the samples from a given site. Bioauthigenic uranium should have been found at approximately the same concentration in all samples if it resulted from uptake of dissolved uranium during sample storage. Bioauthigenic uranium concentrations decreased with depth at Sites E and P, suggesting that it is a real phenomenon.

Uranium appears to be a conservative element in open ocean oxygenated seawater (Turekian and Chan, 1971; Ku et al., 1977). Bioauthigenic uranium concentrations in trapped particles decreased by over 50% with

TABLE 3-8

Bioauthigenic Uranium Content of Sediment Trap Material - Sites E and P.

Depth (m)	Site E Bioauthigenic Uranium $^{238}\text{U}$ dpm/g	Depth (m)	Site P Bioauthigenic Uranium $^{238}\text{U}$ dpm/g
389 - A	0.61	378	--
389 - B	0.53	978	0.57
988	0.45	2778	0.32
3755	0.42	4280	0.25
5086	0.17	5582	0.26

depth at both sites, presumably due to regeneration with very labile particulate carrier phases. This is in contrast to the behaviors of  $^{230}\text{Th}$  and  $^{231}\text{Pa}$  which are scavenged throughout the water column. A decrease in  $U_{\text{BA}}$  with depth is consistent with its incorporation into biogenic materials at the sea surface rather than scavenging of uranium from seawater. It is of interest to determine whether measurable concentration gradients should result from the rate of regeneration of bioauthigenic uranium in the deep sea. If  $U_{\text{BA}}$  is taken as 0.5 dpm/g in particles originating at the surface (Table 3-8), and typical particle fluxes are  $0.5\text{--}2.0 \text{ g/cm}^2 10^3 \text{ yr}$  (Table 3-1), then the bioauthigenic uranium flux is  $0.25\text{--}1.0 \text{ dpm/cm}^2 10^3 \text{ yr}$ . Regeneration of this uranium evenly throughout 2500 m of deep ocean changes the uranium concentration by  $0.001\text{--}0.004 \text{ dpm/l-}10^3 \text{ years}$ , an insignificant change compared to the uranium concentration in seawater of 2.5 dpm/l (Turekian and Chan, 1971; Ku et al., 1977) if the maximum mixing time of the deep ocean is 1000-2000 years.

#### Actinium

The immediate decay product of  $^{231}\text{Pa}$  is  $^{227}\text{Ac}$  (Figure 1-1), which is itself radioactive with a half life of 21.7 years. Three processes could account for  $^{227}\text{Ac}$  found in trapped particles. First, if particles act as a closed system with respect to  $^{231}\text{Pa}$  daughters, Ac will begin to grow into equilibrium once protactinium is adsorbed. Second, sediments older than 100 years incorporated into sediment-trap samples would have a  $^{227}\text{Ac}/^{231}\text{Pa}$  ratio equal to one if both elements are retained by the particles. Third, since most of the protactinium in seawater is dissolved (Chapter 5), there is significant production of dissolved actinium which may itself be scavenged by particles.



It appears that the bulk of the material caught in sediment traps settles very rapidly through the water column, perhaps in less than a year. Very little  $^{227}\text{Ac}$  would have been produced by decay of  $^{231}\text{Pa}$  on these particles, and the first process above would be negligible. Plutonium results indicated that there was minimal contribution to the trapped material by resuspended sediments greater than 100 years old. Therefore, the third process above may be the dominant source of particulate Ac in the sediment trap samples. If particulate Ac (Table 3-9) is derived entirely by scavenging of dissolved Ac, then the steady state distribution of particulate Ac can be represented by

$$dX_{\text{Ac}}/dt = \psi_{\text{Ac}} A_{\text{Ac}} - \lambda_{\text{Ac}} X_{\text{Ac}} - S(dX_{\text{Ac}}/dz) \quad (7)$$

where:  $X_{\text{Ac}}$  = concentration of particulate Ac

$\psi_{\text{Ac}}$  = scavenging rate constant for dissolved Ac

$A_{\text{Ac}}$  = concentration of dissolved Ac

$\lambda_{\text{Ac}}$  = radioactive decay constant of  $^{227}\text{Ac}$

$S$  = average particle settling rate

$z$  = depth

Then:

$$X_{\text{Ac}} = (\psi_{\text{Ac}} A_{\text{Ac}} / \lambda_{\text{Ac}}) (1 - e^{-\lambda_{\text{Ac}} z / S}) \quad (8)$$

Similarly for Pa:

$$X_{\text{Pa}} = (\psi_{\text{Pa}} A_{\text{Pa}} / \lambda_{\text{Pa}}) (1 - e^{-\lambda_{\text{Pa}} z / S}) \quad (9)$$

Thus

$$\frac{X_{\text{Ac}}}{X_{\text{Pa}}} = \frac{\lambda_{\text{Pa}} \psi_{\text{Ac}} A_{\text{Ac}} (1 - e^{-\lambda_{\text{Ac}} z / S})}{\lambda_{\text{Ac}} \psi_{\text{Pa}} A_{\text{Pa}} (1 - e^{-\lambda_{\text{Pa}} z / S})} \quad (10)$$

TABLE 3-9

$^{227}\text{Ac}/^{231}\text{Pa}$  Ratios at PARFLUX Site P.

Sample	$^{227}\text{Ac}$	$^{231}\text{Pa}$	$^{227}\text{Ac}/^{231}\text{Pa}$
	(dpm/g)		Activity Ratio
P - 978 m	< 0.012	0.105 $\pm$ .009	< 0.117
P - 4280 m	0.204 $\pm$ .018	0.476 $\pm$ .021	0.429 $\pm$ .042
P - 5582 m	0.519 $\pm$ .035	0.907 $\pm$ .043	0.572 $\pm$ .046
KKI Core 1, 3.8-5.1 cm	2.17 $\pm$ .19	2.23 $\pm$ .05	0.973 $\pm$ .088

which for large, rapidly settling particles (i.e.  $\lambda z/S \ll 1.0$ )

reduces to

$$\frac{X_{Ac}}{X_{Pa}} = \frac{\psi_{Ac} A_{Ac}}{\psi_{Pa} A_{Pa}} \quad (11)$$

If the only source of dissolved Ac is by decay of dissolved Pa, then

$$A_{Ac}/A_{Pa} \leq 1.0 \quad (12)$$

Combining Equations 11 and 12,

$$X_{Ac}/X_{Pa} \leq \psi_{Ac}/\psi_{Pa} \quad (13)$$

or

$$\psi_{Ac} \leq \psi_{Pa} (X_{Ac}/X_{Pa}) = (0.1-0.6)\psi_{Pa} \quad (14)$$

The residence time of protactinium ( $\tau_{Pa}$ ) at Site P is about 130 years (Chapter 4), and scavenging represents about 40% of the removal of the Pa produced by uranium decay (Table 3-7). Then:

$$\psi_{Pa} = 0.4(1/\tau_{Pa}) = (1/325) \text{ years}^{-1} \quad (15)$$

and

$$\psi_{Ac} = (0.1-0.6)(1/325) \text{ years}^{-1} \quad (16)$$

or the minimum residence time of actinium with respect to scavenging at Site P,  $\tau_{Ac} = 1/\psi_{Ac}$ , is 540-3250 years. A range of values is derived for the minimum scavenging residence time of Ac because

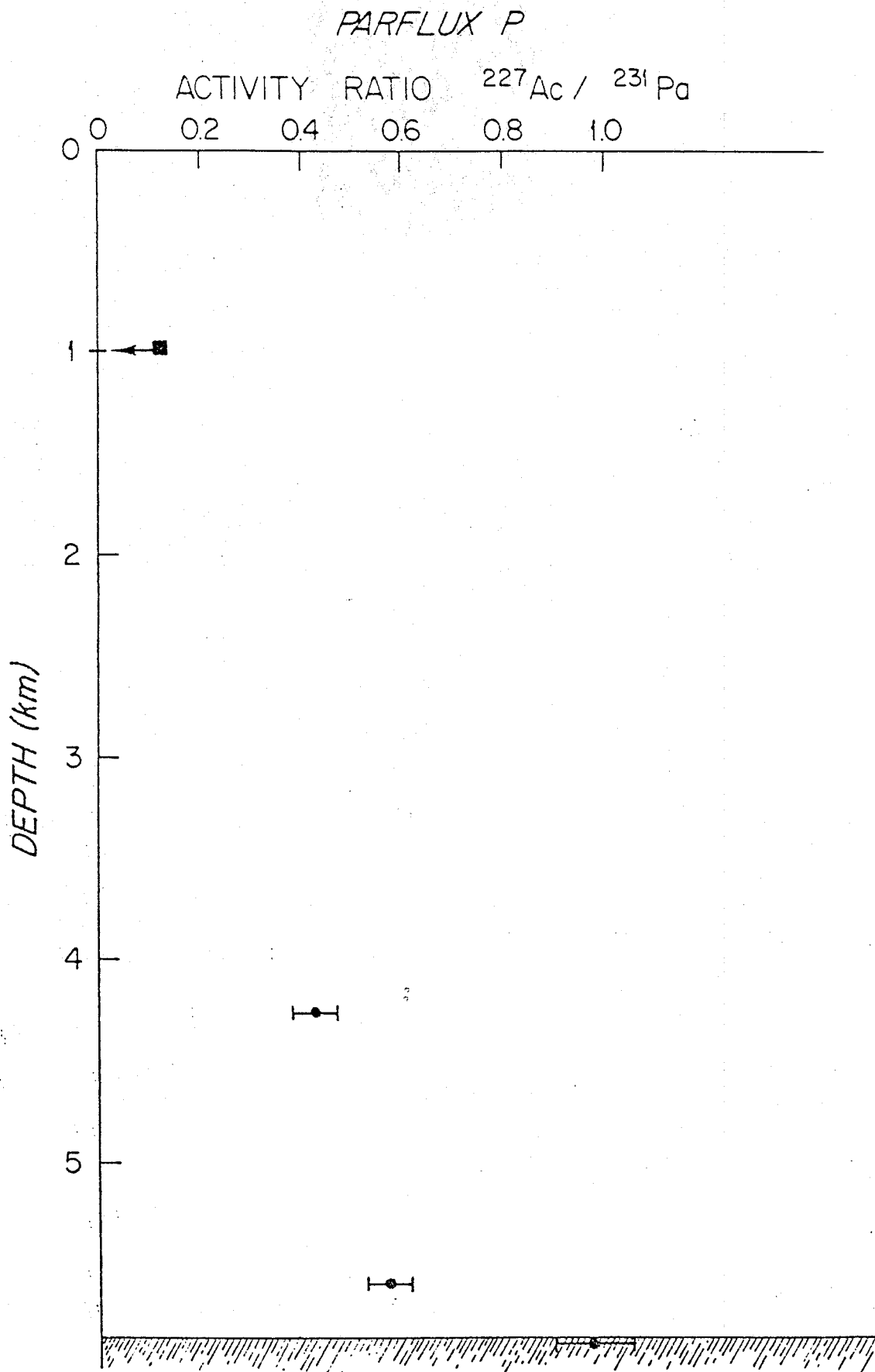
$X_{Ac}/X_{Pa}$  increases with depth (Figure 3-14).  $X_{Ac}/X_{Pa}$  should be constant with depth if 1) the approximation used to derive Equation 11 from Equation 10 is valid, 2) scavenging is the only source of  $X_{Ac}$ , 3)  $\psi_{Ac}/\psi_{Pa}$  is constant with depth, and 4)  $A_{Ac}/A_{Pa}$  is constant with depth. Since  $X_{Ac}/X_{Pa}$  increases with depth, one of the above criteria is not fulfilled. If some of the particulate Ac is derived by resuspension of old sediments or by decay of Pa on the particles, then the scavenging residence time of Ac is longer than calculated above, and 540-3250 years must be viewed as a lower limit for the scavenging residence time of Ac.

#### COMPARISON OF FILTERED AND TRAPPED PARTICLES

Specific activities of excess  $^{230}\text{Th}$  and  $^{231}\text{Pa}$  were higher in filtered particles than trapped particles at all depths at Site E (Table 3-5). Thorium-230 and  $^{231}\text{Pa}$  are present in samples of suspended particles primarily adsorbed at particle surfaces and particles collected by filtration tend to be smaller than particles collected with sediment traps. The greater specific surface area of smaller particles provides a greater number of sites for adsorption, resulting in the higher specific activities of  $^{230}\text{Th}$  and  $^{231}\text{Pa}$  in the filtered particles.

Unsupported  $^{230}\text{Th}/^{231}\text{Pa}$  ratios were nearly identical at Site E among two trapped and two filtered particle samples above 1500 m (Figure 3-5); at about 12±1.5. Particles trapped at 3755 m and 5086 m had ratios of 22 and 30. Some of the  $^{230}\text{Th}$  and  $^{231}\text{Pa}$  contained by the particles trapped at these depths was scavenged above 1500 m at a ratio of about 12. The ratio at which  $^{230}\text{Th}$  and  $^{231}\text{Pa}$  were actually scavenged at depths of 3000-5000 m by trapped particles must have been

Figure 3-14. Particulate  $^{227}\text{Ac}/^{231}\text{Pa}$  Ratio in Sediment-Trap Samples



much greater than the measured ratios of 22 and 30. Particles filtered at 3600 m and 5000 m had probably been at depth for considerably longer than the trapped particles, and may have obtained most of their scavenged Th and Pa at those depths. Unsupported  $^{230}\text{Th}/^{231}\text{Pa}$  ratios of 40-50 measured on filtered particles (Table 3-5) may be a more accurate representation of the ratio at which these isotopes are scavenged in the deep ocean, and are consistent with conclusion that trapped particles must have scavenged  $^{230}\text{Th}$  and  $^{231}\text{Pa}$  between 3000-5000 m at a ratio greater than 22-30. Therefore,  $^{230}\text{Th}$  and  $^{231}\text{Pa}$  are scavenged at similar ratios by filtered and trapped ("small" and "large") particles at all depths at Site E, although the ratio increases by a factor of 2.5-4 between 1000 m and 5000 m.

#### CONCLUSIONS

(1) Sediment traps catch large particles formed near the sea surface which scavenge significant amounts of reactive elements from seawater. The average transit time of the particles through the water column is less than a year.

(2) Settling particles preferentially scavenge  $^{230}\text{Th}$  relative to  $^{231}\text{Pa}$  from seawater, resulting in the high  $^{230}\text{Th}/^{231}\text{Pa}$  ratios found in many deep-sea sediments. Unsupported  $^{230}\text{Th}/^{231}\text{Pa}$  ratios as high as 50 were measured in suspended particles.

(3) The high  $^{230}\text{Th}/^{231}\text{Pa}$  ratios in suspended particles did not result from resuspension of sediments.

(4) Settling particles in low-particle-flux, deep open-ocean environments remove  $^{231}\text{Pa}$  at rates less than its production by uranium decay in the water column. This is probably true for other elements such as  $^{230}\text{Th}$  and  $^{210}\text{Pb}$  as well.

(5) Reactive elements that are not removed from seawater by settling particles are transported horizontally to environments where scavenging rates are greater than in most of the open ocean. At the open ocean sites studied, horizontal transport is relatively more important for removal of  $^{231}\text{Pa}$  whereas scavenging by settling particles is relatively more important for removal of  $^{230}\text{Th}$  produced by uranium decay. Sediments in environments with especially high rates of scavenging contain inventories of  $^{230}\text{Th}$  and  $^{231}\text{Pa}$  greater than would be expected from their rates of production by uranium decay in the overlying water column because of their input by horizontal mixing processes.

(6) Suspended particles near the sea floor have higher  $^{230}\text{Th}/^{232}\text{Th}$  and  $^{231}\text{Pa}/^{232}\text{Th}$  ratios but identical unsupported  $^{230}\text{Th}/^{231}\text{Pa}$  ratios compared to nearby surface sediments at Sites E and P. This is best explained by regeneration of most of the excess  $^{230}\text{Th}$  and excess  $^{231}\text{Pa}$  associated with suspended particles before they are incorporated into sediments.

(7) Thorium-232 in sediment trap samples is associated with detrital minerals in a Th/Al ratio suggestive of an average shale composition at Sites E and P. Atmospheric transport of Saharan Dust, with a shale-like composition, probably acts as the source of the detrital minerals at Site E.

(8) A bioauthigenic form of uranium is incorporated into particles collected with sediment traps. Bioauthigenic uranium is remineralized in the water column at Sites E and P. This flux of uranium to the deep sea is insufficient to cause measurable concentration gradients of uranium within the mixing time of the oceans.

(9) Estimates of the scavenging residence time of actinium are not well-constrained. However, results from sediment-trap samples show that the scavenging residence time of actinium is much greater than that of protactinium, by as much as an order of magnitude.



CHAPTER 4.

CONCENTRATIONS OF THORIUM AND PROTACTINIUM IN SEAWATER  
DETERMINED BY ADSORPTION ONTO MANGANESE-OXIDE-COATED FABRIC

INTRODUCTION

Sources of  $^{234}\text{Th}$ ,  $^{228}\text{Th}$ ,  $^{230}\text{Th}$  and  $^{231}\text{Pa}$  in seawater by decay of dissolved uranium and radium parents are well-defined. Rates of removal of these isotopes from seawater can then be determined from the degree of radioactive disequilibrium between the reactive daughter and soluble parent. The thorium isotopes listed above have a wide range of radioactive half-lives ( $^{234}\text{Th}$ : 24d;  $^{228}\text{Th}$ : 1.9yr;  $^{230}\text{Th}$ : 75200yr) and thus are useful in the study of scavenging processes occurring at rates varying over several orders of magnitude. Several studies have been made of the  $^{234}\text{Th}$ - $^{238}\text{U}$  and  $^{228}\text{Th}$ - $^{228}\text{Ra}$  disequilibria in surface seawater and nearshore environments (Bhat et al., 1969; Broecker et al., 1973; Matsumoto, 1975; Knauss et al., 1978; Li et al., 1979; Santschi et al., 1979; Minagawa and Tsunogai, 1980), where thorium residence times of days to months have been observed.

Scavenging is much slower in the deep ocean, where  $^{230}\text{Th}$  is the best isotope to use in the studies of processes removing thorium from seawater. Its source is well known, and its half-life is long enough that the  $^{230}\text{Th}/^{234}\text{U}$  ratio can be used to accurately determine the removal rate of thorium from the deep ocean, typically on the time scale of a few decades (Moore and Sackett, 1964; Brewer et al., 1980; this work). Few reliable  $^{230}\text{Th}$  data are available because of the large volumes of seawater required to accurately measure its extremely low concentration. The recent work of Nozaki (in preparation) is an

exception, where  $^{230}\text{Th}$  was measured with sufficient precision to show systematic trends with depth in the  $^{230}\text{Th}$  concentration.

One means of measuring the concentration of  $^{230}\text{Th}$  without processing large volumes of seawater is to employ an adsorber which extracts thorium in situ. Several investigators have used  $\text{MnO}_2$ -impregnated fibers to extract Ra and Th isotopes from seawater (Moore, 1976; Knauss et al., 1978; Reid et al., 1979a,b); however, thorium measurements were only made to depths of 150 m. This work was initiated with the following objectives:

1) To measure the concentration of thorium isotopes in the deep ocean, and calculate residence times of thorium from the measured concentrations.

2) To determine whether the method could be accurately used to measure the concentration of  $^{231}\text{Pa}$  as well as  $^{230}\text{Th}$ .

3) To compare residence times of Th and Pa, after successful measurement of  $^{231}\text{Pa}$ , and test for consistency with the conclusions derived from sediment trap results (Chapter 3).

#### LABORATORY ADSORPTION EXPERIMENTS

A natural isotope yield monitor for the efficiency of extraction of thorium from seawater onto  $\text{MnO}_2$  exists in  $^{234}\text{Th}$ , which is in radioactive equilibrium with its parent  $^{238}\text{U}$  in the deep ocean at 2.5 dpm/l (Amin et al., 1974; Bacon, unpublished results). Activity ratios of  $^{228}\text{Th}/^{234}\text{Th}$  and  $^{230}\text{Th}/^{234}\text{Th}$  on  $\text{MnO}_2$  adsorbers can then be used with the known  $^{234}\text{Th}$  concentration to calculate the concentrations of the other isotopes, which are present at much lower specific activities.

No suitable natural isotope yield monitor of protactinium exists in seawater. However,  $^{234}\text{Th}$  can be used as a yield monitor for Pa if it can be shown that Th and Pa adsorb to  $\text{MnO}_2$  without fractionation. Scott and Nuzzo (1975) found no fractionation of thorium and protactinium during adsorption to  $\text{MnO}_2$  in a laboratory experiment. Additional laboratory experiments were carried out to confirm that Th and Pa are not fractionated during adsorption to the  $\text{MnO}_2$ -coated Nitex adsorbers used in this work. Adsorbers were prepared by precipitation of  $\text{MnO}_2$  (cryptomelane) on acid-leached Nitex nylon fabric from a  $\text{KMnO}_4$  solution (Chapter 2).

Approximately 10 liters of natural, pH  $\sim$  8, filtered ( $\sim$  1  $\mu$  glass fiber filter) Vineyard Sound seawater was spiked with  $^{234}\text{Th}$  and  $^{233}\text{Pa}$ . The pH was measured before and after addition of the spikes to insure that the pH was not significantly changed. Several hours were allowed for spike equilibration. Strips of  $\text{MnO}_2$ -Nitex were then placed in the seawater for various lengths of time. Thorium and protactinium adsorbed to the Nitex were measured by gamma counting (93 keV for  $^{234}\text{Th}$  and 312 keV for  $^{233}\text{Pa}$ ) on Ge(Li) detectors coupled to a 4096-channel analyzer. The thorium and protactinium remaining in the seawater and adsorbed to the container walls at the end of the experiment were also counted. Counting was semi-quantitative, since counting geometries were not identical in each case. As the only concern was possible fractionation of thorium and protactinium during adsorption to  $\text{MnO}_2$ , determination of Th/Pa ratios was sufficient. Ratios were first measured on the mixed spikes before addition to the seawater. Seawater was contained in an acid-washed plastic (Rubbermaid No. 29634) bucket and was stirred with a magnetic stir-bar throughout the experiments. At the end

of the adsorption period (one-half to two hours) the  $\text{MnO}_2$ -Nitex was removed and counted. The seawater was then transferred to another plastic container to which 30 ml concentrated  $\text{HNO}_3$  and  $\text{FeCl}_3$  carrier were added. The pH was adjusted to 7 with  $\text{NH}_4\text{OH}$  to precipitate  $\text{Fe}(\text{OH})_3$ . Activity ratios in the  $\text{Fe}(\text{OH})_3$  were used to indicate the Th/Pa ratio in solution at the end of the experiment, and the counting rate was used to compare approximately the amounts of thorium and protactinium in solution with the amounts adsorbed to the Nitex. Finally, the bucket used in the adsorption experiment was washed with a mixture of  $\text{HNO}_3 + \text{HF}$ , and the acid wash was evaporated to a small volume and gamma counted.

Results from two adsorption experiments are shown in Table 4-1. There is a peak in the gamma spectrum of  $^{233}\text{Pa}$  at 95 keV that is not resolvable from the 93 keV  $^{234}\text{Th}$  peak. The 95 keV peak is equal to 73% of the activity in the 312 keV  $^{233}\text{Pa}$  peak with the detectors used in this work. Sufficient  $^{234}\text{Th}$  was used so that the contribution by  $^{234}\text{Th}$  to the 93-95 keV peak could be easily resolved.

The Th/Pa activity ratio in solution did not remain constant throughout the adsorption experiments, as can be seen by comparing the activity ratio in the initial spike solution with the ratio in the  $\text{Fe}(\text{OH})_3$  (Table 4-1). The change is caused by adsorption of thorium to the plastic container with very little corresponding adsorption of protactinium. Significant amounts of the thorium added to the seawater were adsorbed by the containers, perhaps as much as 20%, as indicated semi-quantitatively by the count rates given in Table 4-1. Thus thorium and protactinium were adsorbing onto  $\text{MnO}_2$  from a solution with a continuously changing Th/Pa ratio. The final ratios found on the Nitex

TABLE 4-1

Adsorption of  $^{234}\text{Th}$  and  $^{233}\text{Pa}$  onto  $\text{MnO}_2$ -Coated Nitex.

Run No.	Fraction	Activity Ratio		
		$^{234}\text{Th}/^{233}\text{Pa}$	$^{234}\text{Th}$	$^{233}\text{Pa}$
1	Initial Spikes <sup>b</sup>	1.70+.07	1.35	0.79
2	Initial Spikes <sup>b</sup>	1.62+.08	0.86	0.53
1	$\text{MnO}_2$ -Nitex <sup>c</sup>	1.64+.03	0.40	0.24
2	$\text{MnO}_2$ -Nitex <sup>d</sup>	1.13+.08	0.054	0.048
1	$\text{Fe}(\text{OH})_3$ <sup>e</sup>	1.25+.03	0.44	0.36
2	$\text{Fe}(\text{OH})_3$ <sup>e</sup>	0.95+.04	0.37	0.39
1	Container Wash <sup>f</sup>	25+5	0.45	0.013
2	Container Wash <sup>f</sup>	$\sim 40$	0.33	0.0085
	Background		0.005+.004	-0.0006+.0018

	Run No. 1	Run No. 2
<u>Nitex (Th/Pa)<sup>g</sup></u> Solution (Th/Pa)	0.97-1.32	0.70-1.19

<sup>a</sup>Activity ratio of the 93-95 KeV peak to the 312 KeV peak. The 93-95 KeV peak is corrected for the contribution by  $^{233}\text{Pa}$  of 0.728+.020 times the 312 KeV peak.

<sup>b</sup>Before addition to the seawater.

<sup>c</sup>Two-hour exposure to seawater, 2 x 12 cm strip of Nitex.

<sup>d</sup>One-half-hour exposure to seawater, 2 x 12 cm strip of Nitex.

<sup>e</sup>Represents Th/Pa ratio in solution at end of adsorption experiment.

<sup>f</sup>Represents Th and Pa adsorbed to the walls of the container in which the adsorption experiment was carried out.

<sup>g</sup>The range of values is derived by substitution of the initial spikes and the  $\text{Fe}(\text{OH})_3$  Th/Pa ratios for the solution Th/Pa ratio.

were between the initial and final values in solution. The variation of the Th/Pa ratio in solution limits the precision with which fractionation of thorium and protactinium can be estimated. However, comparison of the activity ratios on the Nitex with the initial and final values in solution (Table 4-1) indicates that the fractionation effect is less than 20%.

#### METHODS AND SAMPLING LOCATIONS

Passive adsorbers were prepared by rolling or folding approximately 40 X 60 cm sheets of MnO<sub>2</sub>-coated Nitex to fit into a 6 x 40 cm acrylic tube perforated with 30 1-cm holes. Polycarbonate Swin-Lok (Nuclepore) 47-mm filter holders were fixed to the ends of the tube to allow seawater to pass through the ends and to allow easy replacement of the Nitex sheets during sequential deployments. In every case, acrylic tubes containing sheets of MnO<sub>2</sub>-coated Nitex were attached at a depth of 3200 m on a sediment trap mooring deployed for approximately 2 months.

Results from samples obtained at two sites are reported here. The first sample was taken as part of the PARFLUX Program at Site P (Honjo, 1980; 15°21'N, 151°28'W, 5792 m). The other five samples were obtained from sequential two-month deployments at a site 25 nautical miles southeast of Bermuda (Site D, 4200 m; Deuser and Ross, 1980). The first sequential sample was recovered in July, 1979, and the last in April, 1980. Upon recovery at sea, samples were stored wet in plastic bags and returned to Woods Hole for analysis by the procedure in Chapter 2.

#### RESULTS

##### Calculation of Volumes Sampled

Measured <sup>234</sup>Th activities, A<sub>Th</sub>, were corrected for radioactive decay according to Equation (1):

$$A_0 = A_{Th} (e^{\lambda t_1}) / (1 - e^{-\lambda t_2}) \quad (1)$$

where  $A_0$  is the amount of  $^{234}\text{Th}$  adsorbed,  $\lambda$  is the radioactive decay constant of  $^{234}\text{Th}$ ,  $t_1$  is the time elapsed between recovery of the sample and the measurement of the  $^{234}\text{Th}$  activity, and  $t_2$  is the duration of the deployment. Calculated values of  $A_0$  were divided by 2.5 (dpm/l) to arrive at the effective volume sampled (Table 4-2). Approximately 0.05-0.10 dpm/l of the total  $^{234}\text{Th}$  is particulate (Chapter 5). If particulate thorium is not sampled by the Nitex adsorbers (see discussion below), then the calculated volumes may be too low by 2-4%. Variations in the uranium content of seawater are small compared to other sources of error, and amounts of uranium adsorbed on the Nitex were negligible as a source of  $^{234}\text{Th}$ .

A constant rate of adsorption of thorium during exposure of the Nitex to seawater is assumed by the use of Equation (1). Since all of the deployments were for about the same length of time, this assumption cannot be tested. It is possible that the  $\text{MnO}_2$  comes into an adsorption-desorption equilibrium with seawater on a time scale of a few days or less. The maximum error in the calculated total amount of  $^{234}\text{Th}$  adsorbed would be the factor  $\lambda t_2 / (1 - e^{-\lambda t_2})$  used to correct for decay of  $^{234}\text{Th}$  during deployment. For a two-month deployment this correction would cause the calculated volumes to be too high by a factor of approximately two. The concentration of each of the long-lived isotopes calculated from the  $^{234}\text{Th}$  effective volumes is affected equally by any error resulting from the assumption of a constant uptake rate. Therefore, isotope ratios are not affected by this uncertainty.

Dates of deployment of the  $\text{MnO}_2$ -Nitex adsorbers and fluxes of particulate matter through the water column at the time of each deployment are given in Table 4-2 along with the effective volumes sampled.

TABLE 4-2

MnO<sub>2</sub>-Nitex Samples Analyzed for Thorium and Protactinium Isotopes.

Site/Sample	Deployment Date	Effective Volume <sup>a</sup> Sampled (liters)	Particle Flux <sup>b</sup> mg/m <sup>2</sup> ·yr
P	9/17-11/20/78	2240 <sub>±</sub> 169	16.6
D-A	5/31-7/30/79	1452 <sub>±</sub> 97	23.6
D-B	8/3-10/5/79	647 <sub>±</sub> 43	NA
D-C	10/12-12/5/79	325 <sub>±</sub> 17	19.9
D-D	12/5/79-2/6/80	601 <sub>±</sub> 32	48.8
D-E	2/6-4/15/80	590 <sub>±</sub> 30	49.8

<sup>a</sup>See text for method used to calculate volumes sampled.

<sup>b</sup>Total fluxes were measured at Site D. Fluxes of the less than 1 mm size fraction were measured at Site P.

NA = Data not available because of malfunction of sediment trap.



Concentrations of Thorium and Protactinium

Concentrations of thorium and protactinium isotopes in seawater (Table 4-3) are calculated for each sample from the total amount of each isotope adsorbed to the sheet of Nitex and the effective volume of seawater sampled. Few reliable data are available in the literature with which to compare the  $^{230}\text{Th}$  and  $^{231}\text{Pa}$  results. Reported concentrations of  $^{230}\text{Th}$  and  $^{231}\text{Pa}$  in seawater are presented in Table 4-4. Values for  $^{230}\text{Th}$  activities in the deep ocean range from 0.5 to 3.5 dpm/ $10^3$  l. Concentrations of  $^{230}\text{Th}$  determined by means of the  $\text{MnO}_2$ -Nitex samples (Table 4-3) fall within the lower third of the range of values in the literature. Part of the variability may be geographical, as the concentration varies by about a factor of two between Sites D and P. Concentrations of  $^{231}\text{Pa}$  reported by Moore and Sackett (1964) (Table 4-4) fall within the range of those in Table 4-3; however, the sample locations and depths are not directly comparable. Concentrations of protactinium in surface seawater measured by Imai and Sakanoue (1973) (Table 4-4) tend to be higher than those in Table 4-3. There is no consistent trend to their data, and the high values are inconsistent with the much greater scavenging rates in surface seawater compared to the deep ocean.

Concentrations of  $^{232}\text{Th}$  measured at Site D are slightly greater than the upper limit for  $^{232}\text{Th}$  of 0.016 dpm/ $10^3$  l in surface seawater analyzed by Kaufman (1969). Turekian et al. (1973) used Th/La ratios in pteropod tests to predict an upper limit of 0.0017 dpm/ $10^3$  l for the concentration of  $^{232}\text{Th}$  (see their Table 3, the value in their text is a misprint). The upper limit of 0.0019 dpm/ $10^3$  l for dissolved  $^{232}\text{Th}$  in the Site P sample is the same as the pteropod data as corrected and is an order of magnitude lower than the upper limit of Kaufman (1969).

TABLE 4-3

Thorium and Protactinium Adsorbed to MnO<sub>2</sub>-Coated Nitex.

Sample	<sup>232</sup> Th	<sup>230</sup> Th	<sup>228</sup> Th	<sup>231</sup> Pa	<sup>228</sup> Th/ <sup>230</sup> Th	<sup>230</sup> Th/ <sup>231</sup> Pa	<sup>230</sup> Th/ <sup>232</sup> Th
P	< 0.0019	1.082±.084	0.174±.020	0.316±.027	0.161±.014	3.42±.16	> 569
D-A	0.015±.004	0.436±.036	1.72±.13	0.083±.007	3.95±.25	5.27±.36	29+8
D-B	0.020±.006	0.556±.047	2.26±.18	0.107±.010	4.06±.28	5.19±.43	28+8
D-C	0.033±.016	0.652±.050	2.18±.16	0.108±.011	3.34±.25	6.06±.62	20+10
D-D	0.015±.008	0.737±.054	2.44±.16	0.129±.011	3.31±.21	5.70±.45	49+26
D-E	0.022±.009	0.661±.048	2.45±.16	0.169±.014	3.70±.24	3.91±.29	30+12

dpm/10<sup>3</sup> liters

Activity Ratio

TABLE 4-4  
Concentrations of  $^{230}\text{Th}$  and  $^{231}\text{Pa}$  in Seawater.

Sample Location	Depth (m)	$^{230}\text{Th}$ dpm/ $10^3$	$^{231}\text{Pa}$	Comments	Reference
13°31'N, 60°39'W	0	0.44±.11	--		
14°20'N, 60°54'W	0	--	0.13±.13	Centrifuged to remove particles.	Moore & Sackett (1964)
32°15'N, 74°48'W	4500	1.6±.2	--	"	"
14°14'N, 64°40'W	0	0.43±.11	--	"	"
17°36'N, 65°16'W	800	0.31±.12	0.22±.10	"	"
13°21'N, 64°20'W	800	--	0.24±.10	"	"
32°57'N, 127°05'W	0	0.55±.10	--	In situ extraction onto Fe(OH) <sub>3</sub> -coated sponges.	Somayajulu & Goldberg (1966)
32°57'N, 127°05'W	2500	1.62±.31	--	"	"
35°34'N, 124°34'W	2500	0.51±.15	--	"	"
33°05'N, 143°15'E	0	0.78±.18	--	Total water - 500 l samples.	Miyake et al. (1970)
33°05'N, 143°15'E	1000	1.24±.51	--	"	"
33°05'N, 143°15'E	3000	0.51±.15	--	"	"
37°54'N, 143°50'E	0	3.17±.69	--	"	"
37°54'N, 143°50'E	500	1.29±.28	--	"	"
37°54'N, 143°50'E	1000	1.38±.97	--	"	"
37°54'N, 143°50'E	3000	3.5±1.0	--	"	"
37°54'N, 143°50'E	5000	1.47±.37	--	"	"
40°36'N, 137°03'E	0	0.51±.09	--	"	"
40°36'N, 137°03'E	1000	1.29±.18	--	"	"
41°16'N, 131°01'E	2000	0.69±.09	--	"	"
41°16'N, 131°01'E	3000	1.15±.14	--	"	"
39°02'N, 169°57'W	0	0.72±.15	5.2±.5	Total water - 1000 l samples.	Imai & Sakanoue (1973)
30°05'N, 170°05'W	0	0.93±.20	--	"	"
31°54'N, 146°06'W	0	0.49±.11	0.7±.2	"	"
Not Given	0	0.66±.21	--	"	"
41°22'N, 175°52'W	0	0.45±.17	0.6±.3	"	"
38°16'N, 156°46'E	0	1.8±.4	0.2±.1	"	"
30°40'N, 129°30'E	0	0.58±.14	--	"	"
30°32'N, 170°39'E	0-700	0.1-0.2	--	Total water - four samples above 700 m. Six samples below 2000 m. Exact values not tabulated.	Nozaki (in preparation)
	2000-5000	0.7-2.0	--		

## DISCUSSION

### $^{230}\text{Th}/^{232}\text{Th}$ Ratios

There is no production of dissolved  $^{232}\text{Th}$  in seawater by decay of a dissolved radioactive parent. However, there must be a finite concentration of dissolved  $^{232}\text{Th}$  as evidenced by its incorporation into authigenic manganese nodules at concentrations greater than in surrounding sediments (Calvert and Price, 1977). Typical  $^{230}\text{Th}/^{232}\text{Th}$  ratios in manganese nodules are compared with ratios in  $\text{MnO}_2$ -Nitex samples in Table 4-5. The  $\text{MnO}_2$ -Nitex sample at Site P has a ratio much greater than that reported for any nodule. Ratios measured at Site D fall within the range of values for nodules. However, the nodule sampled nearest Site D has a ratio much less than the ratios measured in Nitex samples from Site D (Table 4-5). The range of  $^{230}\text{Th}/^{232}\text{Th}$  ratios may represent varying degrees of mixture of dissolved and particulate thorium. The dissolved end member would then be best represented by the ratio at Site P. Lower ratios at Site D may result from inclusion of some particulate material in the Nitex samples. Manganese nodules have even lower ratios because they contain even greater amounts of particulate thorium associated with detrital minerals. The alternative possibility, that the concentration of dissolved  $^{232}\text{Th}$  is greater at Site D than at Site P, cannot be disproven without additional data.

### Particulate Thorium and Protactinium in the Nitex Samples

Several lines of evidence indicate that the  $^{230}\text{Th}$  and  $^{231}\text{Pa}$  adsorbed to the  $\text{MnO}_2$ -Nitex were predominantly dissolved. Most of the  $^{230}\text{Th}$  and  $^{231}\text{Pa}$  in seawater is dissolved. Particulate  $^{230}\text{Th}$  concentrations measured by Krishnaswami et al. (1976) at GEOSECS Station 226 were less than 20% of the total concentrations of  $^{230}\text{Th}$  measured

TABLE 4-5

$^{230}\text{Th}/^{232}\text{Th}$  Activity Ratios<sup>a</sup> in  $\text{MnO}_2$ -Nitex Samples Compared to Ratios in Deep-Sea Manganese Nodules.

Sample Location/Reference	$^{230}\text{Th}/^{232}\text{Th}$ Activity Ratio Average	Ratio Range
Site P, $\text{MnO}_2$ -Nitex	> 500	
Site D, $\text{MnO}_2$ -Nitex	30	20-50
All oceans - 17 nodules Ku & Broecker (1969)	44	6-200
8°18'N, 153°05'W - 3 nodules Somayajulu et al. (1971)	45	23-59
Equatorial Pacific - 3 nodules Krishnaswami & Cochran (1978)	111(99) <sup>b</sup>	87(86)-149(116) <sup>b</sup>

Individual Nodules Near Sites D and P

	$^{230}\text{Th}/^{232}\text{Th}$	Near Site:
C58 - 100; 33°57'N, 65°47'W Ku & Broecker (1969)	6	D
V21-D4; ~ 13°N, ~ 147°W Ku & Broecker Two Nodules	67 > 34	P
A47-16; 9°2.3'N, 151°11.4'W Krishnaswami & Cochran (1978) Two Nodules	87(86) <sup>b</sup> 149(116) <sup>b</sup>	P

<sup>a</sup>Ratios are extrapolated to nodule surfaces.

<sup>b</sup>Values reported were for unsupported  $^{230}\text{Th}/^{232}\text{Th}$ . There was some uncertainty in the uranium-supported  $^{230}\text{Th}$  value.  $^{230}\text{Th}/^{232}\text{Th}$  ratios would increase by < 5% if total  $^{230}\text{Th}$  activities were used.

during a reoccupation of the site by Nozaki (in preparation).

Measurement of particulate and dissolved  $^{230}\text{Th}$  and  $^{231}\text{Pa}$  on the same water samples in the Panama and Guatemala Basins (Chapter 5) showed that both isotopes are predominantly dissolved.

The Site P Nitex sample had an immeasurably low  $^{232}\text{Th}$  content, and the  $^{230}\text{Th}/^{232}\text{Th}$  activity ratio was greater than 500. The  $^{230}\text{Th}/^{232}\text{Th}$  ratios for trapped particles at a similar depth and in nearby surface sediments were 93 and 50, respectively (Chapter 3). Then, particulate  $^{230}\text{Th}$  could account for at most 10-20% ( $50/500-93/500$ ) of the total  $^{230}\text{Th}$ . The particulate  $^{231}\text{Pa}/^{230}\text{Th}$  activity ratio at Site P was approximately 0.033 (Chapter 3), and the  $^{231}\text{Pa}/^{230}\text{Th}$  ratio in the  $\text{MnO}_2$ -Nitex sample was 0.3 (Table 4-3). Thus, even if all of the  $^{230}\text{Th}$  were particulate, particulate  $^{231}\text{Pa}$  could account for a maximum of about 11% ( $0.033/0.3$ ) of the total. Since at least 80-90% of the  $^{230}\text{Th}$  was dissolved, a maximum of 1-2% of the  $^{231}\text{Pa}$  was particulate.

Similar arguments hold for Site D samples; however, upper limits on contribution by particles to the measured thorium and protactinium can be set only if particulate activity ratios determined at Site  $S_2$  (Chapter 3) are used, as particulate radioisotopes were not measured at Site D. At Site  $S_2$  (3694 m) the particulate  $^{230}\text{Th}/^{232}\text{Th}$  activity ratio was 13.5, and the particulate  $^{231}\text{Pa}/^{230}\text{Th}$  ratio was 0.037. The  $^{230}\text{Th}/^{232}\text{Th}$  ratios in the Nitex samples at Site D range from 20-50. If an average value of about 30 is adopted and it is assumed that all of the  $^{232}\text{Th}$  was particulate, then the maximum particulate  $^{230}\text{Th}$  was slightly less than half ( $13.5/30$ ) of the total. The average ratio of  $^{231}\text{Pa}/^{230}\text{Th}$  in the Nitex samples at Site D was 0.19. If at most ( $13.5/30$ ) of the  $^{230}\text{Th}$  was particulate, the maximum particulate  $^{231}\text{Pa}$  was about 9% of the total.

### $^{230}\text{Th}/^{231}\text{Pa}$ Activity Ratios

Thorium-230 and  $^{231}\text{Pa}$  are produced at a constant rate throughout the open ocean because of the constancy of the concentration and isotopic composition of uranium in seawater (Ku et al., 1977). If thorium and protactinium were scavenged from seawater at the same rates, then dissolved thorium and protactinium would be present at a  $^{230}\text{Th}/^{231}\text{Pa}$  activity ratio of 10.8. Moore and Sackett (1964) found  $^{230}\text{Th}/^{231}\text{Pa}$  ratios in seawater of 1.4 and 3.4, with large uncertainties (Table 4-4). All of the Th/Pa ratios observed in  $\text{MnO}_2$ -Nitex samples fall in the range of 3-6 (Table 4-3).

Deep-sea surface sediments commonly have  $^{230}\text{Th}/^{231}\text{Pa}$  activity ratios of 20-30 or higher (Sackett, 1964; Ku, 1966; Ku et al., 1972; Chapter 3). Manganese nodules also act as a sink for many trace elements in seawater. Nodule surfaces commonly have  $^{230}\text{Th}/^{231}\text{Pa}$  activity ratios less than 10.8, sometimes as low as 3 (Table 4-6). All of the above information is consistent with the conclusion in Chapter 3 that settling particles preferentially scavenge  $^{230}\text{Th}$  relative to  $^{231}\text{Pa}$ , resulting in a dissolved  $^{230}\text{Th}/^{231}\text{Pa}$  ratio less than 10.8. As previously discussed, thorium and protactinium appear to be adsorbed onto  $\text{MnO}_2$  without fractionation. Therefore, the  $^{230}\text{Th}/^{231}\text{Pa}$  ratios in manganese nodules simply reflect adsorption of dissolved thorium and protactinium onto nodule surfaces at the ratio present in seawater.

### Processes Removing Thorium and Protactinium from Seawater

Concentrations of  $^{230}\text{Th}$  and  $^{231}\text{Pa}$  are 2-3 times lower at Site D than at Site P (Table 4-3). Two mechanisms dominate scavenging of reactive elements from the deep ocean: adsorption to settling particles and transport by mixing processes to ocean basin margins (e.g. Brewer et

TABLE 4-6  
 Unsupported  $^{230}\text{Th}/^{231}\text{Pa}$  Ratios in Manganese Nodules.

Nodule	$x_s\text{Th}/x_s\text{Pa}_o^a$	$I_x\text{Th}/I_x\text{Pa}^b$	$(I_x\text{Th}/I_x\text{Pa})/(x_s\text{Th}/x_s\text{Pa}_o)$
Activity Ratio			
Ku and Broecker (1969)			
V21 D 2 A	12.5	30	2.4
V20 D 4 A	4.0	6.1	1.5
V20 D 4 B	< 5.5	6.5	> 1.2
6A	5.0	13	2.6
V18 D 32	~ 5.9	13	~ 2.2
V18 T119 A	< 9.3	20	> 2.2
V18 T119 B	40	40	1.0
C58 100	5.0	9.08	1.8
V16 T 3	9.0	12	1.3
D6253	2.5	5.4	2.2
V16 T 19 A	8.9	20	2.3
V16 T 19 A	8.6	19	2.2
E17 36	7.0	11	1.6
Krishnaswami & Cochran (1978)			
A47 16 2	8.5	14	1.7
C57 58 1	9.2	16	1.7
Moore et al. (in press)			
Mn7601 20 2	14.2	22.1	1.56

<sup>a</sup> $x_s\text{Th}/x_s\text{Pa}$  is the unsupported  $^{230}\text{Th}/^{231}\text{Pa}$  activity ratio extrapolated to the surface of the nodule.

<sup>b</sup> $I_x\text{Th}/I_x\text{Pa}$  is the ratio of the inventory of  $x_s^{230}\text{Th}$  (dpm/cm<sup>2</sup>) to the inventory of  $x_s^{231}\text{Pa}$  (dpm/cm<sup>2</sup>).



al., 1980; Bacon et al., 1976; Chapter 3). Only rough estimates can be made of the relative magnitudes of the two removal processes based on sediment trap data (Chapter 3), since absolute trapping efficiencies of the sediment traps are unknown.

If scavenging of thorium and protactinium occurs predominantly by adsorption to settling particles, then concentrations of thorium and protactinium should correlate inversely with concentrations or fluxes of particles. The flux of particulate matter at Site D was 25-30% greater than at Site P during collection of samples A and C (Table 5-2), while the flux at Site D more than doubled during collection of samples D and E, reflecting seasonal changes in surface biological productivity (Deuser and Ross, 1980). Sediment traps were identical at both sites, so results are comparable even if the absolute fluxes are in error. Concentrations of  $^{230}\text{Th}$  and  $^{231}\text{Pa}$  are lower at Site D, consistent with the higher scavenging rates compared to Site P predicted from the higher flux of particles at Site D.

If scavenging of thorium and protactinium occurs predominantly at ocean basin boundaries, either by vertical mixing to the bottom or horizontal mixing along isopycnals to slope sediments, then the rates of removal should be significantly less at Site P than at Site D.

$\text{MnO}_2$ -Nitex samples were obtained at 3200 m at both sites; however, the total water depth at Site D (4200 m) is much less than at Site P (5800 m). Furthermore, the nearest continental margin is farther from Site P than Site D. The extent of contact of seawater with the sea floor can be shown by calculating the  $^{228}\text{Ra}$  concentration at each site.

Decay of  $^{232}\text{Th}$  in sediments produces  $^{228}\text{Ra}$ , which diffuses into the water column and subsequently decays to  $^{228}\text{Th}$ . Because the

half-life of  $^{228}\text{Ra}$  is only 5.75 years, its distribution in the deep ocean reflects the rate of mixing of the water near the sea floor. If the concentrations of  $^{230}\text{Th}$  and  $^{228}\text{Th}$  are assumed to be at steady state, then the concentration of either isotope can be represented as a balance between production and scavenging plus decay:

$$dA_{\text{Th}}/dt = \lambda_{\text{Th}} A_{\text{P}} - (\psi_{\text{Th}} + \lambda_{\text{Th}}) A_{\text{Th}} = 0 \quad (2)$$

where:  $A_{\text{Th}}$  = activity of  $^{230}\text{Th}$  or  $^{228}\text{Th}$

$A_{\text{P}}$  = activity of parent isotope,  $^{234}\text{U}$  or  $^{228}\text{Ra}$

$\lambda_{\text{Th}}$  = radioactive decay constant of  $^{230}\text{Th}$  or  $^{228}\text{Th}$

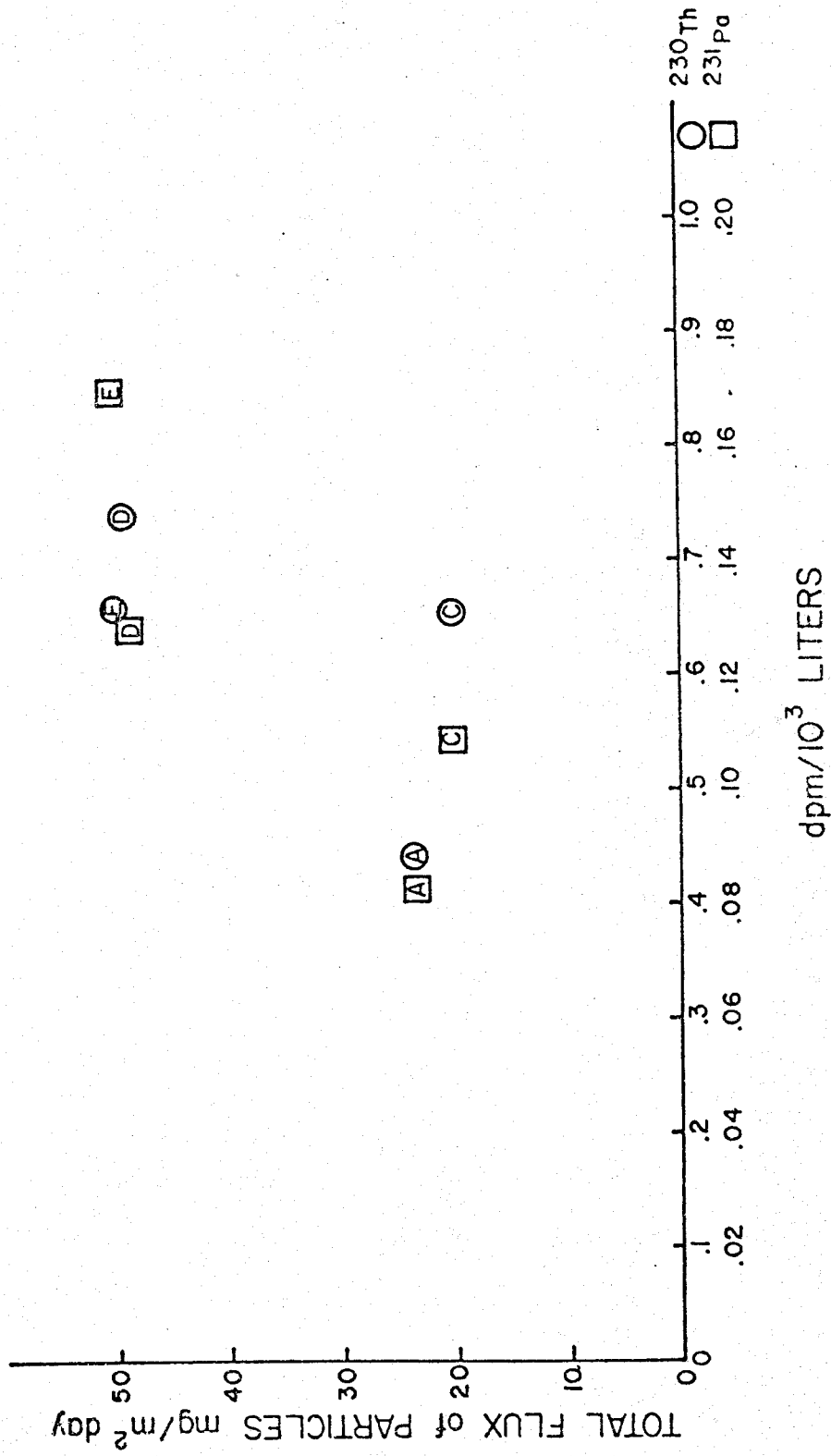
$\psi_{\text{Th}}$  = first order chemical scavenging rate constant

Values of  $\psi_{\text{Th}}$  calculated by substitution of  $A_{^{230}\text{Th}}$  (Table 4-3) and  $A_{^{234}\text{U}}$  (2.85 dpm/l; Ku et al., 1977) into Equation (2) are approximately  $0.04 \text{ yr}^{-1}$  and  $0.025 \text{ yr}^{-1}$  at Sites D and P respectively. As  $\psi_{\text{Th}}$  is much less than  $\lambda_{^{228}\text{Th}}$  ( $0.52 \text{ yr}^{-1}$ ),  $^{228}\text{Th}$  is nearly in radioactive equilibrium with  $^{228}\text{Ra}$ . The concentrations of  $^{228}\text{Ra}$  calculated from Equation (2) are 2.7 and 0.18 dpm/ $10^3 \text{ l}$  at Sites D and P respectively. The much higher  $^{228}\text{Ra}$  concentration at 3200 m at Site D is a direct reflection of the greater extent to which seawater at Site D has been in contact with the sea floor. Therefore, scavenging to settling particles and removal by mixing to the sediment-seawater interface should both be more effective at Site D than at Site P, and it is impossible to determine which process dominates removal of  $^{230}\text{Th}$  and  $^{231}\text{Pa}$  at either site.

#### Short Term Variations in $^{230}\text{Th}$ and $^{231}\text{Pa}$ Concentrations at Site D

There is a slight correlation between the concentrations of  $^{230}\text{Th}$  and  $^{231}\text{Pa}$  and the flux of particles at Site D (Figure 4-1). The correlation is poor, and may be merely coincidental. If, however, the

Figure 4-1. Concentrations of  $^{230}\text{Th}$  (circles) and  $^{231}\text{Pa}$  (squares) determined from the  $\text{MnO}_2$ -Nitex adsorbers at Site D plotted against the flux of particles into a sediment trap at the same depth during each sampling period.



DEUSER TRAP MnO<sub>2</sub> NITEX

Figure 4-1.

the correlation is real, then settling particles act as a source of thorium and protactinium to the deep ocean by regeneration of thorium and protactinium scavenged at shallower depths (Chapter 3).

In order for the observed changes in the concentrations of  $^{230}\text{Th}$  and  $^{231}\text{Pa}$  to result from regeneration of Th and Pa scavenged at shallower depths, the rates of production of these isotopes must be at least as large as the rates of change of their concentrations at depth. A simple calculation for  $^{230}\text{Th}$  shows this not to be the case. A maximum rate of change in the concentration of  $^{230}\text{Th}$  in the deep ocean of  $0.2 \text{ dpm}/10^3 \text{ l-yr}$  is used (Table 4-3), and the ocean is divided into two 2000-m layers, with some fraction of the  $^{230}\text{Th}$  scavenged in the shallow layer regenerated in the deep layer. The rate of production of  $^{230}\text{Th}$  in each layer is  $0.005 \text{ dpm}/\text{cm}^2\text{-yr}$ . The average rate of change in the  $^{230}\text{Th}$  concentration in the deep layer is  $0.04 \text{ dpm}/\text{cm}^2\text{-yr}$ . In the extreme case that all of the  $^{230}\text{Th}$  scavenged in the shallow layer is regenerated in the deep layer and that scavenging ceases completely in the deep layer for that part of the year, the combined input of  $^{230}\text{Th}$  would be only  $0.01 \text{ dpm}/\text{cm}^2\text{yr}$ , a factor of four less than the rate of change of the concentration. Therefore, regeneration and changes in the scavenging rate of thorium in the deep ocean cannot be responsible for the observed rate of change in the concentration of  $^{230}\text{Th}$  at Site D. Some other process, for example the movement of horizontal concentration gradients by mesoscale eddies or some other fluctuation in the general circulation pattern, must be responsible for the concentration changes.

#### Residence Times of Thorium and Protactinium

Residence times for thorium and protactinium ( $\tau_{\text{Th}} = 1/\psi_{\text{Th}}$ ) may be calculated from Equation (2). Use of this equation requires the

assumption that the system is at steady state and that other processes, such as mixing and advection, are negligible. Horizontal mixing may act as a source or a sink for  $^{230}\text{Th}$  and  $^{231}\text{Pa}$  depending on the environment (Chapters 3 and 5). As long as mixing acts as a net removal of  $^{230}\text{Th}$  and  $^{231}\text{Pa}$  from a parcel of water, the residence times of  $^{230}\text{Th}$  and  $^{231}\text{Pa}$  calculated from their concentrations and production rates by uranium decay are valid. As discussed above, the steady state assumption is not strictly valid at Site D, since the concentrations of thorium and protactinium are observed to vary by a factor of two over the time intervals sampled. Since the source of the variability is unknown, it cannot be modeled in Equation (2), and the derived scavenging rates can only be used to qualitatively compare residence times of thorium and protactinium at the two sites.

Residence times calculated for  $^{230}\text{Th}$  and  $^{231}\text{Pa}$  are presented in Table 4-7. An estimate of the residence times of thorium and protactinium in seawater independent of their measured concentrations was made by Brewer et al. (1980) from sediment trap results. Their estimates of  $\tau_{\text{Th}}$  of 22 years (misprinted 27 years in their text) and  $\tau_{\text{Pa}}$  of 31 years pertain to removal of the elements from the entire water column at Site E (Chapter 3). A  $\tau_{\text{Th}}$  of 22 years falls within the range of values determined at Site D, while  $\tau_{\text{Th}}$  determined at Site P was somewhat higher (41 years).

The  $\tau_{\text{Pa}}$  estimated by Brewer et al. is lower than the values in Table 4-7, and consequently their  $\tau_{\text{Pa}}/\tau_{\text{Th}}$  ratio of 1.4 (1.15 in their text is a misprint) is less than the values of 2-3 in Table 4-7. This difference probably results from the assumption in the scavenging model of Brewer et al. that scavenging by settling particles is the only

TABLE 4-7

Residence Times of Thorium and Protactinium.

Sample	$\tau_{Th}$ (years)	$\tau_{Pa}$ (years)	$\tau_{Pa}/\tau_{Th}$
P	41.2 $\pm$ 3.2	130 $\pm$ 11	3.16 $\pm$ .36
D-A	16.6 $\pm$ 1.4	34.2 $\pm$ 2.9	2.06 $\pm$ .25
D-B	21.2 $\pm$ 1.8	44.0 $\pm$ 4.1	2.08 $\pm$ .26
D-C	24.8 $\pm$ 1.9	44.0 $\pm$ 4.5	1.77 $\pm$ .23
D-D	28.1 $\pm$ 2.1	53.1 $\pm$ 4.5	1.90 $\pm$ .22
D-E	25.2 $\pm$ 1.8	69.6 $\pm$ 5.4	2.76 $\pm$ .29

mechanism by which  $^{230}\text{Th}$  and  $^{231}\text{Pa}$  are removed from seawater. Most of the protactinium produced at open ocean Sites E and P is not removed by settling particles but is removed by horizontal mixing to other environments (Chapters 3 and 5). Residence times for thorium in Table 4-7 and calculated by Brewer et al. are in better agreement than the residence times of protactinium because complete removal by scavenging onto settling particles is a better approximation for  $^{230}\text{Th}$  than for  $^{231}\text{Pa}$ .

The residence time of thorium in most of the deep, open ocean falls in the range of 15-40 years, and the residence time of protactinium is 1.5-3.0 times longer than that of thorium. Since  $\tau_{\text{Th}}$  and  $\tau_{\text{Pa}}$  are much shorter than the mixing time of the oceans, they do not represent ocean-wide residence times, but vary geographically in accord with local scavenging rates.

Radioactive decay in the water column is a negligible sink for  $^{230}\text{Th}$  and  $^{231}\text{Pa}$  as their residence times in seawater are orders of magnitude less than their radioactive half-lives. Virtually all of the  $^{230}\text{Th}$  and  $^{231}\text{Pa}$  produced in seawater is removed to some depositional sink which must be found to make a mass balance for  $^{230}\text{Th}$  and  $^{231}\text{Pa}$  in the oceans.

#### Speculation About Growth Rates of Manganese Nodules

Distributions of  $^{230}\text{Th}$  and  $^{231}\text{Pa}$  in manganese nodules have been commonly used as a means of determining nodule growth rates, although there is some controversy about the validity of the method (Krishnaswami and Cochran, 1978; Glasby, 1978; Halbach et al., 1978; Lalou and Brichet, 1978). The popular opinion is that manganese nodules in the deep ocean grow slowly, at a rate of a few mm/ $10^6$  yr. It is assumed that thorium



and protactinium adsorb from seawater onto nodules at a constant rate, and that their specific activities at a nodule surface remain approximately constant with time. Then the decrease with depth in the specific activities of  $^{230}\text{Th}$  and  $^{231}\text{Pa}$  can be used to determine the rate at which a nodule has grown. The alternative view is that manganese nodules grow rapidly, and adsorption of thorium and protactinium occurs after growth has ceased. Distributions of  $^{230}\text{Th}$  and  $^{231}\text{Pa}$  with depth in nodules would then result from diffusion into the interior of the nodules, or from an artifact of the sampling procedure. However, Krishnaswami and Cochran (1978) have used  $^{210}\text{Pb}$  distributions in manganese nodules to show that the  $^{230}\text{Th}$  and  $^{231}\text{Pa}$  distributions do not result from an artifact of the sampling procedure.

The inventories of  $^{230}\text{Th}$  or  $^{231}\text{Pa}$  in a nodule,  $I(\text{dpm}/\text{cm}^2)$ , are a function of their rates of adsorption,  $R(\text{dpm}/\text{cm}^2 10^3 \text{yr})$ , and time:

$$dI/dt = R - \lambda I \quad (3)$$

If  $dR/dt=0$ , then:

$$I = (R/\lambda)(1 - e^{-\lambda t}) \quad (4)$$

Two examples will be considered:

Case 1). Nodules grow, or grew, rapidly. Thorium-230 and  $^{231}\text{Pa}$  adsorb to nodule surfaces after growth ceases, and subsequently diffuse into the interiors of nodules. Protactinium must then diffuse faster than thorium to produce concordant growth rates calculated from distributions of  $^{230}\text{Th}$  and  $^{231}\text{Pa}$  (Ku and Broecker, 1969; Krishnaswami and Cochran, 1978). If an arbitrary maximum nodule age of  $2 \times 10^4$  years is assumed for the rapid growth model, then Equation (4) written for  $^{230}\text{Th}$  and  $^{231}\text{Pa}$  can be combined to yield

$$1.0 \leq (I_{\text{Th}}/I_{\text{Pa}})/(R_{\text{Th}}/R_{\text{Pa}}) \leq 1.12 \quad (5)$$

Since  $^{231}\text{Pa}$  is lost from the nodule surface faster than  $^{230}\text{Th}$  by diffusion into the nodule, and from Equation 5

$$[\text{xsTh}/\text{xsPa}]_0 > R_{\text{Th}}/R_{\text{Pa}} \approx (0.9-1.0)(I_{\text{Th}}/I_{\text{Pa}}) \quad (6)$$

or

$$I_{\text{Th}}/I_{\text{Pa}} < (1.1)([\text{xsTh}/\text{xsPa}]_0) \quad (7)$$

where  $[\text{xsTh}/\text{xsPa}]_0$  is the unsupported  $^{230}\text{Th}/^{231}\text{Pa}$  activity ratio extrapolated to the nodule surface. Results from three studies are presented in Table 4-6 showing that  $I_{\text{Th}}/I_{\text{Pa}}$  is considerably more than a factor of 1.1 larger than  $[\text{xsTh}/\text{xsPa}]_0$ . These results are not consistent with the rapid growth of nodules.

Case 2). Nodules grow slowly. Adsorption of  $^{230}\text{Th}$  and  $^{231}\text{Pa}$  at nodule surfaces and their decay within nodules is at a steady state, and the distributions of  $^{230}\text{Th}$  and  $^{231}\text{Pa}$  with depth in nodules reflect the growth rate of the nodules. Then,

$$R_{\text{Th}}/R_{\text{Pa}} \approx [\text{xsTh}/\text{xsPa}]_0 \quad (8)$$

and combining Equation (4) written for  $^{230}\text{Th}$  and  $^{231}\text{Pa}$  for very large  $t$ ,

$$I_{\text{Th}}/I_{\text{Pa}} = 2.3(R_{\text{Th}}/R_{\text{Pa}}) \approx 2.3([\text{xsTh}/\text{xsPa}]_0) \quad (9)$$

Several nodules in Table 4-6 have  $(I_{\text{Th}}/I_{\text{Pa}})/([\text{xsTh}/\text{xsPa}]_0)$  ratios of about 2.3, consistent with the slow growth rate model. Furthermore, if the ratio at which  $^{230}\text{Th}$  and  $^{231}\text{Pa}$  adsorb to  $\text{MnO}_2$ -coated Nitex is representative of  $R_{\text{Th}}/R_{\text{Pa}}$ , then the  $^{230}\text{Th}/^{231}\text{Pa}$  ratios in Table 4-3 are more consistent with  $[\text{xsTh}/\text{xsPa}]_0$  (Case 2, Equation (8)) than with  $I_{\text{Th}}/I_{\text{Pa}}$  (Case 1, Equation (5)).

Many of the nodules in Table 4-6 have  $I_{\text{Th}}/I_{\text{Pa}}$  less than 2.3 times  $[\text{xsTh}/\text{xsPa}]_0$ . This may indicate that some nodules are not at a steady state with respect to accumulation and decay of  $^{230}\text{Th}$  and  $^{231}\text{Pa}$ .

However, the low ratios may also result from sampling difficulties arising from the necessity of sampling nodules over depth ranges of tenths of millimeters. Nevertheless, the results discussed above are all more consistent with the slow growth model than with the rapid growth model.

#### CONCLUSIONS

(1) Artificially prepared  $\text{MnO}_2$  adsorbers may be used to extract thorium isotopes and protactinium from seawater. Little or no fractionation occurred during adsorption of thorium and protactinium to  $\text{MnO}_2$  in a laboratory experiment. Therefore  $^{234}\text{Th}$  may be used as a yield monitor for Pa as well as Th isotopes to indicate effective volumes of seawater sampled.

(2) Thorium-230 and  $^{231}\text{Pa}$  collected by passive  $\text{MnO}_2$  adsorbers were predominantly dissolved, with very minor contributions by particulate isotopes.

(3) Dissolved  $^{230}\text{Th}/^{231}\text{Pa}$  activity ratios ranged from 3-6, compared to ratios of 30-50 measured in suspended particles (Chapter 3). High  $^{230}\text{Th}/^{231}\text{Pa}$  ratios commonly found in deep-sea sediments result from preferential adsorption of Th relative to Pa by settling particles. In contrast, low ratios in manganese nodules result from adsorption of Th and Pa from seawater with little or no fractionation.

(4) The residence time of thorium in the deep ocean is 15-40 years, while the residence time of protactinium ranged from 34-130 years. The longer residence time for protactinium is consistent with the conclusion in Chapter 3 that  $^{230}\text{Th}$  is more rapidly removed from seawater than  $^{231}\text{Pa}$  by scavenging onto settling particles.

(5) The ratio at which  $^{230}\text{Th}$  and  $^{231}\text{Pa}$  are adsorbed to  $\text{MnO}_2$ -Nitex adsorbers is more consistent with slow growth rates of manganese nodules than rapid growth rates.

CHAPTER 5.

PROCESSES REMOVING THORIUM AND PROTACTINIUM FROM SEAWATER:

OCEAN-MARGIN ENVIRONMENTS

INTRODUCTION

Particulate material in the open ocean preferentially scavenges Th relative to Pa (Chapter 3). Particulate  $^{230}\text{Th}/^{231}\text{Pa}$  activity ratios as high as 35 in trapped particles at Site P and 50 in filtered particles at Site E were measured. These ratios are much greater than dissolved  $^{230}\text{Th}/^{231}\text{Pa}$  activity ratios of 3-6 and the ratio of 10.8 that would be expected from the isotopic composition of uranium in seawater if Th and Pa were scavenged from seawater without fractionation. Fluxes of particulate  $^{230}\text{Th}$  and  $^{231}\text{Pa}$  into sediment traps at Sites S<sub>2</sub>, E and P were less than their rates of production in the overlying water column. Low fluxes may have resulted in part from undertrapping the true flux of particles. However, the  $^{230}\text{Th}/^{231}\text{Pa}$  activity ratios of 30-35 could only occur if there is a mechanism locally removing Pa from seawater other than scavenging by settling particles. Radioactive decay is not a significant sink for dissolved  $^{230}\text{Th}$  or  $^{231}\text{Pa}$  (Chapter 4). Manganese nodules have long been acknowledged as a preferential sink for  $^{231}\text{Pa}$  relative to  $^{230}\text{Th}$ . However, it is doubtful that there are sufficient quantities of manganese nodules in the ocean to balance the deficiency of  $^{231}\text{Pa}$  relative to  $^{230}\text{Th}$  observed in most deep-sea sediments (Ku and Broecker, 1969). Some other Pa sink is required to balance production of Pa in seawater.

Bacon et al. (1976) concluded that removal of  $^{210}\text{Pb}$  from the deep ocean, like  $^{231}\text{Pa}$ , does not occur entirely by scavenging onto settling particles. They found that  $^{210}\text{Pb}/^{226}\text{Ra}$  disequilibria increased

approaching ocean margins from the open ocean. From this they concluded that ocean margins act as a sink for much of the  $^{210}\text{Pb}$  produced in the open ocean. Since ocean margins act as sinks for  $^{210}\text{Pb}$  produced in the open ocean, it seemed reasonable to investigate ocean margins as potential sinks for  $^{230}\text{Th}$  and  $^{231}\text{Pa}$  produced in the open ocean, and more specifically, as preferential sinks for  $^{231}\text{Pa}$  relative to  $^{230}\text{Th}$ .

High fluxes of organic matter in some margin environments cause reducing conditions in sediments to occur at or very near the sediment-seawater interface. Precipitation of  $\text{MnO}_2$ , an efficient adsorber of many reactive elements, at the sediment surface is one means of making margin environments an efficient sink for reactive elements in seawater that comes into contact with the sediments. Concentrations and fluxes of particles may also be higher in margin environments, further increasing scavenging efficiencies relative to the open ocean. Bottom currents are generally more intense near ocean margins than in the open ocean. Resuspension of sediments by intense bottom currents could result in high particle concentrations that would act as an efficient sink for dissolved reactive elements. Input of terrigenous material near continental margins can further increase particle fluxes relative to the open ocean. Finally, upwelling along certain margins causes extremely high biological productivity with its ensuing high flux of biogenic particulate debris. Therefore, several factors may work in combination to cause ocean margins to act as efficient sinks for reactive elements produced in the open ocean. It remains to be shown whether these factors may also cause the preferential removal of Pa relative to Th.

The objectives of this study were to determine whether a particular ocean margin environment, in the Panama and Guatemala Basins, acts as a sink for  $^{230}\text{Th}$  and  $^{231}\text{Pa}$  transported from the open ocean, and if the area acts as a preferential sink for Pa relative to Th.

#### Sample Locations

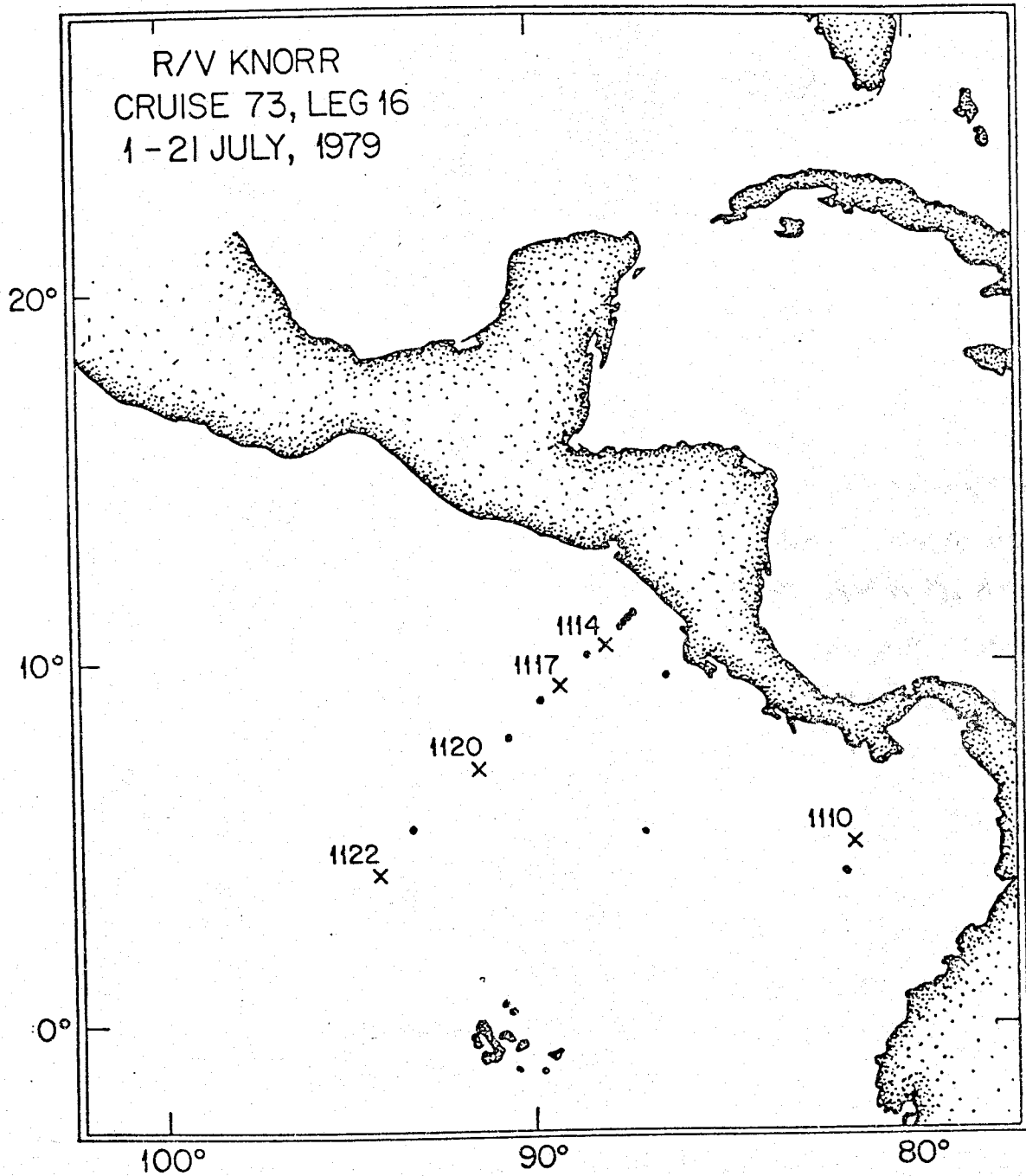
Two opportunities occurred almost simultaneously to sample in a near-margin environment. First, in July, 1979, R/V KNORR, Cruise 73, Leg 16 was carried out to sample in a transect from the Coast of Nicaragua into the Guatemala Basin (Figure 5-1). Second, sediment traps were deployed in August, 1979, on Leg 17 of R/V KNORR, Cruise 73 as part of the Sediment Trap Intercomparison Experiment (STIE) in the Panama Basin. A station was occupied during Leg 16 at the STIE site (Station 1110 in Figure 5-1) to make hydrographic measurements and sample suspended particulate matter for comparison with material obtained in the sediment traps.

The STIE Site was located in an area of very rough bottom topography, only about 20 km from the Coiba Ridge. Water depths less than 1000 m were observed near the STIE Site (J. Bishop, personal communication). STIE moorings were set at depths of 3865 to 3893 m. Thus, the STIE samples below about 1000 m may contain particulate material winnowed off of nearby topographic highs. There is evidence that this actually occurred with most of the material being derived from slope sediments to the northwest of the STIE Site (S. Honjo, personal communication).

#### Sampling Methods

Sediment trap samples from the STIE site were collected with the same traps used at PARFLUX Sites S, E, and P (Chapter 3; Honjo, 1978, 1980). Handling and distribution of sediment trap material were carried out as for the PARFLUX samples (Chapter 3; Brewer et al., 1980; Honjo, 1980).

Figure 5-1. Locations of stations occupied during KN73-16, including the STIE Site (Station 1110).





Battery-powered pumps used to filter seawater in situ were the same systems as were used during R/V OCEANUS, Cruise 78, Leg 1 (Chapter 3). Seawater was filtered through 293-mm diameter, 1.0-micron pore size Nuclepore filters. The only difference between the filtering procedure during KN 73-16 and OC 78-1 was that the KN 73-16 samples were prefiltered through 62-micron mesh Nitex fabric. This procedure was adopted in part to prevent clogging of the filters by large particles. It was determined on OC 78-1 (subsequent to KN73-16) that Nuclepore filters did not clog any faster without prefilters than with them, so the practice of prefiltering has been discontinued.

Sheets of  $MnO_2$ -Nitex identical to those described in Chapter 4 were packed into cartridges in the pumping systems between the filters and the pumps. The plumbing sequence of the filtering systems used on KN 73-16 was: prefilter - Nuclepore filter -  $MnO_2$  cartridge - battery powered pump - flow meter - exit. Effective volumes of seawater from which Th and Pa isotopes were scavenged onto  $MnO_2$  were calculated from the amounts of  $^{234}Th$  adsorbed (Chapter 4).

Analytical procedures for the analysis of radioisotopes in sediment trap material, Nuclepore filters and  $MnO_2$ -Nitex adsorbers are described in Chapter 2.

## RESULTS

Fluxes of material recovered in STIE sediment traps are presented in Table 5-1 along with other basic information on the deployment. Results of radiochemical analyses of the trapped material are presented in Table 5-2. Errors given in Table 5-2 are  $\pm 1\sigma$  counting statistics.

Locations and water depths of stations occupied during KN 73-16 are presented in Table 5-3, along with sample depths, volumes of seawater

TABLE 5-1

Fluxes of Particulate Material into STIE Sediment Traps<sup>a</sup>.

Mooring	Depth (m)	Flux (< 1-mm Size Fraction) <sup>b</sup> mg/m <sup>2</sup> ·day	g/cm <sup>2</sup> ·1000 yr	Percent of Total Flux <sup>c</sup>
C	667	96.5	3.52	84.4
C	1268	104.6	3.82	95.8
D	2265-RT 3 <sup>d</sup>	116.9	4.27	97.7
D	2265-RT 4 <sup>d</sup>	156.0	5.69	95.4
D	2265-RT 5 <sup>d</sup>	219.5	8.01	98.3
A	2869	152.6	5.57	95.6
A	3769	175.3	6.40	97.1
B	3791	177.7	6.49	96.3

<sup>a</sup>STIE deployment: 5°21'N, 81°53'W; 112-day deployment, August-November, 1979.

<sup>b</sup>All radioisotope analyses were performed on the less than 1-mm size fraction of the trapped material.

<sup>c</sup>Percent of total flux is the flux of < 1-mm particles, given here, divided by the total flux, including the > 1-mm particles.

<sup>d</sup>RT indicates Rotating Trap; 3,4, and 5 represent sequential four-week sampling periods.

TABLE 5-2  
 Radioisotope Content of Sediment Trap Material: STIE Site.

Depth (m)	Mooring	dpm/g										Activity Ratio		
		<sup>232</sup> Th	<sup>230</sup> Th	<sup>228</sup> Th	<sup>238</sup> U	<sup>231</sup> Pa	<sup>239+240</sup> Pu	<sup>234</sup> U/ <sup>238</sup> U	<sup>230</sup> Th/ <sup>231</sup> Pa					
667	C	0.0879±.0070	0.451±.018	2.028±.056	0.788±.047	0.0642±.0034	0.421±.026	1.34±.10	7.02±.47	1.267±.063	1.255±.051	1.268±.061	1.364±.067	8.34±.43
1268	C	0.103±.010	0.955±.031	2.671±.072	Lost	0.1777±.0081	Lost	Lost	5.37±.30	1.267±.063	1.255±.051	1.268±.061	1.364±.067	8.34±.43
2869	A	0.191±.013	2.295±.057	4.68±.11	0.878±.037	0.2811±.0089	0.420±.024	1.267±.063	8.16±.33	1.267±.063	1.255±.051	1.268±.061	1.364±.067	8.34±.43
3769	A	0.276±.017	3.058±.075	6.28±.14	0.889±.031	0.544±.041	0.287±.017	1.255±.051	5.62±.24	1.267±.063	1.255±.051	1.268±.061	1.364±.067	8.34±.43
3791	B	0.265±.017	3.458±.084	7.16±.16	0.913±.037	0.802±.023	0.318±.025	1.268±.061	4.31±.16	1.267±.063	1.255±.051	1.268±.061	1.364±.067	8.34±.43
2265-RT 5	D	0.189±.014	2.091±.056	3.73±.10	0.716±.039	0.285±.012	0.461±.030	1.364±.067	7.34±.37	1.267±.063	1.255±.051	1.268±.061	1.364±.067	8.34±.43
2265-RT 4	D	0.163±.016	1.598±.045	2.978±.082	0.815±.035	0.1916±.0084	0.505±.029	1.219±.066	8.34±.43	1.267±.063	1.255±.051	1.268±.061	1.364±.067	8.34±.43
2265-RT 3	D	0.166±.014	1.901±.054	3.66±.10	0.861±.034	Lost	0.543±.030	1.443±.070	-	1.267±.063	1.255±.051	1.268±.061	1.364±.067	8.34±.43

TABLE 5-3  
 KN 73-16 In Situ Filtration Samples: Station Locations and  
 Sample Sizes.

Station	Location	Water Depth (m)	Sample Depth (m)	Volume Filtered (liters)	Weight of Particles Collected (mg)
1110	05°06'N, 81°32'W	3440-4290 <sup>a</sup>	1500 2250 3000	3005 2190 1413	65.5 34.5 26.8
1114	11°09.4'N, 87°35.2'W	5369	2000 3000 4700	3530 1945 1732	70.4 38.0 33.2
1117	09°35.7'N, 89°08.1'W	3470	1500 2250 2900	2487 1909 3347	30.0 18.3 41.7
1120	07°04.1'N, 91°41.4'W	3620	1000 1500 2250 3100	3195 2591 2112 4265	21.7 24.5 17.3 35.5
1122	04°08.3'N, 94°22.1'W	3100-3500	1100 1600 2100 2600	2877 3888 1928 1755	22.9 31.0 27.1 27.8

<sup>a</sup>Depth changed because of ship drift during sampling.

filtered, and amounts of particulate material collected. Effective volumes of seawater sampled by scavenging dissolved Th and Pa onto the  $MnO_2$ -Nitex adsorbers are given in Table 5-4. Scavenging efficiencies in Table 5-4 are the ratios of the effective volumes sampled to the total volumes of seawater pumped through the  $MnO_2$ -Nitex cartridges.

In some cases two Nitex adsorbers were placed in tandem. Scavenging efficiencies of the Nitex were low (5-15%) and were nearly the same for front and back adsorbers where two were used.  $MnO_2$ -coated Nitex was originally designed for use as a passive adsorber (Chapter 4), and was not intended to scavenge elements efficiently from seawater when placed in line behind filters<sup>(1)</sup>. The method was chosen because of its ready availability. Concentrations of  $^{230}Th$  determined on front and back adsorbers for samples 1110 - 1500 m and 1122 - 2600 m are in good agreement (Table 5-5). Agreement is also good for  $^{228}Th$  in the 1122 - 2600 m sample. The discrepancy between the  $^{228}Th$  concentration determined on the front and back adsorber in sample 1110 - 1500 m cannot as yet be explained.

Radioisotopes were measured in the less than 1-mm size fraction of samples from all sediment trap sites. The greater than 1-mm size fraction constituted less than 5% of all but the 667-m STIE samples (Table 5-1). Fluxes of isotopes calculated later in the discussion may therefore be low by a few percent, although this will not change any of the conclusions drawn from the results.

---

(1) A much more efficient system, in which seawater is pumped through a cartridge filled with  $MnO_2$ -coated fibers, has been developed by Reid et al. (1979).

TABLE 5-4

Effective Volumes of Seawater Sampled by MnO<sub>2</sub>-Nitex Adsorbers.

Station	Depth (m)	Volume Filtered (liters)	Volume <sup>a</sup> Sampled (liters)	Scavenging Efficiency (percent)
1110	1500 (front)	3005	212+19	7.1
	1500 (back)	3005	311+22	10.4
	2250	2190	178+24	8.1
	3000	1413	151+13	10.7
1114	2000	3530	563+49	15.9
	3000	1945	203+17	10.4
	4700	1732	244+19	14.1
1117	1500	2487	170+15	6.8
	2250	1909	444+37	23.3
	2900	3347	492+37	14.7
1120	1000	3195	170+15	6.8
	1500	2591	139+11	5.4
	2250	2112	193+15	9.1
	3100	4265	248+25	5.8
1122	1100	2877	444+27	15.4
	1600	3888	393+20	10.1
	2100	1928	362+23	18.8
	2600 (front)	1755	311+28	17.7
	2600 (back)	1755	202+14	11.5

<sup>a</sup>Volume sampled was calculated as  $(^{234}\text{Th dpm}) / (2.5 - P)$ ,  
where P was the concentration of particulate <sup>234</sup>Th.

TABLE 5-5

KN 73-16: Dissolved Radioisotopes.

Sample Station/Depth	$^{232}\text{Th}$	$^{230}\text{Th}$	$^{228}\text{Th}$	$^{231}\text{Pa}$	$^{230}\text{Th}/^{231}\text{Pa}$
	(dpm/ $10^6$ liters)				Activity Ratio
1110-1500 (front)	-3+11	133+25	348+57	Lost	---
1110-1500 (back)	-8+8	151+21	505+55	42.8+6.0	3.54+0.60
1110-2250	89+21	420+67	865+135	51+11	8.2+1.6
1110-3000	54+21	181+31	1130+120	47+10	3.85+0.59
1114-2000	9.6+4.8	223+25	247+32	41.6+6.3	5.35+0.78
1114-3000	15+12	306+39	412+54	40.4+8.1	7.6+1.6
1114-4700	1890+160	615+57	1630+140	37.7+6.0	16.3+2.3
1117-1500	49+21	442+68	235+62	ND	---
1117-2250	47+12	439+45	435+97	ND	---
1117-2900	12+8	337+33	508+50	35.6+5.0	9.5+1.3
1120-1000	29+16	262+41	587+82	ND	---
1120-1500	84+22	477+64	395+111	49+11	9.7+2.3
1120-2250	19+13	545+59	104+44	40.4+8.9	13.5+2.9
1120-3100	38+12	285+38	141+42	40.7+7.6	7.0+1.3
1122-1100	7+6	300+27	180+51	93+10	3.22+0.36
1122-1600	13+6	328+27	100+24	75.6+8.5	4.34+0.52
1122-2100	7+7	365+33	182+32	104+12	3.49+0.39
1122-2600 (front)	9+9	297+35	370+49	56+10	5.3+1.0
1122-2600 (back)	7+12	268+37	345+56	ND	---

ND = Not Determined.

Concentrations of particulate radioisotopes in KN 73-16 samples are presented in two ways. Specific activities in dpm/g of particles are presented in Table 5-6 for comparison with STIE samples. Concentrations in dpm/ $10^6$  l are presented in Table 5-7 for comparison with concentrations of dissolved isotopes measured on the  $MnO_2$  adsorbers (Table 5-5).

Total  $^{230}Th/^{231}Pa$  activity ratios in STIE samples are listed in Table 5-2. Detrital, uranium-supported  $^{230}Th$  and  $^{231}Pa$  were calculated for STIE samples assuming that all of the  $^{232}Th$  is detrital and that the detrital  $^{238}U/^{232}Th$  activity ratio is  $0.8 \pm 0.4$ . This ratio was chosen as a best estimate from a survey of the literature. Sediment samples were not available from the STIE site to estimate the detrital U/Th ratio as was done at Sites E and P. Unsupported  $^{230}Th$  and  $^{231}Pa$  values calculated with the above detrital uranium correction are presented in Table 5-8. Activity ratios are decreased only a little from those in Table 5-2.

Particulate  $^{232}Th$  concentrations were too low to be accurately measured in many of the samples of filtered particles. Therefore,  $^{230}Th$  and  $^{231}Pa$  activities in these samples were not corrected for detrital, uranium-supported contributions. However, the corrections would be small, and would not have a significant effect on the Th/Pa ratios.

## DISCUSSION

### Scavenging of Thorium and Protactinium in the Panama Basin

Specific activities of  $^{230}Th$  and  $^{231}Pa$  in trapped particles both increased with depth at the STIE Site (Figures 5-2 and 5-3), similar to patterns observed at other sediment trap sites (Chapter 3). The linear



TABLE 5-6

KN 73-16 Particulate Radioisotope Concentrations - dpm/g.

Sample Station/Depth	$^{232}\text{Th}$	$^{230}\text{Th}$	$^{228}\text{Th}$	$^{231}\text{Pa}$	$^{238}\text{U}$	$^{230}\text{Th}/^{231}\text{Pa}$
	(dpm/g)				Activity Ratio	
1110-1500	0.133 $\pm$ .056	3.01 $\pm$ .23	4.63 $\pm$ .37	0.377 $\pm$ .061	1.08 $\pm$ .20	8.0 $\pm$ 1.4
1110-2250	0.043 $\pm$ .055	2.99 $\pm$ .21	5.25 $\pm$ .38	0.296 $\pm$ .054	0.55 $\pm$ .17	10.1 $\pm$ 2.0
1110-3000	0.257 $\pm$ .082	3.44 $\pm$ .29	12.05 $\pm$ .71	1.17 $\pm$ .11	0.78 $\pm$ .22	2.95 $\pm$ .38
1114-2000	0.206 $\pm$ .031	3.20 $\pm$ .16	2.36 $\pm$ .14	0.428 $\pm$ .043	Lost	7.47 $\pm$ .83
1114-3000	0.107 $\pm$ .045	2.69 $\pm$ .20	2.92 $\pm$ .23	0.403 $\pm$ .062	0.63 $\pm$ .19	6.7 $\pm$ 1.1
1114-4700	36.9 $\pm$ 1.8	12.23 $\pm$ .66	26.4 $\pm$ 1.3	1.57 $\pm$ .11	0.88 $\pm$ .20	7.78 $\pm$ .69
1117-1500	-.007 $\pm$ .067	2.72 $\pm$ .26	1.99 $\pm$ .26	0.353 $\pm$ .062	0.73 $\pm$ .21	7.7 $\pm$ 1.6
1117-2250	0.08 $\pm$ .10	5.85 $\pm$ .45	2.72 $\pm$ .38	0.464 $\pm$ .087	0.89 $\pm$ .32	12.6 $\pm$ 2.6
1117-2900	0.122 $\pm$ .043	6.40 $\pm$ .36	5.78 $\pm$ .41	0.935 $\pm$ .074	0.91 $\pm$ .26	6.85 $\pm$ .67
1120-1000	0.05 $\pm$ .14	3.00 $\pm$ .29	3.04 $\pm$ .46	0.166 $\pm$ .060	0.59 $\pm$ .25	18.1 $\pm$ 6.3
1120-1500	0.08 $\pm$ .09	5.39 $\pm$ .36	3.34 $\pm$ .34	0.322 $\pm$ .069	0.77 $\pm$ .10	16.7 $\pm$ 3.8
1120-2250	0.06 $\pm$ .12	9.13 $\pm$ .53	2.50 $\pm$ .40	0.54 $\pm$ .11	0.91 $\pm$ .35	17.0 $\pm$ 3.6
1120-3100	0.14 $\pm$ .11	8.87 $\pm$ .59	7.07 $\pm$ .82	1.363 $\pm$ .082	0.94 $\pm$ .21	6.51 $\pm$ .58
1122-1100	0.017 $\pm$ .061	4.19 $\pm$ .31	4.35 $\pm$ .39	0.205 $\pm$ .087	1.02 $\pm$ .43	20.4 $\pm$ 8.8
1122-1600	0.087 $\pm$ .071	8.42 $\pm$ .48	3.50 $\pm$ .35	0.452 $\pm$ .061	0.91 $\pm$ .22	18.6 $\pm$ 2.7
1122-2100	0.074 $\pm$ .081	7.12 $\pm$ .52	2.94 $\pm$ .39	0.657 $\pm$ .092	0.90 $\pm$ .25	10.8 $\pm$ 1.7
1122-2600	0.050 $\pm$ .061	6.37 $\pm$ .43	3.60 $\pm$ .39	0.647 $\pm$ .086	0.50 $\pm$ .22	9.8 $\pm$ 1.5

TABLE 5-7

KN-73-16 Particulate Radioisotope Concentrations - dpm/10<sup>6</sup> l.

Sample Station/Depth	<sup>232</sup> Th	<sup>230</sup> Th	<sup>228</sup> Th	<sup>231</sup> Pa	<sup>238</sup> U	<sup>234</sup> Th
	(dpm/ 10 <sup>6</sup> liters)					(dpm/l)
1110-1500	2.9+1.2	55.6+5.0	107+9	8.2+1.3	23.6+4.3	0.172+.019
1110-2250	0.7+.9	47.0+3.3	82.6+5.5	4.65+.85	8.7+2.7	0.100+.006
1110-3000	4.9+1.6	65.3+5.6	229+13	22.2+2.2	14.7+4.2	0.209+.013
1114-2000	4.1+.62	63.7+3.1	47.0+2.7	8.53+.85	Lost	0.101+.013
1114-3000	1.70+.72	42.4+3.1	46.2+3.7	6.38+.98	9.9+3.1	0.0643+.0072
1114-4700	707+34	234+13	507+25	30.1+2.1	16.9+3.9	0.153+.013
1117-1500	-.08+.80	32.8+3.1	24.0+3.1	4.26+.75	8.8+2.5	0.0523+.0058
1117-2250	0.73+.94	56.1+4.3	26.0+3.6	4.45+.84	8.5+3.1	0.0432+.0092
1117-2900	1.52+.54	79.8+4.5	72.0+5.1	11.7+.92	11.4+3.3	0.1113+.0095
1120-1000	0.3+.9	20.4+2.0	20.7+3.1	1.13+.41	4.0+1.7	0.0486+.0030
1120-1500	0.8+.9	50.9+3.4	31.6+3.2	3.05+.66	7.3+2.4	0.0663+.0068
1120-2250	0.5+1.0	74.8+4.4	20.5+3.3	4.40+.90	7.4+2.8	0.0413+.0058
1120-3100	1.2+1.0	73.9+4.9	58.9+6.8	11.35+.68	7.8+1.8	0.104+.018
1122-1100	0.14+.48	33.4+2.4	34.7+3.1	1.63+.70	8.1+3.4	0.049+.005
1122-1600	0.69+.57	67.1+3.9	27.9+2.8	3.60+.49	7.3+1.7	0.057+.007
1122-2100	1.0+1.1	100+7	41.3+5.5	9.2+1.3	12.7+3.5	0.117+.011
1122-2600	0.08+.10	101+7	57.0+6.2	10.3+1.4	7.7+3.4	0.122+.015

TABLE 5-8  
 Unsupported  $^{230}\text{Th}$  and  $^{231}\text{Pa}$  in STIE Sediment Trap Samples.

Depth (m)	$^{230}\text{Th}$	$^{231}\text{Pa}$	$^{230}\text{Th}/^{231}\text{Pa}$
	$x_s$ (dpm/g)	$x_s$ (dpm/g)	(Activity Ratio)
667	0.381 $\pm$ .039	0.0610 $\pm$ .0038	6.25 $\pm$ .75
1268	0.873 $\pm$ .051	0.1739 $\pm$ .0083	5.02 $\pm$ .38
2869	2.142 $\pm$ .096	0.2741 $\pm$ .0096	7.81 $\pm$ .44
3769	2.84 $\pm$ .13	0.534 $\pm$ .020	5.31 $\pm$ .32
3791	3.25 $\pm$ .14	0.792 $\pm$ .024	4.10 $\pm$ .21
2265-RT-5	1.940 $\pm$ .094	0.278 $\pm$ .012	6.98 $\pm$ .45
2265-RT-4	1.468 $\pm$ .079	0.186 $\pm$ .009	7.91 $\pm$ .57
2265-RT-3	1.768 $\pm$ .086	Lost	--

Unsupported activities were calculated assuming that the uranium series were in radioactive equilibrium in detrital phases and that the detrital  $^{238}\text{U}/^{232}\text{Th}$  activity ratio was 0.8 $\pm$ 0.4.

Figure 5-2. Thorium-230 content of sediment-trap samples collected at the STIE Site.

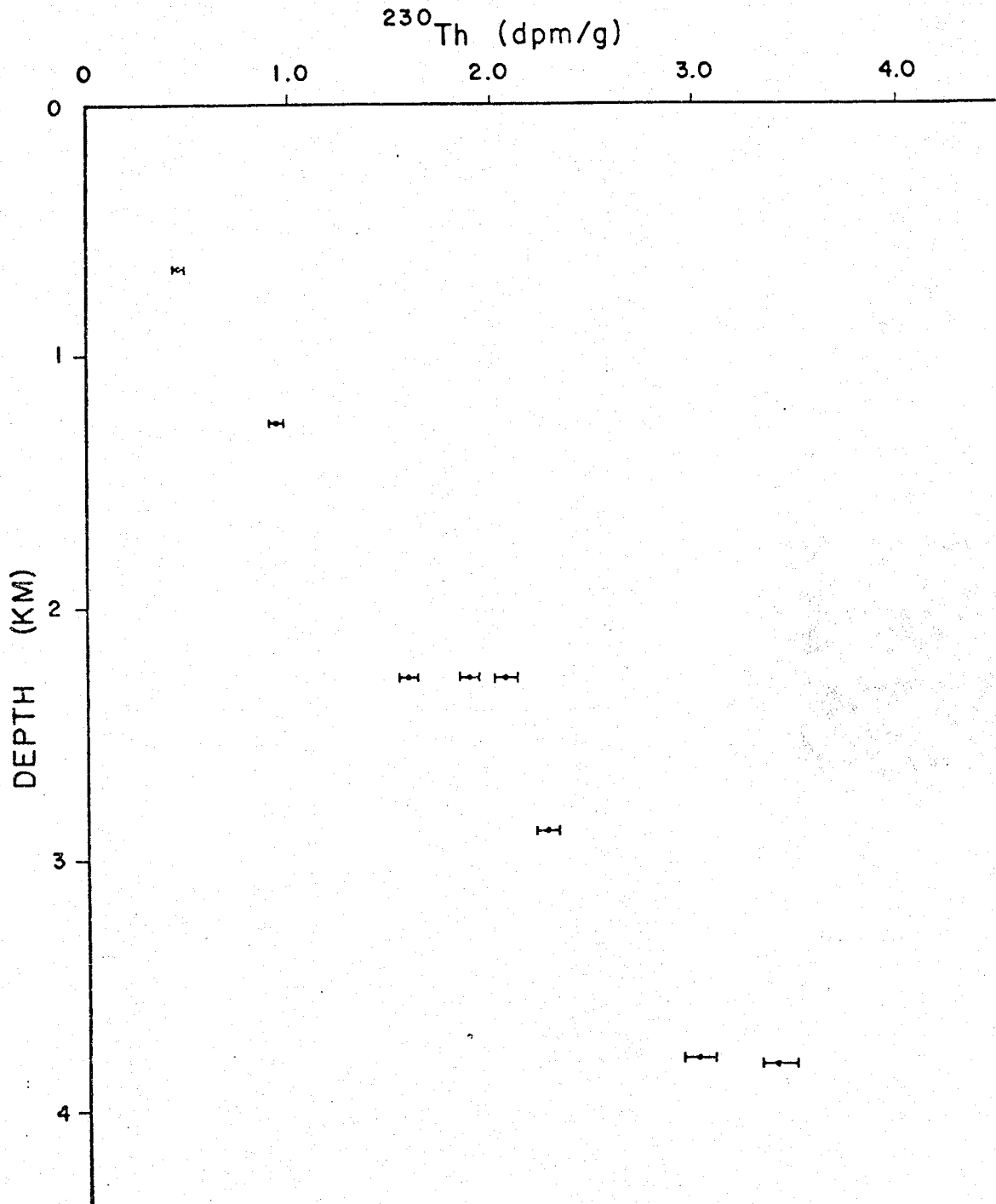


Figure 5-3. Protactinium-231 content of sediment-trap samples collected at the STIE Site.

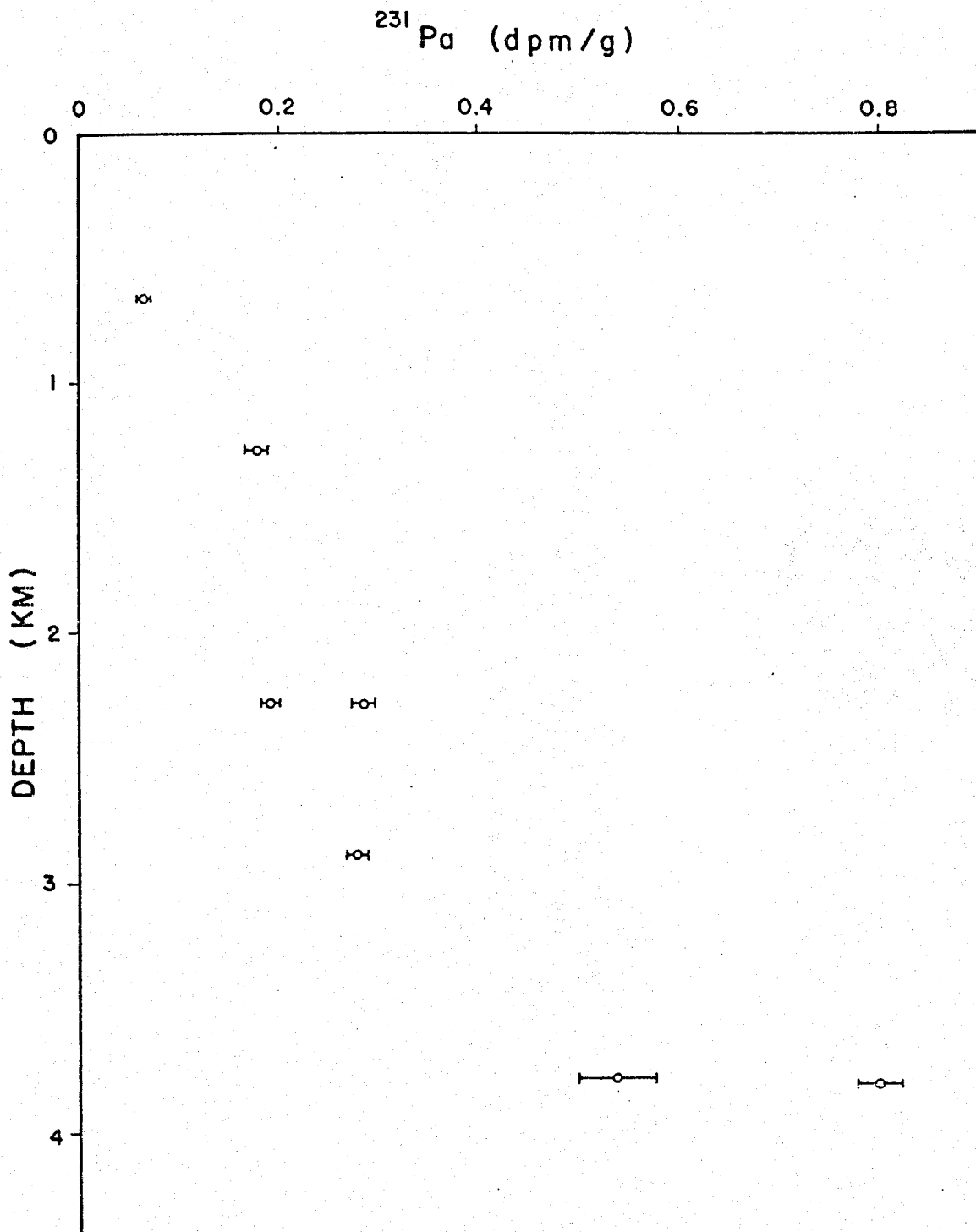
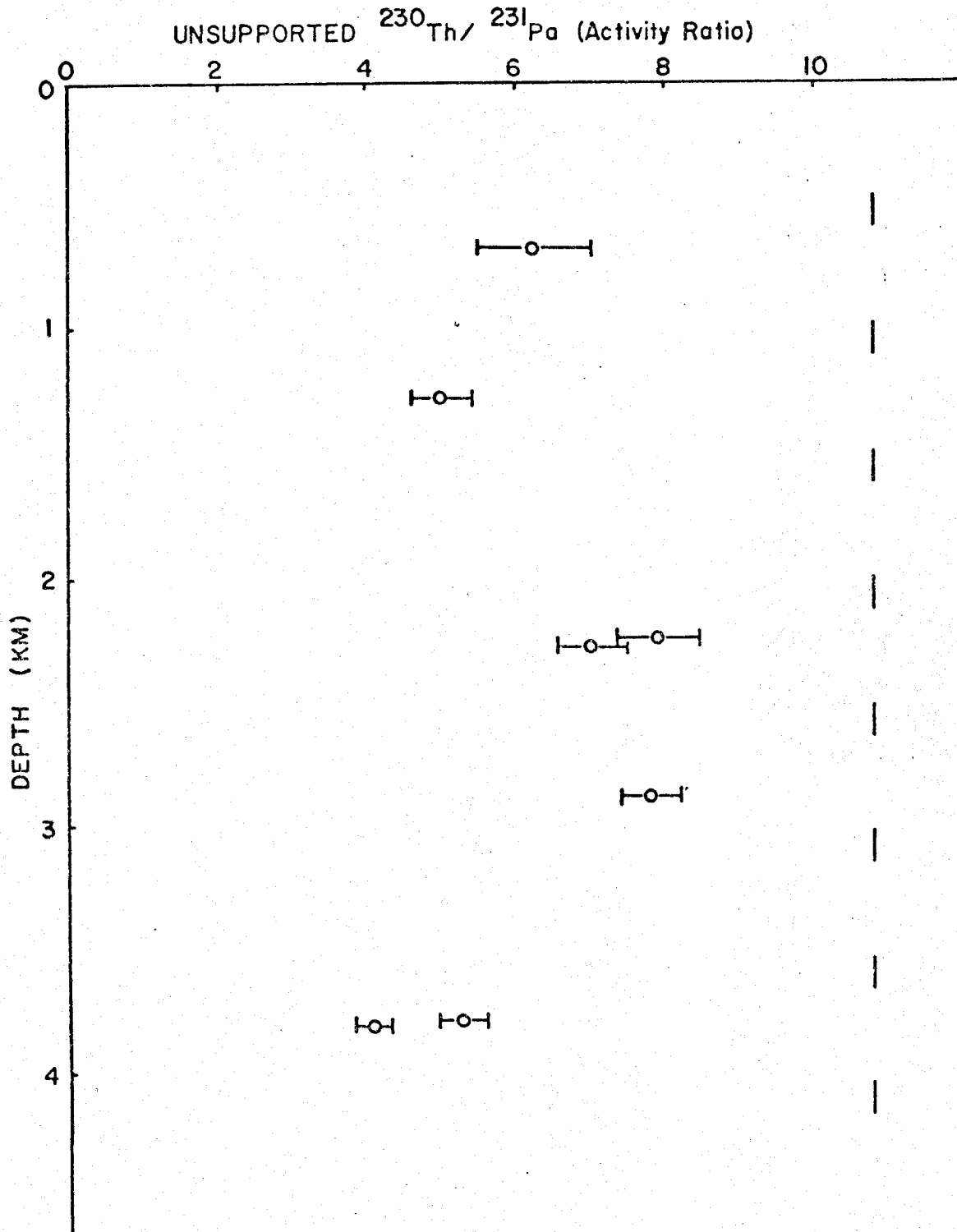


Figure 5-4. Unsupported  $^{230}\text{Th}/^{231}\text{Pa}$  activity ratio in sediment-trap samples from the STIE Site. The dashed line indicates the ratio at which  $^{230}\text{Th}$  and  $^{231}\text{Pa}$  are produced by uranium decay.



increase with depth in the specific activities of  $^{230}\text{Th}$  and  $^{231}\text{Pa}$  is consistent with continuous scavenging of dissolved  $^{230}\text{Th}$  and  $^{231}\text{Pa}$  by settling particles. The major contrast in radiochemical results between STIE samples and those from Sites S<sub>2</sub>, E, and P is found in the  $^{230}\text{Th}/^{231}\text{Pa}$  ratio. Ratios were less than 8, and as low as 4 (Table 5-8; Figure 5-4) in the STIE samples, approaching values of dissolved  $^{230}\text{Th}$  and  $^{231}\text{Pa}$  ratios (Chapter 4; Table 5-5). At the open ocean PARFLUX sites,  $^{230}\text{Th}/^{231}\text{Pa}$  ratios increase with depth in trapped material, while at the STIE site the deepest sample had the lowest ratio, although there was no real trend with depth.

Particle fluxes at the STIE Site are 2-4 times greater than at Site E and an order of magnitude greater than at Site P (Table 3-1 and 5-1). Particulate  $^{230}\text{Th}$  fluxes at the STIE Site were roughly three times greater than at corresponding depths at Sites S<sub>2</sub>, E, and P, while the fluxes of particulate  $^{231}\text{Pa}$  were about an order of magnitude higher than at the other sites (Table 5-9; Figures 3-7 and 3-8).

Ratios of the fluxes of particulate  $^{230}\text{Th}$  and  $^{231}\text{Pa}$  to their rates of production by uranium decay in the overlying water column increased with depth at the STIE Site (Table 5-9; Figures 5-5 and 5-6). This may have resulted from one or more of four processes: 1) input of sediments resuspended locally from the sea floor may have increased with depth, 2) incorporation of winnowed particulate material from areas where the sea floor is shallower than the traps may have increased with depth, 3) although all of the traps were identical, trapping efficiencies of the sediment traps may have increased with depth, and 4) loss of material due to zooplankton grazing in the traps may have decreased with depth. None of these processes can be proven as solely responsible for the increase in the flux to production ratios.

TABLE 5-9

Fluxes of Unsupported  $^{230}\text{Th}$  and  $^{231}\text{Pa}$  into STIE Sediment Traps<sup>a</sup>.

Depth (m)	Flux: $\text{dpm/cm}^2 \cdot 10^3 \text{ y}$		Ratio: Flux/Production <sup>b</sup>	
	$^{230}\text{Th}$	$^{231}\text{Pa}$	$^{230}\text{Th}$	$^{231}\text{Pa}$
667	1.34 $\pm$ .14	0.215 $\pm$ .013	0.773	1.34
1268	3.33 $\pm$ .19	0.664 $\pm$ .032	1.01	2.18
2869	11.93 $\pm$ .52	1.527 $\pm$ .053	1.60	2.14
3769	18.15 $\pm$ .86	3.42 $\pm$ .13	1.85	3.78
3791	21.05 $\pm$ .88	5.14 $\pm$ .16	2.13	5.65
2265-RT-5	15.54 $\pm$ .75	2.227 $\pm$ .096	2.64	4.09
2265-RT-4	8.36 $\pm$ .45	1.057 $\pm$ .051	1.42	1.94
2265-RT-3	7.54 $\pm$ .37	Lost	1.28	--

<sup>a</sup>Measurements were made on the less than 1-mm size fraction of trapped particles. See Table 1.

<sup>b</sup>Integrated production by decay of uranium in the overlying water column.



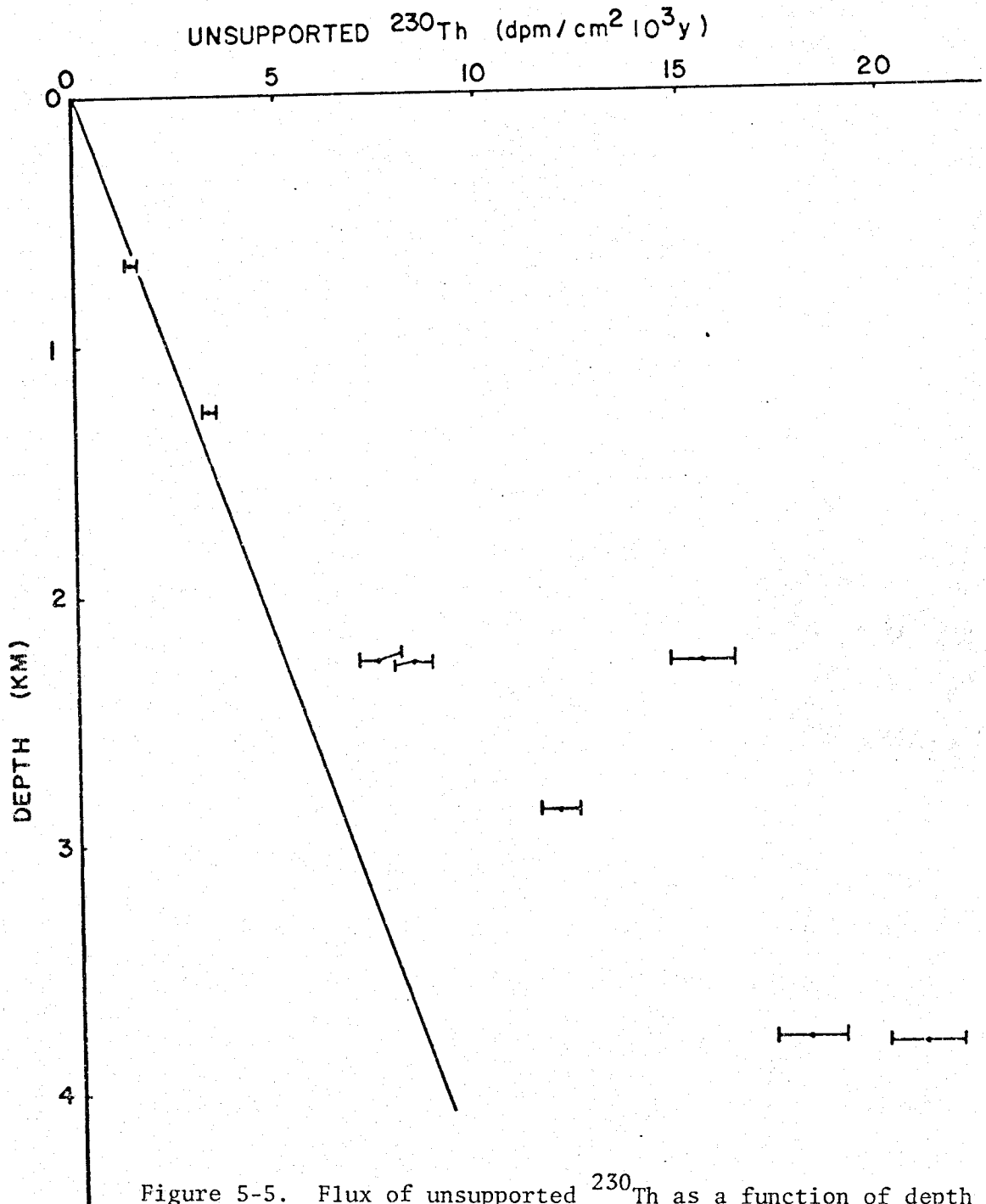


Figure 5-5. Flux of unsupported  $^{230}\text{Th}$  as a function of depth at the STIE Site. The solid line indicates the integrated rate of supply by uranium decay in the water column as a function of depth.

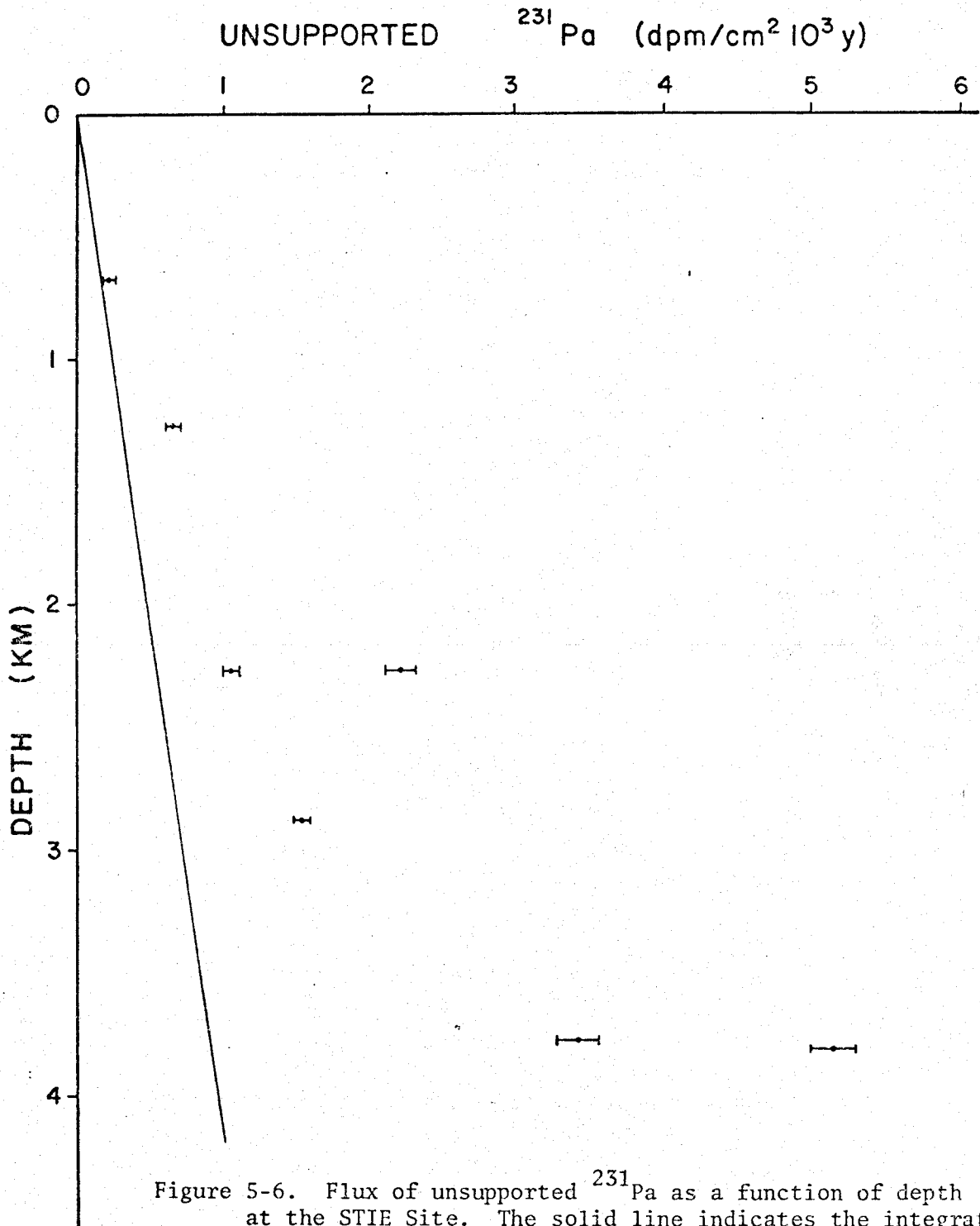


Figure 5-6. Flux of unsupported  $^{231}\text{Pa}$  as a function of depth at the STIE Site. The solid line indicates the integrated rate of supply by uranium decay as a function of depth.

Current meters placed on the sediment trap moorings below 2000 m showed velocities of only a few cm/sec (Honjo, personal communication), probably not high enough to erode and resuspend sediment from the sea floor. However, much greater current velocities were measured above 2000 m. Particle fluxes increased by a factor of two with depth (Table 5-1), and mineralogical evidence indicates that much of the increase resulted from incorporation of sediments winnowed from the slope area to the north and nothwest of the site (S. Honjo, personal communication).

Plutonium and organic matter contents of the trapped material indicate that the winnowed particles may be recently derived from the sea surface. The plutonium concentration in trapped material in the deepest sample was 75% of the concentration in the shallowest sample (Table 5-2). Plutonium has a source near the sea surface, and does not exist in sediments greater than about 30 years old. The organic matter content of trapped material also remained high in the deepest samples (S. Honjo, personal communication), more like the shallower trap samples than typical surface sediments.

As it is reasonably certain that the sediment traps at the STIE Site collected particles winnowed from local topographic highs, it is impossible to determine from sediment-trap results the extent to which the Panama Basin is acting as a sink for  $^{230}\text{Th}$  and  $^{231}\text{Pa}$  introduced by horizontal mixing from the open ocean. However, concentrations of dissolved  $^{230}\text{Th}$  and  $^{231}\text{Pa}$  are lower at the STIE Site than at Site P (see discussion below), so mixing should result in a net transfer of dissolved  $^{230}\text{Th}$  and  $^{231}\text{Pa}$  from the open ocean to the Panama Basin. The low  $^{230}\text{Th}/^{231}\text{Pa}$  ratios in the STIE samples indicates that a

greater proportion of the  $^{231}\text{Pa}$  than the  $^{230}\text{Th}$  in the trapped particles had a source by mixing from the open ocean, consistent with the conclusions of Chapter 3 that more  $^{231}\text{Pa}$  than  $^{230}\text{Th}$  is removed from the open ocean by horizontal mixing.

Particles filtered at the STIE Site (Station 1110, Figure 5-1) had  $^{230}\text{Th}/^{231}\text{Pa}$  ratios similar to ratios measured in trapped particles (Tables 5-2 and 5-6). As filtration tends to sample smaller particles than sediment traps, particle size is not a factor in the ratio at which  $^{230}\text{Th}$  and  $^{231}\text{Pa}$  are scavenged at the STIE Site. The same conclusion was reached from Site E samples (Chapter 3).

A  $^{230}\text{Th}/^{231}\text{Pa}$  ratio of  $3.0 \pm .4$  was measured in particles filtered at 3000 m at Station 1110 (Table 5-6). The deepest trap sample also had the lowest unsupported  $^{230}\text{Th}/^{231}\text{Pa}$  ratio ( $4.1 \pm .2$ ; Table 5-8). Neither value is significantly different from the dissolved ratio of  $3.9 \pm .6$  in the deepest sample at Station 1110 (Table 5-5).

Adsorption of thorium and protactinium to particles without measurable fractionation is suggestive of the adsorptive behavior of  $\text{MnO}_2$  (Chapter 4). Redox processes in the sediments in the area of the STIE Site may cause the precipitation of  $\text{MnO}_2$  at the sediment surface (Lynn and Bonatti, 1965; Bonatti et al., 1971). Higher manganese contents were found in some of the STIE samples than in any of the samples from Sites S<sub>2</sub>, E, and P, presumably as  $\text{MnO}_2$ . Manganese and aluminum contents of sediment-trap samples are given in Table 5-10. Excess Mn (xsMn) is calculated as

$$\text{xs Mn} = \text{Mn}_T - (\text{Mn/Al})_L \times \text{Al}_T \quad (1)$$

where  $\text{Mn}_T$  and  $\text{Al}_T$  are the total Mn and Al contents in the samples and  $(\text{Mn/Al})_L$  is the lithogenous, or detrital, Mn/Al ratio, which

TABLE 5-10

Calculated MnO<sub>2</sub> in Sediment Trap Samples.

Sample Depth (m)	Al <sup>a</sup> (ppm)	Mn <sup>a</sup>	Mn/Al (Weight Ratio)	MnO <sub>2</sub> <sup>b</sup> (ppm)	<sup>xs</sup> 230Th/ <sup>xs</sup> 231Pa (Activity Ratio)
<u>STIE</u>					
667	11800	191	0.016	211	6.25+.75
1268	14500	186	0.013	182	5.02+.38
2265-RT 4	17600	253	0.014	264	7.91+.57
2265-RT 5	24400	370	0.015	397	6.98+.45
2869	27200	1610	0.059	2358	7.81+.44
3769	37000	9880	0.267	15512	5.31+.32
3791	38700	9240	0.239	14474	4.10+.21
<u>Site S<sub>2</sub></u>					
3694	21800	780	0.036	1073	27+2
<u>Site E</u>					
389	7600	56	0.0073	29	12+2
988	13100	78	0.0060	20	12.4+1.1
3755	28900	330	0.0114	297	21.7+1.2
5086	36400	460	0.0126	445	29.6+1.8
<u>Site P</u>					
978	1400	63	0.045	90	18.3+1.7
2778	2900	69	0.024	87	30.0+1.0
4280	2900	53	0.018	62	34.9+1.7
5582	9400	404	0.043	571	30.3+1.6

<sup>a</sup>Al and Mn results from Brewer et al. (1980) and Brewer et al. (in preparation).

<sup>b</sup>MnO<sub>2</sub> is calculated as 1.6 (xsMn), where xsMn is calculated from Equation ( 1 ).

unfortunately is not well defined. The average crustal Mn/Al ratio is 0.0123 (Krauskopf, 1979), greater than or equal to the ratios found in many of the sediment trap samples. The lowest ratio found in any sediment-trap sample was about 0.006, nearly the same as the minimum values found in particles filtered in Atlantic surface seawater (Krishnaswami and Sarin, 1976). A value of  $(\text{Mn}/\text{Al})_L$  of 0.005 was assumed considering the above information, and to avoid zero or negative values of  $x_{\text{Mn}}$ . Values of  $\text{MnO}_2$ , calculated as  $1.6(x_{\text{Mn}})$ , are presented in Table 5-10.

A negative correlation between unsupported  $^{230}\text{Th}/^{231}\text{Pa}$  ratios and  $\text{MnO}_2$  would be expected if  $\text{MnO}_2$  accounts for a significant proportion of the total scavenged  $^{230}\text{Th}$  and  $^{231}\text{Pa}$ . There is a negative correlation for the data in Table 5-10, however the correlation coefficient is only -0.44, slightly less than the correlation coefficient of -0.497 required to be significant at the 5% level of confidence, and this is largely determined by the two deepest STIE samples. When these two samples are excluded from the calculation, the correlation coefficient is reduced to -0.12, which is not significant.

The minimal effect of the  $\text{MnO}_2$  content of trapped particles on the  $^{230}\text{Th}/^{231}\text{Pa}$  ratios can be shown by another calculation using two STIE samples as examples. It is assumed for the calculation that  $^{230}\text{Th}$  and  $^{231}\text{Pa}$  are adsorbed to  $\text{MnO}_2$  to the same extent as to the surfaces of manganese nodules, which have  $^{230}\text{Th}$  contents as high as 1000 dpm/g and  $^{230}\text{Th}/^{231}\text{Pa}$  activity ratios as low as 3 (Ku and Broecker, 1969; Krishnaswami and Cochran, 1978). Then the 2265-m RT5 sample, with 397 ppm  $\text{MnO}_2$  should have 0.397 dpm  $^{230}\text{Th}$  and 0.132 dpm  $^{231}\text{Pa}$  per gram of sample associated with the  $\text{MnO}_2$ . The  $^{230}\text{Th}$  and  $^{231}\text{Pa}$  associated

with the remainder of the sample ( $^{230}\text{Th} = 2.091 - 0.397 = 1.694$  dpm/g;  $^{231}\text{Pa} = 0.285 - 0.132 = 0.153$  dpm/g) are present at an activity ratio of 10.4.

The same conditions for adsorption of  $^{230}\text{Th}$  and  $^{231}\text{Pa}$  to  $\text{MnO}_2$  can be applied to the 3769-m sample, which had 15500 ppm  $\text{MnO}_2$ . This sample would then contain 15.5 dpm  $^{230}\text{Th}$  and 5.2 dpm  $^{231}\text{Pa}$  per gram associated exclusively with the  $\text{MnO}_2$ , much more than the total  $^{230}\text{Th}$  and  $^{231}\text{Pa}$  contents of 3.06 and 0.54 dpm/g respectively. Thus the quantities of  $^{230}\text{Th}$  and  $^{231}\text{Pa}$  estimated above to be associated with the  $\text{MnO}_2$  in the 2265-m RT5 sample were much too large. STIE samples above 2300 m all had  $\text{MnO}_2$  contents and  $^{230}\text{Th}/^{231}\text{Pa}$  ratios similar to the 2265-m RT5 sample. Therefore, particles other than  $\text{MnO}_2$  are adsorbing  $^{230}\text{Th}$  and  $^{231}\text{Pa}$  at low  $^{230}\text{Th}/^{231}\text{Pa}$  ratios in the Panama Basin. The effect of particle composition on  $^{230}\text{Th}/^{231}\text{Pa}$  ratios will be discussed further in Chapter 6.

#### Scavenging of Thorium and Protactinium in the Guatemala Basin

Profiles of particulate  $^{230}\text{Th}$  and  $^{231}\text{Pa}$  concentrations along the transect into the Guatemala Basin are shown in Figure 5-7a and b. Particulate  $^{230}\text{Th}$  concentrations increased with depth (Figure 5-8), in a pattern similar to that found by Krishnaswami et al. (1976) farther to the west in the Pacific. Krishnaswami et al. used a one-dimensional, steady-state scavenging model to derive an average particle settling rate of 300-900 m/y from the increase with depth in their measured particulate  $^{230}\text{Th}$  concentration. It is assumed in their model that  $^{230}\text{Th}$  is removed from the water column exclusively by irreversible scavenging to settling particles. Thus their model predicts a linear increase with depth in the particulate  $^{230}\text{Th}$  concentration. Mid-depth minima in

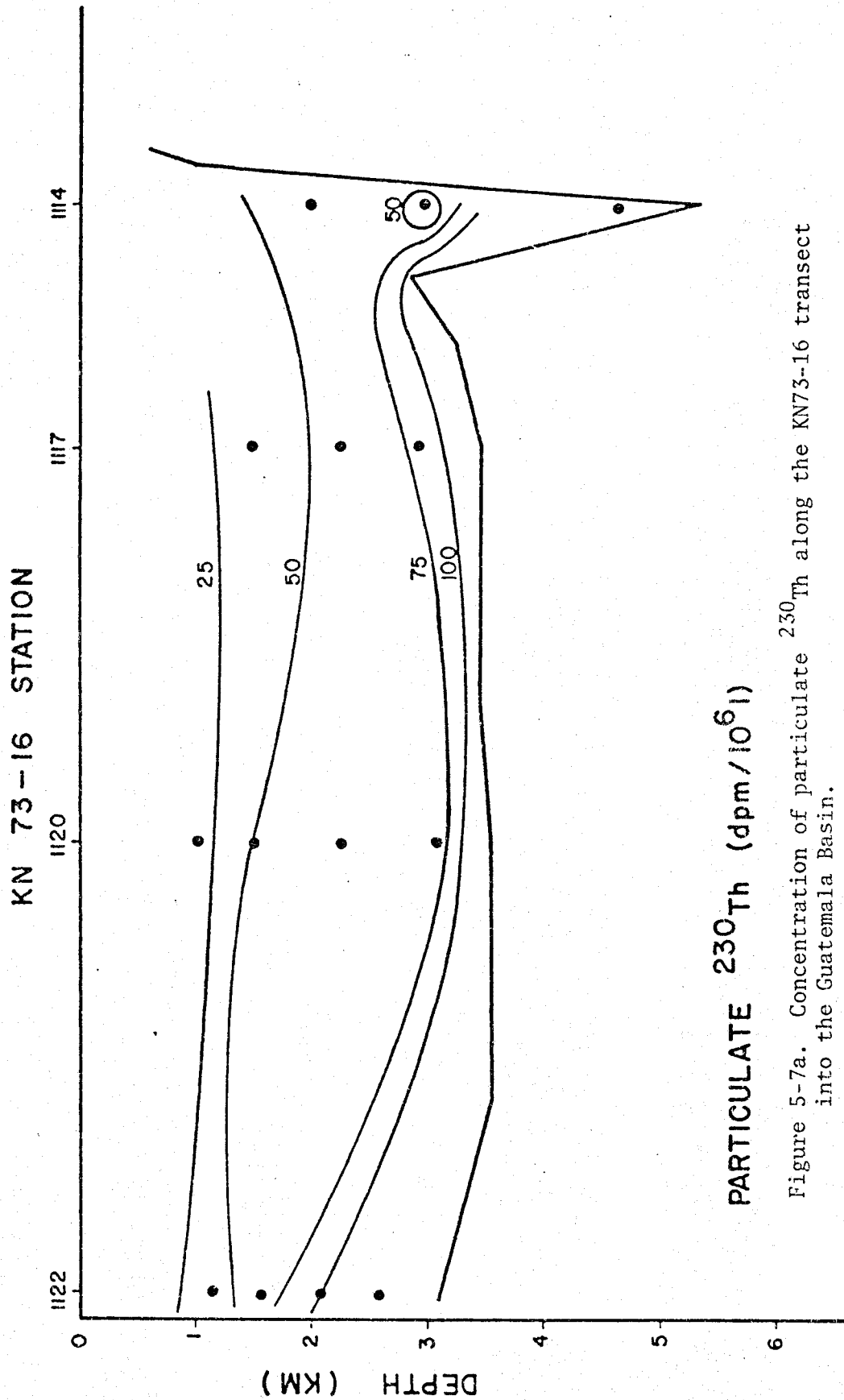
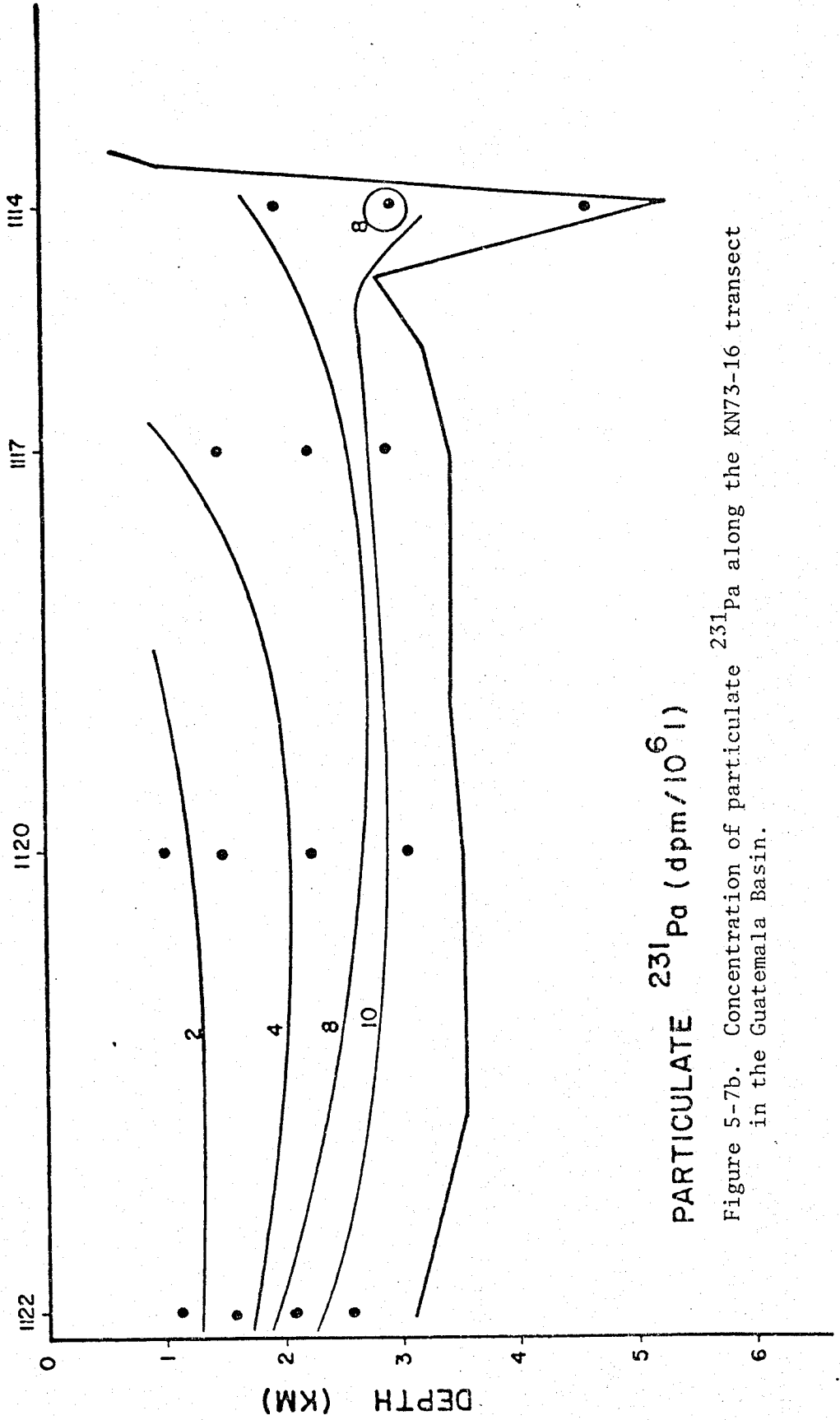


Figure 5-7a. Concentration of particulate  $^{230}\text{Th}$  along the KN73-16 transect into the Guatemala Basin.



KN 73-16 STATION

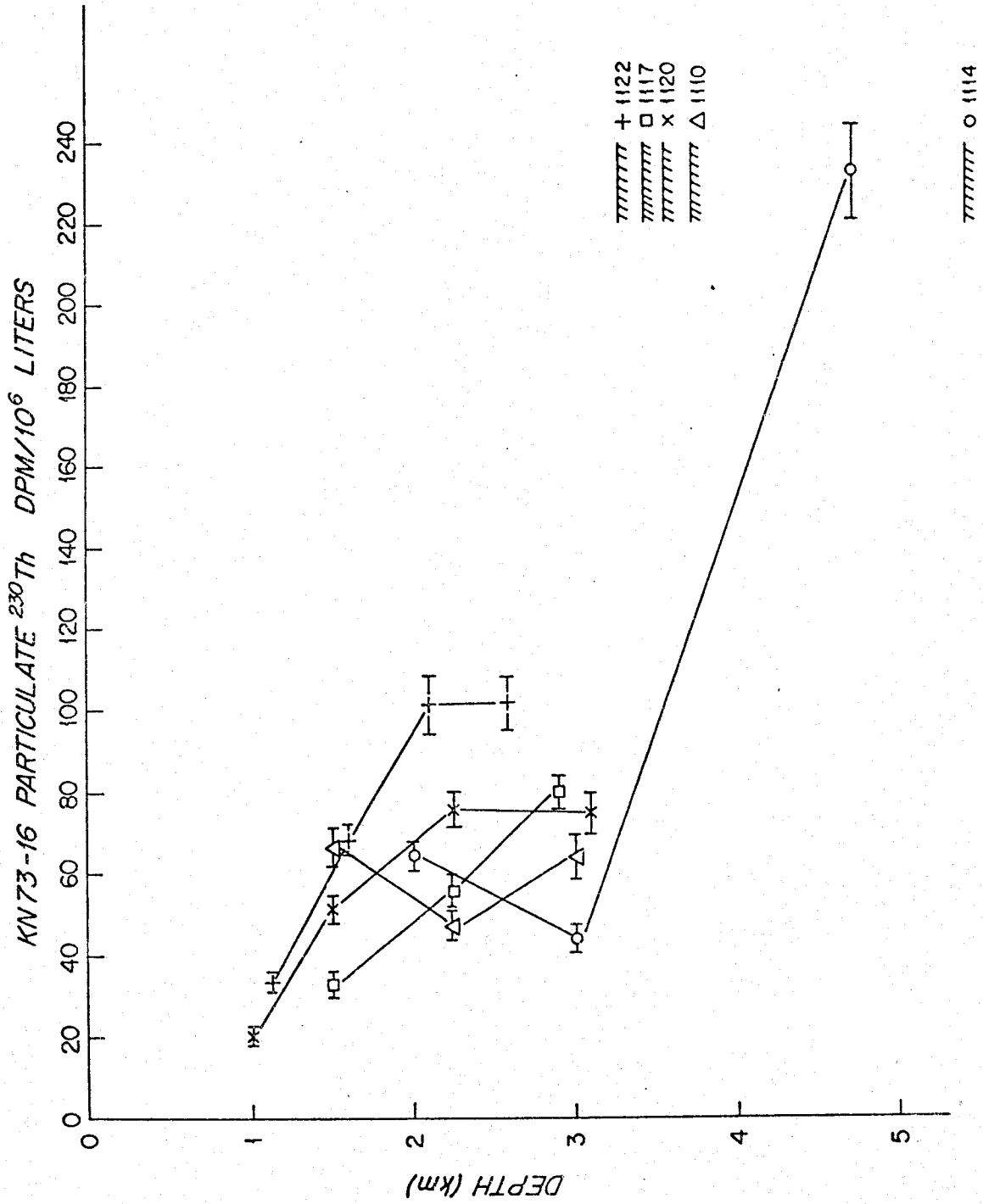


PARTICULATE  $^{231}\text{Pa}$  ( $\text{dpm}/10^6 \text{ l}$ )

Figure 5-7b. Concentration of particulate  $^{231}\text{Pa}$  along the KN73-16 transect in the Guatemala Basin.

Figure 5-8. Concentration of particulate  $^{230}\text{Th}/^{231}\text{Pa}$  at the KN 73-16 stations. The trend of the data, although strongly influenced by the point at Station 1114-4700 m, is the same as was found by Krishnaswami et al. (1976). The hatched areas indicate the depth at each station.

Figure 5-8



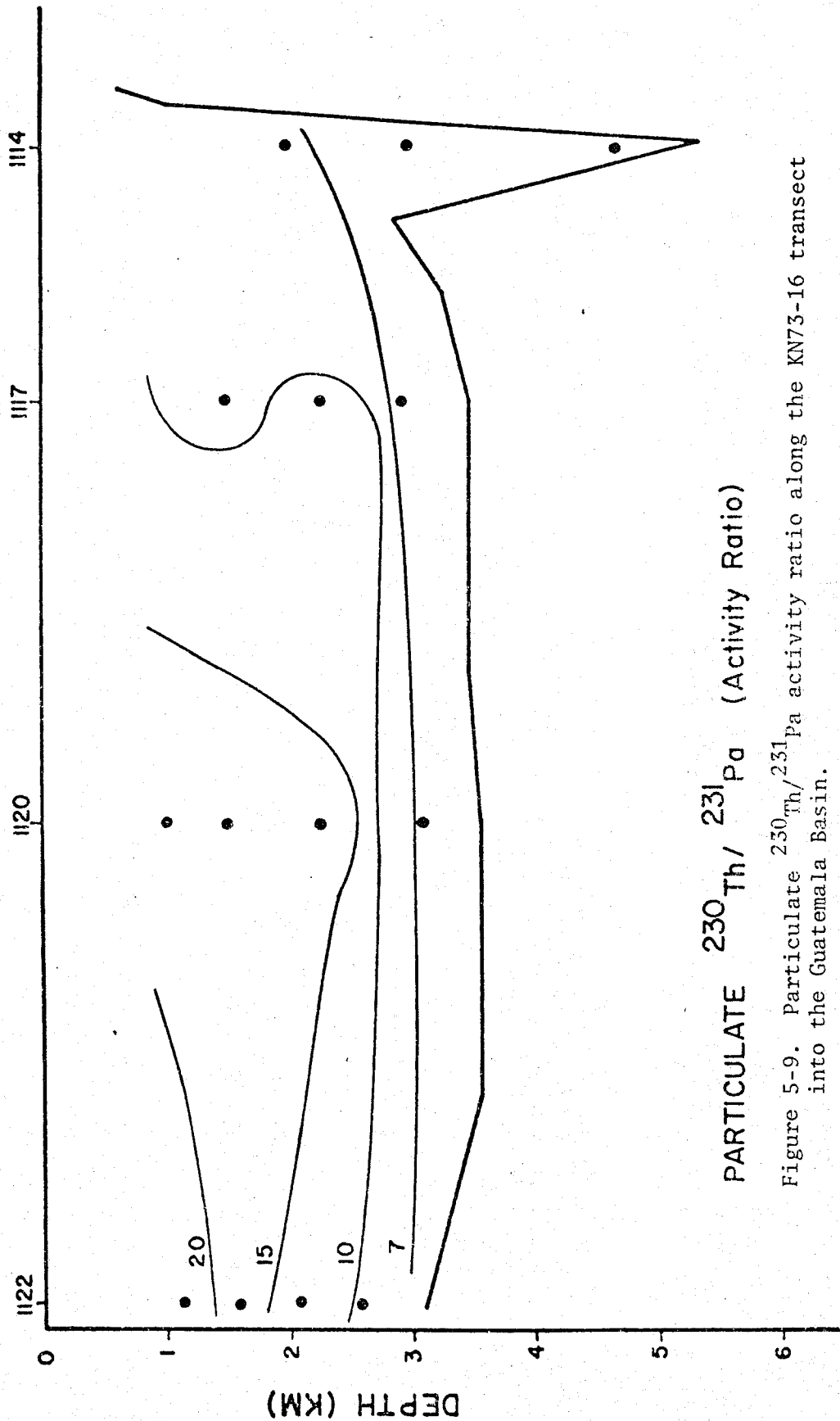
particulate  $^{230}\text{Th}$  concentrations at Station 1110 - 2250 m and 1114 - 3000 m, and at some of the stations sampled by Krishnaswami et al., indicate that the model is not strictly valid. Thorium-230 is redistributed by mixing processes from the open ocean to areas with higher scavenging rates. Current directions and velocities varied with depth and with time at the STIE Site (S. Honjo, personal communication). If a similar variability in current direction with depth is a common feature in the ocean, then horizontal mixing may affect the distributions of dissolved  $^{230}\text{Th}$ , and  $^{230}\text{Th}$  associated with the fine fraction of particles collected by filtration, to different extents at different depths, resulting in the observed mid-depth minima in the concentration of particulate  $^{230}\text{Th}$ .

The settling rate calculated by Krishnaswami et al. (1976) is much less than the apparent settling rates of particles collected with sediment traps (Chapter 3; Brewer et al., 1980; Deuser and Ross, 1980). Particles samples by in situ filtration tend to be smaller than particles collected with sediment traps. Particles greater than 62  $\mu$  were excluded by prefiltration from the KN 73-16 samples, and generally constitute a small portion of the total particulate material sampled by filtration. In contrast, the 62  $\mu\text{m}$ -1 mm size fraction constituted 25-55% of the trapped particles collected at Sites S<sub>2</sub>, E, and P (Honjo, 1980). Some disaggregation of large particles collected by sediment traps occurred prior to their size determination (Honjo, 1980), so particles greater than 62  $\mu$  constituted an even greater proportion of the trapped material than the amount determined by sieving. Therefore the greater settling rates inferred for the trapped particles compared with the filtered particles are consistent with the known differences in their size distributions.

Particulate  $^{230}\text{Th}/^{231}\text{Pa}$  activity ratios are shown in Figure 5-9. Two trends are immediately obvious: 1) the ratio increases into the open ocean and 2) the ratio decreases with depth, particularly at Stations 1120 and 1122. The first trend is predicted from the conclusions of Chapter 3. Thorium is preferentially scavenged by settling particles in the open ocean. Open ocean conditions are approached at stations 1120 and 1122 and the  $^{230}\text{Th}/^{231}\text{Pa}$  ratios there are similar to values found in sediment trap samples at similar depths at Sites E and P. The second trend is opposite to that observed at the open-ocean sediment trap sites, where  $^{230}\text{Th}/^{231}\text{Pa}$  ratios increased with depth. The dissolved  $^{230}\text{Th}/^{231}\text{Pa}$  ratio does not decrease with depth at Stations 1120 and 1122 (Table 5-5). Therefore, particles near the sea floor are chemically different from those at shallower depths, having less preference for adsorption of Th (Chapter 6).

A mid-depth maximum was found for the concentration of dissolved  $^{230}\text{Th}$  (Figure 5-10). Since production of  $^{230}\text{Th}$  by uranium decay occurs at a constant rate throughout the section, the rate of removal must be lowest at mid-depth. This is not unexpected, as very rapid removal rates have been found for Th isotopes in surface waters, presumably as a result of biological activity and higher concentrations of particulate matter (Bhat et al., 1969; Broecker et al., 1973; Matsumoto, 1975; Knauss et al., 1978). Scavenging rates may increase near the sea floor, either because of increased concentrations and fluxes of particle caused by resuspension of bottom sediments, or because of direct contact of the water with the sea floor. A near-bottom decrease in the  $^{230}\text{Th}$  concentration was not observed at an open-ocean site ( $30^{\circ}32'\text{N}$ ,  $170^{\circ}39'\text{E}$ ) studied by Nozaki (in preparation). Bacon et al. (1976)

### KN 73-16 STATION



### PARTICULATE $^{230}\text{Th}/^{231}\text{Pa}$ (Activity Ratio)

Figure 5-9. Particulate  $^{230}\text{Th}/^{231}\text{Pa}$  activity ratio along the KN73-16 transect into the Guatemala Basin.

KN 73-16 STATION

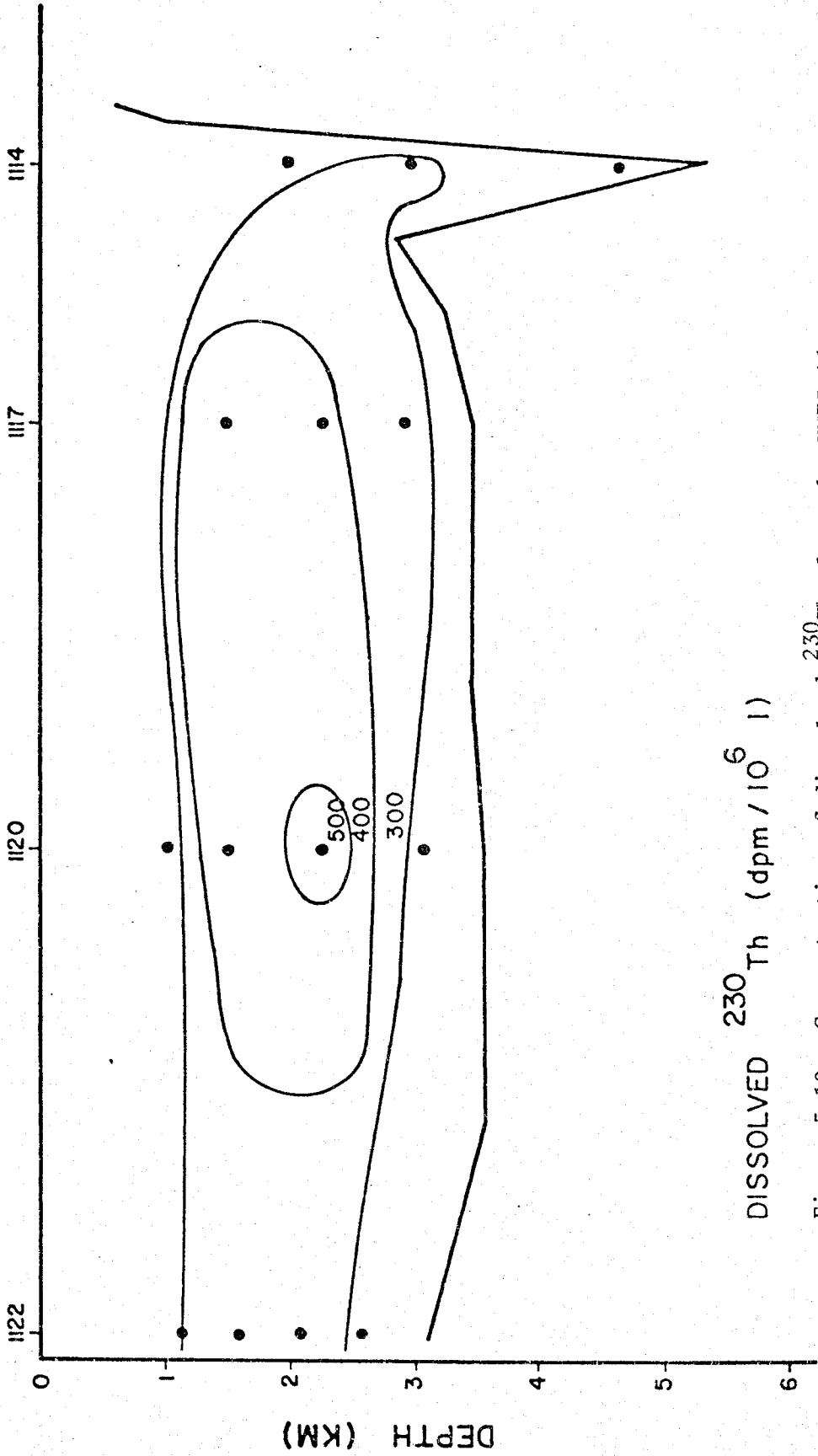


Figure 5-10. Concentration of dissolved  $^{230}\text{Th}$  along the KN73-16 transect into the Guatemala Basin.

suggested that  $^{210}\text{Pb}$  may be scavenged at the sediment-seawater interface in ocean margin environments by iron and manganese oxides precipitating in surface sediments. Manganese oxides are precipitating at or near the sediment-seawater interface in the area of the transect (Lynn and Bonatti, 1965; Bonatti et al., 1971), which could account for the greater scavenging efficiency of the sea floor in this area compared to the open-ocean site studied by Nozaki (in preparation). Scavenging to manganese dioxide would also partially explain the lower particulate  $^{230}\text{Th}/^{231}\text{Pa}$  ratios near the sea floor (Chapter 6), although as discussed in regard to the STIE Site, manganese oxides may not be the only factor affecting the ratio.

The model of Bacon et al. (1976) predicts that the lowest mid-depth concentrations of  $^{230}\text{Th}$  would be found near the continental margin and that concentrations would increase with distance into the open ocean. There is a tendency for the  $^{230}\text{Th}$  concentration to decrease toward the margin, but it also decreases at mid-depth at the seaward end of the transect (Figure 5-10). This implies that there may be another sink for  $^{230}\text{Th}$  at mid-depth beyond the seaward end of the transect. There does not appear to be a similar mid-depth sink for Pa at the seaward end of the transect as dissolved protactinium concentrations were highest at Station 1122 (Table 5-5) and were nearly constant at the other stations at values about half the concentration measured at Station 1122. If the data reflect a real sink for Th and not for Pa, then this may result from a change in the concentration and composition of suspended particles (Chapter 6). Higher biological productivity at the equator, off the seaward end of the transect, may increase the flux of biogenic particles enough to significantly increase the rate of scavenging of Th. Particles



at Site P were predominantly biogenic, and had high  $^{230}\text{Th}/^{231}\text{Pa}$  ratios. The influence of the particles responsible for the low  $^{230}\text{Th}/^{231}\text{Pa}$  ratios near the continental margin decreases into the open ocean, as evidenced by the increasing particulate  $^{230}\text{Th}/^{231}\text{Pa}$  ratios. The decreasing influence of these particles may offset the increased scavenging of  $^{231}\text{Pa}$  by the higher flux of biogenic particles. The combined effect of the increasing flux of biogenic particles and the decreasing influence of margin-related particles could result in a lower concentration of dissolved  $^{230}\text{Th}$ , without a corresponding decrease in the concentration of dissolved  $^{231}\text{Pa}$ , at the seaward end of the transect. The above discussion is largely speculation given the limited amount of data. It is included to suggest where future sampling should be carried out to study the effect of particle composition on the fractionation of Th and Pa during adsorption from seawater.

Dissolved  $^{230}\text{Th}/^{231}\text{Pa}$  ratios are presented in Table 5-5. Ratios measured at Station 1122 are typical of open ocean values observed at Sites P and D (Chapter 4). Ratios tend to be higher at other stations, although no consistent pattern emerges. Sample 1114 - 4700 m, with an anomalously high ratio, will be discussed later. Within the counting errors, the other samples all have ratios less than or equal to the seawater production ratio of 10.8. Near-margin dissolved  $^{230}\text{Th}/^{231}\text{Pa}$  ratios greater than or equal to ratios in the open ocean prove that the low particulate  $^{230}\text{Th}/^{231}\text{Pa}$  ratios do not simply result from greatly increased scavenging rates compared to the open ocean. Particulate  $^{230}\text{Th}/^{231}\text{Pa}$  ratios would equal the ratio at which  $^{230}\text{Th}$  and  $^{231}\text{Pa}$  are supplied if scavenging rates were rapid enough to completely remove

all of the dissolved  $^{230}\text{Th}$  and  $^{231}\text{Pa}$  supplied to the area.

Thorium-230 and  $^{231}\text{Pa}$  are supplied at a ratio of 3-6 by horizontal transport from the open ocean and a ratio of 10.8 by uranium decay.

Particulate  $^{230}\text{Th}/^{231}\text{Pa}$  ratios are about a factor of ten greater than dissolved  $^{230}\text{Th}/^{231}\text{Pa}$  ratios in the open ocean (Chapters 3 and 4). If similar fractionation of Th and Pa during adsorption occurred in margin environments, then dissolved  $^{230}\text{Th}/^{231}\text{Pa}$  ratios less than one would be found. The results in Table 5-5 clearly show this not to be the case. Even if there is a small, systematic fractionation of Th and Pa during adsorption to  $\text{MnO}_2$ , the dissolved  $^{230}\text{Th}/^{231}\text{Pa}$  ratios at the STIE Site and at the landward end of the transect in the Guatemala Basin are greater than or equal to the dissolved ratios at Sites P and D. Therefore, the low particulate  $^{230}\text{Th}/^{231}\text{Pa}$  ratios do not result from increased scavenging rates, but must be caused by differences in the compositions of the particles between open-ocean and ocean-margin environments.

#### Reversibility of Scavenging Processes

Scavenging is generally assumed to be an irreversible process, where the steady state distribution of a dissolved reactive daughter isotope is expressed as

$$dA_d/dt = \lambda A_d^P - (\lambda + \psi) A_d = 0 \quad (2)$$

where:  $A_d$  is the activity of dissolved reactive daughter isotope

$\lambda$  is the radioactive decay constant of the daughter isotope

$A_d^P$  is the activity of the dissolved parent isotope

$\psi$  is the rate constant for removal by scavenging

Then  $\psi$  is calculated from measured values of  $A_d$  and  $A_d^P$ , and scavenging residence times,  $\tau_d$ , are calculated as  $1/\psi$ .

This can be shown to be in error. Approximately 4% of the total  $^{234}\text{Th}$  concentration in the deeper samples in the Guatemala Basin is particulate (Figures 5-11). Using Equation (2) with a  $^{238}\text{U}$  concentration of 2.5 dpm/l and a dissolved  $^{234}\text{Th}$  concentration of 2.4 dpm/l, a residence time for dissolved  $^{234}\text{Th}$  of 2.3 years is calculated. If this uptake is irreversible, and if  $\psi$  is the same for all Th isotopes, then dissolved  $^{230}\text{Th}$  should be present at 60 dpm/ $10^6$ -l in samples with 0.1 dpm/l particulate  $^{234}\text{Th}$ . The average dissolved  $^{230}\text{Th}$  concentration in samples with approximately 0.1 dpm/l of particulate  $^{234}\text{Th}$  was 370 dpm/ $10^6$ -l, clearly much greater than predicted by the irreversible uptake model. Therefore, there must be some mechanism by which  $^{230}\text{Th}$  is returned to solution, either by desorption from particles or by redissolution upon remineralization of labile carrier phases (Chapter 3). Recent work of Bacon (personal communication) indicates that the Th isotopes were in an adsorption-desorption equilibrium in the samples taken in the Panama and Guatemala Basins. Therefore, desorption and regeneration (Chapter 3) may both operate to return scavenged thorium to solution.

#### Residence Times of Thorium and Protactinium

Reactive isotopes such as  $^{230}\text{Th}$ ,  $^{228}\text{Th}$ ,  $^{234}\text{Th}$ ,  $^{231}\text{Pa}$ ,  $^{210}\text{Pb}$ , and  $^{210}\text{Po}$  are predominantly in the dissolved state in the deep open ocean in spite of their short residence times (this work; Bacon et al., 1976; Somayajulu and Craig, 1976). This is true even in areas near continental margins where scavenging rates are higher than in open-ocean environments. Particulate  $^{230}\text{Th}$  and  $^{231}\text{Pa}$  constitute less than a quarter of their total concentrations in the Guatemala Basin (Figure 5-12a and b). Therefore, particle concentrations greater than those

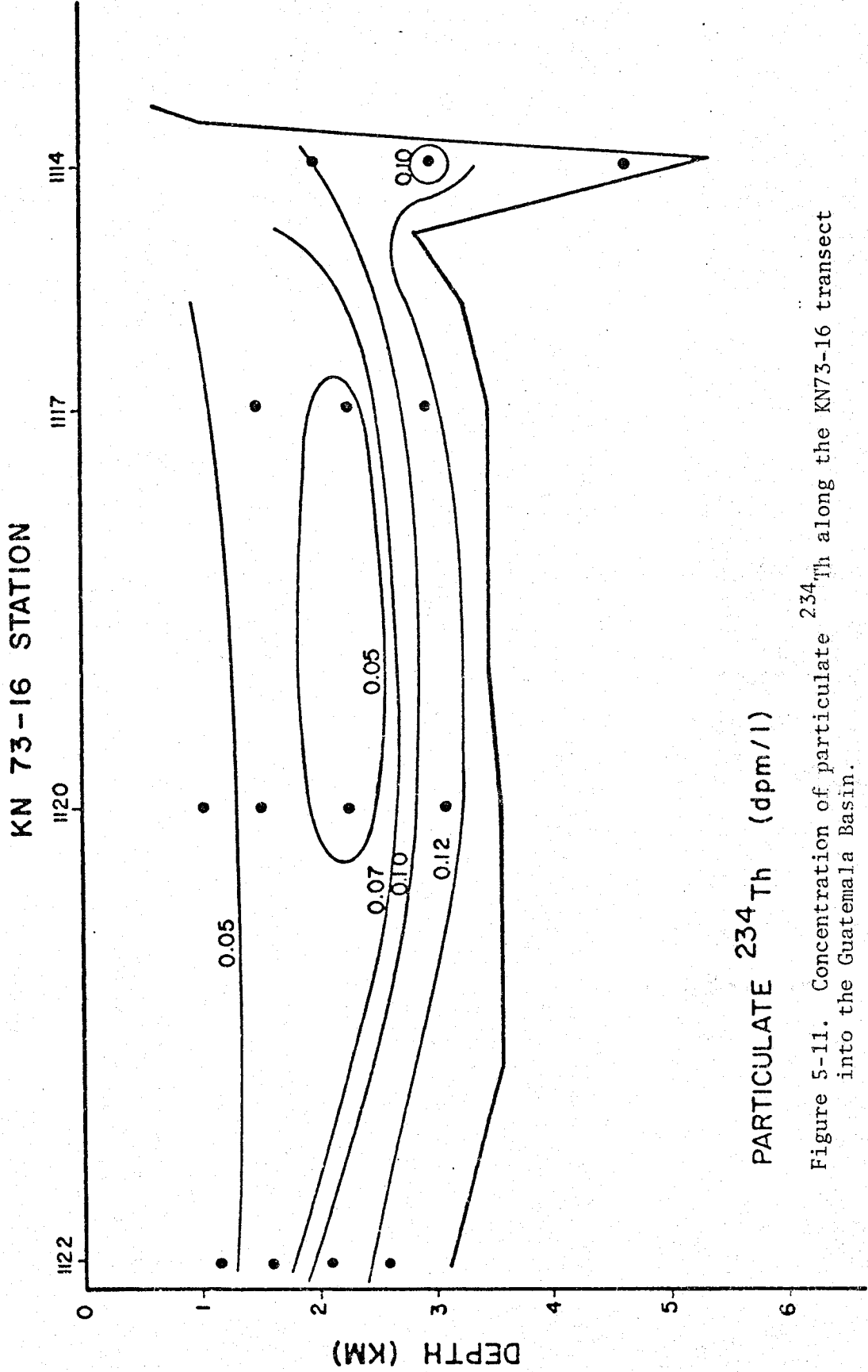


Figure 5-11. Concentration of particulate  $^{234}\text{Th}$  along the KN73-16 transect into the Guatemala Basin.

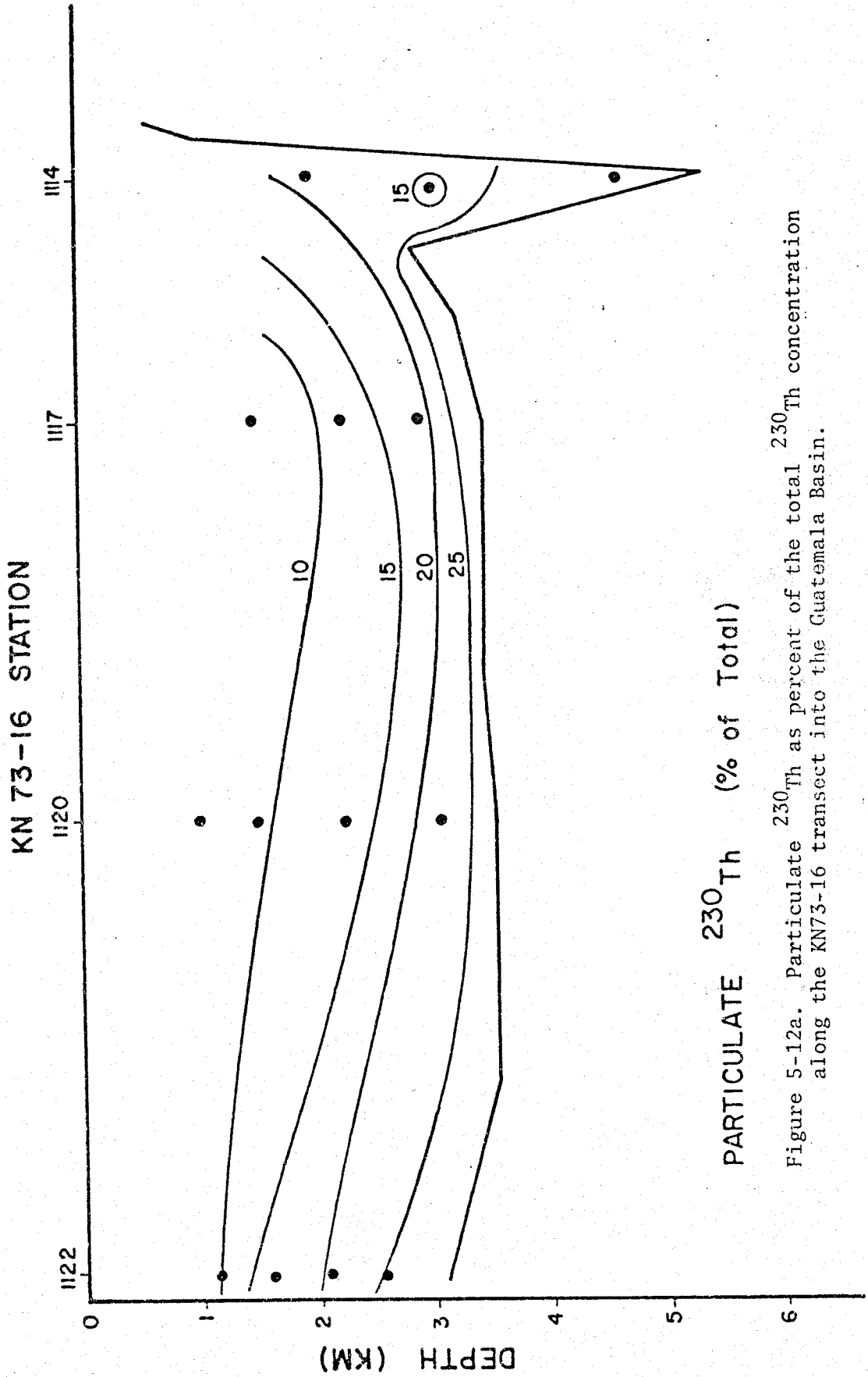
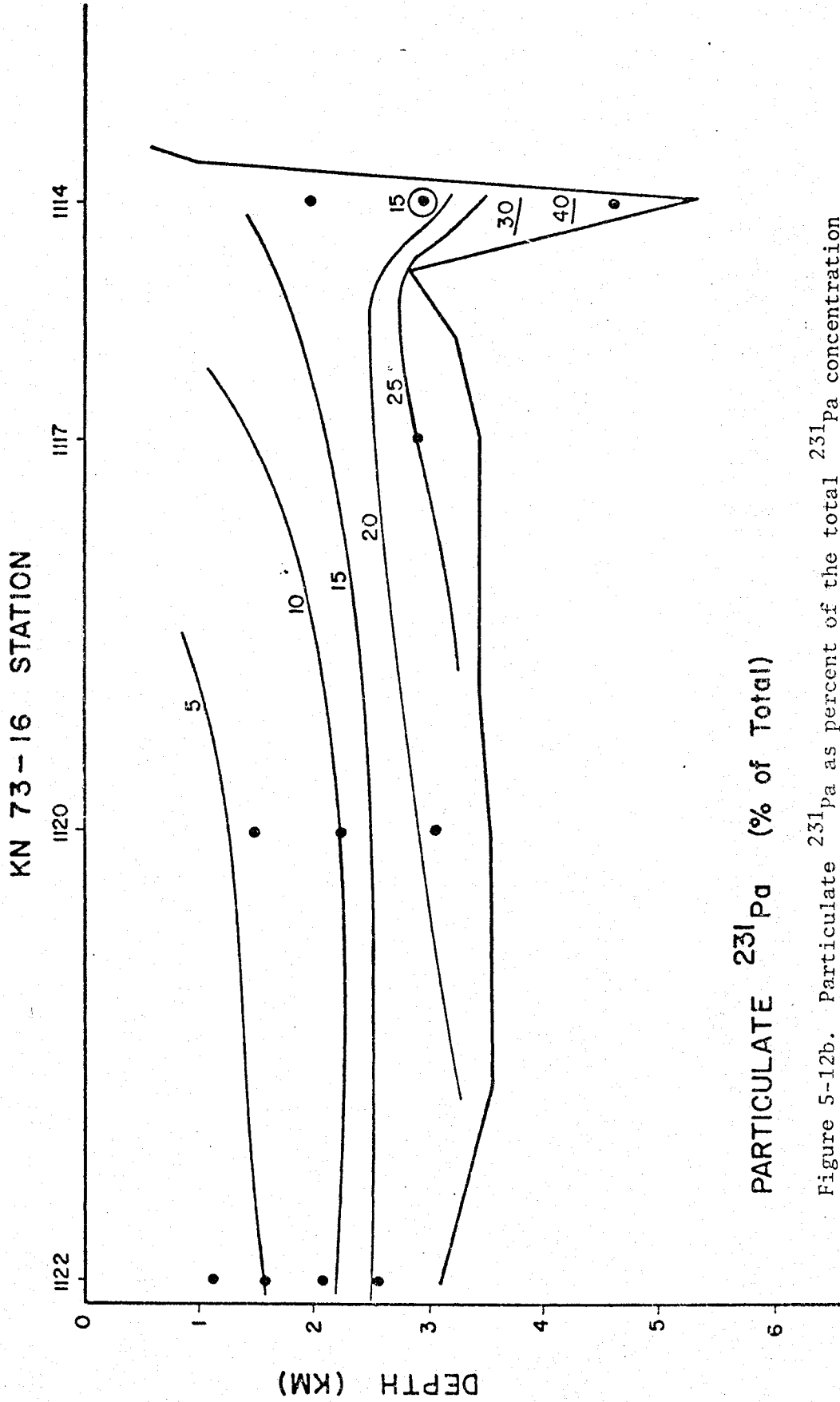


Figure 5-12a. Particulate  $^{230}\text{Th}$  as percent of the total  $^{230}\text{Th}$  concentration along the KN73-16 transect into the Guatemala Basin.



PARTICULATE  $^{231}\text{Pa}$  (% of Total)

Figure 5-12b. Particulate  $^{231}\text{Pa}$  as percent of the total  $^{231}\text{Pa}$  concentration along the KN73-16 transect into the Guatemala Basin.

measured at these stations (10-20  $\mu\text{g}/\text{l}$ ; Figure 6-1) are required before the rates of removal of  $^{230}\text{Th}$  and  $^{231}\text{Pa}$  will be limited by the settling rate of particles rather than their rates of adsorption to particles.

It is of interest to compare the concentrations of dissolved  $^{230}\text{Th}$  and  $^{231}\text{Pa}$ , and their corresponding residence times, measured during KN 73-16 with those measured at open ocean Sites P and D (Chapter 4). The simplest approach would be to calculate residence times from measured concentrations of  $^{230}\text{Th}$  and  $^{231}\text{Pa}$  and their known production rates by uranium decay

$$\tau_d = A_d / (\lambda A_U) \quad (3)$$

where:  $\tau_d$  is the residence time of Th or Pa,  $A_d$  is the dissolved activity of  $^{230}\text{Th}$  or  $^{231}\text{Pa}$ ,  $\lambda$  is the radioactive decay constant of  $^{230}\text{Th}$  or  $^{231}\text{Pa}$ , and  $A_U$  is the activity of  $^{234}\text{U}$  or  $^{235}\text{U}$ .

Residence times calculated in this way from data obtained in the Panama and Guatemala Basins are presented in Table 5-11 along with a summary of the results from Sites D and P. Residence times of  $^{230}\text{Th}$  and  $^{231}\text{Pa}$  are both lower in the Panama and Guatemala Basins than at Sites D and P, although the maximum residence times found in the Guatemala Basin are within the lower part of the range of values observed at Site D. More rapid rates of removal of  $^{230}\text{Th}$  and  $^{231}\text{Pa}$  in the Panama and Guatemala Basins than in the open ocean would be expected from the reasons discussed at the beginning of this chapter.

If production by uranium decay is the only source of dissolved  $^{230}\text{Th}$  and  $^{231}\text{Pa}$ , then Equation (3) gives an accurate representation of their residence times. If scavenging is the only process removing dissolved Th and Pa from seawater, then the residence times from

TABLE 5-11

Residence Times of Dissolved  $^{230}\text{Th}$  and  $^{231}\text{Pa}$ <sup>a</sup>.

Sample Station/Depth	$^{230}\text{Th}$	$^{231}\text{Pa}$
	(Years)	
1110-1500 (front)	5.1	---
1110-1500 (back)	5.7	18
1110-2250	16	21
1110-3000	6.9	19
1114-2000	8.5	17
1114-3000	12	17
1114-4700	23	16
1117-1500	17	---
1117-2250	18	---
1117-2900	13	15
1120-1000	10	---
1120-1500	18	20
1120-2250	21	16
1120-3100	11	17
1122-1100	11	38
1122-1600	13	31
1122-2100	14	43
1122-2600 (front)	11	23
1122-2600 (back)	10	---
Site P, 3200 <sup>b</sup>	41	130
Site D, 3200 <sup>b</sup>	23 (16-28)	49 (34-69)

<sup>a</sup>Residence times were calculated from Equation 3 in the text and are directly proportional to the dissolved concentrations in Table 5-5.

<sup>b</sup>Results from Site P and average and range of results from Site D are given for comparison. From Chapter 4.



Equation (3) are appropriately designated scavenging residence times. However, Equation (3) neglects the effects of horizontal mixing. If scavenging and horizontal transport are the only processes that remove dissolved  $^{230}\text{Th}$  and  $^{231}\text{Pa}$  from the water column, then a more accurate representation of the scavenging residence time is

$$\tau_d' = A_d / (\lambda A_U + K_H \partial^2 A_d / \partial X^2) \quad (4)$$

where  $K_H$  is the horizontal eddy diffusivity and  $X$  is the horizontal distance. Therefore, the residence times in Table 5-11,  $\tau_d$ , are in error by the amount

$$\tau_d = [(\lambda A_U + K_H \partial^2 A_d / \partial X^2) / \lambda A_U] \tau_d' \quad (5)$$

At the open-ocean sites, where mixing acts as a sink for dissolved  $^{230}\text{Th}$  and  $^{231}\text{Pa}$ ,  $K_H \partial^2 A_d / \partial X^2 < 0$ , and  $\tau_d < \tau_d'$ .

Conversely, at the STIE Site, where horizontal transport acts as a source of  $^{230}\text{Th}$  and  $^{231}\text{Pa}$ ,  $K_H \partial^2 A_d / \partial X^2 > 0$ , and  $\tau_d > \tau_d'$ .

Horizontal transport acts as a sink for over half of the  $^{231}\text{Pa}$  produced by uranium decay at Sites  $S_2$ , E, and P, while it is less important as a sink for  $^{230}\text{Th}$  (Chapter 3). Therefore,  $^{231}\text{Pa}$  will be used in the following discussion to emphasize the importance of horizontal transport on the calculated scavenging residence times. If most of the  $^{231}\text{Pa}$  produced in the open ocean is removed by horizontal transport, then  $-K_H \partial^2 A_d^{Pa} / \partial X^2 > 0.5 (\lambda A_U)$ , and the true scavenging residence time,  $\tau_d'$ , is underestimated by at least a factor of two. Conversely, if the Panama Basin acts as a net sink for horizontally transported  $^{230}\text{Th}$  and  $^{231}\text{Pa}$ , then particulate  $^{230}\text{Th}/^{231}\text{Pa}$  ratios of 5-6 (Table 5-8) indicate that at least half of the  $^{231}\text{Pa}$  is derived by horizontal mixing from the open ocean. In this case, values of  $\tau_{Pa}$  in Table 5-11 are too high by a factor of at

least two at Station 1110. Therefore, because of horizontal transport of  $^{231}\text{Pa}$ ,  $\tau_{\text{Pa}}'(\text{Site P})/\tau_{\text{Pa}}'(\text{STIE})$  is at least four times greater than  $\tau_{\text{Pa}}(\text{Site P})/\tau_{\text{Pa}}(\text{STIE})$  calculated from residence times in Table 5-11. Then the actual scavenging rate of  $^{231}\text{Pa}$  in the Panama Basin is about 25 times greater than at Site P. Horizontal transport of  $^{230}\text{Th}$  and  $^{231}\text{Pa}$  is not well quantified, so true scavenging residence times,  $\tau_d'$ , cannot be determined like the easily calculated values of  $\tau_d$  in Table 5-11. Nevertheless, the values of  $\tau_d$  in Table 5-11 are useful as (1) they provide lower limits for the scavenging residence times in the open ocean, (2) they accurately represent the total residence times in open ocean areas where production by uranium decay is the only source of dissolved  $^{230}\text{Th}$  and  $^{231}\text{Pa}$ , and (3) they provide upper limits for scavenging residence times in areas like the Panama Basin which act as sinks for reactive elements transported from the open ocean.

One implication of these results is that very reactive elements, such as Pa, with an average oceanic residence time of less than 100 years, can be redistributed within the ocean by mixing processes when scavenging rates vary by an order of magnitude between two environments. Other reactive elements, including those of pollutant origin, may be similarly redistributed. The extent of redistribution of  $^{231}\text{Pa}$  would not have been predicted from the behavior of  $^{230}\text{Th}$ . Thus it is possible that redistribution of other elements may occur to an even greater extent than for Pa, the extent of redistribution being determined by the degree to which the efficiency of removal of the element in certain environments is enhanced relative to removal rates in the open ocean.

Geochemical Behavior of Other Isotopes

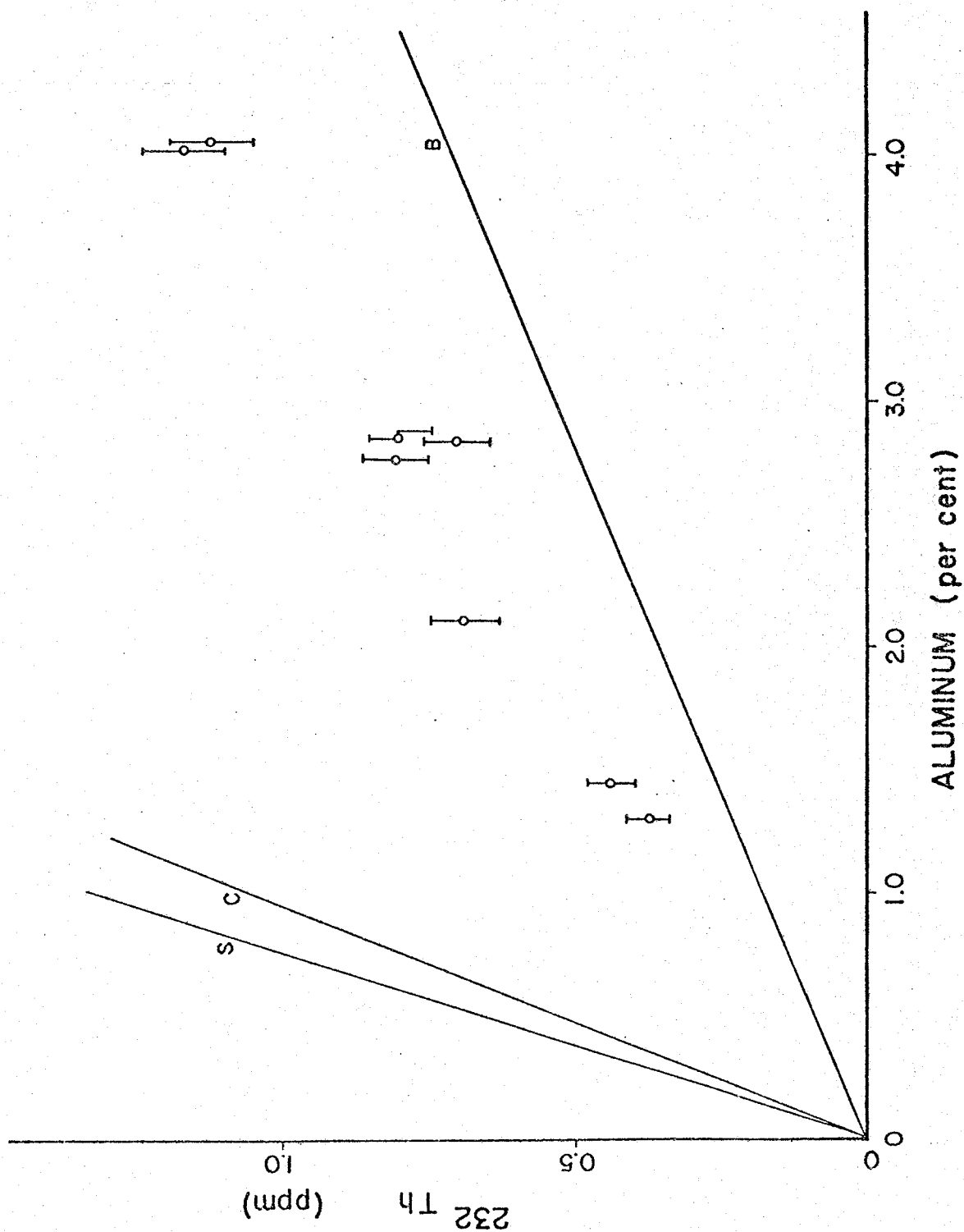
Thorium-232

Detrital minerals formed an increasing percent of the total trapped material with depth at the STIE Site, as they did at Sites S<sub>2</sub>, E, and P (Chapter 3: Honjo, 1980; Brewer et al., 1980). A strong correlation of all of the detrital elements with Al was observed at Site E, including <sup>232</sup>Th (Figure 3-11). The <sup>232</sup>Th/Al ratio in the trapped particles and underlying sediments at Site E was very close to the average ratio for shales. A strong positive correlation between <sup>232</sup>Th and Al was also found in samples from the STIE Site (Figure 5-13); however, the <sup>232</sup>Th/Al ratio is about a factor of four lower than at Site E. A major source of detrital material at Site E is atmospheric dust of Saharan origin with typical crustal or shale composition (Rydell and Prospero, 1972; Glaccum and Prospero, 1980). Detrital material at the STIE site is probably derived from Central America, which consists in large part of uplifted basalts. While the Th/Al ratio is somewhat greater than for average basalts (Figure 5-13), a contribution by basalts is clearly indicated. This suggests that Th/Al ratios may be a good indicator of sources of detrital minerals in deep sea sediments.

Concentrations of dissolved and particulate <sup>232</sup>Th are given in Tables 5-5 and 5-7, respectively. Several of the samples have levels of <sup>232</sup>Th significantly greater than blanks. While it is difficult to find trends in data so close to detection limits, it does appear that particulate <sup>232</sup>Th concentrations increase with depth and also increase near the continental margins (Stations 1110 and 1114). This distribution is reasonable since <sup>232</sup>Th is expected to be associated with detrital material supplied by resuspension and by input from the continent.

Figure 5-13. Thorium content plotted against aluminum for STIE sediment trap samples. The solid lines indicate average ratios for shales (S), crust (C), and basalts (B), from Krauskopf (1979). For comparison, samples at Sites E and P fell approximately on the line for average shales.

Figure 5-13.



Stations 1110 and 1114 near the continental margin have concentrations of particulate  $^{232}\text{Th}$  of a few  $\text{dpm}/10^6 \text{ l}$  (Table 5-7). Specific activities of  $^{232}\text{Th}$  in filtered particles at Stations 1110 and 1114 (Table 5-6) are similar to values measured in STE sediment-trap samples. At stations farther from the continent, the concentrations of particulate  $^{232}\text{Th}$  are lower, and only upper limits of about 1-2  $\text{dpm}/10^6 \text{ l}$  can be set.

Dissolved  $^{232}\text{Th}$  concentrations measured with the  $\text{MnO}_2$ -Nitex adsorbers are highly variable. Some of the samples are not above the detection limit of about 0.005  $\text{dpm } ^{232}\text{Th}$  (approximately 20 ng). However, many of the samples contain amounts of  $^{232}\text{Th}$  in excess of blank levels. Values of dissolved  $^{232}\text{Th}$  are less than  $100 \text{ dpm}/10^6 \text{ l}$ , and average about  $30 \text{ dpm}/10^6 \text{ l}$  (excluding Station 1114 - 4700 m), close to the range of five values found at Site D of 15-33  $\text{dpm}/10^6 \text{ l}$  (Chapter 4).

One sample taken deep in the Middle America Trench off the coast of Nicaragua (Station 1114 - 4700 m) contained extremely high concentrations of dissolved and particulate  $^{232}\text{Th}$  (Tables 5-5 and 5-7). Since these are the only samples with such high Th concentrations, it is necessary to consider the possibility of contamination. All of the filters were stored together until their use at sea. Nitex sheets were prepared in batches of 15, and stored in contact with each other. It is highly unlikely that a single randomly contaminated filter and one randomly contaminated Nitex sheet should be chosen for use on the same sample. Laboratory analysis of the filter was performed three weeks prior to analysis of the Nitex, with many other samples run before, between and after these two. It is highly unlikely that two laboratory contamination

events should occur on the same filter-Nitex pair. The only time that the filter and Nitex were together was during the sampling at sea. No  $^{232}\text{Th}$  was taken to sea as a tracer or for any other purpose. The same pumping systems were used at every station, so contamination could not have resulted from a component of one of the pumping systems. No other plausible source of contamination can be imagined. Therefore, it appears that the high concentration of  $^{232}\text{Th}$  at the bottom of the trench is real.

Concentrations of other radioisotopes in the Station 1114 - 4700 m sample are not unusually high. The dissolved  $^{230}\text{Th}$  concentration is less than two times greater than at the other stations and is approximately equal to values found at the open-ocean Site D (Chapter 4). Particulate  $^{230}\text{Th}$  is only 3-4 times greater than at the other stations and is equal to values found at similar depths farther west in the Pacific (Krishnaswami et al., 1976). The particulate uranium concentration is similar to concentrations in other samples on the transect. The dissolved  $^{230}\text{Th}/^{231}\text{Pa}$  ratio is the highest observed at any of the stations, and this sample is the only one with a ratio significantly greater than 10.8. Particulate Pa comprises the greatest percentage of total Pa of any of the KN 73-16 samples, so the particulate  $^{230}\text{Th}/^{231}\text{Pa}$  ratio at 4700 m is identical to the ratio in other samples at Station 1114. The anomalously high dissolved  $^{230}\text{Th}/^{231}\text{Pa}$  ratio is consistent with the unusually high  $^{232}\text{Th}$  concentration, which must result from an unknown process preferentially stabilizing dissolved Th and an unknown source of dissolved  $^{232}\text{Th}$ .

#### Thorium-228

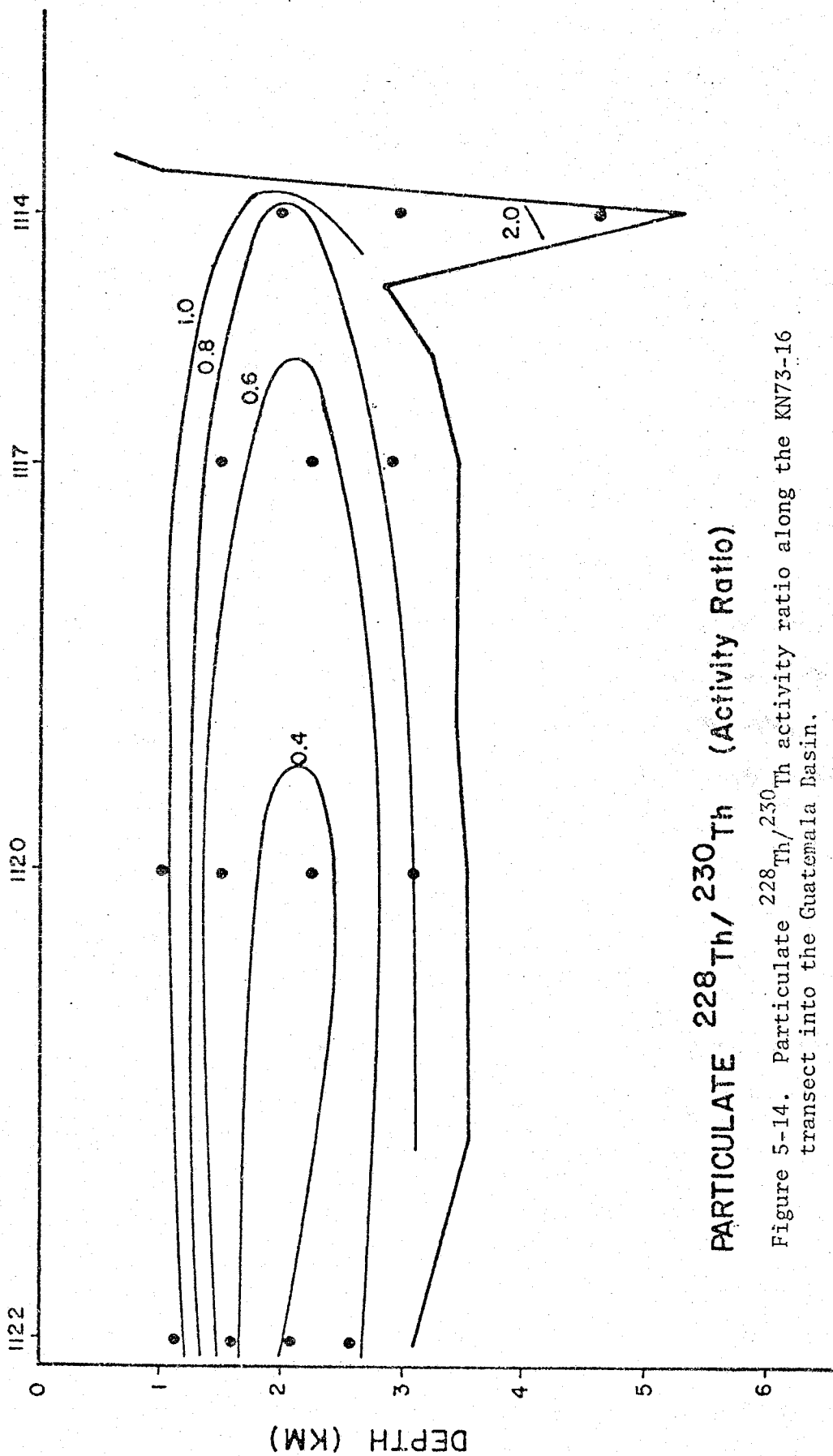
In the open ocean  $^{228}\text{Th}$  is produced near the sea surface and near the sea floor as a result of the distribution of its parent  $^{228}\text{Ra}$

(Trier et al., 1972). Specific activities of  $^{228}\text{Th}$  in trapped material were constant through mid-depths at Sites E and P because of the lack of a mid-depth source and the high settling velocity of the surface-derived particles. Specific activities of  $^{228}\text{Th}$  in trapped particles increase with depth at the STIE Site (Table 5-2). This suggests that the STIE Site is close enough to the continental slope (approximately 20 km from the Coiba Ridge) that  $^{228}\text{Ra}$  can diffuse horizontally from slope sediments to the STIE site before it is depleted from the water by radioactive decay. Production of dissolved  $^{228}\text{Th}$  throughout the water column at the STIE Site would explain the similarity of the  $^{228}\text{Th}$  distribution with depth in the STIE samples to the distributions of  $^{230}\text{Th}$  and  $^{231}\text{Pa}$  with depth at all of the sediment-trap sites.

The  $^{228}\text{Th}$  distribution in the Guatemala Basin (Tables 5-5 and 5-7) is consistent with its source by decay of  $^{228}\text{Ra}$ . The highest particulate  $^{228}\text{Th}$  concentrations were found at Station 1114 near the continental margin and near the sea floor, similar to the near-bottom increases in specific activity of particulate  $^{228}\text{Th}$  observed at Sites E and P. Processes affecting the  $^{228}\text{Th}$  distribution are best illustrated by particulate  $^{228}\text{Th}/^{230}\text{Th}$  activity ratios (Figure 5-14). The distribution is a function of the sources of these two isotopes. Production of  $^{230}\text{Th}$  occurs at a constant rate throughout the water column, whereas  $^{228}\text{Th}$  production is limited to water which has been in contact with the sea floor within a few half-lives of  $^{228}\text{Ra}$ . These sources are reflected in the higher particulate  $^{228}\text{Th}/^{230}\text{Th}$  ratios near the sea surface, near the sea floor, and near the continental margin. The observed mid-depth minimum in the open ocean is expected because the time scale for mixing this water into contact with sediments is much greater than the half-life of  $^{228}\text{Ra}$ .



KN 73-16 STATION



PARTICULATE  $^{228}\text{Th}/^{230}\text{Th}$  (Activity Ratio)

Figure 5-14. Particulate  $^{228}\text{Th}/^{230}\text{Th}$  activity ratio along the KN73-16 transect into the Guatemala Basin.

The distribution of dissolved  $^{228}\text{Th}$  is similar to that of particulate  $^{228}\text{Th}$ , and again reflects the source of  $^{228}\text{Th}$  by decay of  $^{228}\text{Ra}$ . Concentrations of dissolved  $^{228}\text{Th}$  in the mid-depth minimum at the open ocean end of the transect are approximately equal to the concentrations measured at Site P (Chapter 4). Concentrations of dissolved  $^{228}\text{Th}$  increase toward the bottom along the KN 73-16 transect, but values at approximately 3000 m only reach about 20% of those at Site D (Chapter 4). Either the flux of  $^{228}\text{Ra}$  out of the sediments is lower in the Guatemala Basin than at Site D, or greater scavenging rates in the Guatemala Basin reduce the  $^{228}\text{Th}$  concentration to levels much below that found at Site D. The former possibility is expected from the lower  $^{232}\text{Th}$  contents in STIE samples compared to samples from Sites S<sub>2</sub> and E, while the latter explanation is supported by the higher scavenging rates calculated for the Panama Basin compared to Site D from the  $^{230}\text{Th}$  data (Table 5-11). Both factors work together to produce the lower  $^{228}\text{Th}$  concentrations in the Guatemala Basin compared to Site D.

#### Uranium

Uranium contents in STIE samples are nearly constant with depth (Table 5-2), and the  $^{238}\text{U}/^{232}\text{Th}$  ratios are much higher than in typical deep-sea sediments. Both of these aspects of the uranium distribution have been observed at Sites E and P and result from a bioauthigenic uranium component in the trapped material greater than the amount of detrital uranium (Chapter 3). An average basalt  $^{238}\text{U}/^{232}\text{Th}$  ratio was assumed for the detrital minerals in the STIE samples since the  $^{232}\text{Th}/\text{Al}$  ratio approached that for basalt (Figure 5-14). Bioauthigenic uranium ( $U_{\text{BA}}$ ) (Table 5-12) accounts for 70-90% of the uranium in the STIE samples, so possible errors in the assumed detrital U/Th ratio would have a small effect on the calculated  $U_{\text{BA}}$  contents.

Bioauthigenic uranium contents of the STIE samples are equal to those measured in the 389-m sample at Site E and in the 978-m sample at Site P (Chapter 3). Fluxes of  $U_{BA}$  at Sites E and P ranged from 0.25-1.0 dpm/cm<sup>2</sup>10<sup>3</sup>y (Chapter 3), nearly an order of magnitude less than the fluxes measured in the STIE samples (Table 5-12). If the entire flux of  $U_{BA}$  at the STIE Site, including the flux from winnowed sediments, were regenerated in a 500-m layer of bottom water, the dissolved uranium concentration would change at a rate of 0.08 dpm/l-10<sup>3</sup>y, compared to a uranium concentration of 2.5 dpm/l (Turekian and Chan, 1971; Ku et al., 1977). Therefore, the conclusion reached in Chapter 3, that the  $U_{BA}$  flux at the open-ocean sites should not measurably alter the conservative behavior of uranium, also applies in the Panama Basin, where  $U_{BA}$  fluxes are an order of magnitude greater than in the open ocean.

Bioauthigenic uranium contents of trapped material decreased with depth at Sites E and P, in contrast to the constant  $U_{BA}$  contents of the STIE samples. The carrier of  $U_{BA}$  appears not to be significantly remineralized in the water column in the Panama Basin. Since sediment samples were not obtained at the STIE Site, the <sup>238</sup>U/<sup>232</sup>Th ratios in the sediments could not be used to determine the extent of  $U_{BA}$  remineralization before burial.

Hemipelagic sediments in a core studied by Kraemer (1975; 29°17'N, 87°15'W, 747 m) are qualitatively similar to the 667-m STIE sample. Kraemer (1975) found a <sup>238</sup>U/<sup>232</sup>Th activity ratio of about two in surface (9-23 cm) sediments, about a factor of two greater than the U/Th ratio in fluvial particles introduced to the area. Kraemer also found a <sup>230</sup>Th/<sup>238</sup>U ratio less than one and a <sup>231</sup>Pa/<sup>235</sup>U ratio greater than one. For comparison, the 667-m STIE sample contained a

TABLE 5-12

Bioauthigenic Uranium in STIE Samples.

Depth (m)	$^{238}\text{U}^a$	$^{232}\text{Th}^a$ dpm/g	$\text{U}_{\text{BA}}^a$	$\text{U}_{\text{BA}}\text{-Flux}$ dpm/cm <sup>2</sup> ·10 <sup>3</sup> y	Detrital-U % of Total U
667	0.788	0.089	0.699	2.46	11
1268	Lost	--	--	--	--
2265-RT 3	0.861	0.166	0.695	2.97	19
2265-RT 4	0.815	0.163	0.652	3.71	20
2265-RT 5	0.716	0.189	0.527	4.22	26
2869	0.878	0.191	0.687	3.83	22
3769	0.889	0.276	0.613	3.92	31
3791	0.913	0.265	0.648	4.20	29

<sup>a</sup>From Table 5-2.

<sup>b</sup>Calculated assuming approximate basalt composition of detrital minerals, with a  $^{238}\text{U}/^{232}\text{Th}$  activity ratio of 1.0 (Krauskopf, 1979).

$^{230}\text{Th}/^{238}\text{U}$  ratio of 0.57 and a  $^{231}\text{Pa}/^{235}\text{U}$  ratio of 1.78. The similarity in the isotope distribution between the 667-m STIE sample and the sediments studied by Kraemer indicates that hemipelagic sediments may act as a sink for seawater-derived uranium (see Veeh, 1967), and may act as a preferential sink for  $^{231}\text{Pa}$  relative to  $^{230}\text{Th}$  (Chapter 6).

Kolodny and Kaplan (1973) concluded that removal of uranium from anoxic waters of Saanich Inlet occurred primarily by formation of complexes with organic matter. The organic matter content of the sediment-trap samples was about the same in the shallowest sample at each of the sites; however, it decreased with depth to a much greater extent at Sites E and P than at the STIE Site (Honjo, 1980, personal communication). This is consistent with the more extensive remineralization of  $\text{U}_{\text{BA}}$  at Sites E and P than at the STIE site, and suggests that organic matter is the carrier phase for  $\text{U}_{\text{BA}}$ , supporting the conclusion of Kolodny and Kaplan (1973).

If the measured  $\text{U}_{\text{BA}}$  flux of about  $4 \text{ dpm/cm}^2 10^3 \text{ y}$  (Table 5-12) is representative of the whole Panama Basin, then the residence time of uranium in an average 3000 m water column in the basin with respect to this removal process is about  $2 \times 10^5$  years. This is not much less than the average residence time of uranium in the oceans ( $4 \times 10^5$  years; Brewer, 1975), which suggests that while uranium is removed from surface seawater to hemipelagic sediments, this process does not account for the removal of uranium from large areas of the open ocean.

Concentrations of particulate uranium (Table 5-7) are extremely low in seawater, in the range of  $10^{-5}$  to  $10^{-6}$  of the total uranium concentration. Precision of the measurements was not particularly good because of the small amounts of particulate uranium measured. Uranium is

not scavenged to a significant extent onto marine particles because of the stability of the soluble  $\text{UO}_2(\text{CO}_3)_3^{-4}$  complex (Starik and Kolyadnin, 1957; Langmuir, 1978). Under reducing conditions uranium is reduced from the hexavalent to the tetravalent state in which it is very particle reactive, much like tetravalent thorium. Uranium (VI) reduction in seawater should occur at a slightly higher Eh than reduction of Fe(III) (Langmuir, 1978). Therefore, while U(VI) reduction may occur in sulfide-bearing sediments, it would not be expected to occur in seawater except in basins with restricted circulation where sulfate reduction is occurring, or possibly in microenvironments where the Eh is lower than in the surrounding seawater. An intense  $\text{O}_2$  minimum occurred at all of the stations occupied during KN 73-16, where  $\text{O}_2$  concentrations were below a few  $\mu\text{M}/\text{kg}$  (unpublished data). While samples were not taken in the  $\text{O}_2$  minimum, concentrations of particulate uranium below the minimum are no higher than at Site E (Table 3-2), and the concentration of  $\text{U}_{\text{BA}}$  in the STIE samples was no greater than in the shallow sediment-trap samples at Sites E and P. These results support the predictions from the physical chemical data that U(VI) reduction should not occur at the Eh in  $\text{O}_2$  minima, and removal by scavenging onto settling particles in  $\text{O}_2$  minima is not a sink for uranium in seawater.

#### CONCLUSIONS

(1) The Panama and Guatemala Basins act as a preferential sink for  $^{231}\text{Pa}$  compared to  $^{230}\text{Th}$ . In contrast to the open ocean, where adsorption strongly favors Th, particles in these ocean-margin environments adsorb  $^{230}\text{Th}$  and  $^{231}\text{Pa}$  with little or no fractionation.

(2) Particle size is not a factor in the ratio at which  $^{230}\text{Th}$  and  $^{231}\text{Pa}$  are scavenged in the Panama Basin, to the extent that particles

collected by filtration and with sediment traps represent different size distributions.

(3) Adsorption to  $MnO_2$  is not entirely responsible for the low particulate  $^{230}Th/^{231}Pa$  ratios in the Panama Basin. Other types of particles must also adsorb Th and Pa without fractionation.

(4) Scavenging rates in the Panama and Guatemala Basins are at least an order of magnitude higher than in the open ocean. The increased scavenging rates result from a higher flux of particles and more intense scavenging at the sediment-seawater interface. However, even in this environment of intense scavenging,  $^{230}Th$  and  $^{231}Pa$  are predominantly dissolved.

(5) Because of the higher scavenging rates in the Panama and Guatemala Basins, concentrations of  $^{230}Th$  and  $^{231}Pa$  are lower than in the open ocean. Horizontal mixing processes result in a net transport of  $^{230}Th$  and  $^{231}Pa$  down concentration gradients. Thus, these basins are acting as a sink for  $^{230}Th$  and  $^{231}Pa$  produced in the open ocean. Horizontal transport redistributes  $^{231}Pa$  in the ocean to a greater extent than  $^{230}Th$ .

(6) The distributions of particulate and dissolved thorium isotopes showed that scavenging of thorium is not an irreversible process.

(7) The sea floor is a much more efficient scavenger of  $^{230}Th$  in the Panama and Guatemala Basins than in the open ocean, probably as a result of scavenging by freshly precipitated  $MnO_2$  at the sediment-seawater interface.

(8) Thorium-232 is associated with detrital minerals in the Panama Basin, showing a strong correlation with Al in a Th/Al ratio indicating a source from basalts.

(9) Bioauthigenic uranium contents of trapped material in the Panama Basin are about the same as in trapped material at shallow depths at Sites E and P. However, bioauthigenic uranium is not regenerated in the water column in the Panama Basin. Hemipelagic sediments may therefore act as a sink for surface seawater-derived uranium. Results from the sediment-trap samples are consistent with the conclusion of Kolodny and Kaplan (1973) that removal of dissolved uranium from seawater results from association with organic matter.



CHAPTER 6.

GENERAL SUMMARY

INTRODUCTION

The speciation of an element in seawater is an important factor determining its geochemical behavior. Elaborate computer models have been developed to predict the distribution of elements among various dissolved species and particulate phases (Nordstrom et al., 1979). Balistrieri et al. (1980) developed a model to predict the rate of removal of a reactive element from seawater from known constants for association with dissolved ligands and from constants for adsorption to various solid surfaces. Thorium was included in their model, and it fit well with the trend of the other elements. However, as they pointed out, a lack of stability constants for Pa prevented its inclusion in the model. The chemistry of thorium has been more extensively studied than that of protactinium because of the greater abundance of thorium on earth and because of its importance as a nuclear fuel. Stability constants for the hydrolysis and complexation behavior of thorium have been determined (Sillen and Martell, 1971; Smith and Martell, 1976; Baes and Mesmer, 1976). In contrast, the solution chemistry of protactinium is poorly understood.

This chapter consists of three sections. Some aspects of the solution chemistry of thorium and protactinium will be discussed in the first section. The second section consists of some speculation about the mechanisms producing the  $^{230}\text{Th}/^{231}\text{Pa}$  ratios found in different depositional environments. The conclusions derived from this thesis work are summarized in the final section.

SOME ASPECTS OF THE SOLUTION CHEMISTRY OF THORIUM AND PROTACTINIUM

Reviews of the solution chemistry of protactinium have been compiled by Keller (1966) and Guillaumont et al. (1968). The latter is far more comprehensive and summarizes most of the available information on stability constants for protactinium. Other reviews of the analytical (Pal'shin et al., 1970; Myasoedov et al., 1979) and preparative (Brown, 1969) chemistry of protactinium contain a little additional information on its solution chemistry. Little work has been done on the speciation of pentavalent protactinium since 1970 as evidenced by the lack of more recent information in a review by Bulman (1980) and in compilations of stability constants (Smith and Martell, 1976; Baes and Mesmer, 1976).

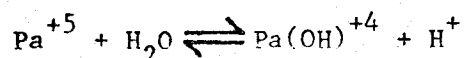
Thorium and protactinium have been described as having dual chemical natures (Pal'shin et al., 1970; Cotton and Wilkinson, 1972; Bulman, 1980). Thorium exhibits some chemical similarities to Group IV-B elements Zr and Hf, while protactinium is chemically similar to Group V-B elements Nb and Ta. Thorium and protactinium are also members of the actinide series, which involves filling the 5f electron shell. However, tetravalent thorium and pentavalent protactinium, the ionic forms stable in natural environments, both lack 5f electrons. It is because of the lack of 5f electrons that Th(IV) and Pa(V) have chemical behaviors similar to the IV-B and V-B elements as well as behaviors indicative of actinide series elements. Tetravalent protactinium contains one 5f electron, and although it is not stable with respect to oxidation in aerated solutions, it behaves chemically more like a true actinide than Th(IV) or Pa(V).

An important difference between Pa and the other pentavalent actinides is that  $\text{PaO}_2^+$  is much less stable than the  $\text{MO}_2^+$

actinyl ions of U, Np, and Pu (Cotton and Wilkinson, 1972).  $\text{PaO}_2^+$  is probably in equilibrium with  $\text{PaO}(\text{OH})_2^+$  or  $\text{Pa}(\text{OH})_4^+$  (Guillaumont et al., 1968). If the speciation of Th and Pa were predicted by analogy with the known behavior of Pu(IV) and Pu(V), Th would be expected to be strongly hydrolyzed as  $\text{Th}(\text{OH})_n^{(4-n)+}$  while Pa would form the stable and weakly hydrolyzed  $\text{PaO}_2^+$  (Cleveland, 1979). By further analogy with uranium, which forms the stable  $\text{UO}_2^{+2}$  ion, Pa would be expected to be much more resistant to scavenging from seawater than Th. Guillaumont (in Guillaumont et al., 1968) has shown that in 1-3N acid solutions ( $3\text{N ClO}_4^-$ ,  $\text{H}^+ + \text{Li}^+ = 3\text{N}$ ,  $\text{H}^+ = 1-3\text{N}$ ), Pa is present as a divalent ion, either  $\text{PaOOH}^{+2}$  or  $\text{Pa}(\text{OH})_3^{+2}$ . Guillaumont prefers the former because of the strength of the  $\text{Pa}=\text{O}$  bond. A tripositive species,  $\text{PaO}^{+3}$ , was suggested at greater than 6-8N  $\text{HClO}_4$ . In contrast to the results of Guillaumont et al., (1968), Liljenzin (1970) found evidence for a tripositive Pa species at pH less than 0.5 and reported that dipositive species did not form a significant portion of the dissolved Pa at any acid concentration. Liljenzin did not discuss the discrepancy with the results of Guillaumont et al. (1968).

Guillaumont (in Guillaumont et al., 1968) studied the fourth and fifth hydrolyses of Pa in  $3\text{N}(\text{Li}+\text{H})\text{ClO}_4$ , and reported values of  $K_4=9\times 10^{-2}$  and  $K_5=3.2\times 10^{-5}$ . He also found little variation in  $K_4$  between ionic strengths of 0.1 and 3.0. Therefore, at pH greater than about one, concentrations of the monovalent species  $\text{PaO}_2^+$ ,  $\text{PaO}(\text{OH})_2^+$ , or  $\text{Pa}(\text{OH})_4^+$  exceed the concentration of dipositive ions, and at pH greater than about 4.5 the neutral species  $\text{Pa}(\text{OH})_5$  is formed. The existence of a neutral species leads to the formation of colloids, which occurs at pH 5 even at Pa concentrations as low as  $10^{-11}\text{M}$  (Guillaumont et al., 1968).

Mikhailov (1958) estimated from theoretical considerations that the first hydrolysis constant for  $\text{Pa}^{+5}$ ,



is  $10^{3+1}$ . Thus, significant amounts of  $\text{Pa}^{+5}$  should not occur in aqueous solutions. Estimates of the second hydrolysis constant are not available. In contrast, the first hydrolysis constant for Th is about  $10^{-3}$  (Baes and Mesmer, 1976). At pH 2, it is therefore possible to have  $\text{Th}^{+4}$  coexisting with monovalent Pa species such as  $\text{PaO}_2^+$ ,  $\text{PaO}(\text{OH})_2^+$ , and  $\text{Pa}(\text{OH})_4^+$ .

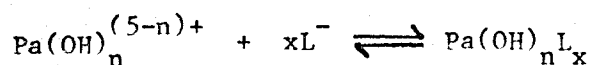
According to the model of Balistrieri et al. (1980), the rate at which a reactive element is scavenged from seawater is proportional to the magnitude of its first or second hydrolysis constant. It is necessary to know the proper reference species for the hydrolysis of Pa, i. e. the species that forms the Pa-hydroxyl bond ( $\text{Pa}^{+5}$ ,  $\text{PaO}^{+3}$ , or  $\text{PaO}_2^+$ ), in order to include Pa in the model. If the first hydrolysis constant for  $\text{Th}^{+4}$  is compared with the first hydrolysis constant for  $\text{Pa}^{+5}$ , then Pa should be scavenged much more rapidly than Th. This may not be an appropriate comparison. For example, by analogy with uranium, if a first hydrolysis constant could be estimated for  $\text{U}^{+6}$ , it would likely be even greater than for  $\text{Pa}^{+5}$ . However, the reference species for hydrolysis of uranium in solution is  $\text{UO}_2^{+2}$ , which is weakly hydrolyzed, rather than  $\text{U}^{+6}$ .

If the reference species for hydrolysis of Pa is  $\text{PaO}^{+3}$ , then the first hydrolysis constant for Pa is about 0.3 - 8 (Liljenzin, 1970; Guillaumont et al. 1968). The first hydrolysis constant for  $\text{PaO}^{+3}$  is still much greater than that of  $\text{Th}^{+4}$ . However, if  $\text{PaO}_2^+$  is the

stable reference species for the hydrolysis of Pa, with a hydrolysis stability constant of  $3.2 \times 10^{-5}$  (Guillaumont et al., 1968), then hydrolysis of Pa would be weaker than for Th, and the model of Balistrieri et al. (1980) would predict that Pa is scavenged less rapidly than Th. Regardless of which is the correct reference species for the hydrolysis of Pa, at the pH of seawater Pa should exist as the neutral species  $\text{Pa}(\text{OH})_5$ ,  $\text{PaO}(\text{OH})_3$ , or  $\text{PaO}_2\text{OH}$  in the absence of complexation by other ligands and Th should likewise exist as the neutral  $\text{Th}(\text{OH})_4$ .

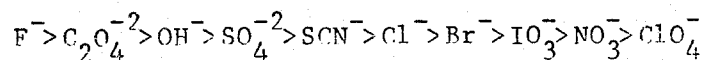
Uncertainty in the reference species for hydrolysis of Pa is only one of the problems in determining its speciation. Guillaumont et al. (1968) pointed out that some of the inconsistencies in the stability constants determined by different investigators may result in part from the difficulty in preventing the formation of Pa colloids. Another problem is that the speciation of Pa in solution seems to depend on the method of preparation of the solution.

Thorium-230 and  $^{231}\text{Pa}$  are adsorbed onto particles in the deep ocean at a ratio about an order of magnitude greater than their ratio in solution. If the first hydrolysis constant of Pa is in fact much greater than that of Th ( $\text{PaO}^{+3}$  is the proper reference species), and if the model of Balistrieri et al. (1980) is valid for Pa, then this behavior requires the formation of stable dissolved complexes of Pa to prevent adsorption. Most of the stability constants for organic complexes of Pa were determined by Gelateanu and coworkers (see Gelateanu, 1966). The speciation of Pa during their experiments was uncontrolled, and only the ligand:Pa ratios were determined for the reactions



Thus, these constants, which are the ones reported by Keller (1966), Guillaumont et al. (1968), and Sillen and Martell (1971), are of little value in determining the extent of complexation of Pa by organic matter in seawater.

Some stability constants for the formation of inorganic complexes of Pa have been determined. Much of the information on the relative stability of various Pa complexes has been determined empirically by noting the stability of solutions of Pa with respect to formation of colloids and adsorption to containers. The following series of decreasing strength of Pa complexes



(Myasoedov et al., 1979), was largely determined in this way. Most of the available data is pre-1970 and has been summarized by Guillaumont et al. (1968). In some cases, only ligand:Pa ratios were determined, as was the case with the organic complexes. Kolarich et al. (1967) presented constants for the reaction of  $\text{Pa}^{+5}$  with various ligands to form unhydrolyzed species such as  $\text{PaCl}^{+4}$  and  $\text{PaNO}_3^{+4}$ , which would not exist in their 1N  $\text{HClO}_4$  reaction medium. The hydrolysis behavior of Pa in their studies must be assumed before their constants can be used. Constants have not been determined for neutral or negatively charged mixed hydroxy-ligand species that might form in seawater, and based on the available constants in Guillaumont et al. (1968), it is unlikely that positively charged species can be formed with  $\text{Cl}^-$ ,  $\text{SO}_4^{2-}$ , or  $\text{NO}_3^-$  at their concentrations in seawater.

SPECULATION ABOUT PROCESSES REMOVING THORIUM AND PROTACTINIUM  
FROM SEAWATER

A. The Influence of Scavenging Rates on Particulate  $^{230}\text{Th}/^{231}\text{Pa}$

Ratios

With one exception (Ku, 1966), at all of the locations where  $^{230}\text{Th}/^{231}\text{Pa}$  ratios less than 10.8 have been found in sediments,  $^{230}\text{Th}$  and  $^{231}\text{Pa}$  are both accumulating in the sediments at rates greater than their rates of production in the overlying water column. Sediment samples were not obtained in the Panama Basin; however, fluxes of both isotopes into sediment traps were also greater than or equal to their rates of production in the water column above each trap. Thus environments where scavenging rates are greater than in the open ocean are not only acting as sinks for  $^{230}\text{Th}$  and  $^{231}\text{Pa}$  supplied by horizontal transport from the open ocean, but these environments also act as preferential sinks for  $^{231}\text{Pa}$  relative to  $^{230}\text{Th}$ .

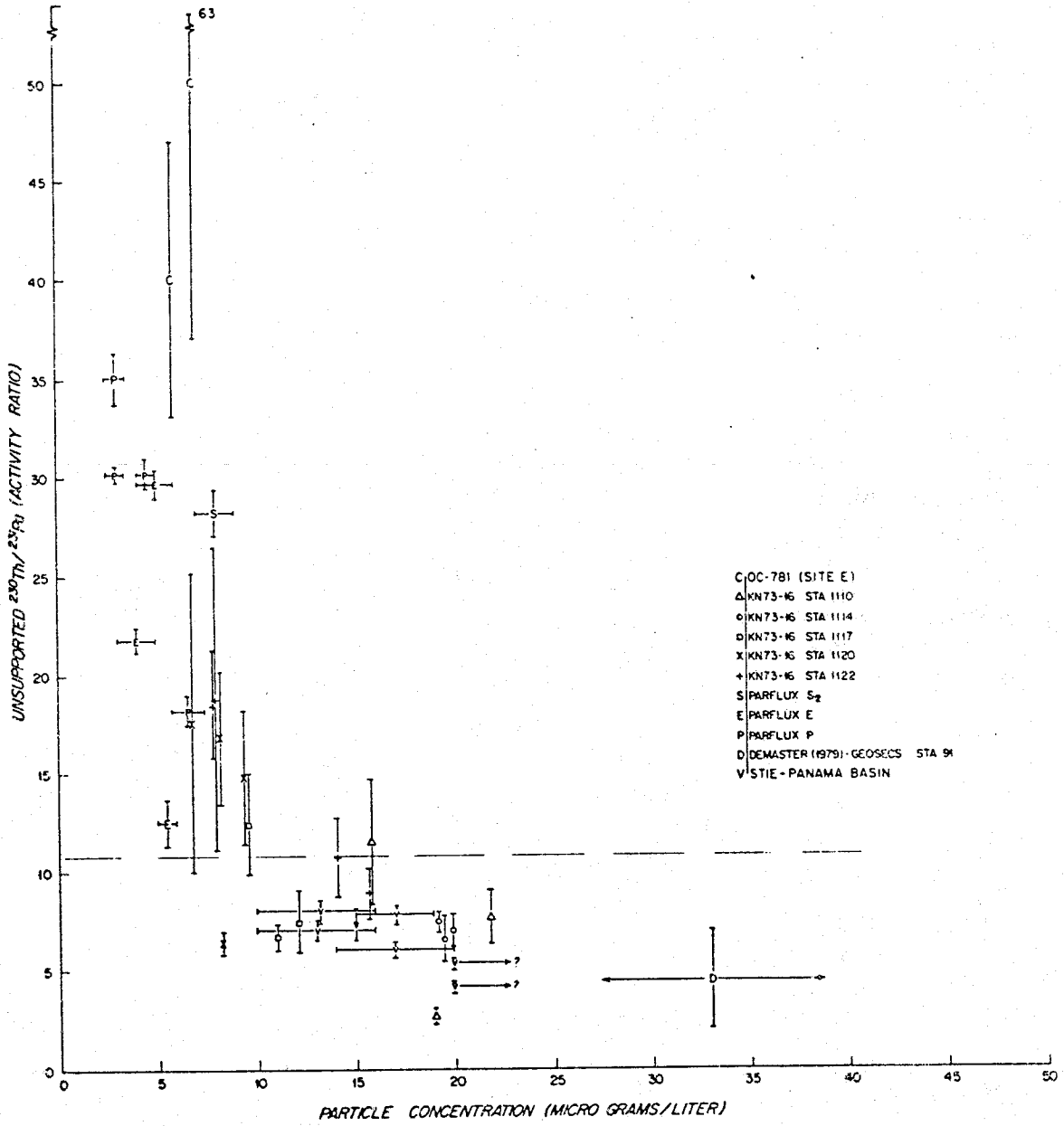
Particulate  $^{230}\text{Th}/^{231}\text{Pa}$  ratios from samples collected with sediment traps and by in situ filtration and from one set of cores are plotted against particle concentration in Figure 6-1. GEOSECS Station 91 was used to determine an average particle concentration in the area where the cores were taken. Concentrations of particles were determined from hydrocasts at each of the sediment trap sites (Spencer et al., 1978; Brewer et al., 1980; in preparation), and ranges of particle concentrations measured at depths near each sediment trap are used in Figure 6-1.

The variables plotted in Figure 6-1 do not show exclusively the relationship between scavenging rate and the resulting ratio at which  $^{230}\text{Th}$  and  $^{231}\text{Pa}$  are adsorbed. Sediment trap samples represent

Figure 6-1. Particulate  $^{230}\text{Th}/^{231}\text{Pa}$  activity ratios plotted against the concentration of suspended particles. Results are from samples analyzed during this work and Antarctic siliceous sediments from DeMaster (1979). GEOSECS Station 91 was used to determine an average particle concentration in the area where the cores were taken. Concentrations of particles were determined from hydrocasts at each of the sediment trap sites. Ranges of particle concentrations at depths near each sediment trap are shown. Samples are identified in the key in the upper right corner of the figure.



Figure 6-1.



integrated  $^{230}\text{Th}/^{231}\text{Pa}$  ratios collected by particles over the depth of the water column above the traps. Since  $^{230}\text{Th}$  and  $^{231}\text{Pa}$  tend to be scavenged at lower ratios at shallower depths, the true ratios at which  $^{230}\text{Th}$  and  $^{231}\text{Pa}$  are scavenged at the depths where the samples were collected are greater than the measured integrated ratios (Chapter 3). Furthermore, the flux of particles, which may determine scavenging rates to a greater extent than the concentration of particles, is not always proportional to the concentration of particles in the water column (Chapter 3). Nevertheless, there is a clear negative correlation between particle concentration and particulate  $^{230}\text{Th}/^{231}\text{Pa}$  ratios. As particle concentrations become very high, particulate  $^{230}\text{Th}/^{231}\text{Pa}$  ratios approach the open ocean dissolved  $^{230}\text{Th}/^{231}\text{Pa}$  ratio. Thus there are two lines of evidence linking scavenging rates with particulate  $^{230}\text{Th}/^{231}\text{Pa}$  ratios: 1) sediments with low  $^{230}\text{Th}/^{231}\text{Pa}$  ratios are accumulating excess  $^{230}\text{Th}$  and  $^{231}\text{Pa}$  at rates greater than their rates of production by uranium decay in the overlying water column, and 2) particulate  $^{230}\text{Th}/^{231}\text{Pa}$  ratios are negatively correlated with the concentration of particles.

As scavenging rates increase to the point where adsorption to particles is the only sink for dissolved  $^{230}\text{Th}$  and  $^{231}\text{Pa}$ , the particulate  $^{230}\text{Th}/^{231}\text{Pa}$  ratio must approach the ratio at which  $^{230}\text{Th}$  and  $^{231}\text{Pa}$  are supplied in the dissolved state. However, it was shown in Chapter 5 that increased scavenging rates alone cannot account for the low particulate  $^{230}\text{Th}/^{231}\text{Pa}$  ratios in the Panama and Guatemala Basins. Therefore, it is necessary to consider how the chemical properties of the particles scavenging thorium and protactinium at low  $^{230}\text{Th}/^{231}\text{Pa}$  ratios are different from the chemical properties of particles in the open ocean.

B. Composition of Particles as a Factor Controlling  $^{230}\text{Th}/^{231}\text{Pa}$  Ratios

Some data on the composition of trapped particles at PARFLUX Sites S<sub>2</sub>, E and P and the STIE Site are presented in Table 6-1. Various types of surfaces are represented by Al (clay), Fe (Fe(OH)<sub>3</sub>), Mn (MnO<sub>2</sub>), Si (SiO<sub>2</sub>), organic matter and CaCO<sub>3</sub>. Sites S, E and P are in typical open-ocean environments with high particulate  $^{230}\text{Th}/^{231}\text{Pa}$  ratios (below 1500 m at Site E), whereas  $^{230}\text{Th}/^{231}\text{Pa}$  ratios are uniformly low at the STIE site.

Sediment-trap samples from Site P have by far the lowest Al contents, while STIE samples and samples from Sites S<sub>2</sub>, and E have similar Al contents. Iron contents of STIE samples are also very similar to those at Site E; however, both are an order of magnitude greater than at Site P. Organic matter content is generally the same at all sites, although the organic matter content decreases with depth to a greater extent at Sites E and P than at the STIE site. CaCO<sub>3</sub> is significantly lower in STIE samples, although it is still the dominant component. Total Si is somewhat lower at Sites S and P and is highest at the STIE site. A better indicator of biogenic Si is the Si/Al ratio, which is lowest at Site S and is by far the highest at Site P. Concentrations of several elements were also determined by neutron activation of aliquots of the samples of filtered particulate matter from the Panama and Guatemala Basins (Figures 6-2, 6-3, 6-4, 6-5, 6-6).

It is difficult to explain the measured particulate  $^{230}\text{Th}/^{231}\text{Pa}$  ratios in terms of the available information about the composition of the particles to which they are adsorbed. The following discussion consists of a series of hypotheses based on certain observations, and contradictions to the hypotheses based on other data. It is intended

TABLE 6-1

Compositions of Particles Collected at Four Sediment Trap Sites<sup>a</sup>.

Component	S <sub>2</sub>	E	P	STIE
	(Sediment Trap Site)			
Al (%)	2.2	0.76-3.8	0.1-0.95	1.5-4.0
Fe (%)	0.75	0.2-1.9	0.01-0.24	0.9-2.0
Mn (ppm)	780	40-460	40-370	120-1320 <sup>b</sup> 9000-10000 <sup>c</sup>
Organic Matter (%)	10	20-10	16-10	22-12
CaCO <sub>3</sub> (%)	68	62-50	72-61	40-25
Si (%)	7	9-15	5-10	15-20
Si/Al (weight ratio)	3.2	11-4	34-11	13-5
Particle Flux (g/cm <sup>2</sup> 10 <sup>3</sup> y)	0.74	1.6-1.9	0.2-0.6	3.5-8.0

<sup>a</sup>Results are included here only for samples on which <sup>230</sup>Th and <sup>231</sup>Pa were measured. The first number of the range represents the shallowest sample at each site and the second number represents the deepest sample, except for particle fluxes. Data are from Honjo (1980) and Brewer et al. (1980; in preparation).

<sup>b</sup>All samples except 3769 m and 3791 m.

<sup>c</sup>Samples from 3769 m and 3791 m.

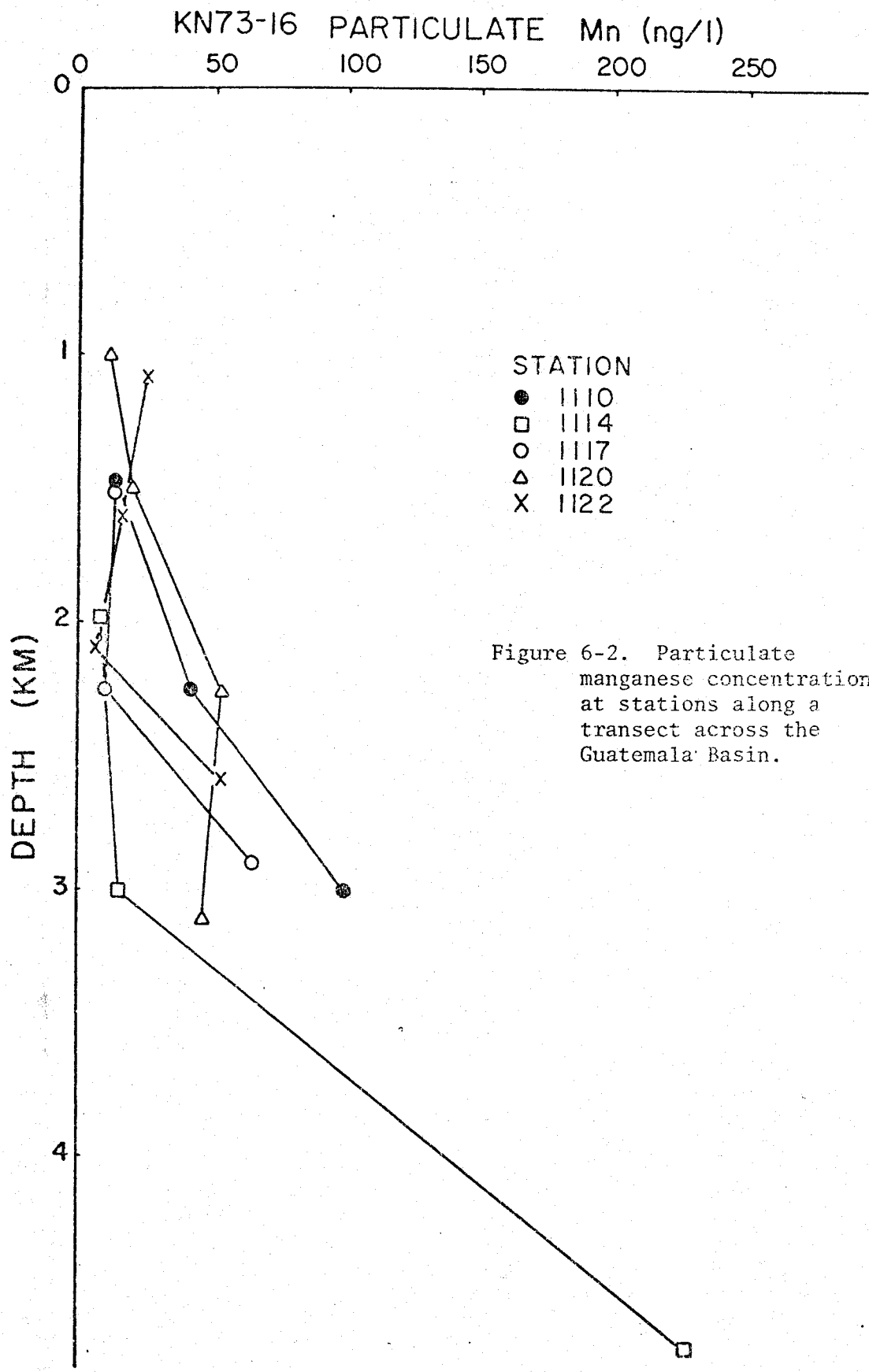


Figure 6-2. Particulate manganese concentrations at stations along a transect across the Guatemala Basin.

that this discussion should suggest areas for future research on the adsorption chemistries of thorium and protactinium.

#### Manganese Dioxide

Particles other than  $\text{MnO}_2$  must be adsorbing  $^{230}\text{Th}$  and  $^{231}\text{Pa}$  from solution at a ratio less than 10 in the Panama Basin (Chapter 5). This does not, however, prove that the  $\text{MnO}_2$  content of particulate matter has no effect on the ratio at which Th and Pa are adsorbed from seawater. One of the features of the particulate  $^{230}\text{Th}/^{231}\text{Pa}$  ratio distribution in the Panama and Guatemala Basins that is most different from the open ocean sites studied is that the ratio decreases near the sea floor compared to shallower depths (Table 5-6, Figure 5-9). The concentration of particulate Mn also increases toward the bottom (Figure 6-2), suggesting that the lower particulate  $^{230}\text{Th}/^{231}\text{Pa}$  ratios in the deepest samples may be partly caused by the higher Mn concentrations. Resuspension of  $\text{MnO}_2$  precipitated in the surface sediments (see Chapter 5) or precipitation of dissolved Mn that has diffused out of the sediments would cause the higher particulate Mn concentrations near the sea floor. However, other factors must also be involved, as some of the samples near the margin (Station 1114-2000 m and 3000 m, Station 1117-1500 m) have low particulate  $^{230}\text{Th}/^{231}\text{Pa}$  ratios and low particulate Mn concentrations. Particles other than  $\text{MnO}_2$  near the margin must also adsorb Th and Pa without fractionation, in agreement with the conclusion expressed in Chapter 5 that the low  $^{230}\text{Th}/^{231}\text{Pa}$  ratios in the STIE samples were not caused entirely by adsorption to the  $\text{MnO}_2$  in the trapped material.

#### Detrital Minerals Versus Biogenic Particles

It might be expected from the preferential association of  $^{230}\text{Th}$  with deep-sea sediments and  $^{231}\text{Pa}$  with manganese nodules that

Figure 6-3. Particulate Mn/Al ratios at stations along the transect across the Guatemala Basin.

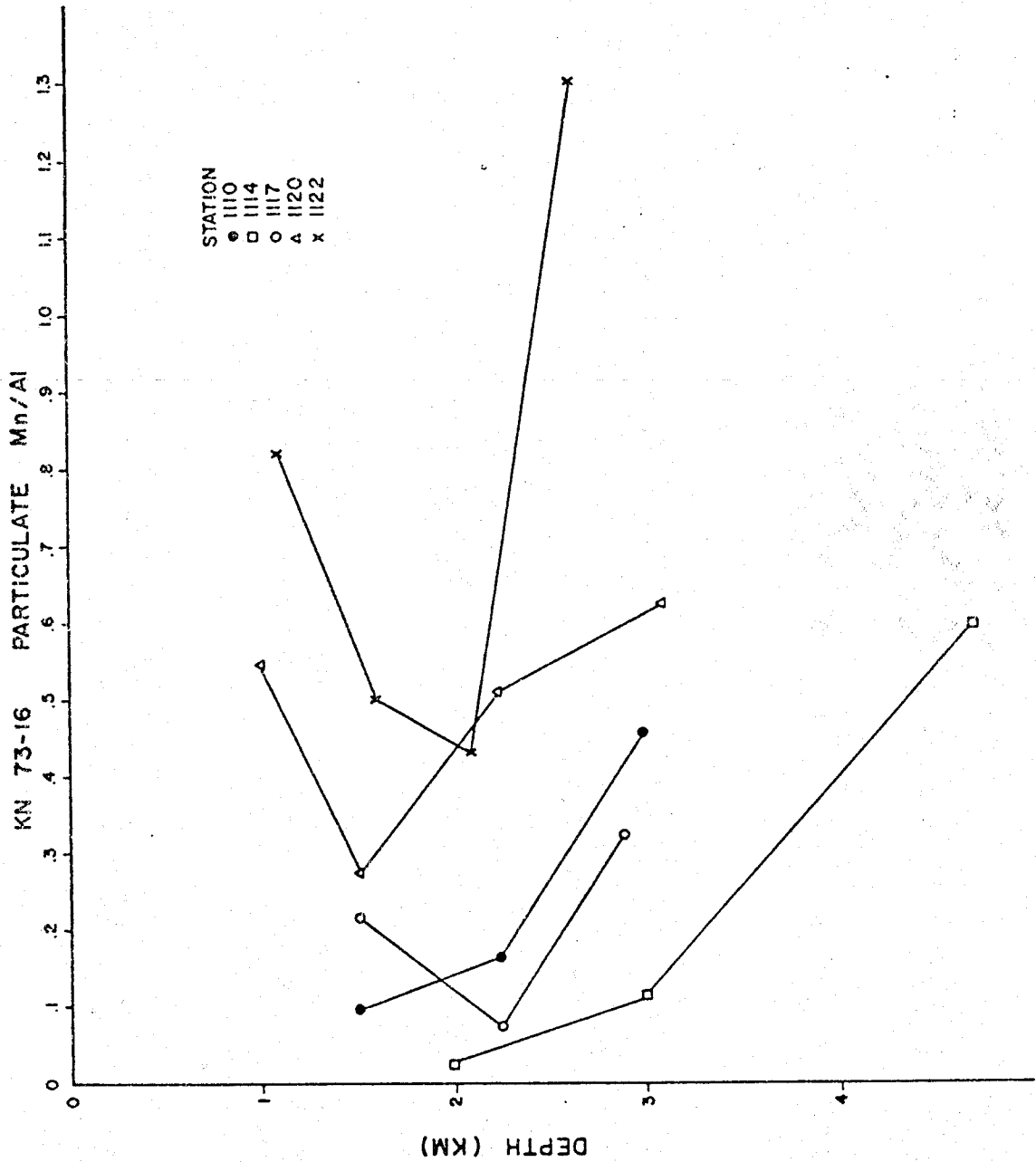
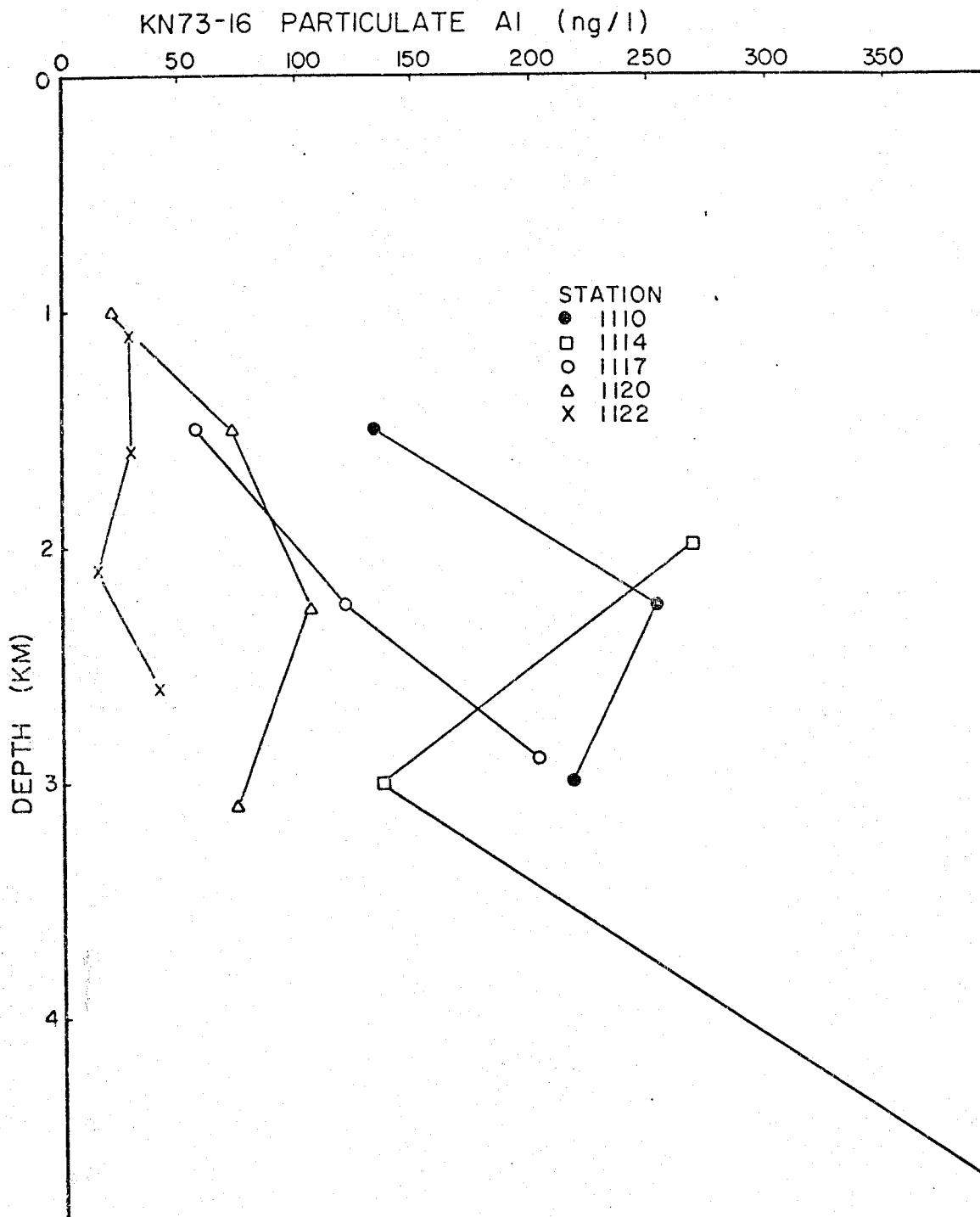


Figure 6-4. Particulate aluminum concentrations at stations along a transect across the Guatemala Basin.





### KN73-16 PARTICULATE Ca (ng/l)

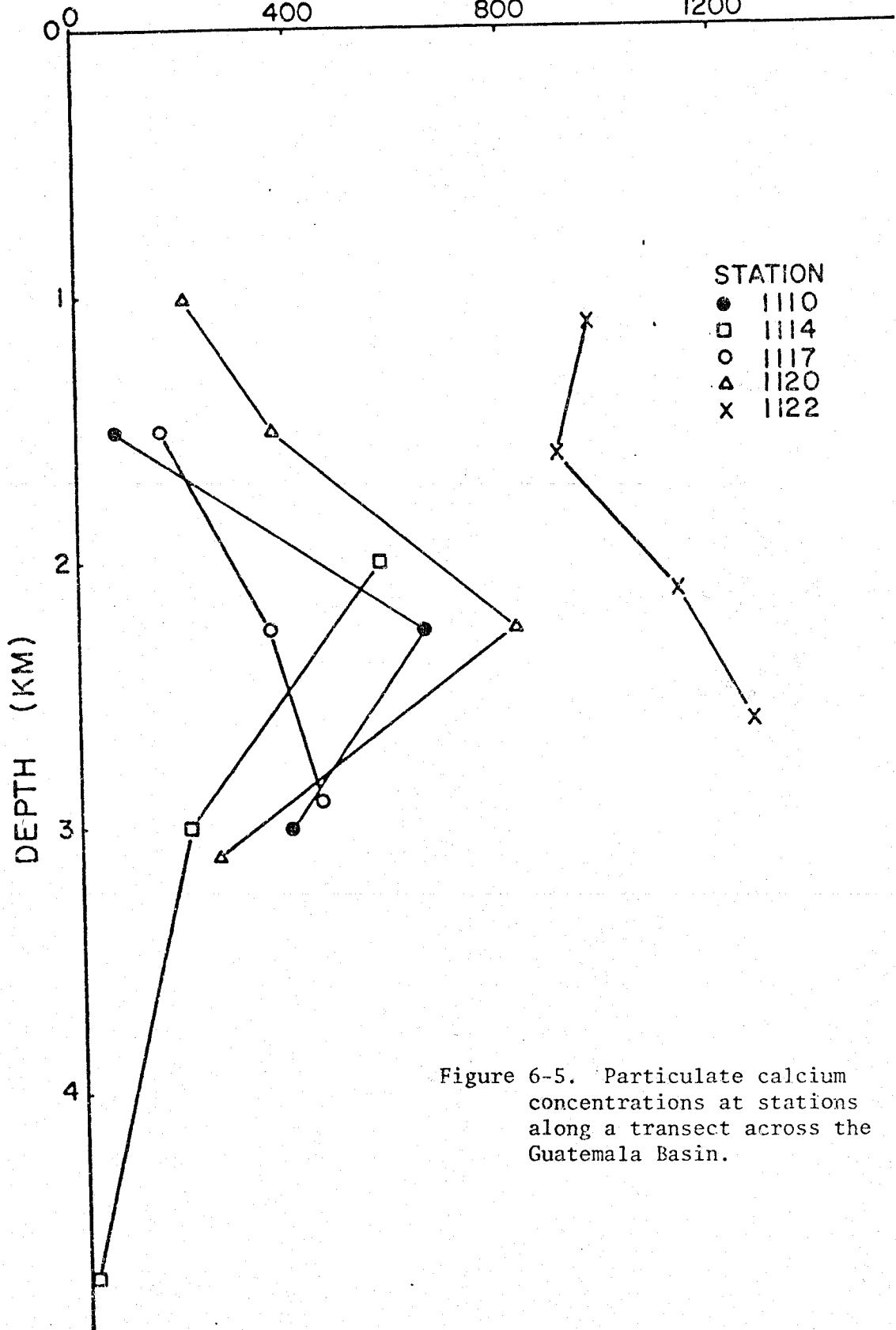
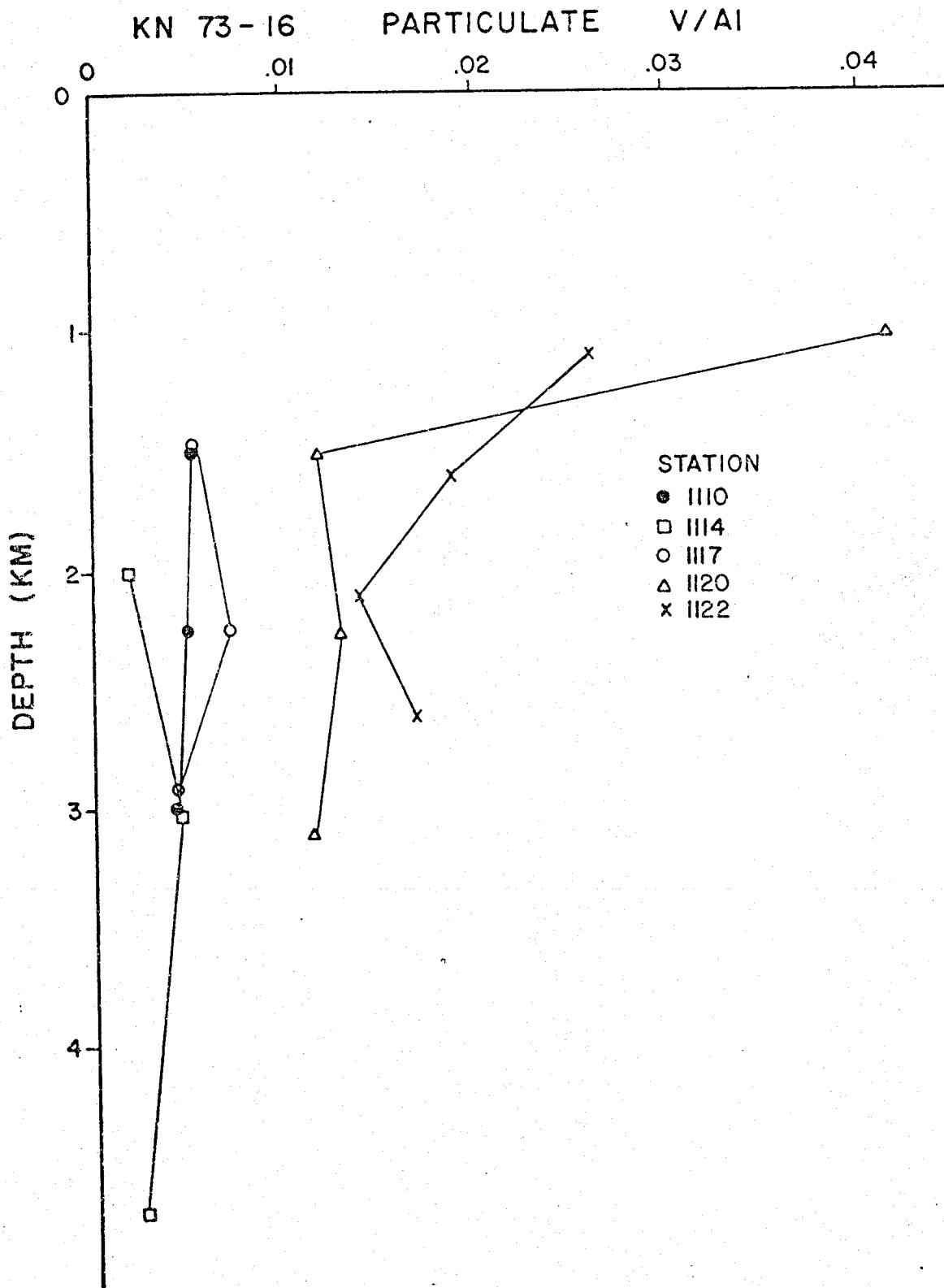


Figure 6-5. Particulate calcium concentrations at stations along a transect across the Guatemala Basin.

Figure 6-6. Particulate V/Al ratios at stations along a transect across the Guatemala Basin.



particulate  $^{230}\text{Th}/^{231}\text{Pa}$  ratios would correlate inversely with the particulate Mn/Al ratios. The opposite trend is, in fact, observed for the shallower samples in the Guatemala Basin. Samples at the seaward end of the transect have both the highest Mn/Al ratios (Figure 6-3) and the highest particulate  $^{230}\text{Th}/^{231}\text{Pa}$  ratios (Figure 5-9). The increase in the Mn/Al ratio away from the margin is not caused by an increase in the concentration of particulate Mn (Figure 6-2), but rather by a decrease in the concentration of particulate Al (Figure 6-4). It can be inferred from these results that the high  $^{230}\text{Th}/^{231}\text{Pa}$  ratios in deep-sea sediments and in the shallower samples at the seaward end of the transect are caused by preferential adsorption of  $^{230}\text{Th}$  by particles other than clays.

The change in the nature of the particulate matter along the transect in the Guatemala Basin is best illustrated by the decrease in the concentration of particulate Al away from the continent, noted above, and the increase in the concentration of particulate Ca towards the seaward end of the transect (Figure 6-5). These elemental distributions indicate a general decrease in the concentration of detrital minerals and an increase in the concentration of biogenic particles. Further evidence of the open-ocean nature of the particles at the seaward end of the transect is provided by the V/Al ratios (Figure 6-6), which equal values typically measured in open-ocean particulate material (R. Collier, personal communication).

The increase in the particulate  $^{230}\text{Th}/^{231}\text{Pa}$  ratio toward the seaward end of the transect would be expected from the results in Chapter 3. The particulate Al and Ca concentrations and V/Al ratios discussed above all indicate a decreasing proportion of detrital

particles and increasing proportion of biogenic particles with distance away from the margin. Sediment-trap samples at Site P, which generally contained higher  $^{230}\text{Th}/^{231}\text{Pa}$  ratios than samples at Sites  $S_2$  and E at similar depths, also had the highest biogenic/detrital particle ratio (Table 6-1; Honjo, 1980, personal communication). Preferential adsorption of Th relative to Pa by biogenic particles and adsorption without fractionation by  $\text{MnO}_2$  and detrital particles might then be suggested to explain these observations. However, the Site E 5086-m sample had Al and Mn contents as high as most of the STIE samples (Table 6-1), yet the Site E 5086-m sample had a  $^{230}\text{Th}/^{231}\text{Pa}$  ratio of 30 (Chapter 3). Thus, some factor other than the total Al(clay) and Mn( $\text{MnO}_2$ ) contents must determine the ratio at which Th and Pa are scavenged from seawater.

If the detrital particles in the Panama Basin adsorb Th and Pa without fractionation, then they must be compositionally different from the detrital particles at Site E. This is, in fact, the case. Detrital minerals at the STIE Site are dominated by smectite with minor contributions by chlorite and kaolinite whereas detrital minerals at Sites  $S_2$  and E are dominated by illite and kaolinite with minor amounts of smectite (Honjo, 1980, personal communication). While this does not prove that smectites are responsible for the low particulate  $^{230}\text{Th}/^{231}\text{Pa}$  ratios in the Panama Basin, the possibility must be considered. Adsorption studies should be carried out with these minerals to determine the extent to which they are likely to have influenced the particulate  $^{230}\text{Th}/^{231}\text{Pa}$  ratios.

#### Calcium Carbonate

Biogenic particles can be divided in a simple manner into  $\text{CaCO}_3$ , organic matter, and opal. STIE samples have about the same opal contents

(indicated by Si/Al ratios) as samples from Site E (Table 6-1). However, the  $\text{CaCO}_3$  content of STTE samples is significantly lower than for samples from Sites S<sub>2</sub>, E, and P (Table 6-1). Particulate Ca concentrations were highest at the seaward end of the KN73-16 transect (Figure 6-5), where the highest particulate  $^{230}\text{Th}/^{231}\text{Pa}$  ratios were found. These results suggest that fractionation of Th and Pa by  $\text{CaCO}_3$  should be considered.

Lower  $^{230}\text{Th}/^{231}\text{Pa}$  ratios in shallower sediment-trap samples at Sites E and P, which had higher  $\text{CaCO}_3$  contents than the deeper samples, contradict the hypothesis that  $\text{CaCO}_3$  causes the fractionation of Th and Pa in the deep ocean unless there is a change in the chemical nature of the  $\text{CaCO}_3$  with depth. Fresh, whole  $\text{CaCO}_3$  tests in the sediment-trap samples are nearly pure  $\text{CaCO}_3$ , while broken or partially dissolved tests contain associated Si, Al, and other elements (C. C. Wu, personal communication). Fragmentation and dissolution of  $\text{CaCO}_3$  particles may increase with depth, so the per cent of the total  $\text{CaCO}_3$  acting to remove other elements from seawater also increases with depth, which could account for the increasing  $^{230}\text{Th}/^{231}\text{Pa}$  ratios with depth in sediment-trap samples.

Two cores studied by Cochran (1979) provide further evidence contradicting the hypothesis that  $\text{CaCO}_3$  causes the initial fractionation of Th and Pa during adsorption by deep-sea particles. Both cores were from the FAMOUS area on the crest of the Mid Atlantic Ridge and contained sediments with  $^{230}\text{Th}/^{231}\text{Pa}$  ratios of eight or less. The sediments consisted of 50-60% and 68-80%  $\text{CaCO}_3$ , and the core with the higher  $\text{CaCO}_3$  content had the lower  $^{230}\text{Th}/^{231}\text{Pa}$  ratios. Finally, cores in the Caribbean and equatorial Atlantic studied by

Rosholt et al. (1961) and Ku (1966) contained 50-75%  $\text{CaCO}_3$ , yet the surface sediments had  $^{230}\text{Th}/^{231}\text{Pa}$  ratios near 10.8. Therefore, the hypothesis that  $\text{CaCO}_3$  causes the fractionation of Th and Pa by deep-sea particles, which was suggested from suspended-particle data, must be rejected on the basis of these results from sediments.

#### Organic Matter

Hemipelagic sediments studied by Kraemer (1975) from the Gulf of Mexico had an excess  $^{230}\text{Th}/^{231}\text{Pa}$  ratio less than 10.8. These sediments also had a Mn/Al ratio of 0.007, indicating that they contained little  $\text{MnO}_2$  (see discussion of xs Mn in Chapter 5) in the sediments. Therefore, the low ratios must have been caused by adsorption to some type of particle other than  $\text{MnO}_2$  which does not preferentially adsorb Th, similar to the situation in the Panama Basin. Kraemer studied the clay mineral composition of the sediments, but made no note of whether or not there was a significant amount of smectite. He did not report the organic matter content of the sediments; however, the major elements were determined, and the major mineral components sum to about 92%, allowing for the possibility of a high organic matter content. Since organic matter seems to be responsible for the presence of bio-authigenic uranium in sediment-trap samples, and since the sediments studied by Kraemer contained bio-authigenic uranium (see Chapter 5), organic matter may also partly account for the low  $^{230}\text{Th}/^{231}\text{Pa}$  ratios at the STIE Site and in the sediments studied by Kraemer. The organic matter content was about the same in the shallowest samples at all of the sediment-trap sites (Table 6-1); however, it decreased with depth to a much greater extent at Sites E and P than at the STIE Site (Honjo, 1980, personal communication). If organic matter preferentially adsorbs Pa, or adsorbs

Th and Pa without fractionation, then the decreasing organic matter content with depth at the open-ocean sites may account for the increase in the  $^{230}\text{Th}/^{231}\text{Pa}$  ratio with depth.

The content of certain extremely labile organic compounds decreased with depth to a much greater extent than the total organic matter in the Site E samples (Wakeham et al., 1980). Preferential complexation of Pa by the more labile organic compounds, which may be better preserved in the STIE samples than at the other sites, or preferential complexation of Th by the more resistant organic matter, could account for the increasing particulate  $^{230}\text{Th}/^{231}\text{Pa}$  ratios with depth. Thus, while the possibility of an influence of organic matter on the extent of fractionation of Th and Pa is suggested, the evidence is not conclusive.

#### Biogenic Silica

Six cores studied by DeMaster (1979) in an area of rapidly accumulating Antarctic siliceous oozes consistently contained sediments with  $^{230}\text{Th}/^{231}\text{Pa}$  ratios less than 10.8, and three cores had ratios of five or less. Biogenic opal constituted 48-60% of these sediments, suggesting that silica may preferentially adsorb Pa, or adsorb Th and Pa without fractionation. These cores are from an area of extremely high particle flux (Figure 6-1; DeMaster, 1979), and the increased scavenging rate in this environment (see discussion above), rather than adsorption to silica, may account for the low  $^{230}\text{Th}/^{231}\text{Pa}$  ratios.

Of the cores studied by Ku (1966), the two with the lowest  $^{230}\text{Th}/^{231}\text{Pa}$  ratios in the surface sediments, 8.6 and 12, were diatom-radiolarian oozes from the equatorial Indian Ocean and from the Pacific Antarctic respectively. These cores did not show abnormally high sedimentation rates, about  $0.5$  and  $1.0 \text{ cm}/10^3 \text{ yr}$  respectively.

Furthermore, the sediments contained inventories of excess  $^{230}\text{Th}$  and  $^{231}\text{Pa}$  nearly equal to that expected from their rates of production by uranium decay in the overlying water column. Ku did not measure the biogenic silica contents of these sediments, but the  $\text{CaCO}_3$  contents were less than 6%, allowing for potentially high silica contents. While these ratios are not as low as those observed by DeMaster (1979) or Cochran (1979) or in the Panama and Guatemala Basins, they do suggest that biogenic silica adsorbs Th and Pa without fractionation even in areas of normal open-ocean scavenging rates.

Kuznetsov et al. (1967) measured the  $^{230}\text{Th}$  and  $^{231}\text{Pa}$  contents of surface sediments from a suite of cores from the Indian and Pacific Oceans. Surface sediments in five cores from areas of siliceous oozes in the Indian Antarctic contained an average  $^{230}\text{Th}/^{231}\text{Pa}$  ratio of about 10, and only one core had a ratio greater than 10. The average ratio for five cores containing foram ooze from the southern Indian Ocean was about 17 and the average ratio for seven cores of Pacific red clay was about 41, although this average ratio may be biased too high by bioturbation in an area of extremely slow sediment deposition (see Chapter 1 for a discussion of the effect of bioturbation on  $^{230}\text{Th}/^{231}\text{Pa}$  ratios). These results add further support to the hypothesis that biogenic silica adsorbs Th and Pa without fractionation.

While the sediment results indicate that biogenic silica adsorbs Th and Pa without fractionation, this is not apparent from the sediment-trap data. The flux of biogenic silica did not change much with depth at the open ocean sediment-trap sites (Honjo, 1980), where the particulate  $^{230}\text{Th}/^{231}\text{Pa}$  ratio increased by nearly a factor of three with depth. Furthermore, the biogenic silica content of the trapped material at the



STIE Site was no greater than at the open-ocean sites (Table 6-1).

Therefore, while biogenic silica appears to affect the distribution of thorium and protactinium in sediments, other factors must also influence the  $^{230}\text{Th}/^{231}\text{Pa}$  ratios in the sediment-trap samples.

#### Particle Composition-Summary

No clear correlation of particulate  $^{230}\text{Th}/^{231}\text{Pa}$  ratios with particle composition emerges from a survey of the available data. As discussed above, several types of particles may influence the extent to which Th and Pa are fractionated during adsorption in the deep sea. Particles other than  $\text{MnO}_2$  adsorb Th and Pa at a low  $^{230}\text{Th}/^{231}\text{Pa}$  ratio in certain environments, while clays and  $\text{CaCO}_3$  appear not to be the phases fractionating Th and Pa in the deep ocean. Biogenic silica, smectites, and organic matter are suggested as phases which potentially adsorb Th and Pa without fractionation or which preferentially adsorb Pa. Studies should be carried out to determine the degree of fractionation of Th and Pa during adsorption to these particulate phases. Selection of sediments for future study from environments chosen for better control of these variables would lead to a better understanding of the mechanisms removing these elements from seawater.

#### C. Depth Dependent Factors

Sediments on the crest of the Mid Atlantic Ridge and the slope of Molokai Island have much lower  $^{230}\text{Th}/^{231}\text{Pa}$  ratios than nearby deeper sediments. This suggests the possibility that the lower ratios result from better preservation of labile biogenic particles in the shallower sediments. Sediment trap samples from Site P can be used to argue against this possibility. Particles trapped at approximately the same depth as the core from the slope of Molokai Island (KK1-Core 4; 2701m)

had a  $^{230}\text{Th}/^{231}\text{Pa}$  ratio three times greater than the ratio in the sediments (30 vs. 10). Particles trapped at 1000 m had a ratio of 18. As the trapped material was recently derived from the surface, remineralization was minimal, and better preservation of labile carrier phases is not responsible for lower ratios in KKI Core 4 (2701 m) compared to KKI Cores 1 and 2 (approximately 5800 m, Chapter 3). Therefore, either particles formed at the sea surface have different compositions near Molokai Island than at Site P, or the low ratios in the slope sediments result from near bottom processes.

There is no reason why particles formed at the sea surface over the crest of the Mid Atlantic Ridge should be different from particles formed over the flanks of the ridge. However,  $^{230}\text{Th}/^{231}\text{Pa}$  ratios were a factor of 2-4 lower in surface sediments on the ridge crest than in nearby deeper surface sediments (Cochran, 1979; Ku et al., 1972). Therefore, lower ratios in ridge-crest sediments cannot be attributed to differences in the composition of surface-derived particles.

If variable composition of surface-derived particles and preferential preservation of labile biogenic particles can be ruled out as means of producing the low ratios in KKI-Core 4 and in sediments from the crest of the Mid Atlantic Ridge, then the low ratios must be caused by some near-bottom process. There must be some chemical properties that distinguish the slope and ridge-crest sediments from nearby deeper sediments and trapped particles. Concentrations of all of the major elements were not determined for sediments from the Mid Atlantic Ridge or from Molokai Island. The  $\text{CaCO}_3$  content of the ridge-crest sediments was determined to be 50-80% (Cochran, 1979) and the total Si and K contents of KKI Core 4 were measured (A. Fleer, personal communication),

from which the biogenic silica content was estimated to be a maximum of 15%. Therefore, biogenic silica is not the phase responsible for the low  $^{230}\text{Th}/^{231}\text{Pa}$  ratios in these cores. Both cores are near sites of volcanic activity and could therefore contain hydrothermally derived  $\text{MnO}_2$ . A detailed chemical analysis of these sediments would indicate probable particulate phases responsible for the low  $^{230}\text{Th}/^{231}\text{Pa}$  ratios.

#### D. Scavenging in Surface Seawater

Particulate  $^{230}\text{Th}/^{231}\text{Pa}$  ratios in shallow sediment trap samples approached 10.8 at Site F and decreased toward the surface at Site P. This suggests that  $^{230}\text{Th}$  and  $^{231}\text{Pa}$  are adsorbed to particles at the sea surface at the ratio at which they are produced by uranium decay. This is reasonable as residence times with respect to scavenging in surface seawater are a few months, too short for other processes, such as horizontal mixing to other environments, to be effective. Measurement of dissolved  $^{230}\text{Th}/^{231}\text{Pa}$  ratios in surface seawater would indicate whether particles in surface seawater fractionate Th and Pa to the same extent as particles in the deep sea. If dissolved ratios are about 10.8, then surface particles do not fractionate Th and Pa during adsorption. Alternatively, if surface particles adsorb  $^{230}\text{Th}$  and  $^{231}\text{Pa}$  at a ratio about 10 times greater than the dissolved ratio, as is the case in the deep ocean, then the dissolved  $^{230}\text{Th}/^{231}\text{Pa}$  ratio in surface seawater must be about one.

Only a few samples of surface seawater have been analyzed for  $^{230}\text{Th}$  and  $^{231}\text{Pa}$ , and as noted in Chapter 4, the measured concentrations seem unreasonably high. Imai and Sakanoue (1973) determined total concentrations (dissolved plus particulate) in several samples from

various locations across the Pacific. There is a great deal of variability in their results, but with one exception,  $^{230}\text{Th}/^{231}\text{Pa}$  ratios were less than one. If the variability is due to patchiness in the concentration, composition, and residence time of particles in surface seawater, and if their values prove to be valid estimates for concentrations of dissolved  $^{230}\text{Th}$  and  $^{231}\text{Pa}$ , then their results suggest that surface particles preferentially scavenge Th relative to Pa much like particles in the deep ocean. If, however, it is shown that dissolved  $^{230}\text{Th}/^{231}\text{Pa}$  ratios in surface seawater are approximately 10.8, then the compositional differences between particles in surface seawater and in the deep-sea may indicate which particulate phases preferentially adsorb Th and which adsorb Th and Pa without fractionation.

#### E. Solution Chemistry

Only factors pertaining to the chemistry of the particulate phases have been considered. Adsorption of metals onto particles is in competition with complexation reactions which form nonadsorbable species. Variations in the concentrations of complexing ligands with depth or with location may influence the ratio at which Th and Pa are scavenged. Unfortunately, as was discussed earlier in this chapter, stability constants for the formation of probable Pa species in seawater do not exist.

Dissolved organic matter is ubiquitous in the oceans. Complexes with organic matter could act either to maintain an element in solution or to enhance the adsorption of an element to particle surfaces (Elliott and Huang, 1979). Organic matter has been shown to coat virtually any solid surface placed in seawater (Neihof and Joeb, 1972, 1974; Loeb and Neihof,

1977; Hunter and Liss, 1979). Surface properties of particulate matter may therefore be derived in large part from the chemical properties of adsorbed organic matter. It is conceivable then that the adsorption of Th and Pa to particles is controlled by the types of organic matter in solution and adsorbed onto the particles. Balistrieri et al. (1980) concluded that scavenging of reactive elements by particles collected in sediment traps is best explained by adsorption to humic-like organic matter. With the exception of the theoretical consideration by Balistrieri et al. (1980), the effect of organic matter on the geochemical behaviors of Th and Pa has been neglected. This topic requires further study.

GENERAL SUMMARY OF INFORMATION DERIVED FROM THIS THESIS RESEARCH

From the above discussion it is clear that the marine geochemistries of thorium and protactinium are by no means simple, and are far from being manifest. However, this work has revealed some important new insight into the marine geochemical behavior of these elements.

Fractionation of Th and Pa occurs in the water column throughout most of the open ocean. Settling particles in the deep open ocean preferentially scavenge Th relative to Pa, so that particulate  $^{230}\text{Th}/^{231}\text{Pa}$  ratios are about an order of magnitude greater than the dissolved ratios in the seawater with which they are in contact. High  $^{230}\text{Th}/^{231}\text{Pa}$  ratios commonly found in deep-sea sediments are a result of this preferential adsorption of Th relative to Pa.

In contrast to the fractionation by suspended particles, manganese dioxide adsorbs Th and Pa from seawater without measurable fractionation. Low  $^{230}\text{Th}/^{231}\text{Pa}$  ratios commonly found in manganese nodules result from the adsorption of dissolved Th and Pa at approximately the dissolved  $^{230}\text{Th}/^{231}\text{Pa}$  ratio in seawater.

Gradients in the concentrations of  $^{230}\text{Th}$  and  $^{231}\text{Pa}$  exist between different areas of the ocean with different scavenging rates. Horizontal mixing acts to redistribute  $^{230}\text{Th}$  and  $^{231}\text{Pa}$  from areas with low scavenging rates to areas with high scavenging rates. Preferential removal of  $^{230}\text{Th}$  by adsorption to settling particles in the open ocean is counterbalanced by more extensive redistribution of  $^{231}\text{Pa}$  from the open ocean to areas of enhanced scavenging rates. Fluxes of particulate  $^{230}\text{Th}$  into sediment traps can be used to set limits on the extent of redistribution of  $^{231}\text{Pa}$  by horizontal mixing. More than half of the  $^{231}\text{Pa}$  produced by decay of dissolved uranium at the open-ocean sites

studied is removed from the water column by horizontal mixing. Conversely, more than half of the flux of  $^{231}\text{Pa}$  into sediment traps in the Panama Basin was derived by horizontal transport from the open ocean.

Studies by other investigators support the conclusion that  $^{231}\text{Pa}$  is redistributed by mixing processes to a greater extent than  $^{230}\text{Th}$ . In areas where sediments have low  $^{230}\text{Th}/^{231}\text{Pa}$  ratios, both isotopes are accumulating in the sediments at rates greater than their rates of production by uranium decay in the overlying water column. Thus, environments which act as sinks for horizontally transported  $^{230}\text{Th}$  and  $^{231}\text{Pa}$ , i. e. environments where scavenging rates are greater than in the open ocean, also act as preferential sinks for  $^{231}\text{Pa}$ .

A negative correlation between particle concentration, which is one factor determining scavenging efficiency, and particulate  $^{230}\text{Th}/^{231}\text{Pa}$  ratios was found. This is further evidence that the preference for adsorption of Th by marine particles is less in areas of high scavenging rates.

Fractionation of Th and Pa during adsorption to marine particles, defined as the particulate  $^{230}\text{Th}/^{231}\text{Pa}$  ratio divided by the dissolved  $^{230}\text{Th}/^{231}\text{Pa}$  ratio, decreases by an order of magnitude from the open-ocean Site P to the Panama Basin, where measurable fractionation does not occur. Fractionation also decreases, although to a lesser extent, from the seaward edge of the Guatemala Basin toward the continental margin. Therefore, while there is a negative correlation between particulate  $^{230}\text{Th}/^{231}\text{Pa}$  ratios and scavenging rates, the decreasing extent of fractionation as the continental margin is approached indicates that the composition of the particles must also change, as they lose their preference for adsorption of Th.

It was shown that particles other than  $MnO_2$  are scavenging Th and Pa in the Panama Basin without fractionation. However, particulate  $^{230}Th/^{231}Pa$  ratios in near-bottom samples at the seaward part of the Guatemala Basin may be lowered relative to the shallower samples by the higher concentration of particulate  $MnO_2$ . No other clear correlations between particulate  $^{230}Th/^{231}Pa$  ratios and particle composition could be determined from the results of this work or from a survey of the literature. Biogenic silica, smectites, and organic matter were suggested as phases that adsorb Th and Pa without fractionation, although the evidence is inconclusive.

At least half of the flux of particulate  $^{230}Th$  and  $^{231}Pa$  collected with sediment traps is regenerated along with labile biogenic carrier phases. Thorium and protactinium are regenerated from trapped particles without measurable fractionation at two open-ocean sites studied. Thus Th and Pa may have distributions in the oceans similar to copper or other reactive trace metals that are released into solution upon dissolution or decomposition of their biogenic carrier phases at the sea floor (Boyle et al., 1977; Bruland, 1980). If other aspects of the geochemical behavior of Th and Pa hold for reactive elements in general, then ocean margins and areas of high particle flux may act as sinks for reactive elements introduced into the open ocean.

Thorium and protactinium isotopes may be extracted from seawater by adsorption to  $MnO_2$ -coated fabric. Thorium and protactinium sampled in this way are predominantly dissolved, although inclusion of a small amount of particulate isotopes cannot be disproven. An upper limit for the concentration of dissolved  $^{232}Th$  of  $1.9 \times 10^{-6}$  dpm/l ( $8 \times 10^{-12}$  g/l) was determined at one of the open-ocean sediment-trap sites,



where the dissolved  $^{230}\text{Th}/^{232}\text{Th}$  activity ratio was greater than 500. This upper limit for the  $^{232}\text{Th}$  concentration is nearly an order of magnitude lower than previous estimates of the upper limit, and the low concentration is consistent with the lack of a source of dissolved  $^{232}\text{Th}$ . Higher  $^{232}\text{Th}$  concentrations measured at other sites may indicate a greater rate of solubilization of  $^{232}\text{Th}$  at these sites, although inclusion of small amounts of particulate material in the samples cannot be disproven.

Thorium-232 correlates strongly with Al in sediment-trap samples, indicating that all of the  $^{232}\text{Th}$  can be accounted for by its association with detrital minerals. Samples collected at Site E had a Th/Al ratio near that for average shales, in agreement with the known source of detrital minerals at Site E by atmospheric transport of Saharan dust, which has a shale-like composition. Particles collected at Site P also had a Th/Al ratio near that of average shales, although there was more variability to the data than at Site E. The Th/Al ratio in particles collected with sediment traps in the Panama Basin is about a factor of four lower than at the other sites, indicating a contribution by detrital minerals with a basalt-like composition.

Trapped particles at shallow depths contained approximately the same amounts of bio-authigenic uranium at all of the sites studied. However, bio-authigenic uranium is remineralized in the water column to a much greater extent at open-ocean Sites E and P than in the Panama Basin. Hemipelagic sediments, such as occur in the Panama Basin, may therefore act as a sink for uranium incorporated into particles at the sea surface. The flux of bio-authigenic uranium to the deep sea is insufficient to measurably alter the conservative behavior of uranium in

the mixing time of the oceans. The observed behavior of bio-authigenic uranium is consistent with its formation by association with organic matter.

There is no evidence for removal of uranium from seawater by reduction of U(VI) to U(IV) with subsequent scavenging to settling particles in the intense oxygen minimum that occurs in the eastern tropical North Pacific. This is consistent with the known physical chemistry of uranium, which suggests that reduction of U(VI) should occur at about the same Eh as the reduction of Fe(III). Particulate uranium constitutes only  $10^{-5}$  to  $10^{-6}$  of the total uranium concentration in seawater.

It is difficult to create conditions in laboratory experiments that accurately reproduce the natural environment. One approach to the study of the environmental chemistry of elements such as thorium and protactinium is to sample different natural environments where chemical conditions vary in a well defined manner. Artificially introduced factors such as the presence of container walls and more importantly the non steady-state nature of laboratory systems can be avoided in this way. A simple example of such a study is presented in Appendix A, where the results of the measurement of natural and fallout actinides in a saline, alkaline lake (Mono Lake) are presented. The results of this study strongly suggest that carbonate ions effectively compete with adsorption processes in the lake, maintaining high concentrations of Th, Pa, U, and Pu isotopes compared to seawater.

REFERENCES

- Amin, B. S., S. Krishnaswami and B. L. K. Somayajulu (1974).  $^{234}\text{Th}/^{238}\text{U}$  activity ratios in Pacific Ocean bottom waters. *Earth Planet. Sci. Lett.*, 21: 342-344.
- Andelmann, J. B. and T. C. Rozzell (1970). Plutonium in the water environment. I. Characteristics of aqueous plutonium. In: *Radionuclides in the Environment*, Robert F. Gould, ed. American Chemical Society, Advances in Chemistry Series No. 93. Washington, D. C.
- Anonymous (1975). "Transuranic Elements". In: *Reference Methods for Marine Radioactivity Studies. II. Iodine, Ruthenium, Silver, Zirconium, and the Transuranic Elements*. IAEA Tech. Rept. Ser., 69: 5.
- Bacon, M. P., D. W. Spencer and P. G. Brewer (1976).  $^{210}\text{Pb}/^{226}\text{Ra}$  and  $^{210}\text{Po}/^{210}\text{Pb}$  disequilibria in seawater and suspended particulate matter. *Earth Planet. Sci. Lett.*, 32: 277-296.
- Baes, C. F. and R. F. Mesmer (1976). *The hydrolysis of cations*. John Wiley and Sons, Inc., New York, 489 pp.
- Balistrieri, L., P. G. Brewer and J. W. Murray (1980). Scavenging residence times and surface chemistry. *Deep-Sea Res.*, in press.
- Baranov, V. I. and L. A. Kuzmina (1957). Content of radioactive elements in bottom sediments of Pacific Ocean in the area of Japanese Islands. *Geochemistry*, 1: 25-36.
- Baranov, V. I. and L. A. Kuzmina (1958). The rate of silt deposition in the Indian Ocean. *Geochemistry*, 2: 131-140.
- Beasley, T. M., M. Heyraud, J. J. W. Higgo, R. D. Cherry and S. W. Fowler (1978).  $^{210}\text{Po}$  and  $^{210}\text{Pb}$  in zooplankton fecal pellets. *Mar. Biol.*, 44: 325-328.
- Bhat, S. G., S. Krishnaswami, D. Lal, Rama and W. S. Moore (1969).  $^{234}\text{Th}/^{238}\text{U}$  ratios in the ocean. *Earth Planet. Sci. Lett.*, 5: 483-491.
- Bishop, J. K. B. and J. M. Edmond (1976). A new large volume filtration system for the sampling of oceanic particulate matter. *J. Mar. Res.*, 34: 181-198.
- Bishop, J. K. B., J. M. Edmond, D. R. Ketten, M. P. Bacon and W. B. Silker (1977). The chemistry, biology and vertical flux of particulate matter from the upper 400m of the Equatorial Atlantic Ocean. *Deep-Sea Res.*, 24: 511-548.

- Bishop, J. K. B., D. R. Ketten and J. M. Edmond (1978). The chemistry, biology and vertical flux of particulate matter from the upper 400m of the Cape Basin in the southeast Atlantic Ocean. *Deep-Sea Res.*, 25: 1121-1161.
- Bonatti, E., D. E. Fisher, O. Joensuu and H. S. Rydell (1971). Postdepositional mobility of some transition elements, phosphorus, uranium and thorium in deep sea sediments. *Geochim. Cosmochim. Acta*, 35: 189-201.
- Bondiatti, E. A. and J. R. Trabalka (1980). Evidence for plutonium /V/ in an alkaline freshwater pond. *Radiochem. Radioanal. Lett.* 42: 169-176.
- Bowen, V. T., H. D. Livingston and J. C. Burke (1976). Distributions of transuranic nuclides in sediments and biota of the North Atlantic Ocean. In: *Transuranium Nuclides in the Environment*. International Atomic Energy Agency, Vienna.
- Bowen, V. T., V. E. Noshkin, H. D. Livingston and H. L. Volchok (1980). Fallout nuclides in the Pacific Ocean - vertical and horizontal distributions, largely from GEOSECS stations. *Earth Planet. Sci. Lett.*, 49: 411-434.
- Boyle, E. A., F. R. Sclater and J. M. Edmond (1977). The distribution of dissolved copper in the Pacific. *Earth Planet. Sci. Lett.*, 37: 38-54.
- Brewer, P. G. (1975). Minor elements in seawater. In: *Chemical Oceanography*. J. P. Riley and G. Skirrow, eds. Vol. 1, second edition. Academic Press, New York.
- Brewer, P. G., Y. Nozaki, D. W. Spencer and A. P. Fleer (1980). A sediment trap experiment in the deep sub-tropical Atlantic: Isotopic and elemental fluxes. *J. Mar. Res.*, in press.
- Broecker, W. S. and T. L. Ku (1969). Caribbean cores P6304-8 and P6304-9: New analysis on absolute chronology. *Science*, 166: 404-406.
- Broecker, W. S., A. Kaufman and R. M. Trier (1973). The residence time of thorium in surface seawater and its implications regarding the rate of reactive pollutants. *Earth Planet. Sci. Lett.*, 20: 35-44.
- Brown, D. (1969). Some recent preparative chemistry of protactinium. In: *Advances in Inorganic and Nuclear Chemistry*, H. J. Emeleus and A. G. Sharpe, eds. Vol. 12: 1-
- Bruland, K. W. (1980). Oceanographic distributions of cadmium, zinc, nickel, and copper in the North Pacific. *Earth Planet. Sci. Lett.*, 47: 176-198.
- Bulman, R. A. (1980). Some aspects of the bioinorganic chemistry of the actinides. *Coord. Chem. Rev.*, 31: 221-250.

- Calvert, S. E. and N. B. Price (1977). Geochemical variation in ferromanganese nodules and associated sediments from the Pacific Ocean. *Mar. Chem.*, 5: 43-74.
- Cherry, R. D., S. W. Fowler, T. M. Beasley and M. Heyraud (1975). Polonium-210: Its vertical oceanic transport by zooplankton metabolic activity. *Mar. Chem.*, 3: 105-110.
- Cleveland, J. M. (1979). Critical review of plutonium equilibria of environmental concern. pp. 321-338. In: *Chemical Modeling in Aqueous Systems*, E. A. Jenne, ed. ACS Symposium 93, American Chemical Society, Washington, D. C. 914 pp.
- Cochran, J. K. and J. K. Osmond (1976). Sedimentation patterns and accumulation rates in the Tasman Basin. *Deep-Sea Res.*, 23: 193-210.
- Cochran, J. K. (1979). The geochemistry of  $^{226}\text{Ra}$  and  $^{228}\text{Ra}$  in marine deposits. Ph. D. Thesis. Yale University, New Haven, Connecticut.
- Cochran, J. K. (1980). The flux of  $^{226}\text{Ra}$  from deep-sea sediments. *Earth Planet. Sci. Lett.*, 49: 381-392.
- Cotton, F. P. and G. Wilkinson (1972). *Advanced Inorganic Chemistry*, third edition. Interscience Publishers, New York. 1145 pp.
- DeMaster, D. J. (1979). The marine budgets of silica and  $^{32}\text{Si}$ . Ph. D. Thesis. Yale University, New Haven, Connecticut.
- Deuser, W. G. and E. H. Ross (1980). Seasonal change in the flux of organic carbon to the deep Sargasso Sea. *Nature*, 283: 364-365.
- Deuser, W. G., E. H. Ross and R. F. Anderson. Seasonality in the supply of sediment to the deep Sargasso Sea, and implications for the rapid transfer of matter to the deep ocean. Submitted to *Deep-Sea Research*.
- Elliott, H. A. and C. P. Huang (1979). The effect of complex formation on the adsorption characteristics of heavy metals. *Environ. Internat.*, 2: 145-155.
- Fleischer, R. L. and O. G. Raabe (1978). Recoiling alpha-emitting nuclei. Mechanisms for uranium-series disequilibrium. *Geochim. Cosmochim. Acta* 42: 973-978.
- Fleischer, R. L. (1980). Isotopic disequilibrium of uranium: Alpha-recoil damage and preferential solution effects. *Science* 207: 979-981.
- Foyn, E. B. Karlik, H. Pettersson and E. Rona (1939). The uranium, radium, and thorium content of sea water. *Goteb. K. Vetensk. Vitterect. Handl.*, Ser. B, No. 12., 1-44.
- Friedlander, G., J. W. Kennedy and J. M. Miller (1964). *Nuclear and Radiochemistry*. John Wiley and Sons, Inc., New York. Second Edition.

- Gelateanu, I. (1966). Etude de la formation des complexes du protactinium avec les acides di- et poly-carboxyliques par la method d'echange d'ions. *Can. J. Chem.*, 44: 647-655.
- Glaccum, R. A. and J. M. Prospero (1980). Saharan aerosols over the tropical North Atlantic - mineralogy. *Mar. Geol.*, 37: 295-321.
- Glasby, G. P. (1978). Comments on the publication by C. Lalou and E. Bricet - On some relationships between the oxide layers and the cores of deep-sea manganese nodules. *Mineralium Deposita*, 13: 131-136.
- Goldberg, E. D. and K. Bruland (1974). Radioactive geochronologies. In: *The Sea*. E. D. Goldberg, ed. Vol. 5. John Wiley and Sons, New York.
- Guillaumont, R., G. Boussieres and R. Muxart (1968). Chimie du protactinium I. Solutions aqueuses de protactinium penta- et tetravalent. *Actinides Reviews*, 1: 135-163.
- Halbach, P., V. Marchig and W. Schellmann (1978). Comments on the publication by C. Lalou and E. Bricet - On some relationships between the oxide layers and the cores of deep-sea manganese nodules. *Mineralium Deposita*, 13: 137-138.
- Hardy, E. P., P. W. Krey and H. L. Volchock (1973). Global inventory and distribution of plutonium. *Nature*, 241: 444-445.
- Honjo, S. (1978). Sedimentation of material in the Sargasso Sea at a 5367 m deep station. *J. Mar. Res.*, 36: 469-492.
- Honjo, S. (1980). Material fluxes and modes of sedimentation in the mesopelagic and bathypelagic zones. *J. Mar. Res.*, 38: 53-97.
- Hunter, K. A. and P. S. Liss (1979). The surface charge of suspended particles in estuarine and coastal waters. *Nature*, 282: 823-825.
- Imai, T. and M. Sakanoue (1973). Content of plutonium, thorium and protactinium in seawater and recent coral in the North Pacific. *J. Oceanogr. Soc. Japan*, 29: 76-82.
- Isaac, N. and E. Picciotto (1953). Ionium determination in deep-sea sediments. *Nature*, 171: 742-743.
- Johnson, D. A. (1972). Ocean-floor erosion in the Equatorial Pacific. *Geol. Soc. Am. Bull.*, 83: 3121-3144.
- Joly, J. J. (1908). On the radium content of deep sea sediments. *Philos. Mag.*, 6 Series, 16: 190-197.
- Joshi, L. U. and A. K. Ganguly (1976a). Studies on thorium and uranium disequilibrium on the surface layers of the coastal sediments and their absolute concentrations in the sediments. *J. Radioanal. Chem.*, 34: 299-308.

- Joshi, L. U. and A. K. Ganguly (1976b). Anomalous behavior of uranium isotopes in coastal marine environment of the west coast of India. *Geochim. Cosmochim. Acta.*, 40: 1491-1496.
- Kaufman, A. (1969). The Th<sup>232</sup> concentration of surface ocean water. *Geochim. Cosmochim. Acta.*, 33: 717-724.
- Keller, C. (1966). The chemistry of protactinium. *Angew. Chem. Internat. Edit.*, 5: 23-35.
- Kharkar, D. P., J. Thomson, K. K. Turekian and W. O. Forster (1976). Uranium and thorium decay series nuclides in plankton from the Caribbean. *Limnol. Oceanogr.*, 21: 294-299.
- Kolarich, R. T., V. A. Ryan and R. P. Schuman (1967). Association constants of anionic-protactinium (V) complexes. *J. Inorg. Nucl. Chem.*, 29: 783-797.
- Knauss, K. G., T. L. Ku and W. S. Moore (1978). Radium and thorium isotopes in the surface waters of the East Pacific and coastal Southern California. *Earth Planet. Sci. Lett.*, 39: 235-249.
- Koczy, F. F., E. Picciotto, G. Poulart and S. Wilgain (1957). Mesure des isotopes du thorium dans l'eau de mer. *Geochim. Cosmochim. Acta.*, 11: 103-129.
- Kolodny, Y. and I. R. Kaplan (1973). Deposition of uranium in the sediment and interstitial water of an anoxic fjord. In: *Proc. Symposium on Hydrogeochemistry and Biogeochemistry*, E. Ingerson, ed. Vol. 1, 418-442. The Clarke Co., Washington, D. C.
- Kraemer, T. F. (1975). Geochemical investigation of Pleistocene sediments from the American Mediterranean. Ph.D. Thesis, University of Miami, Coral Gables, Florida.
- Krauskopf, K. B. (1979). *Introduction to Geochemistry*. Second Edition. McGraw-Hill Book Co., New York.
- Krishnaswami, S. and M. M. Sarin (1976). Atlantic surface particulates: composition, settling rates and dissolution in the deep sea. *Earth Planet. Sci. Lett.*, 32: 430-440.
- Krishnaswami, S., D. Lal, B. L. K. Somayajulu, R. F. Weiss and H. Craig (1976). Large volume in-situ filtration of deep Pacific waters: mineralogical and radioisotope studies. *Earth Planet. Sci. Lett.*, 32: 420-429.
- Krishnaswami, S. and J. K. Cochran (1978). Uranium and thorium series nuclides in oriented ferromanganese nodules: Growth rates, turnover times and nuclide behavior. *Earth Planet. Sci. Lett.*, 40: 45-62.
- Kroll, V. S. (1953). Vertical distribution of radium in deep-sea sediments. *Nature*, 171: 742.

- Kroll, V. S. (1954). On the age-determination in deep-sea sediments by radium measurements. *Deep-Sea Res.*, 1: 211-215.
- Ku, T. L. (1966). Uranium series disequilibrium in deep-sea sediments. Ph. D. Thesis. Columbia University.
- Ku, T. L. and W. S. Broecker (1969). Radiochemical studies on manganese nodules of deep-sea origin. *Deep-Sea Res.*, 16: 625-637.
- Ku, T. L., J. L. Bischoff and A. Boersma (1972). Age studies of Mid-Atlantic Ridge sediments near 42°N and 20°N. *Deep-Sea Res.*, 19: 233-247.
- Ku, T. L. (1976). The uranium-series methods of age determination. *Ann. Rev. Earth Planet. Sci.* 4: 347-379.
- Ku, T. L., K. G. Knauss and G. G. Mathieu (1977). Uranium in open ocean: concentration and isotopic composition. *Deep-Sea Res.* 24: 1005-1017.
- Kurbatov, M. H., H. B. Webster and J. D. Kurbatov (1950). Some properties of thorium in very dilute solutions. *J. Phys. Colloid Chem.* 54: 1239-1250.
- Kuznetsov, Y. V., Z. N. Simonyak, A. N. Elizarova and A. P. Lisitzin (1956). Content of protactinium and thorium isotopes in ocean waters. *Radiokhimiya*, 8: 455-458.
- Kuznetsov, Yu. V., A. N. Elizarova and M. S. Frenklich (1967). Investigation of the mechanism of the precipitation of Pa<sup>231</sup> and Th<sup>230</sup> from ocean waters. *Soviet Radiochemistry* (1967): 425-432. Translated from *Radiokhimiya*, (1966), 8: 459-468.
- Labeyrie, L. D., H. D. Livingston and A. G. Gordon (1975). Measurement of <sup>55</sup>Fe from nuclear fallout in marine sediments and seawater. *Nucl. Inst. Meth.*, 128: 575-580.
- Labeyrie, L. D., H. D. Livingston and V. T. Bowen (1976). Comparison of the distributions in marine sediments of the fall-out derived nuclides <sup>55</sup>Fe and <sup>239,240</sup>Pu. In: *Transuranium Nuclides in the Environment*. International Atomic Energy Agency, Vienna.
- Lal, D and D. R. Schink (1960). Low background thin wall flow-counter for measuring beta activity of solids. *Rev. Sci. Instrum.*, 31: 395.
- Lalou, C and E. Brichet (1978). Replies on the comments of G. P. Glasby and E. Halbach on the publication by C. Lalou and E. Brichet - On some relationships between the oxide layers and the cores of deep-sea manganese nodules. *Mineralium Deposita*, 13: 131-136.
- Langmuir, D. (1978). Uranium solution - mineral equilibria at low temperatures with applications to sedimentary ore deposits. *Geochim. Cosmochim. Acta*, 42: 547-569.



- Lederer, C. M. and V. S. Shirley, eds. (1978). Table of Isotopes. John Wiley and Sons, New York.
- Li, Y. H., H. W. Feely and P. H. Santschi (1979).  $^{228}\text{Th}$ - $^{228}\text{Ra}$  radioactive disequilibrium in the New York Bight and its implications for coastal pollution. *Earth Planet. Sci. Lett.*, 42: 13-26.
- Liljenzin, J. O. (1970). Stability constants for protactinium (V)-acetylacetonate complexes. *Acta Chem. Scand.*, 24: 1655-1661.
- Livingston, H. D., D. R. Mann and V. T. Bowen (1975). Analytical procedures for transuranic elements in seawater and marine sediments. In: Thomas R. P. Gibb Jr. ed., *Analytical Methods in Oceanography*. American Chemical Society, Washington, D. C.
- Livingston, H. D., D. L. Schneider and V. T. Bowen (1975).  $^{241}\text{Pu}$  in the marine environment by a radiochemical procedure. *Earth Planet. Sci. Lett.*, 25: 361-367.
- Livingston, H. D. and V. T. Bowen (1976). Americium in the marine environment - relationship to plutonium. In: *Environmental Toxicity of Aquatic Radionuclides: Models and Mechanisms*. Ann Arbor Sci. Publ. Inc., Ann Arbor, Mich. pp. 107-130.
- Loeb, G. I. and R. A. Neihof (1977). Adsorption of an organic film at the platinum-seawater interface. *J. Mar. Res.*, 35: 283-291.
- Lynn, D. C. and E. Bonatti (1965). Mobility of manganese in diagenesis of deep-sea sediments. *Mar. Geol.*, 3: 457-474.
- Mangini, A. and C. Sonntag (1977).  $^{231}\text{Pa}$  dating of deep-sea cores via  $^{227}\text{Th}$  counting. *Earth Planet. Sci. Lett.*, 37: 251-256.
- Matsumoto, E. (1975). Th-234/U-238 disequilibrium in the surface layer of the ocean. *Geochim. Cosmochim. Acta*, 39: 205-212.
- McCave, I. N. (1975). Vertical flux of particles in the ocean. *Deep-Sea Res.*, 22: 491-502.
- Mikhailov, V. A. (1958). *Zhur. Fiz. Khim.*, 32: 1421. Referenced in Guillaumont et al., 1968.
- Minagawa, M. and S. Tsunogai (1980). Removal of  $^{234}\text{Th}$  from a coastal sea: Funaka Bay, Japan. *Earth Planet. Sci. Lett.*, 47: 51-64.
- Miyake, Y., Y. Sugimura and T. Yasujima (1970). Thorium concentration and the activity ratios  $^{230}\text{Th}/^{232}\text{Th}$  and  $^{228}\text{Th}/^{232}\text{Th}$  in seawater in the Western North Pacific. *J. Oceanogr. Soc. Japan*, 26: 130-136.

- Mo, T., A. D. Suttle and W. M. Sackett (1973). Uranium concentrations in marine sediments. *Geochim. Cosmochim. Acta*, 37: 35-51.
- Moore, W. S. and W. M. Sackett (1964). Uranium and thorium series inequilibrium in seawater. *J. Geophys. Res.*, 69: 5401-5405.
- Moore W. S. and D. F. Reid (1973). Extraction of radium from natural waters using manganese-impregnated acrylic fibers. *J. Geophys. Res.*, 78: 8880-8886.
- Moore, W. S. (1976). Sampling  $^{228}\text{Ra}$  in the deep ocean. *Deep-Sea Res.*, 23: 647-651.
- Moore, W. S., T. L. Ku, J. D. Macdougall, V. M. Burns, R. Burns, J. Dymond, M. W. Lyle and D. Z. Piper (in press). Fluxes of metals to a manganese nodule: radiochemical, chemical, structural, and mineralogical studies. *Earth Planet. Sci. Lett.*
- Murray, C. N. and R. Fukai (1975). Adsorption-desorption characteristics of plutonium and americium with sediment particles in the estuarine environment. Studies using plutonium-237 and americium-241. In: *Impacts of Nuclear Releases into the Environment*. International Atomic Energy Agency, Vienna.
- Myasoedov, B. F., A. V. Davydov and V. V. Nekrasova (1979). Analytical chemistry of protactinium. *Soviet Radiochemistry*, July, 1979, 726-732. Translated from: *Radiokhimiya*, (1978), 20: 851-858.
- Neihof, R. A. and G. Loeb (1972). The surface charge of particulate matter in seawater. *Limnol. Oceanogr.*, 17: 7-16.
- Neihof, R. A. and G. Loeb (1974). Dissolved organic matter in seawater and the electric charge of immersed surfaces. *J. Mar. Res.*, 32: 5-12.
- Nelson, D. M. and M. B. Lovett (1978). Oxidation state of plutonium in the Irish Sea. *Nature* 276: 599-601.
- Nikolayev, D. S., N. S. Okunev, V. M. Drozhzhnin, Ye. I. Yefimova and B. N. Belayayev (1979).  $^{234}\text{U}/^{238}\text{U}$  ratios for seas and rivers. *Geochem. Internat.*, 16: 134-144.
- Nordstrom, D. K., L. N. Plummer, T. M. L. Wiggley, T. J. Wolery, J. W. Ball, E. A. Jenne, R. L. Bassett, D. A. Crerar, T. M. Florence, B. Fritz, M. Hoffman, G. R. Holdren, Jr., G. M. Lafon, S. V. Mattigod, R. E. McDuff, F. Morel, M. M. Reddy, G. Sposito and J. Thrailkill (1979). Comparison of computerized chemical models for equilibrium calculations in aqueous systems, pp. 857-892. In: *Chemical Modeling in Aqueous Systems*, E. A. Jenne, ed. ACS Symposium 93, American Chemical Society, Washington, D. C. 914 pp.

- Nozaki, Y., J. Thomson and K. K. Turekian (1976). The distribution of  $^{210}\text{Pb}$  and  $^{210}\text{Po}$  in the surface waters of the Pacific Ocean. *Earth Planet. Sci. Lett.*, 32: 304-312.
- Nozaki, Y., J. K. Cochran, K. K. Turekian and G. Keller (1977). Radiocarbon and  $^{210}\text{Pb}$  distribution in submersible-taken deep-sea cores from Project FAMOUS. *Earth Planet. Sci. Lett.*, 34: 167-173.
- Nozaki, Y. (in preparation). Thorium-230 and thorium-228 profile in the North Pacific. Submitted to *Earth Planet. Sci. Lett.*
- Osmond, J. K. (1979). Accumulation models of  $^{230}\text{Th}$  and  $^{231}\text{Pa}$  in deep sea sediments. *Earth Sci. Rev.*, 15: 95-150.
- Pal'shin, E. S., B. F. Myasoedov and A. V. Davydov (1970). Analytical Chemistry of Protactinium. Halsted Press, New York. 233 pp.
- Pettersson, H. (1930). In: *Camp. Scient. du Prince de Monaco LXXXI*. Reference from Foyn et al., 1939.
- Pettersson, H. (1937). Der Verhaltnis Thorium zu Uran in den Gesteinen und un Meer. *Anz. Akad. Wiss. Wein, Math-Naturwiss. Kl., Ser. B*, 6: 127-128.
- Picciotto, E. and S. Wilgain (1954). Thorium determination in deep-sea sediments. *Nature*, 173: 632-633.
- Piggot, C. S. (1933). Radium content of ocean bottom sediments. *Am. J. Sci.*, 5 Series, 25: 229-238.
- Piggot, C. S. and W. D. Urry (1939). The radium content of an ocean bottom core. *J. Wash. Acad. Sci.*, 29: 405-410.
- Piggot, C. S. and W. D. Urry (1941). Radioactivity of ocean sediments III. Radioactive relations in ocean water and bottom sediments. *Am. J. Sci.*, 239: 81-91.
- Piggot, C. S. and W. D. Urry (1942a). Time relations in ocean sediments. *Bull. Geol. Soc. Am.*, 53: 1187-1210.
- Piggot, C. S. and W. D. Urry (1942b). Radioactivity of ocean sediments IV. The radium content of sediments of the Cayman Trough. *Am. J. Sci.*, 240: 1-12.
- Reid, D. F., R. M. Key and D. R. Schink (1979). Radium, thorium, and actinium extraction from seawater using an improved manganese-oxide-coated fiber. *Earth Planet. Sci. Lett.*, 43: 223-226.
- Reid, D. F., W. S. Moore and W. M. Sackett (1979). Temporal variation of  $^{228}\text{Ra}$  in the near-surface Gulf of Mexico. *Earth Planet. Sci. Lett.*, 43: 227-236.

- Richardson, M. J. (1980). Composition and characteristics of particles in the ocean: Evidence for present day resuspension. Ph. D. Thesis. Massachusetts Institute of Technology-Woods Hole Oceanographic Institution Joint Program in Oceanography, Woods Hole, Massachusetts.
- Riedel, W. R. and B. M. Funnell (1964). Tertiary sediment cores and microfossils from the Pacific Ocean floor. *Geol. Soc. London Quart. J.*, 120: 305-368.
- Rosholt, J. N., C. Emiliani, J. Geiss, F. F. Koczy and P. J. Wangersky (1961). Absolute dating of deep-sea cores by the  $^{231}\text{Pa}/^{230}\text{Th}$  method. *J. Geol.*, 69: 162-185.
- Rosholt, J. N. and B. J. Szabo (1969). Determination of protactinium by neutron activation and alpha spectrometry. In: *Modern Trends in Activation Analysis*. J. F. DeVoe and P. D. LaFleur, eds. Nat. Bur. Stan. Spec. Pub. 312, Vol. 1: 327-333.
- Rosholt, J. N., Prijana and D. C. Noble (1971). Mobility of uranium and thorium in glassy and crystallized silicic volcanic rocks. *Econ. Geol.*, 66: 1061-1069.
- Rydell, H. S. and J. M. Prospero (1972). Uranium and thorium concentrations in wind-borne Saharan dust over the Western Equatorial North Atlantic Ocean. *Earth Planet. Sci. Lett.*, 14: 397-402.
- Sackett, W. M. (1960). The protactinium-231 content of ocean water and sediments. *Science*, 132: 1761-1762.
- Sackett, W. M. (1964). Measured deposition rates of marine sediments and implications for accumulation rates of extraterrestrial dust. *Ann. N. Y. Acad. Sci.*, 119: 339-346.
- Sackett, W. M. (1966). Manganese nodules: thorium-230: protactinium-231 ratios. *Science*, 154: 646-647.
- Sackett, W. M., T. Mo, R. F. Spalding and M. E. Exner (1973). A reevaluation of the marine chemistry of uranium. In: *Radioactive Contamination in the Marine Environment*. International Atomic Energy Agency, Vienna.
- Santschi, P. H., Y. H. Li and J. Bell (1979). Natural radionuclides in the water of Narragansett Bay. *Earth Planet. Sci. Lett.*, 45: 201-213.
- Sarmiento, J. L., H. W. Feely, W. S. Moore, A. E. Bainbridge and W. S. Broecker (1976). The relationship between vertical eddy diffusion and buoyancy gradient in the deep sea. *Earth Planet. Sci. Lett.*, 32: 357-370.
- Sarmiento, J. L. and C. G. H. Rooth (1980). A comparison of vertical and isopycnal mixing models in the deep sea based on Radon 222 measurements. *J. Geophys. Res.*, 85: 1515-1518.

- Scholl, D. W., R. Von Huene, P. St.-Amand and J. B. Ridlon (1967). Age and origin of topography beneath Mono Lake, a remnant Pleistocene lake, California. *Geol. Soc. Am. Bull.* 78: 583-600.
- Scott, M. R. (1968). Thorium and uranium concentrations and isotope ratios in river sediments. *Earth Planet. Sci. Lett.*, 4: 245-252.
- Scott, M. R. and M. L. Nuzzo (1975). Adsorption chemistry of thorium and protactinium in the marine environment. Unpublished abstract from the Fall 1975 meeting of the American Geophysical Union.
- Sill, C. W. (1978). Radiochemical determination of protactinium-231 in environmental and biological materials. *Anal. Chem.*, 50: 1559-1571.
- Sillen, L. G. and A. E. Martell (1971). Stability Constants of Metal Ion Complexes. Spec. Pub. No. 25, Supplement to Spec. Pub. No. 17. The Chemical Society, London. 865 pp.
- Simpson, H. J. and T. Takahashi (1973). Interstitial water studies, Leg 15 - Chemical model of seawater and saline waters. In: Heezen, B. C., MacGregor, I. D. et al., Initial Reports of the Deep Sea Drilling Project, Vol. 20. U. S. Government Printing Office, Washington, D. C.
- Simpson, H. J., R. M. Trier, C. R. Olsen, D. E. Hammond, A. Ege, L. Miller and J. M. Melack (1980). Fallout plutonium in an alkaline, saline lake. *Science* 207: 1071-1073.
- Smith, R. M. and A. E. Martell (1976). Critical stability constants. Vol. 4: Inorganic Complexes. Plenum Press, New York. 257 pp.
- Somayajulu, B. L. K. and E. D. Goldberg (1966). Thorium and uranium isotopes in sea water and sediments. *Earth Planet. Sci. Lett.*, 1: 102-106.
- Somayajulu, B. L. K., G. R. Heath, T. C. Moore and D. S. Cronan (1971). Rates of accumulation of manganese nodules and associated sediments from the equatorial Pacific. *Geochim. Cosmochim. Acta*, 35: 621-624.
- Spencer, D. W. and P. L. Sachs (1970). Some aspects of the distribution, chemistry, and mineralogy of suspended matter in the Gulf of Maine. *Mar. Geol.*, 9: 117-136.
- Spencer, D. W., P. G. Brewer, A. P. Fleer, S. Honjo, S. Krishnaswami and Y. Nozaki (1978). Chemical fluxes from a sediment trap experiment in the deep Sargasso Sea. *J. Mar. Res.*, 36: 493-523.
- Starik, I. E. and L. B. Kolyadnin (1957). The occurrence of uranium in ocean water. *Geochemistry*, 2: 245-256.
- Starik, I. E., et al. (1967). *Radiokhimiya* 9: 105. From Andelmann and Rozzell, 1970.

- Thomson, J. and A. Walton (1972). Natural radioactive decay series elements in the oceans and sediments. Proc. R. Soc. Edinb., Ser. B, 72/73, 15: 167-182.
- Trier, R. M., W. S. Broecker and H. W. Feely (1972).  $^{228}\text{Ra}$  profile at the second GEOSECS station 1970 in the North Atlantic. Earth Planet. Sci. Lett., 16: 141-145.
- Turekian, K. K. and L. H. Chan (1971). The marine geochemistry of the uranium isotopes,  $^{230}\text{Th}$  and  $^{231}\text{Pa}$ . In: Activation Analysis in Geochemistry and Cosmochemistry. A. O. Brunfelt and E. Steinnes, eds. pp. 311-320. Universitetsforlaget: Oslo, Norway.
- Turekian, K. K., A. Katz and L. Chan (1973). Trace element trapping in pteropod tests. Limnol. Oceanogr., 18: 240-249.
- Turekian, K. K., D. P. Kharkar and J. Thomson (1974). The fates of  $\text{Pb}^{210}$  and  $\text{Po}^{210}$  in the ocean surface. J. Rech. Atmos., 8: 639-646.
- Veeh, H. H. (1967). Deposition of uranium from the ocean. Earth Planet. Sci. Lett., 3: 145-150.
- Wakeham, S. G., J. W. Farrington, R. B. Gagosian, C. Lee, H. DeBaar, G. E. Nigrelli, B. W. Tripp, S. O. Smith and N. M. Frew (1980). Organic matter fluxes from sediment traps in the equatorial Atlantic Ocean. Nature, 286: 798-800.
- Whitehead, H. C. and J. H. Feth (1961). Recent chemical analyses of waters from several closed-basin lakes and their tributaries in the western United States. Geol. Soc. Am. Bull. 72: 1421-1426.
- Wong, K. M., V. E. Noshkin and V. T. Bowen (1970). Radiochemical procedures used at WHOI for the analyses of Sr, Sb, rare earths, Cs, and Pu in seawater samples. In: Reference Methods for Marine Radioactivity Studies. IAEA, Vienna, Tech. Rep. Ser. No. 118: 119-127.

APPENDIX A

CONCENTRATION OF ACTINIDES IN MONO LAKE WATER

Introduction

Mono Lake is a saline, highly alkaline lake in eastern central California, located in a closed basin so that the only mechanism of water loss from the lake is evaporation. The salt content of Mono Lake water is more than twice that of seawater. Concentrations of the major ions in Mono Lake water are compared with average seawater values in Table A-1. Mono Lake is currently drying up (Simpson et al., 1980), and the salt content of the lake water increased significantly between the times of the two analyses referenced in Table A-1.

The geochemical behavior of the natural uranium- and thorium-series isotopes in seawater has been the focus of this thesis work, and Mono Lake offers the opportunity to study the effects of varying chemical compositions of natural waters on the chemistry of these elements. For example, one concern is the ability of major anions to act as solubilizing ligands for reactive elements, including the actinides. Simpson et al. (1980) found unexpectedly high concentrations of dissolved plutonium in Mono Lake. Therefore, it seemed that Mono Lake would be an ideal place to study the chemical behavior of the other actinides as well.

Expected Chemical Behavior of the Actinides

Plutonium normally exhibits a very high distribution coefficient with respect to uptake from the dissolved state onto particles. In most fresh water lakes nearly all of the plutonium inventory is found in the sediments (Simpson et al., 1980). In contrast with this, Simpson et al.

TABLE A-1

Composition of Mono Lake Water and Average Open Ocean Seawater.

	<u>Mono Lake</u>		<u>Seawater</u>
	(a)	(b)	(mM/l)
Cl <sup>-</sup>	409	536	540
SO <sub>4</sub> <sup>2-</sup>	82	107	28
HCO <sub>3</sub> <sup>-</sup>	87	-	2.13
CO <sub>3</sub> <sup>2-</sup>	187	-	0.17
Total CO <sub>2</sub>	-	357	-
Na <sup>+</sup>	944	1240	470
K <sup>+</sup>	29.4	38.5	10
Ca <sup>+2</sup>	0.108	0.146	10
Mg <sup>+2</sup>	1.52	1.99	52
pH	9.7 <sup>a</sup> ; 10 <sup>c</sup> ; 9.5 <sup>d</sup>		8

- a. Whitehead and Feth (1961).
- b. Simpson and Takahashi (1973).
- c. Simpson et al., (1980).
- d. This work.



found that about half of the plutonium inventory in Mono Lake was present in the water. The concentration of plutonium was about 100 times greater than in other lakes they had studied, and the distribution coefficient for uptake on sediments was about 100 times lower. One possible reason for the high plutonium concentration is complexation and solubilization by the high concentration of carbonate ions in the highly alkaline water (Table A-1). The results of Simpson et al. are not inconsistent with this possibility; however, they felt that the oxidation state of plutonium in the water could also be an important factor responsible for the high concentration of plutonium. The various oxidation states of plutonium decrease in their tendency to hydrolyze in the order  $\text{Pu}^{+4} > \text{PuO}_2^{+2} > \text{Pu}^{+3} > \text{PuO}_2^+$  (Cleveland, 1979).

Adsorption of metal ions is strongly a function of their tendency to hydrolyze (Balistrieri et al., 1980). Therefore, the rate at which plutonium is removed from Mono Lake water by adsorption to settling particles would be dependent on its oxidation state, which was not measured in Mono Lake.

Plutonium in the hexavalent oxidation state is chemically similar to uranium in the same state, forming stable  $\text{MO}_2^{+2}$  ions (Andelman and Rozzell, 1970; Cleveland, 1979) which would be much more soluble than tetravalent plutonium. Tetravalent plutonium has been shown to adsorb onto particulate matter to a greater extent than hexavalent plutonium (Murray and Fukai, 1975). Most of the plutonium from Windscale effluent that remains in solution in seawater appears to be in the hexavalent oxidation state (Nelson and Lovett, 1978). More recently, as a result of a study of dissolved plutonium in an alkaline (pH approximately 9) fresh water pond at Oak Ridge, Bondietti and Trabalka (1980) have suggested

that pentavalent plutonium is the dominant dissolved form. However, the high pH and high alkalinity of the Oak Ridge pond again present the possibility of solubilization of plutonium by carbonate complexation.

There is evidence in the literature for enhanced solubility of actinides in three oxidation states as a result of complexation by carbonate ions. The relatively high concentration of uranium (VI) in oxygenated seawater is a result of complexation of the uranyl ion by carbonate to form the stable species  $UO_2(CO_3)_3^{-4}$  (Starik and Kolyadnin, 1957; Starik et al., 1967; Langmuir, 1978). Solubility enhancement by carbonate complexation has also been observed for thorium (Kurbatov et al., 1950), which exists only in the tetravalent oxidation state, and for both tetravalent and hexavalent plutonium (Andelman and Rozzell, 1970). While complexation by carbonate ions is an important factor in the speciation of plutonium in natural waters, Pu-carbonate complexes are difficult to study because of the extent of hydrolysis of Pu at a pH high enough for  $CO_3^{-2}$  to be present (Cleveland, 1979). Thorium (IV) and protactinium (V) are rapidly adsorbed from seawater onto particulate material. However, adsorption of both elements from seawater onto various types of particle surfaces was reduced in the presence of 20-50 mM bicarbonate concentration (Scott and Nuzzo, 1975), presumably by carbonate ion complexation.

In view of the possible importance of carbonate complexation with respect to the solubility and general geochemical behavior of the actinides in natural waters, this study was initiated to measure the concentrations of several actinides in different, known oxidation states in a single sample of Mono Lake water. The natural actinides, actinium, thorium, protactinium and uranium, should be present in Mono Lake water

only in the (III), (IV), (V) and (VI) oxidation states, respectively. Therefore, the ambiguity in the results of Simpson et al. (1980) with respect to the relative importance of carbonate complexation and oxidation state for the solubilization of plutonium will not be a problem.

#### Sampling and Methods

In August, 1979, a sample of approximately 11 liters was obtained from Mono Lake in a plastic cubitainer and was shipped to Woods Hole for analysis without any pretreatment. The pH of the sample when it arrived at Woods Hole was 9.5, somewhat lower than reported previously (Table A-1). Visible amounts of particulate material were present in the sample. No attempt was made to remove the particles for fear of losing some of the dissolved actinides.

Two 500 ml portions of the sample were archived for possible future analysis, one acidified and one not. The remainder of the sample was acidified with concentrated  $\text{HNO}_3$  to  $\text{pH} < 1$ , and the water was allowed to degas for several days to remove all of the carbonate and bicarbonate. Isotope yield monitors  $^{236}\text{U}$ ,  $^{229}\text{Th}$ ,  $^{233}\text{Pa}$ ,  $^{242}\text{Pu}$ , and  $^{243}\text{Am}$  were added along with  $\text{FeCl}_3$  carrier. Several days were allowed for equilibration. The pH was then adjusted to approximately 7 with concentrated  $\text{NH}_4\text{OH}$  to precipitate the Fe as  $\text{Fe}(\text{OH})_3$ , which carries the actinides with it. Actinides were purified by ion exchange chromatography and solvent extraction (Chapter 2), and plated as thin sources suitable for alpha spectrometry.

Actinium is quantitatively isolated free of thorium isotopes during the course of this procedure. The  $^{227}\text{Th}$  daughter is then allowed to grow into radioactive equilibrium with  $^{227}\text{Ac}$  for a period of 3-5

months. A  $^{230}\text{Th}$  yield monitor is added, and thorium is separated from actinium on an anion exchange column. Thorium isotopes are plated and counted to determine the  $^{227}\text{Th}$  activity, from which the Ac activity can be calculated.

### Results

Actinide activities determined in Mono Lake water are presented in Table A-2 along with corresponding results reported in the literature for seawater. Errors reported in Table 2 are  $\pm 1\sigma$  counting statistics. The poor sensitivity for actinium (i.e., high counting errors) is due to corrections required to remove contributions to the alpha spectrum of  $^{227}\text{Th}$  by  $^{228}\text{Th}$  and  $^{229}\text{Th}$  daughters present as recoil contaminants on the detector surface.

Insufficient  $^{236}\text{U}$  spike was added to the primary sample, so that a large correction was required to remove the contribution by the  $^{234}\text{U}$  peak tail to the  $^{236}\text{U}$  peak. To more precisely determine the uranium concentration, the acidified archive subsample was analyzed for uranium using an appropriate amount of  $^{236}\text{U}$  tracer. Uranium concentrations determined on the primary sample and the archived subsample are both given in Table A-2. Calculations of residence times for thorium and protactinium presented later are based on the uranium concentration determined in the subsample.

The concentration of plutonium determined here for Mono Lake water is about a factor of two lower than found by Simpson et al. (1980) (Table A-2). This difference may simply be due to sampling at different times and locations within the lake. The difference does not change the conclusion that some factor enhances the concentration of plutonium in Mono Lake relative to other natural waters.

TABLE A-2

Actinide Activities in Mono Lake Water and Seawater.

<u>Isotope (Valence)</u>	<u>Mono Lake<sup>a</sup></u>	<u>Seawater</u>	<u>Seawater References</u>
	(dpm/10 <sup>3</sup> liters)		
232Th (IV)	886 <sub>±</sub> 29	0.002-.03 0.016	Chapter 4 Kaufman, 1969
230Th (IV)	1674 <sub>±</sub> 43	0.4-1.0 0.3-1.3 0.5-1.6	Chapter 4 Moore and Sackett 1964 Somayajulu and Goldberg
1966			
228Th (IV)	966 <sub>±</sub> 36	0.2-2.0 0.05-0.8 <sup>b</sup> 1-7 <sup>c</sup>	Chapter 4 Knauss et al., 1978 Knauss et al., 1978
238U (VI)	(2.6 <sub>±</sub> .2)X10 <sup>5d</sup> (2.40 <sub>±</sub> .05)X10 <sup>5d</sup>	2.5X10 <sup>3</sup>	Ku et al., 1977
231Pa (V)	79.4 <sub>±</sub> 2.9	0.1-0.3 0.13-0.24	Chapter 4 Moore and Sackett 1964
239+240Pu (?)	24.8 <sub>±</sub> 2.4 ~ 44 <sup>e</sup>	1-5	Bowen et al., 1980
227Ac (III)	< 6 (1.5 <sub>±</sub> 4.2)	ND <sup>f</sup>	
241Am (III)	2.7 <sub>±</sub> .6	0.3-0.7	Livingston and Bowen, 1976

a. This work.

b. Open ocean surface water.

c. Nearshore surface water.

d. First value from main sample. Second value from acidified archive subsample.

e. Simpson et al., 1980.

f. Not determined.

## Discussion

Uranium is about 100 times more concentrated in Mono Lake water than in seawater, but uranium is present at a relatively high concentration in seawater due to formation of a soluble carbonate complex. Thorium and protactinium show the greatest increases in concentration relative to seawater, ranging from  $10^3$  to  $10^5$  or more times higher. Plutonium is present in a concentration only 5-20 times greater than found in seawater. However, the plutonium concentration is probably not at a steady state in Mono Lake. Residence times for thorium and protactinium calculated for Mono Lake are a few hundred years (Table A-3, see discussion below). While the residence time for plutonium may be expected to be similar, it has only been present in the environment for less than 30 years, not nearly long enough to have reached a steady state concentration. If plutonium were to be released into the environment for the next few hundred years, its concentration in Mono Lake water might be expected to reach a steady state value much greater than in seawater, similar to the concentration enhancement observed for the natural actinides.

There is no ambiguity about the effect of oxidation state on the concentrations of the natural actinides in Mono Lake. Thorium, protactinium and uranium (IV, V, and VI oxidation states, respectively) are all present at a much higher concentration than in seawater. Therefore, any oxidation state in which plutonium is likely to be found in the environment should show similar enhanced solubility in Mono Lake. It is still not proven that complexation by carbonate ions is the mechanism responsible for the high concentrations of actinides in Mono Lake. However, considerable evidence for solubilization by carbonate

TABLE A-3

Radioisotope Activity Ratios and Residence Times in Mono Lake Water  
and Seawater.

	<u>Mono Lake</u> <sup>a</sup>	<u>Seawater</u>	<u>Seawater References</u>
$^{234}\text{U}/^{238}\text{U}$	1.14 $\pm$ .01 <sup>b</sup>	1.14 $\pm$ .03	Ku et al., 1977
$^{228}\text{Th}/^{232}\text{Th}$	1.19 $\pm$ .05	50-100+	Chapter 4
$^{230}\text{Th}/^{231}\text{Pa}$	21.08 $\pm$ .95	3-5 1.4; 3.4	Chapter 4 Moore and Sackett 1964
$^{227}\text{Ac}/^{231}\text{Pa}$	<.08	ND <sup>c</sup>	
$^{241}\text{Am}/^{239+240}\text{Pu}$	0.109 $\pm$ .026	0.2-0.3	Livingston and Bowen, 1976
$\tau_{\text{Th}}$ (yr)	668 $\pm$ 23	15-40	Chapter 4 Brewer et al., 1980 Moore and Sackett 1964 Somaya julu and Goldberg 1966
$\tau_{\text{Pa}}$ (yr)	343 $\pm$ 15	30-130	Chapter 4 Brewer et al., 1980 Moore and Sackett 1964
$\tau_{\text{Th}}/\tau_{\text{Pa}}$	1.95 $\pm$ .11	0.13-0.87	See above

a. This work.

b. From acidified archived subsample.

c. Not determined.

complexes was discussed earlier. Furthermore, of all of the major ions, carbonate is the most enriched in Mono Lake relative to seawater (Table A-1). Further work is required to resolve the specific mechanism responsible for the higher actinide concentrations.

It is interesting to note that a similar high concentration for  $^{227}\text{Ac}$  was not observed. If the residence time for trivalent actinides in Mono Lake water was as great as found for thorium and protactinium (Table A-3 and discussion below),  $^{227}\text{Ac}$ , with a half-life of 21.8 years, would be expected to be in radioactive equilibrium with its parent  $^{231}\text{Pa}$ . Only an upper limit for the concentration of  $^{227}\text{Ac}$  could be set for Mono Lake water, but the Ac/Pa ratio is clearly much less than one (Table A-3). Similarly, the  $^{241}\text{Am}/^{239+240}\text{Pu}$  activity ratio (Table A-3) is less than half the ratio observed in seawater and in atmospheric fallout (Livingston et al., 1975; Livingston and Bowen, 1976). Concentrations of trivalent actinides in Mono Lake are therefore not enhanced to nearly the same extent relative to seawater as are the higher valent actinides.

Enrichment of  $^{234}\text{U}$  relative to  $^{238}\text{U}$  is commonly observed in natural waters (Nikolayev et al., 1979). The  $^{234}\text{U}/^{238}\text{U}$  activity ratio in seawater is constant at  $1.14 \pm .03$  (Ku et al., 1977). Mono Lake has an activity ratio indistinguishable from seawater (Table A-3). Preferential loss of  $^{234}\text{U}$  from rocks into solution results from selective oxidation of  $^{234}\text{U}$  during the process of radioactive decay from  $^{238}\text{U}$  to  $^{234}\text{U}$  or preferential leaching of  $^{234}\text{U}$  from mineral lattices damaged by radioactive decay (Fleischer and Raabe, 1978; Fleischer, 1980).



No source of dissolved  $^{232}\text{Th}$  by radioactive decay of a dissolved parent isotope exists in nature. Virtually all  $^{232}\text{Th}$  in the environment is bound in detrital mineral lattices, and any found in solution must arrive through weathering or leaching from rocks. As a result, the concentration of  $^{232}\text{Th}$  in seawater is extremely low. Concentration enhancement in Mono Lake is best illustrated by  $^{232}\text{Th}$ , which is present at a concentration  $3 \times 10^4 - 4 \times 10^5$  greater than in seawater (Table A-2).

The daughter of  $^{232}\text{Th}$  is  $^{228}\text{Ra}$ , which is relatively soluble and eventually decays to  $^{228}\text{Th}$ . Because of this source of dissolved  $^{228}\text{Th}$ ,  $^{228}\text{Th}/^{232}\text{Th}$  activity ratios in seawater as high as 100 or more are found (Table A-3). In Mono Lake the ratio is only slightly greater than one, indicating that the mechanism responsible for the higher concentrations of actinides in Mono Lake does not similarly enhance the radium concentration.

Production of  $^{230}\text{Th}$  and  $^{231}\text{Pa}$  is by the radioactive decay of their uranium isotope parents. Since the  $^{234}\text{U}/^{238}\text{U}$  ratio in Mono Lake is the same as in seawater, the relative rates of production of  $^{230}\text{Th}$  and  $^{231}\text{Pa}$  should also be the same. Recently produced  $^{230}\text{Th}$  and  $^{231}\text{Pa}$  are expected, from their rates of production and radioactive half-lives, to be present in a Th/Pa activity ratio of about 11. It has long been known that there is a fractionation of thorium and protactinium produced in the oceans, with preferential incorporation of  $^{230}\text{Th}$  in deep sea sediments and  $^{231}\text{Pa}$  in manganese nodules (Ku, 1976). In the open ocean, settling marine particulate matter preferentially scavenges thorium relative to protactinium from seawater (Chapter 3), resulting in a  $^{230}\text{Th}/^{231}\text{Pa}$  activity ratio in solution significantly less than 11

(Table A-3). The situation is reversed in Mono Lake, with a  $^{230}\text{Th}/^{231}\text{Pa}$  activity ratio of about 21, nearly two times the ratio expected from production by uranium decay and 4-5 times the ratio in seawater.

Perhaps it is merely a coincidence, but a  $^{230}\text{Th}/^{231}\text{Pa}$  activity ratio of 21 is the same as would be found in rocks greater than one million years old, where the uranium series would be in radioactive equilibrium. This ratio could be derived by leaching of  $^{230}\text{Th}$  and  $^{231}\text{Pa}$  from old rocks over a long period of time during which their concentrations have simply built up in Mono Lake water, kept in solution by complexation. Scholl et al. (1967) determined a salt budget for Mono Lake and concluded that salt has been accumulating over a minimum period of 37,000 years, and perhaps as long as a few hundred thousand years. If thorium and protactinium were simply accumulating as soluble salts, their rates of accumulation would be much less than their rates of production by decay of uranium in solution. Therefore, it is reasonable to model Mono Lake in a manner similar to seawater, where the only significant source of  $^{230}\text{Th}$  and  $^{231}\text{Pa}$  is decay of uranium, and the primary removal process is by chemical scavenging.

Residence times (Table A-3) are calculated by a steady-state model for the concentrations of  $^{230}\text{Th}$  and  $^{231}\text{Pa}$  according to the equation

$$dN_d/dt = (\lambda_d + \psi_d)N_d$$

where:  $N_d$  = concentration of daughter atoms ( $^{230}\text{Th}$  or  $^{231}\text{Pa}$ )

$N_p$  = concentration of parent atoms ( $^{234}\text{U}$  or  $^{235}\text{U}$ )

$\lambda_d$  = radioactive decay constant of daughter isotope

$\lambda_p$  = radioactive decay constant of parent isotope

$\psi_d$  = first order chemical scavenging rate constant.

Residence times,  $\tau_d$ , are defined as  $1/\psi_d$ , and are calculated by substituting known values for the parameters in Equation (1) and solving for  $\psi_d$ . If river input to Mono Lake is a significant source of  $^{230}\text{Th}$  and  $^{231}\text{Pa}$ , then the residence times calculated here are too large. Simpson et al. (1980) found that the inventory of plutonium in Mono Lake was approximately equal to the amount expected from atmospheric fallout. Therefore, river input is not a significant source of plutonium to Mono Lake, adding confidence to the assumption that river input of  $^{230}\text{Th}$  and  $^{231}\text{Pa}$  is insignificant compared to production by uranium decay. The residence times of thorium and protactinium in Mono Lake are clearly much greater than in seawater (Table A-3), reflecting the solubilizing effect of complexation, presumably by carbonate ions.

#### Conclusions

Results of this work are in agreement with the conclusion of Simpson et al. (1980) that certain actinides are present at much higher concentrations in Mono Lake than in other natural waters. Evidence has been presented to support the hypothesis that concentrations of carbonate ions attainable in nature are capable of greatly enhancing the concentrations of IV-, V-, and VI-valent actinides relative to seawater. As suggested by Simpson et al., this information should be considered when making decisions regarding disposal of radioactive wastes. Concentrations of trivalent actinides (Ac and Am) are not enhanced in Mono Lake to nearly the same extent as the higher-valent actinides.

BIOGRAPHICAL NOTE

The author was born in Everett, Washington, and lived in nearby Lake Stevens through his high school years. He graduated from Lake Stevens High School in 1971. In September, 1971 he enrolled at the University of Washington, from which he received a Bachelor of Science Degree (Summa Cum Laude) in chemistry and chemical oceanography in 1975. Since June, 1975, he has been a student in the Massachusetts Institute of Technology - Woods Hole Oceanographic Institution Joint Program in Oceanography. He is a member of Phi Beta Kappa, the American Geophysical Union, and the American Society of Limnology and Oceanography.

Publications

- Denham, C. R., R. F. Anderson and M. P. Bacon (1977). Paleomagnetism and radiochemical age estimates for late-Brunhes polarity episodes. *Earth Planet. Sci. Lett.*, 32: 277-296.
- Farrington, J. W., S. M. Henrichs and R. F. Anderson (1977). Fatty acids and Pb-210 geochronology of a sediment core from Buzzards Bay, Massachusetts. *Geochim. Cosmochim. Acta*, 41: 289-296.
- Deuser, W. G., E. H. Ross and R. F. Anderson. Seasonality in supply of sediment to the deep Sargasso Sea, and implications for the rapid transfer of matter to the deep ocean. Submitted to *Deep-Sea Research*.